UNIVERSITÄTSKLINIKUM HAMBURG-EPPENDORF

Institut für Experimentelle Pharmakologie und Toxikologie

Direktor

Prof. Dr. med. Thomas Eschenhagen

Regulation von zyklischem Adenosinmonophosphat durch Phosphodiesterasen in aus humanen induzierten pluripotenten Stammzellen abgeleiteten Kardiomyozyten: Einfluss der Zellkulturbedingungen

Dissertation

Zur Erlangung des Grades eines PhD
an der Medizinischen Fakultät der Universität Hamburg

vorgelegt von:
Zafar Iqbal
aus Faisalabad, Pakistan

Hamburg (2021)

Angenommen von der

Medizinischen Fakultät der Universität Hamburg am : 23.06.2021

Veröffentlicht mit Genehmigung der

Medizinischen Fakultät der Universität Hamburg.

Prüfungsausschuss, der/die Vorsitzende: PD Dr.Torsten Christ

Prüfungsausschuss, zweite/r Gutachter/in: Prof.Dr. Viacheslav Nikolaev

Table of Contents

1. Introduction

1.1 Cardiovascular diseases an inescapable challenge

The worldwide burden of cardiovascular diseases (CVDs) is substantial (Xu et al., 2015). CVDs are highly diverse and can present themselves in different forms such as coronary artery disease (CAD), ischemic heart disease (IHD), myocardial infarction (MI), heart failure (HF), dilated cardiomyopathy (DCM), atrial fibrillation (AF), stroke, peripheral arterial disease (PAD), rheumatic heart disease (RHD), congenital heart disease (CHD), venous thromboembolism (VTE) and several further types of cardiac and vascular conditions (Naghavi et al., 2015). The high prevalence, a wide range of co-morbidities, and an alarming mortality rate are grave features of CVDs (Benjamin et al., 2019). CVDs make up 31% of all human deaths globally and up to 40% of deaths in the European Union (Nichols et al., 2012). Cardiac arrhythmias are the major cause of sudden death in human beings in developed nations (Wolf and Berul, 2008). They can be the consequence of CHD, which is the most commonly occurring congenital malformation (Van der Linde et al., 2011). If no precautionary measures are taken against CHD, it can lead to arrhythmias and become the cause of death in children (Colan et al., 1984). Different CVDs contribute differently to mortality in human (Fig.1) depending upon factors like age, gender, ethnicity and lifestyle.

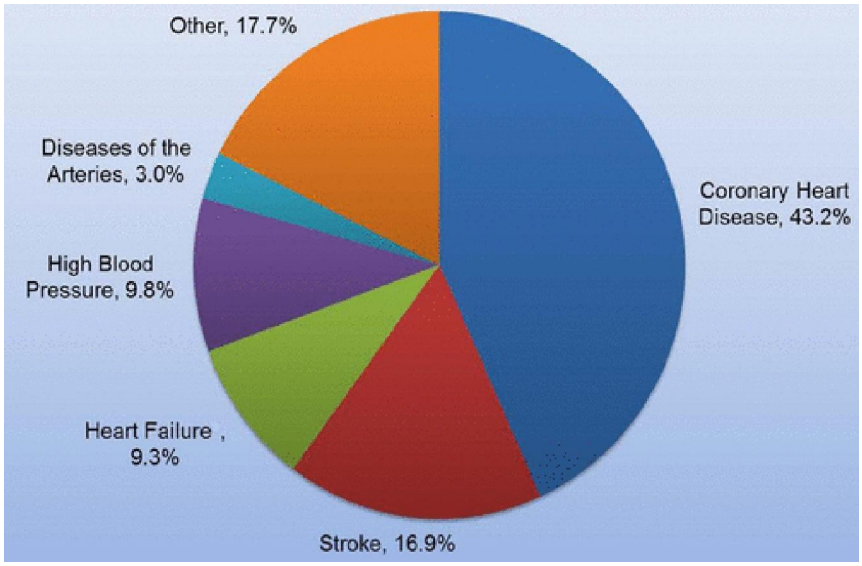

Figure 1: Percentage breakdown of deaths attributable to cardiovascular diseases

The percentage of deaths owing to different CVDs in the United States. Coronary heart disease is by far the most lethal CVD and stroke is the second most deadly. Statistical data about different CVDs and the figure are taken from Benjamin et al., 2019.

1. Introduction

In Europe and the USA, CAD and stroke are the major CVDs with respect to the percentage of mortality they cause. Furthermore, according to a forecasting report about CVDs in the USA, about 92.1 million adults will suffer at least one CVD by 2030 (Benjamin et al., 2017). Currently, about 750,000 people/year become victims of a heart attack in the USA and early measures could reduce this number significantly (Dracup et al., 2008).

A multifactorial aetiological model of CVDs suggested that obesity, a high-fat diet, sedentary lifestyle, alcohol consumption and smoking are among major contributors of CVDs. According to the European cardiovascular disease statistics of 2016 the scope of CVDs and their mortality rate is different in males versus females (Fig.2 A and B). The number of female smokers have been increasing for the last few decades, which may be one of many other contributing factors to the greater risk of developing CVDs in females than males (Bolego et al., 2002; Townsend et al., 2016). The prevalence of CVDs has a direct relationship to family history, so it is important and recommendable to study the genetic makeup of family members (Miller et al., 2014; Veronesi et al., 2014). Austin et al., 2004 has for example reported that there is a direct relationship between familial hypercholesterolemia and CVDs in the family history. Although a lot of studies have tried to reveal the pathophysiology of CVDs there is yet a strong need for further studies and continuous efforts to understand the aetiology and pathophysiology of CVDs and to establish therapeutic regimens to cure them.

Apart from this, drug-related cardiotoxicity is another major cause of cardiac complications. This drug-related cardiotoxicity is major cause of attrition of many pharmaceutical agents during their developmental phases (Abassi et al., 2012; Albini et al., 2009; Laverty et al., 2011). Drug-related cardiotoxicity is usually detected during pre-clinical testing in animals but also during post-marketing phase (Mellor et al., 2011). Number of pharmaceutical agents are increasing and widely available to be used in human beings. So in turn chances of occurrences of unexpected cardiovascular incidences have also increased. Cardiotoxic drugs can be divided into two categories i.e. cardiovascular drugs and non-cardiovascular drugs. Different pharmaceutical agents share different molecular and cellular mechanisms of cardiotoxicity (Murphy and Dargie, 2007). Drug-related cardiotoxicity may affect both structures and functions of cardiomyocytes (Pollard et al., 2010; Force and Kolaja, 2011). Pharmacological agents like β-blockers and calcium channel antagonists which produce negative chronotropic and inotropic effects can precipitate decompensated HF (Goldstein et al., 1991). Use of β_2-ARs agonists, in patients with left ventricular systolic dysfunction and HF may increase chances of necrosis of cardiomyocytes (Libretto, 1994; Cazzola et al., 2005).

1. Introduction

Systemic lupus erytheromatosis often produces pericarditis and some drugs can cause systemic lupus erytheromatosis (Rubin, 2005). Additionally, there are many reports about drugs which may cause pericarditis without any connection to systemic lupus erytheromatosis. For instance, Clozapine (Wehmeier et al., 2005) and 5-aminosalicylic acids (Ishikawa et al., 2001) and antiparkinsonian drugs (bromocriptine and cabergoline) have association with constrictive pericarditis (Champagne et al., 1999; Townsend and MacIver, 2004). Moreover, these ergot-derived dopamine agonist (cabergoline and pergolide) and appetite suppressants (fenfluramine and dexfenfluramine) may cause regurgitant valvular disease (Zanettini et al., 2007; Connolly et al., 1997). Anticancer drugs (Schimmel et al., 2004), antipsychotic drugs (Coulter et al., 2001) and antimalarial drugs (Marquardt and Albertson, 2001) are associated with HF and left ventricular systolic dysfunction. Arrhythmia i.e. tachycardia as well as bradycardia are induced by many drugs. Antiarrhythmic drugs may be considered as proarrhythmic in patients of AF (Lafuente-Lafuente et al., 2006). Pre-existing CVDs make patients more susceptible to drug-induced arrhythmias (Kerin et al., 1994). Polypharmacy, especially proarrhythmic drugs with cytochrome-p450 inhibitors, may induce arrhythmias (Honig et al., 1993). Chao et al., 1996 have reported β_2-agonist-induced torsade de pointes. Many non-cardiovascular drugs can be cardiotoxic, for example high doses of analgesics (Faria et al., 2016), such as diclofenac or celecoxib. Diclofenac can cause repolarization impairment in ventricular muscles (Kristof et al., 2012), while celecoxib produces toxicity by blocking sodium channels, hERG (human Ether-a-go-go Related Gene) and rapidly activating delayed rectifier potassium ion channels (Frolov et al., 2011). Drugs used to treat disturbances in gastrointestinal motility such as metoclopramide and domperidone produce malignant arrhythmia due to toxic interaction with sodium channels (Stoetzer et al., 2017) and hERG channel (Claassen and Zünckler, 2005). Inhibition of the hERG channel by clozapine, an antipsychotic drug, also results in clinically overt cardiotoxicity (Curto et al., 2016, Lee et al., 2006). An extensive list of non-antiarrhythmic drugs (Fig.3) such as antihistamines, which prolong QT intervals due to their intrinsic effects, has been compiled (De Ponti et al., 2001, Ferdinandy et al., 2019). The inhibition of rapidly activating delayed rectifier potassium currents (I_{Kr}), by these drugs, has been shown to be the underlying mechanism of toxicity (Redfern et al., 2003). Known drugs, which can lead to the generation of torsade de pointes include antipsychotics, antimalarial drugs, anti-migraine drugs, macrolides, fluoroquinolone antibiotics and many other drugs, (Balfour and Wiseman, 1999). The aetiology of torsade de pointes is still not fully delineated, but it is clear that cardiotoxic drugs can not only seriously affect their users but also pose high economic risks on their manufacturers. As many drugs face depreciation in preclinical drug development due to cardiotoxicity (Kola and Landis, 2004).

Therefore, reliable tools and systems are needed to study drugs in detail in regards to their cardiotoxic potential and regular benefit risk assessments have to be performed in order to minimize the risk to patients.

Since 1950, about 500 medicinal products have been recalled from the market level as they were producing toxic effects (Onakpoya et al., 2016). Liver, heart, kidney and nervous systems are major targets which were toxically affected by these medicinal products (Bass et al., 2004; Onakpoya et al., 2016). There are many reasons for the occurrence of detrimental pharmaceutical effects. For example, molecular and physiological processes in cardiac tissues react differently to medicinal agents in healthy versus diseased states and the screening methods for novel drugs and tools used to scrutinize their safety during pre-clinical and clinical trials are not suitable or specific enough to identify these detrimental effects on predisposed or particularly vulnerable patients.

Nonetheless, recent advancement in novel drug screening methodology, surgical procedures, medications and better lifestyle have managed to decrease some detrimental aspects of CVDs, particularly in more developed countries. However, CVDs are still a major challenge in low and middle-income countries. Therefore intensive and highly sophisticated in-depth investigations are required to diminish all these existing issues related to CVDs regardless of if they are drug-related or not.

Possible solutions to these problems may include better understanding of the aetiology, origin, distribution and trends of CVDs in all countries, which is essential to improve public health everywhere. The need for the development of better in vitro and in vivo safety testing platforms is undeniable, as existing platforms were unable to detect hidden cardiotoxicity of drugs in the past.

In this context it is also important to develop reliable protocols to better understand multifactorial cardiotoxic mechanisms of drugs, which can in turn lead to the detection of hidden cardiotoxicity at the early pre-clinical stage, thereby preventing clinical trials and marketing of potentially cardiotoxic drugs, which cause more harm than they do well.

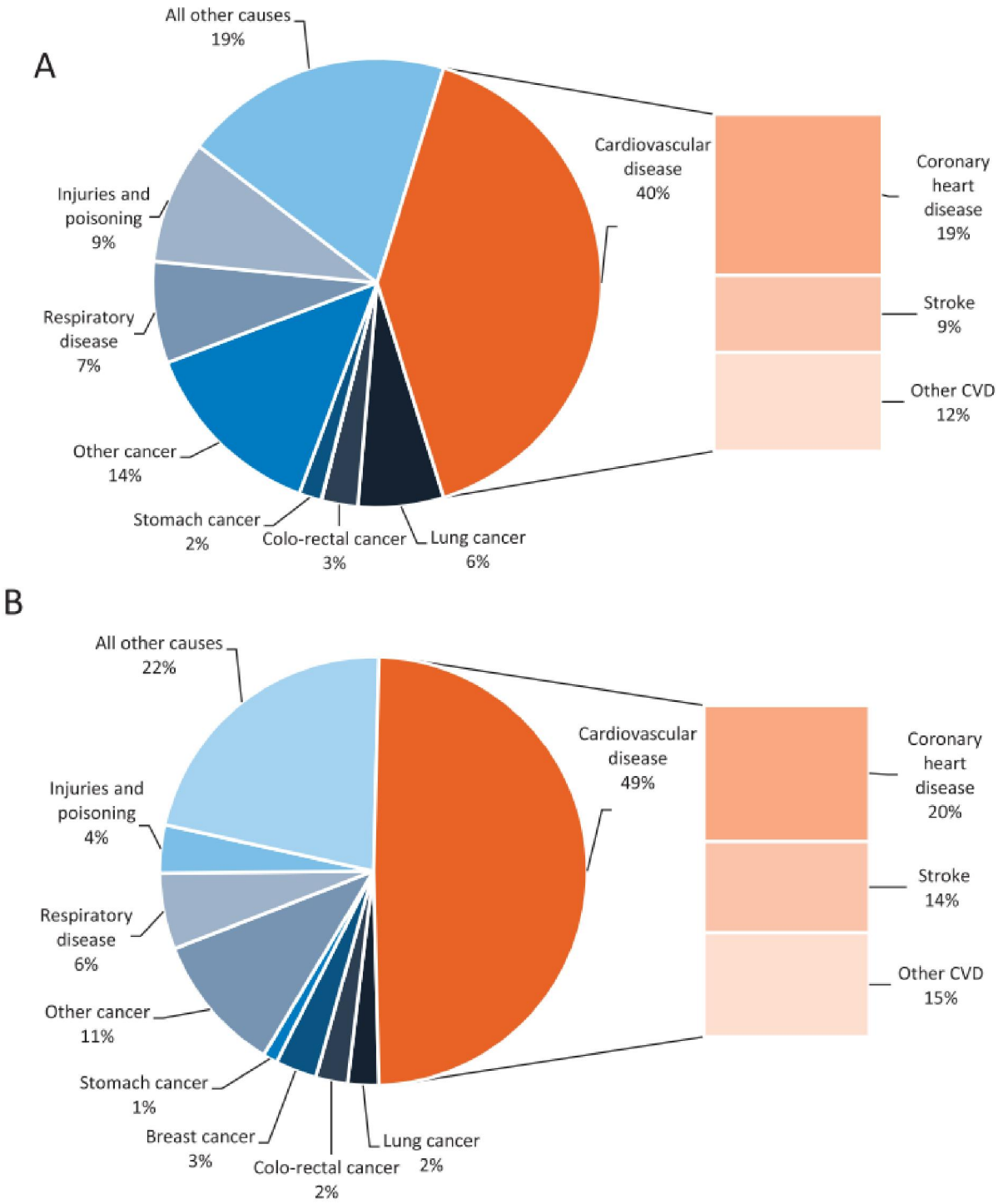

Figure 2: Major causes of death in European citizens (Source; WHO mortality database) The figure depicts the causes of mortality in males (**A**) and females (**B**). CVDs are the major cause of death (49% of all deaths) with females being more prone to die due to CVDs than males in the European population and with different types of cancer causing the second most deaths (17% of all deaths), figure is reproduced from Townsend et al., 2016.

Drug class	Compound	Possible arrhythmogenic mechanism(s)
Antibiotics	Erythromycin, clarithromycin	hERG inhibition
	Grepafloxacine, sparfloxacine	hERG inhibition
Antidepressants	Imipramine	I_{Na}, hERG inhibition
	Fluoxetine	I_{Na}, $I_{Ca,\ L}$, hERG current and trafficking block
	Citalopram	hERG current and trafficking inhibition
Antiepileptics	Retigabine	hERG, I_{Na} inhibition
	Lacosamide	I_{Na} inhibition
Antifungal agents	Fluconazole	hERG current and trafficking inhibition
Antihistamines	Astemizole	hERG inhibition
	Terfenadine	I_{Na}, hERG inhibition
Antimuscarinics	Terodiline	hERG inhibition
Antipsychotics	Haloperidol	hERG inhibition
	Risperidone	hERG inhibition
	Clozapine	hERG inhibition
β_2-agonists	Salbutamol	hERG inhibition
NSAIDs	Diclofenac	I_{Na}, hERG, I_{Ks} inhibition
	Celecoxib	I_{Na}, hERG, I_{Ks} inhibition
Opioid analgesics	Methadone	I_{Na}, hERG inhibition
PDE inhibitors	Milrinone (PDE3 inhibitor)	cAMP dependent SR Ca^{2+} release, I_f activation
	Vardenafil (PDE5 inhibitor)	hERG inhibition
Prokinetics	Cisapride	hERG inhibition
Vasodilators	Bepridil	hERG, I_{Na} inhibition

hERG, human ether-a-go-go-related gene potassium current; I_f, hyperpolarization-activated cyclic nucleotide gated pacemaker 'funny' current; I_{Ks}, slow component of the delayed rectifier potassium current; I_{Na}, voltage-gated sodium current; NSAIDs, non-steroidal anti-inflammatory drugs; PDE, phosphodiesterase; SR, sarcoplasmic reticulum.

Figure 3: List of arrhythmogenic drugs and their possible mechanisms to produce deleterious cardiac effects

Drugs, which affect different ion channels like sodium (I_{Na}), calcium (I_{Ca}), funny current (I_f) and hERG, can produce arrhythmias in patients. Data are taken from Ferdinandy et al., 2019.

1.2 HiPSC-CMs as a bag full of solutions

Cardiovascular research focuses on unmasking the pathophysiology of CVDs, the identification of suitable therapeutic protocols and the establishing of safe and precise models for screening of new pharmacological candidates against CVDs. To study the underlying pathophysiology of CVDs and for drug screening, it would be highly desirable to obtain human cardiac tissue as it would be a perfect tool for in vitro preclinical studies. However, cardiac biopsies are restricted to patients undergoing cardiac surgery, so native adult cardiomyocytes or other cardiac cells are not frequently available for the purpose of cardiovascular research. As a result scientists are forced to search for other options like animal models (rat, mice, and guinea pig etc.) to use in cardiovascular research. Besides these, other alternative tools such as different cell lines, including human embryonic kidney (HEK) cells, and Chinese hamster ovary (CHO) cells are employed (Watanabe et al., 2008). Electrophysiological studies of these cells have shown clear deficits for safety studies as these cells lack important constituents of cardiac channels (Remme et al., 2008). Therefore, the next option is to use other organisms such as transgenic mice. However, despite genetic modification mouse and human cardiomyocytes also have different electrophysiological properties (Watanabe et al., 2011). Furthermore, the generation of such transgenic animals is costly and is associated with further shortcomings as many physiological and pathophysiological mechanisms are species-dependent. The exploitation of somatic stem cells may be the solution of overcoming inter-species related problems. The groundbreaking chapter of pluripotent stem cell research began with the game-changing work of Takahashi and Yamanaka, when they reported the successful transformation of somatic stem cells into induced pluripotent stem cells (iPSCs) in 2006. In their work prime iPSCs were generated from mouse fibroblasts using four retroviral vectors octamer-binding transcription factor 4 (OCT4); sex determining region Y-box 2 (SOX2); Krüppel-like factor (KLF4); and the transcription factor C-MYC (Takahashi and Yamanaka, 2006).

Later on, two groups generated human-induced pluripotent stem cells (hiPSCs) by using these four retroviral vectors OCT4; SOX2; KLF4; and C-MYC (Takahashi and Yamanaka, 2006) or OCT4; SOX2, the RNA-binding protein LIN28; and the transcriptional factor NANOG (Yu et al., 2007). Additionally, hiPSCs can be generated from multiple sources and differentiated into any cell type of the three germinal layers, which includes cardiomyocytes, when suitable growth factors are provided to them (Zhang et al., 2009).

1. Introduction

HiPSCs can be differentiated into hiPSC-CMs as various markers of cardiomyocytes, ion channel-related genes, and genes of several myofilament proteins have been detected in hiPSC-CMs, which were not present in hiPSCs before differentiation into hiPSC-CMs (Honda et al., 2011). Furthermore, hiPSC-CMs express genes of all ion channels, which regulate the shape and duration of the action potential in primary human cardiomyocytes (Honda et al., 2011). Due to all the respective channels being present, hiPSC-CMs give a robust and reproducible response to electrical stimulation and pharmacological agents. Consecutively, the electrophysiology of iPSC-CMs has been thoroughly studied together with calcium (Ca^{2+}) signalling mechanism and excitation-contraction coupling (ECC) in iPSC-CMs by using different pharmacological agents (Marcu et al., 2015). Thus, from the findings of electrophysiological studies of hiPSC-CMs, it has been determined that hiPSC-CMs may be used as a possible model of human cardiomyocytes in cardiovascular research. This realization and the availability of iPSC-CMs have solved many of the striking issues of previously available cardiovascular research models. HiPSC-CMs provide a long list of advantages of which the top most might be that the scarcity of adult human CMs is not hindrance anymore, since reliable and reproducible adult-like cardiomyocytes can be differentiated from hiPSCs. Human adult CMs are notoriously difficult to culture, as alterations in their morphology and ion channels function occur quickly after their isolation (Himmel et al., 2012). Moreover, alterations in t-tubules, which contain ion channels, have been confirmed after culture (Mitcheson et al., 1998). In contrast, hiPSC-CMs can be cultured for several weeks without significant structural modification. Apart from this, there are no ethical issues with generating hiPSC-CMs comparable to the issues which scientists have to face when using embryonic stem cells-derived cardiomyocytes. Additionally significant quantitative differences in interspecies cardiomyocytes models (Lu et al., 2001) have been erased by the usage of hiPSC-CMs as now it is even possible to generate patient-specific hiPSC-CMs. As a consequence genetic, disease and patient-specific molecular and pharmacological screening of drugs has become a feasible possibility and patient-specific hiPSC-CMs have already been utilized to investigate channelopathy (Moretti et al., 2010). In the long run, hiPSC-CMs should be relatively cost and time effective for the screening of novel drugs in comparison to prior testing modalities. Shortcomings of previous safety models for novel drug screening can be compensated by hiPSC-CMs and deleterious effects should become more easily detectable. This should not only alleviate the risks and fears of patients but also those of the pharmaceutical industry as cardiotoxicity is the major reason for withdrawal of drugs even after they went through intensive and costly *in vitro* and *in vivo* screening in animal models (Landis and Kola, 2004; MacDonald and Robertson, 2009).

1. Introduction

Some companies have already embraced hiPSC-CMs as a valuable drug screening tool. For example, The Comprehensive in vitro Proarrhythmia Assay (CiPA) has recognized hiPSC-CMs as a vital component to investigate the arrhythmic effects of many targeted drugs from pharmaceutical companies in their developmental stage (Colatsky et al., 2016). Clinical Trials in a Dish (CTiD) is another practicable tool to judge the safety and efficacy of medical therapies by using hiPSC-CMs collected from a specific sample of human beings (Fermini et al., 2018). This type of testing can be done even before the real clinical trial phase and save trial participants from unnecessary risks and pharmaceutical companies from losing a lot of money (Fig.4).

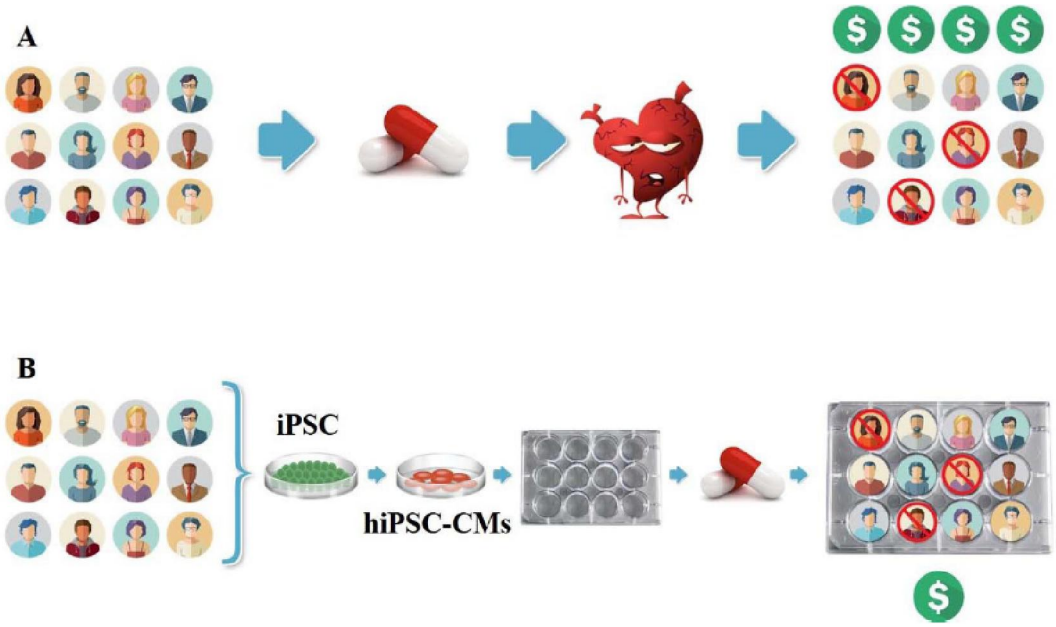

Figure 4: Comparison of conventional clinical trial and clinical trial in a dish
Depiction of the usefulness of hiPSC-CMs to investigate the cardiotoxicity of novel drugs. In phase-I conventional clinical trials the safety of a targeted drug is investigated in healthy humans and putting them at risk of serious cardiac consequences (**A**). HiPSC-CMs from the same healthy humans can be used in an efficacious way (less severe injuries or death-causing and cost-effective) (**B**). Figure is taken from (Fermini et al., 2018).

Last but not the least, certain CVDs, such as myocardial infarction, require transplantation or cell therapy as their last therapeutic approach (Laflamme and Murry, 2011). These hiPSC-CMs could be used for therapy of diseases like congenital heart disease, coronary artery disease and heart valve diseases which require transplantation of heart. But, they have to bring to anatomical, physiological and electrophysiological maturation resembling that of adult human cardiomyocytes. It may not yet be feasible to produce the quantity and maturity of CMs needed for humans, but in-fact approaches of implanting hiPSC-CMs have already shown positive effects in different animal models of myocardial infarction and are worth exploring further (Riegler et al., 2015; Weinberger et al., 2016).

1. Introduction

IPSC-CMs are being investigated as models of pathophysiology to for example investigate hypertrophy as reported by using rat EHTs (Hirt et al., 2012). Moreover iPSC-CMs are not only available as ventricular cell type but also as atrial cell type. Atrial like iPSC-CMs are being used for investigation of electrophysiological changes in atria (Lemme et al., 2018).

Over the last 10 years, enormous progress has been made to characterize iPSC-CMs on the genomic, proteomic, pharmacological, and electrophysiological level, yet there are still many reports that hiPSC-CMs do not show the perfect maturity level of a natural adult cardiomyocyte. This surely is a concern, which needs to be addressed and overcome.

A brief list of potential utilization of hiPSC-CMs depicted in (Fig.5).

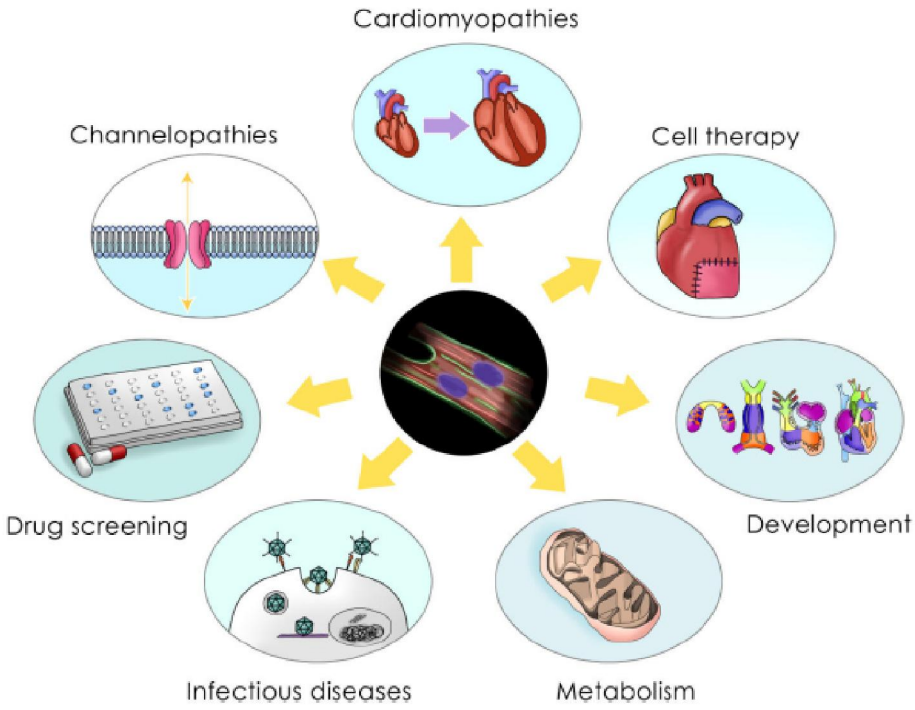

Figure 5: Versatile scope of application of hiPSC-CMs

The wide spectrum of utility of hiPSC-CMs which ranges from creating genetic cardiac disorder models to understanding molecular mechanisms of CVDs and screening of new drugs. The figure is taken from Karakikes et al., 2015.

1.3 Beta-adrenergic receptors (β-ARs) as mastermind of ECC

Excitability is a characteristic feature of cardiomyocytes. The translation of electrical activity into mechanical activity is vital for the contraction of cardiomyocytes. Due to ECC, cardiomyocytes work in a synchronized fashion and collectively pump the blood throughout the body. The body's requirements of oxygen and nutrition are always adapting according to both external and internal stimuli.

The sympathetic part of the autonomic nervous system, of which the adrenergic receptors (ARs) are a vital part, plays an imperative part in ECC in cardiomyocytes (Lymperopoulus et al., 2013). Ahlequist differentiated ARs into α-adrenergic receptors (α-ARs) and β-adrenergic receptors (β-ARs) (Ahlequist, 1948). The neurotransmitter norepinephrine (NE) acts on β-ARs to produce physiological inotropic, lusitropic, and chronotropic effects as depicted in (Fig.6) (Brodde and Michel, 1999; Lindegger et al., 2005; Song et al., 2001). β -ARs have classically been subdivided into three subtypes i.e. β_1-AR, β_2-AR, β_3-AR, and a low-affinity state of the β_1-AR (formerly believed to be a separate receptor, which was called β_4-AR) (Kaumann et al., 1997; Gauthier et al., 1996; Zhu et al., 2012). All three subtypes of β-ARs have different affinities to different agonists and antagonists and have a diverse list of physiological roles (Lohse et al., 2003). The presence and physiological roles of β-ARs in cardiomyocytes have been studied in detail. In normal human heart, β_1-ARs are four times more abundant than β_2-ARs. But this quantitative difference is not uniform throughout the heart, instead it depends upon the state and area of the heart i.e. failing vs non-failing heart, atrial vs ventricular and whole heart vs isolated cardiomyocytes (Bristow et al., 1986). β_1-ARs and β_2-ARs are present in cardiomyocytes throughout the right and left atrial and ventricular tissue in the human heart (Brodde, 1994). In contrast, in mice ventricular tissues β_1-ARs are present in all cardiomyocytes, while β_2-ARs are only marginally present in cardiomyocytes (Myagmar et al., 2017). Myagmar et al., 2017 have found that β_2-ARs & β_3-ARs are mostly absent on isolated cardiomyocytes isolated from adult mice. There are also clear indications that β_2-ARs & β_3-ARs are present on non-cardiomyocytes such as endothelial cells and fibroblasts. Although β_1-ARs and β_2-ARs coexist, the spectrum of their physiological activities is dissimilar. β-ARs are G-protein coupled receptors (GPCRs) and have seven transmembrane-spanning domains (Rockman et al., 2002). Specific roles of major players of ECC are sketched in (Fig.6 A). Briefly, upon stimulation of β_1-ARs the Gαs subunit of the stimulatory G-protein activates adenylyl cyclase (AC), with AC type 5 and 6 being the principal isoforms of adenylyl cyclase in the heart (Chen et al., 2012).

In-turn AC converts adenosine triphosphate (ATP) into cyclic adenosine monophosphate (cAMP). This cAMP triggers PKA to phosphorylate many different and vital downstream proteins, which regulate the intracellular concentration of Ca^{2+} and the sensitivity of myofilament. The direct consequence of all these events collectively is an increase in contractility of cardiomyocytes. Major targets for PKA are L-type Ca^{2+} channels (LTCCs), phospholamban (PLB), troponin I (TnI), ryanodine receptors (RyR2) and many more (Post et al., 1999; Rockman et al., 2002).

1.3.1 Role of Ca^{2+} channels in ECC

The importance of Ca^{2+} in cardiac contraction was discovered in the 19th century (Ringer, 1883). Later on, it was realized that the Ca^{2+} current (I_{Ca}) is a contributor to the plateau of the action potential (AP) of cardiomyocytes (Orkand et al., 1964). The I_{Ca} was also found to advocate the inotropic effect of β-ARs activation in cardiomyocytes (Reuter, 1966). Due to arduous work of researchers I_{Ca} had been recognized as a major part of ECC in cardiomyocytes, as it initiates the process of Ca^{2+}-induced Ca^{2+} release (CICR) from the sarcoplasmic reticulum (Fabiato et al., 1975). Since then, an overwhelming amount of data on the biophysics, pharmacology and pathophysiology of Ca^{2+} channels have been generated (Catterall, 2005). Ca^{2+} homeostasis in cardiomyocytes is regulated by both sarcolemmal Ca^{2+} channels as well as by intracellular Ca^{2+} stores (Bean, 1989; Nilius et al., 1985). The inward current due to sarcolemmal Ca^{2+} channels depolarizes cells and Ca^{2+} entering the cell works as a vital second messenger for ECC (Bers and Perez-Reyes, 1999).

In the late 1980s, two different Ca^{2+} channels were identified in cardiomyocytes, which, based on their voltage dependency and sensitivity to dihydropyridines, were divided into L-type Ca^{2+} channels (LTCCs) and T-type channels (TTCCs) (Isenberg, 1982; Benitah et al., 1992). LTCCs can be blocked or facilitated by dihydropyridines, while TTCCs can be blocked by nickel or mibefradil (Tsien et al., 1987; Mishra et al., 1994). Species, origin of cell and pathophysiology dictate which type of Ca^{2+} channels are present in cardiomyocytes. LTCCs and TTCCs both have been detected in Purkinje cells, pacemaker cells, and some atrial cells while in ventricular cardiomyocytes of most species only LTCCs can be found (Bean, 1989; Hagiwara et al., 1988; Yuan et al., 1994; Hirano et al., 1989).

1. Introduction

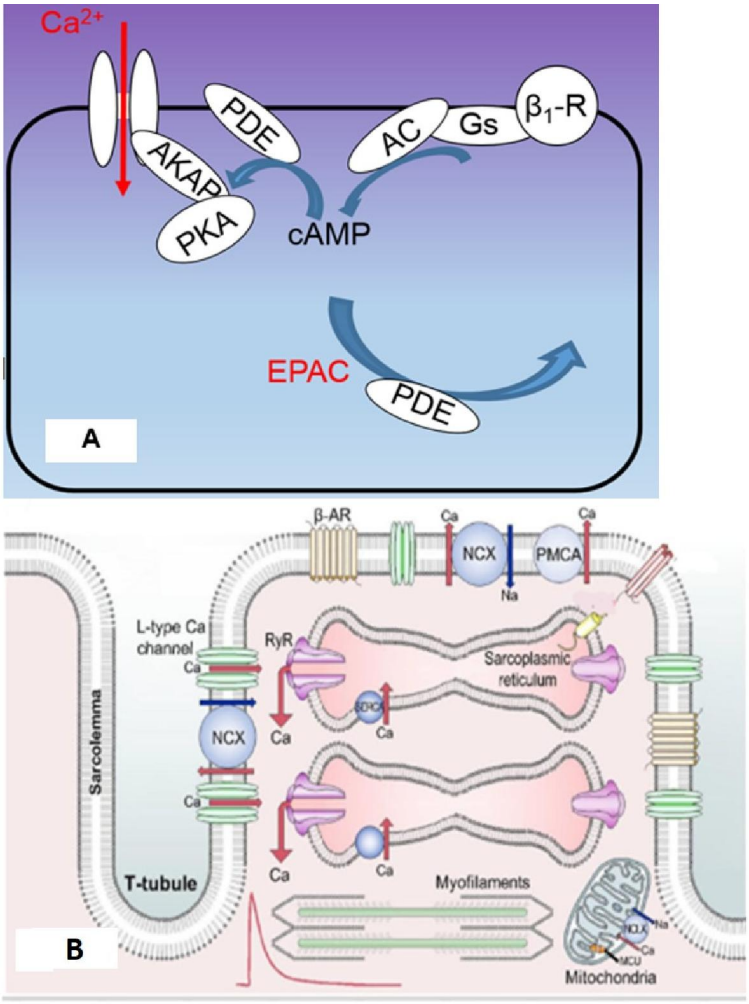

Figure 6: Signal transduction of contraction of cardiomyocyte and regulation by cardiac β-ARs

Synthesis of cAMP via GCPRs and AC and degradation of cAMP by PDEs after stimulation of β-ARs (**A**). Organelles and channels involved in the process of ECC such as LTCCs: L-type Ca^{2+} channel; NKA: Na^{+}, K^{+}-ATPase; PLM: Phospholemman; PLB: Phospholamban; SERCA: Sarcoplasmic/Endoplasmic Reticulum Ca^{2+}-ATPase; RyR: Ryanodine Receptor; NCX: Na^{+}/Ca^{2+} Exchanger. Figures are taken from Eisner et al., 2017 (**B**).

Interestingly, TTCCs are reported as playing a major role in the developmental stages and in hypertrophic ventricular cardiomyocytes, which are devoid of TTCCs under normal circumstances (Nuss and Houser,1993).

1. Introduction

Although two types of Ca^{2+} channels have been identified on cardiomyocytes of some species the I_{Ca} is assumed to be driven mainly by LTCCs as the contribution of TTCCs is negligible in intact cells (Bers, 2008). Therefore, LTCCs are the major gateway of Ca^{2+} from the extracellular fluid into the interior of cardiomyocytes.

Four members of the LTCC family have been reported: Cav1.1, Cav1.2, Cav1.3, and Cav1.4. Out of these four, Cav1.2 is present in ventricular cardiomyocytes and generates the typical $I_{Ca,L}$. Cav1.2 is vital for the development and physiology of the heart as Cav1.2 knockout mice have been shown to suffer cardiovascular failure (Seisenberger et al., 2000). The structure of LTCCs in the cardiovascular system has been fully elucidated. Briefly, α_{1c}, is the most vital subunit and its auxiliary subunits have been cloned (Singer et al., 1991; Catterall 2000). The α_{1c} subunit consists of four homologous domains and each domain has six transmembrane helices. The α_{1c} subunit contains a conduction pore, a voltage sensor, a gating apparatus, and binding sites for ligands (Kobrinsky et al., 2005). During the resting phase a concentration gradient is the driving force for the influx of Ca^{2+} into the cardiomyocytes (Orkand et al., 1964).

The wide range of physiological and pharmacological modulators of LTCCs has been discovered by many different research groups. Important regulators of LTCCs in cardiomyocytes are ligands of GPCRs. These receptors control LTCCs through two kinases protein kinase A (PKA) and protein kinase C (PKC). The endothelin, α_1-ARs, and angiotensin II receptors are coupled to Gq protein. After activation, these receptors initiate a series of downstream reactions. Briefly, Gq activates phospholipase C (PLC) which in turn breaks phosphatidylinositol 4, 5-bisphosphate (PIP2) into inositol trisphosphate (IP3) and diacylglycerol (DAG). IP3 releases Ca^{2+} from the endoplasmic reticulum into the cytosol while DAG activates PKC, which then phosphorylates LTCCs (Puri et al., 1997; Kamp and Hell, 2000; Shistik et all., 1998). In contrast, β-ARs are coupled with Gs protein and the stimulation of β-ARs regulates LTCCs through cAMP-dependent PKA activation (Fig.7)(Kameyame et al., 1986; Hove-Madsen et al., 1996). Liu et al., 2020 have recently reported that PKA regulates LTCCs via Rad proteins.

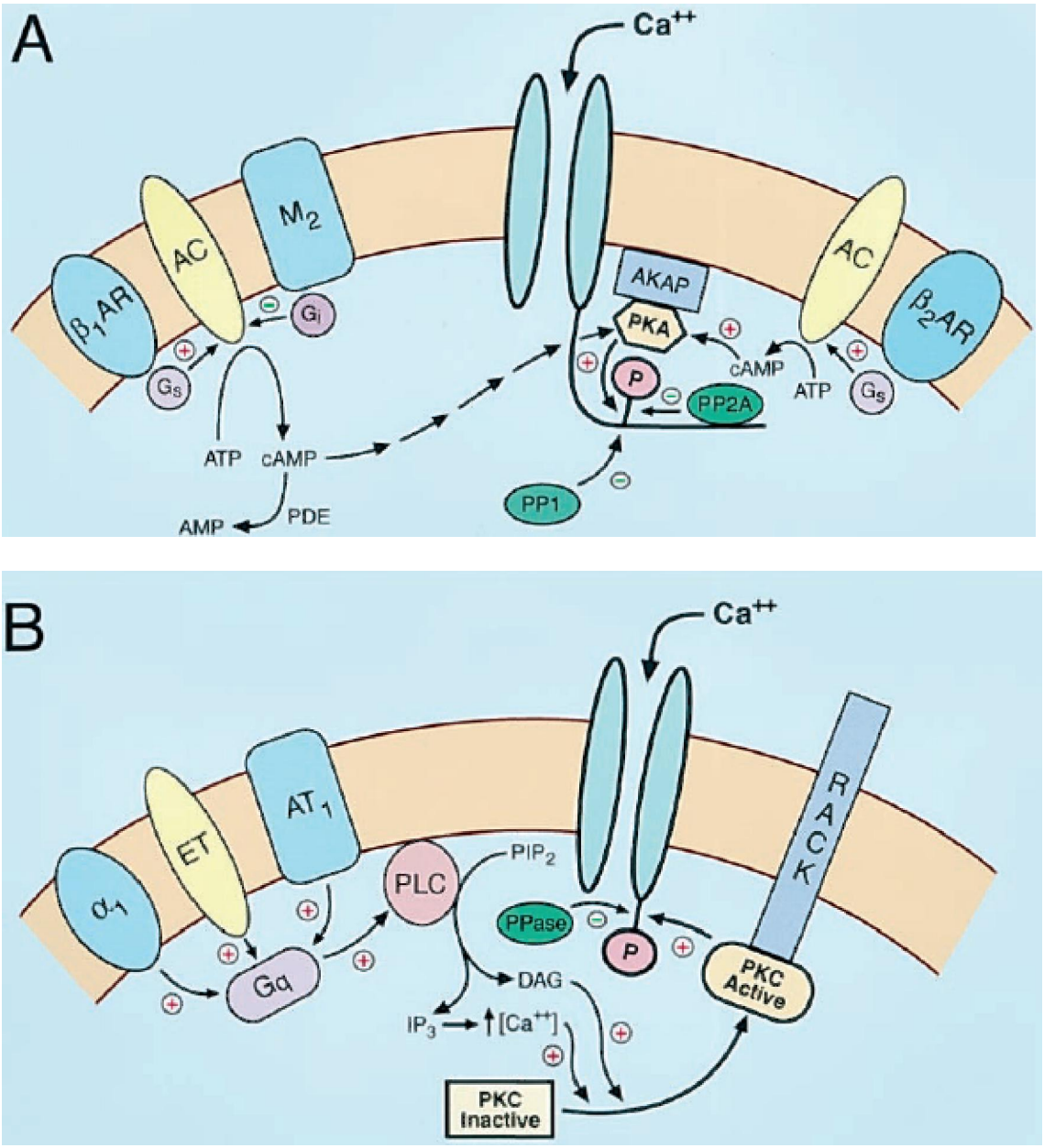

Figure 7: Modulators of LTCCs
G-protein coupled receptors regulating $I_{Ca,L}$ in cardiomyocytes via PKA and PKC pathways. Beta-adrenergic (β-ARs), Alpha-adrenergic (α-ARs), muscarinic receptors (M_2), angiotensin receptors (AT_1) and Endothelin receptors (ET). Figure is taken from Kamp and Hell, 2000.

Once activated, PKA increases the probability of more LTCCs to be opened which produce a collective effect on I_{Ca} (McDonald et al., 1994). In summary, the regulation of LTCCs is a very complex process as multiple key players are involved, which can either exert synergistic or antagonistic effects. The generation of cAMP is described in the next section.

1.3.2 Cyclic adenosine monophosphate (cAMP)

The cyclic nucleotides, cAMP and cGMP, act as secondary intracellular messengers for several hormones, neurotransmitters and inflammatory mediators. In the late 1950s, cAMP was discovered and characterized as a secondary messenger by Sutherland (Rall and Sutherland, 1958). cAMP performs a myriad of physiological roles in almost all types of cells throughout the body, including the cardiovascular system (Antoni, 2000). In cardiomyocytes β-ARs regulate inotropy and lusitropy through cAMP (Guellich et al., 2014) and any aberrations in the level of cAMP can produce drastic consequences such as hypertrophy, HF, and arrhythmias (El-Armouche and Eschenhagen, 2009).

cAMP can elicit a plethora of biological activities which are the aftermath of an enormously complex system of modulators of cAMP i.e. adenylyl cyclase (AC) (Hanoune and Defer, 2001), heterotrimeric G-protein (Marchese et al., 1999), and cyclic nucleotide phosphodiesterase (PDE) protein families (Soderling and Beavo, 2000; Francis and Houslay, 2006; Houslay and Adams, 2003). AC converts ATP into cAMP. Ten closely related isoforms of AC have been characterized but AC5 and AC6 are the dominant isoforms in the heart (Defer et al., 2000). ACs are activated after binding of NE, epinephrine, prostaglandin E1 (PGE1) and prostaglandin E2 (PGE2), glucagon, and glucagon-like peptide-1 to their corresponding receptors (Belmonte and Blaxall, 2011). Effectors of cAMP are PKA, exchange protein activated by cAMP (EPAC) (de Rooij et al., 1998; Lezoualc'h et al., 2016) and cyclic nucleotide-gated ion channels modulated directly by cAMP (Yau, 1994). Cyclic nucleotide PDEs regulate the amount of cAMP in the cell and the propagation of cAMP into different cell regions.

1.3.3 Phosphodiesterases (PDEs) are major modulators of cAMP

PDEs and cAMP were discovered at almost the same time. The diversity of physiological and pathophysiological roles performed by cAMP in almost all cells of the body depends upon the synthesis, propagation and degradation of cAMP and the molecules which are affected by cAMP. Therefore, a strict control of cAMP levels within cells is very important for the correct translation of signals and the consecutive execution of cellular processes. PDEs are the only enzymes which degrade cyclic nucleotides. It is now a well-known fact that within cells there are different pools of cyclic nucleotides in different regions (Steinberg et al., 2001). The density and location of these pools can dictate different cellular activities. The activation of different receptors produces different pools of cyclic nucleotides and in turn different types of physiological reactions within cells (Rochais et al., 2006). An efficient control of cyclic nucleotide pools would not be possible without the presence of PDEs. Due to their unique role as signal regulators and the associated versatile outcomes, PDEs didn't fall under the radar of researchers, who have spent a lot of effort on understanding PDEs and their functions (Berisha. & Nikolaev, 2017; Zaccolo, 2006; Fischmeister and Hartzell, 1991).

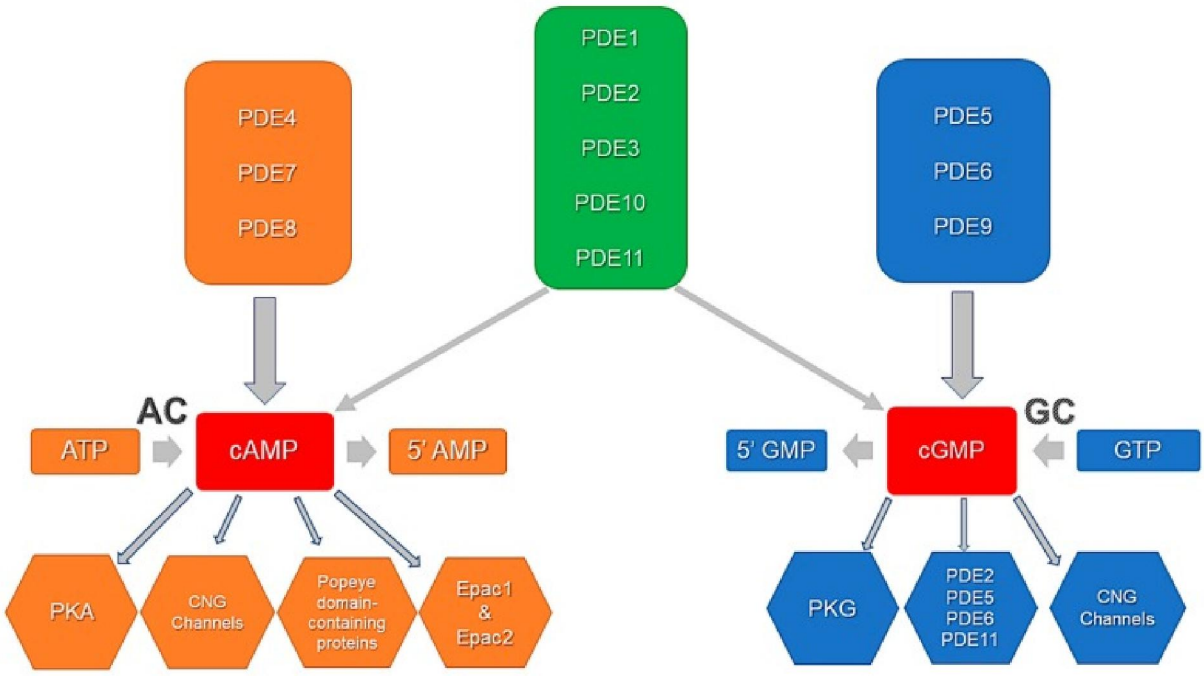

Figure 8: PDE families, their substrates, and targets of cAMP and cGMP
The cAMP-specific PDEs (orange), cGMP specific PDEs (blue), and dual substrate PDEs (green) are depicted. The figure is taken from Ahmed et al., 2015. Abbreviations: Cyclic nucleotide-gated ion channels (CNG Channels) Protein Kinase G (PKG) Protein Kinase A (PKA) Guanosine-5'-triphosphate (GTP) Adenosine triphosphate (ATP), exchange protein activated by cAMP (EPAC).

1. Introduction

The superfamily of cyclic nucleotide hydrolysing phosphodiesterases (PDE) in mammals is subdivided into 11 families of enzymes. This superfamily is classified according to the primary amino acid sequence, overall domain structure, and catalytic and regulatory aspects of their family members (Beavo and Reifsnyder, 1990).

The 11 families can be reclassified in many different ways, but on the basis of substrate specificity they can be regrouped into three classes (Fig. 8). The group of PDEs which are only hydrolyzing cAMP includes PDE4, PDE7 and PDE 8, while the group that hydrolyzes only cGMP is comprised of PDE5, PDE6, and PDE9. The third group incorporates PDE1, PDE2, PDE3, PDE10, and PDE11, which hydrolyze both cGMP and cAMP (Francis et al. 2011). Multiple variants of different PDE families have been confirmed in cardiac tissue as well as in isolated cardiomyocytes and isoforms of the PDE1, PDE2, PDE3, PDE4 and PDE5 families have been reported on an expressional level in cardiac tissue (Movsesian et al., 2009).

1.3.3.1 PDE1

Members of the PDE1 family are dual substrate PDEs which hydrolyze both cAMP and cGMP. The isozymes of PDE1 are known as Ca^{2+}/calmodulin (CaM)-dependent enzymes (Kincaid et al., 1985; Sonnenburg et al., 1993). Three genes for the PDE1 family have been reported by different researchers: PDE1A, PDE1B, and PDE1C. Each of these genes gives birth to different variants. The affinity for cyclic nucleotides varies among different isozymes of PDE1 as PDE1A and PDE1B have more affinity for cGMP than for cAMP (Rybalkin et al., 2003; Dunkern and Hatzelmann, 2007), while PDE1C has equal affinity for both cyclic nucleotides (Nagel et al., 2006; Miller et al., 2009; Yan et al., 1995; Loughney et al., 1996). PDE1C has been found in rat ventricular tissue as well as rat ventricular cardiomyocytes on a mRNA level (Verde et al., 1999). All isoforms of PDE1 are located in the cytosol (Vandeput et al., 2007). In rabbits PDE1A has been reported to control pacemaker activity (Lukyanenko et al., 2016). Isozymes of PDE1 are widely distributed in different tissues. Moreover, different species have different isozymes of PDE1 as PDE1A is the form predominantly expressed in mice (Vandeput et al., 2007) while PDE1C is the predominant form in human cardiomyocytes (Johnson et al., 2012). Hypertrophied rat hearts and both adult and neonatal isolated cardiomyocytes exhibit a higher expression of PDE1A (Miller et al., 2009). Various inhibitors of PDE1 are being used in research to identify roles of PDE1 in cardiomyocytes and different tissues. Vinpocetine, IC224, IC229, IC86340, ITI214, and very high concentrations of sildenafil (1 µM) are among the most often used inhibitors of PDE1.

1.3.3.2 PDE2

PDE2 is a dual substrate enzyme which hydrolyses both cGMP as well as cAMP (Martens et al., 1982). The PDE2 enzyme is known to be allosterically activated by cGMP (Wu et al., 2004). The PDE2 family has only one identified gene from which three variants (PDE2A1/2/3) are translated. PDE2 isozymes are expressed in a variety of tissues and cells such as the brain, platelets, adrenal glomerulosa cells, endothelial cells, macrophages, and heart. Cardiomyocytes express less PDE2 in comparison to other cells of the heart like endothelial cells and fibroblasts. This has been confirmed by using molecular measurements (Vettel et al., 2014). In rat ventricular cardiomyocytes expression of PDE2A has been confirmed by RT-PCR (Verde et al., 1999). Different isozymes of PDE2 are localized preferentially in different compartments of cardiomyocytes. PDE2A1 is expressed in the cytosol while PDE2A2/3 are bound to the membranes (Mongillo et al., 2006). Different studies have reported different isozymes of PDE2 in different species (Stephenson et al., 2009). Only PDE2A1 is widely distributed in the human heart (Sugioka et al., 1994), while in rat ventricle cardiomyocytes contain PDE2A3 (Mongillo et al., 2006). The role of PDE2 in cardiomyocytes depends upon the concentration of cGMP. cGMP induces PDE2 to hydrolyse cAMP at medium concentrations, while at high concentrations cGMP do not induce PDE2 and thereby exhibit no negative regulatory effect on cAMP concentrations (Hambleton et al., 2005). In cardiomyocytes, cGMP-activated PDE2A regulates cAMP in a negative fashion (Martinez et al., 2002). As a result the activity of LTCC is compromised and inotropic response of catecholamines is decreased (Vandecasteele et al., 2001).

PDE2 is reported to be upregulated under circumstances such as chronic stimulation of β-ARs, β-ARs desensitization and as a result of some diseases e.g. HF in humans (Mehel et al., 2013), a finding that was however not confirmed under slightly different experimental conditions (Galindo-Tovar et al., 2018)

PDE2 is not uniformly distributed in all regions of cardiomyocytes, it is compartmentalized instead, as was shown in different studies which investigated PDE2 mediated cGMP/cAMP crosstalk (Mehel et al., 2013; Perera et al., 2017). Inhibition of PDE2 (100 nM BAY 60-7550), in adult rat ventricular cardiomyocytes transduced with PLM-Epac1 (phospholemman) adenovirus, generated even larger cAMP signals than in cells transduced with Epac1-camps (global) adenovirus (Bastug-Özel et al., 2018). Different PDE2 inhibitors are available, which selectively inhibit PDE2 but Erythro-9-(2-hydroxy-3-nonyl) adenine (EHNA) and Bay-60-7550 are two often chosen pharmaceutical agents for the study of PDE2 activities (Maurice et al., 2014).

1.3.3.3 PDE3

Members of the PDE3 family have two substrates i.e. cAMP and cGMP. PDE3 is known to be inhibited by cGMP (Maurice and Haslam, 1990; Meacci et al., 1992). Two genes (PDE3A and PDE3B) of the PDE3 have been reported. There are three different variants of PDE3A (PDE3A 1/2/3) while variants of PDE3B are yet to be reported. Isozymes of the PDE3 family have a greater affinity for cGMP than for cAMP, but PDE3 isozymes have a 10 folds higher maximum rate of reaction for cAMP than cGMP (Weishaar et al., 1986). Both PDE3A and PDE3B are present in the cardiovascular system. PDE3A isozymes are distributed in the cytosol as well associated with membranes while PDE3B is expressed in particulate matter. PDE3A scaffolds with SERCA and PLB at the SR and regulates the reuptake of Ca^{2+} into the SR (Mongillo et al., 2004; Ahmad et al., 2015). PDE3A was detected as major PDE variants in adult rat ventricular cardiomyocytes by immunoprecipitation (Rochais et al., 2006).

PDE3A is one of the major regulators of contractility of cardiomyocytes in human (Hambleton et al., 2005; Wechsler et al., 2002) as only variants of isozymes PDE3A diminish $I_{Ca,L}$ activity, and hence indirectly regulate inotropic responses (Weishaar et al., 1987; Verde et al., 1999). Furthermore, PDE3A knockout mice exhibited greater basal chronotropic responses as compared to wild type, while PDE3B knockout mice failed to do so. Pharmacological inhibition with cilostamide also did not potentiate inotropic and chronotropic responses to isoprenaline in PDE3A knockout mice while it did potentiate them in PDE3B knockout mice. Moreover, a reduction in phosphorylation of pacemaker components in the SA node has been attributed to the activity of PDE3A (Alig et al., 2009; Galindo-Tovar et al., 2009) and Ding et al., 2005 have reported anti-apoptotic activity of PDE3A in cardiomyocytes.

In adult rat ventricular cardiomyocytes PDE3 is one of the major contributors of hydrolysis of cAMP and makes up approximately 31% of the total cAMP hydrolytic activity of PDEs (Rochais et al., 2006). Cilostazol, milrinone, cilostamide, OPC-33540a, and enoximone are widely used inhibitors of PDE3.

1.3.3.4 PDE4

PDE4 represents one of the largest PDE families with four documented genes (PDE4A, PDE4B, PDE4C, and PDE4D). These four genes generate at least 20 to 25 protein variants. Out of these four isoforms, PDE4C is absent in heart (Richter et al., 2005). The hydrolytic activity of all these PDE4 isoforms differs between neonatal rat heart (Mongillo et al., 2004) and adult rat heart (Abi-Gerges et al., 2009). PDE4 is expressed in the ventricle of the human heart (Richter et al., 2011) and atrium (Molina et al., 2012) with PDE4D being most predominant.

Although PDE4 is the major cAMP hydrolysing PDE in rat and mice (Leroy et al., 2008) its inhibition is devoid of inotropic effects on a basal level (Mika et al., 2013). Inhibition of PDE4 produces only an inotropic response in the presence of PDE3 inhibition or of forskolin or isoprenaline stimulation (Molina et al., 2012; Leroy et al., 2008; Mika et al., 2013 and Rochais et al., 2006).

In adult rat ventricular cardiomyocytes PDE4 contributes to 38% of total cAMP hydrolytic activity of PDEs (Rochais et al., 2006). Moreover, the same research group has confirmed that effects of inhibition of PDE4 (Ro 20-1724, 10 µM) on ISO (1 nM)-evoked $I_{Ca,L}$ are much higher than those of inhibition of PDE3 (Cil 1 µM; 34.5% vs 17.5% respectively). During β-ARs stimulation, LTCCs are preferentially regulated by PDE4B (Leroy et al., 2011), while RyR2 is regulated by both PDE4B and PDE4D (Lehnart et al., 2005; Mika et al., 2014).

In transgenic adult mice cardiomyocytes expressing Epac1-camps sensor (global), inhibition of PDE4 (rolipram 10 µM) increases 100 nM ISO-evoked cAMP from β_1 ARs almost 2 folds stronger than inhibition of PDE3 (cilostamide 10 µM) (Perera et al., 2015).

In adult rat ventricular cardiomyocytes transduced either with PLM-Epac1 (phospholemman) or Epac1-camps (global) adenoviruses, PDE4 is the major regulator of cAMP (Bastug-özel et al., 2018). Rolipram, cilomilast, roflumilast, GSK256066, CHF6001, MK0952, and Ro 20–1724 are widely used PDE4 inhibitors in research.

1.3.3.5 PDE5

Members of the PDE5 family are selective cGMP hydrolysing PDEs. Catalytic activities of isozymes of the PDE5 family are triggered by cGMP (Thomas et al., 1990; Rybalkin et al., 2003; Zoraghi et al., 2005). Furthermore, PKG augments the affinity for cGMP and increases hydrolysis of cGMP by PDE5 (Corbin et al., 2000; Francis et al., 2002; Shimizu-Albergine et al., 2003). One gene of PDE5A has been discovered so far, which expresses three variants (PDE5A1, PDE5A2, and PDE5A3) and has been detected in humans, rats, and mice. It is preferentially expressed in smooth muscle and platelets (Lugnier et al., 1986; Francis et al., 1980). PDE5A2 transcripts were expressed and widely distributed in many tissues including heart (Kotera et al., 1999; Giordano et al., 2001). Many reports suggest that expression of PDE5A significantly increases in human and animal cardiovascular disease models (Fisher et al., 2005; Lu et al., 2010; Nagendran et al., 2007; Shan et al., 2012). In the heart, PDE5 is expressed in the cytosol and believed to preferentially regulate the normal physiological NO/cGMP pathway (Castro et al., 2006; Takimoto et al., 2005; Zhang et al., 2008). The effects of PDE5A in adult cardiomyocytes is compartmentalized as activity of PDE5A is increased, only by the NO/PKG/cGMP pathway, but not by the natriuretic peptide-particulate guanylyl cyclase-cGMP (NP-pGC-cGMP) pathway (Castro et al., 2010).

Suppression of the inotropic response to β-AR stimulation in isolated mouse cardiomyocytes and human hearts by PDE5 has been reported (Borlaug et al., 2005; Takimoto et al., 2005; Zhang et al., 2008). Studies with the PDE5 inhibitor sildenafil showed PDE5–PDE2-mediated cross-talk in adult mice as cGMP, which is not degraded by PDE5, activates PDE2 which in turn attenuates cAMP dependant chronotropic response (Isidori et al., 2015). PDE5A has also been shown to play a role in ischemia/reperfusion injury (Zhang et al., 2010) and its inhibition was found to be beneficial in certain heart failure animal models (Ockaili et al., 2002). Sildenafil, tadalafil, vardenafil, udenafil, and avanafil are selective inhibitors of PDE5 and are used both in clinical circumstances as well as in research.

1.3.3.6 PDE11

The PDE11 isoform is a recently discovered member of the phosphodiesterase family which are detectable in mammals. PDE11 originates from only one gene, which expresses four different variants (PDE11A1–4). All isoforms of PDE11 have been cloned (Fawcett et al., 2000; Yuasa et al., 2000). Isoforms of PDE11 are dual substrate hydrolysing enzymes (Baxendale et al., 2005). All have similar affinities for cGMP and cAMP and are activated by cGMP. Isoforms of PDE11 are widely distributed in different species (rat, mouse, and human) and are expressed in many tissues such as skeletal muscle, prostate, testis and salivary glands (Yuasa et al., 2001; Hetman et al., 2000).

PDE11A4 has been reported in rat and human heart by immunohistochemistry but its quantitative expression is very low (Yuasa et al., 2001; Loughney et al., 2005). PDE11 is phylogenetically analogous to the other GAF-containing PDEs (PDE2, PDE5, PDE6 and PDE10) based on sequence homology (Yuasa et al., 2001). Fawcett et al., reported 70% similarity in the catalytic domain between PDE11 and PDE5. Although a selective inhibitor of PDE11 is still unavailable the non-selective PDE inhibitors IBMX, zaprinast, and dipyridamole have been documented to inhibit PDE11. Furthermore, the relatively novel PDE5-selective inhibitor tadalafil is proclaimed as an inhibitor of PDE11 at high concentration (1 μM) (Saenz de Tejada et al., 2002; Gbekor et al., 2002; Weeks et al., 2005; Maw et al., 2003; Bischoff, 2004).

1.4 Approaches to track cAMP in cardiac tissue and cardiomyocytes

Quite a large number of quantitative and qualitative techniques are available for the measurement of cAMP. It is possible to measure the absolute amount of cAMP in tissue or cells and also to measure cAMP in real-time spatially as well as temporally. Highly sophisticated techniques have made it feasible to measure cAMP from different cell compartments and in response to a specific substance. Measurement outcomes, such as precise local detection or accuracy about the amount of cAMP depend upon the choice of method used to record cAMP. Detection techniques can be further divided into subgroups i.e. biochemical methods and fluorescent microscopic methods. Even though biochemical techniques show high sensitivity and specificity they have some demerits. For example biochemical methods need an enormous amount of cells or tissues to measure cAMP. Biochemical methods also lack the capacity to visualize cAMP temporally and spatially. Furthermore by utilizing biochemical methods cAMP in microdomains cannot be mapped.

1.4.1 Radioimmunoassay (RIAs)

Cyclic nucleotides can be detected in different tissues and cells by using radioimmunoassays (RIAs) (Williams, 2004; Brooker et al., 1979). A mixture of radiolabelled cAMP (^{125}I labelled cAMP), specific antibodies as a substrate and cAMP samples are used for RIAs. In brief radioactivity is detected in the RIA procedure when ^{125}I labelled cAMP binds with an anti-cAMP antibody. The intensity of radioactive signals are attenuated when induced cAMP hinders the binding of ^{125}I labelled cAMP with an anti-cAMP antibody. The bound cAMP of the samples is then quantified via a calibration curve.

1.4.2 Enzyme-linked immunoassays (ELISA)

To minimize the possible hazardous effects of radioactive substances non-radioactive techniques, such as enzyme-linked immunoassays (ELISA), were developed as an alternative to RIAs. The ELISA method also utilizes specific antibodies (primary and secondary antibodies) but it requires an enzyme instead of a radioactive substance in order to work. The cAMP from samples and the cAMP linked to the enzymes is poured into the secondary antibody containing multiwall plate. Both cAMP types compete with each other to bind the antibodies in the well. If the cAMP in the sample is low then the cAMP linked to the enzymes binds to the antibodies and dissociates from the enzymes. The free enzymes can then generate specific colors on the addition of specific substrates, which tells you the quantity of cAMP by comparing the signal against a calibration curve for quantification (Williams, 2004).

1.4.3 Cyclic nucleotide gated channels (CNGCs)

Another method to detect cAMP is the use of cyclic nucleotide gated channels (CNGCs). If cAMP is generated within cells containing CNGCs, then it directly activates these plasma membrane channels (Craven and Zagotta, 2006). The dynamics of cAMP is indirectly estimated by measuring I_{CNG} using a patch-clamp technique. Different studies have used these channels to investigate the relationship between $I_{Ca,\ L}$ and the amount of cAMP induced by agonists and inhibitors of PDEs. Furthermore, CGNC based sensors have been generated and successfully utilized to investigate compartmentalization of cAMP in cardiomyocytes (Rich et al., 2001). Though clever, yet this technique possesses drawbacks such as the lack of cAMP/cGMP selectivity, inability to measure cAMP in the cytosolic domain, and the fact that not every type of cell can be patched easily.

1.4.4 Förster Resonance Energy Transfer (FRET)

The historic development of FRET Microscopy can be tracked chronically and tremendous work of multiple contributors led to this sophisticated technique in its present form. The long list of contributions which started from the report of electromagnetic communication, and continued through Faraday's description of force, Maxwell's Dynamical Theory of Electrodynamics Fields, the famous Hertzian oscillating dipole, Planck's quantum mechanics, the London forces (van der Waals) and ended on the exceptional work of Theodor Förster. Theodor Förster published many seminal papers about FRET and facilitated the development of modern-day FRET techniques. FRET is based on the discovery, that fluorescent energy in the form of photons can be transferred from one excited fluorophore to another.

FRET utilizes a pair of fluorophores, one of which acts as a donor while the other acts as acceptor of fluorescent energy. In order to become an ideal pair to create a robust and clear FRET response they have to fulfill very specific physical criteria and conditions.

The distance between donor and acceptor must fall in the range of 10-100 Å. The emission spectrum of the donor must overlap with the absorption spectrum of the acceptor, so it can excite the energy state of the acceptor. Both the donor and acceptor fluorophores must be oriented so that dipole–dipole interaction between the electronic states of the fluorophores can take place. When the donor fluorophore is exposed to radiation of a suitable wavelength by an external source this fluorophore absorbs and attains an excitatory state. During the following relaxing phase, the donor then emits photons and excites the acceptor from the ground state to the excited state. During all these events the fluorescence intensity of the donor attenuates, while the emission intensity of the acceptor increases and this phenomenon can be recorded and used for scientific purposes (Börner et al ., 2011). The principle of the FRET process is illustrated in (Fig.9). In order to give credit to one of his major discoverers, Theodor Förster, the process is renowned as Förster Resonance Energy Transfer.

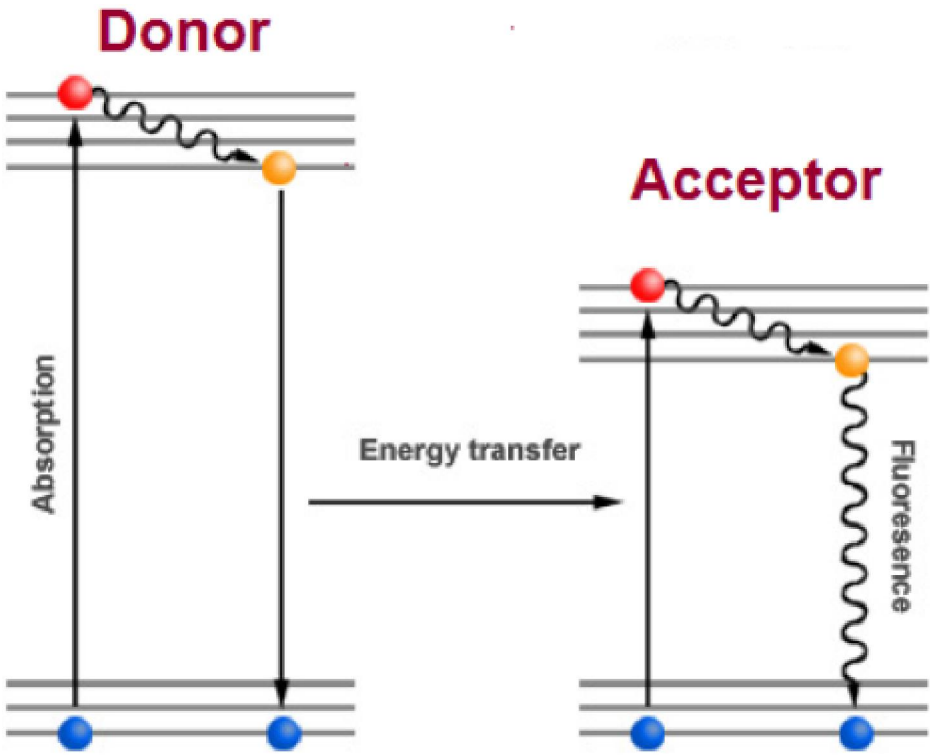

Figure 9: The principle of Förster Resonance Energy Transfer depicted as Jablonski Diagram

The Jablonski diagram is illustrating energy states and transitions between donor and acceptor molecules. Vertical lines illustrate energy state transitions due to absorption or emission of photons. Wavy arrows illustrate vibrational relaxation into lower energy states. Figure adapted from (Ferguson, 2013).

1.4.4.1 Working Principal of FRET

If used in the biomedical research setting FRET can yield temporal and spatial information about molecules of interest, if visualized under a microscope with the necessary equipment. A potential FRET setup for is shown in (Fig.10). To use this type of setup, biosensors have been created, which can be introduced in biological samples and which possess particularly suitable fluorophore acceptor and donor pairs for performing measurements. The fluorophore cyan fluorescent protein (CFP) for example has been established as a good donor for FRET experiments, while yellow fluorescent protein (YFP) has been shown to be a suitable acceptor counterpart to CFP. In the exemplary setup in (Fig.10), the sample is put under the lens of a microscope and the donor fluorophore (CFP) is excited by cool-LED at 400 nm. The excited donor fluorophore transmits part of its energy to the acceptor fluorophore through resonance and the resulting fluorescence of both fluorophores travels through the microscope and is directed through a beam splitter to separate the emitted light. The split light beams are then detect it in separate channels at 480 nm for the donor (CFP) and 535 nm for the acceptor (YFP). The signals in the two channels are captured by a sensitive enough camera and recorded by a computer (Nikolaev et al., 2006).

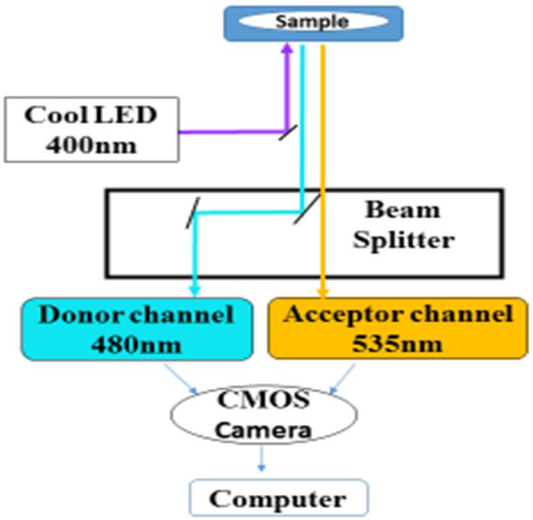

Figure 10: Schematic representation of a FRET recording setup
The sketch shows the various parts of a FRET microscopy setup and how donor and acceptor fluorophores are excited and their emission is recorded separately. Figure adapted from Nikolaev et al., 2006.

1.4.4.2 FRET Biosensors

A diverse range of both donor fluorophores and acceptor fluorophores can be used and can be used in different ways to construct different biosensors for research. So far they can be either flanked covalently onto two dimerizing proteins, one protein, two DNA strands, an antigen and an antibody, or a ligand and its receptor to fit their respective purpose (Nikolaev et al., 2004). In the following paragraphs the types of biosensors are discussed, some of which were used for the work presented in this thesis.

1.4.4.2.1 Protein Kinase A (PKA)-Based cAMP Sensors

PKA is one of the immediate molecular targets of cAMP. After its generation, cAMP binds to PKA to produce multiple downstream effects. By using this known mechanism a pioneering FRET sensor was constructed to measure real-time cAMP (Adams et al., 1991).

The design of this primary PKA-based cAMP sensor incorporates fluorescein (donor) bound to the catalytic subunit and rhodamine (acceptor) bound to the regulatory subunit of PKA. Ligand-induced cAMP segregates the PKA catalytic subunits from this assembly which in turn leads to a decrease in FRET signals. Although several studies utilized this sensor to track cAMP in different cell types, including cardiomyocytes, (Goaillard et al., 2001; Takeda et al., 2006) the inclusion of this FlCRhR biosensor (fluorescein-labelled PKA catalytic subunit and a rhodamine-labelled regulatory subunit) into cells by microinjection is laborious and troublesome. Moreover, the retention of the catalytic ability of PKA makes it complex to use. To overcome the shortcomings of this FlCRhR biosensor, genetically-encoded PKA-based FRET sensors were developed (Zaccolo et al., 2000). These genetically-encoded FRET sensors were used in many studies and went through multiple amendments to yield sensors with better noise to signal ratio (Zaccolo and Pozzan, 2002; Warrier et al., 2005). PKA-based FRET sensors and genetically-encoded FRET sensors have relatively slow kinetics and can have expressional issues. Therefore, Nikolaev and colleagues designed sensors with just the cAMP binding domain of the PKA, which lead to significantly faster kinetics and was devoid of off-target effects (Nikolaev et al., 2004).

Later on, a new generation of sensor based on the A-kinase activity reporter (AKAR) was created these sensors facilitated the simultaneous real time measurement of cAMP and PKA activity in cells (Allen and Zhang, 2006).

1.4.4.2.2 Epac-Based cAMP Sensors

Exchange protein activated by cAMP (Epac) is another direct target of cAMP and as such was also used to create FRET biosensors. In Epac-based FRET sensors, the fluorophores, usually CFP as donor and YFP as acceptor, are linked to the cAMP binding domains of Epac1 or Epac2 to generate single-chain Epac-based cAMP biosensors (Nikolaev et al., 2004; DiPilato et al., 2004; Ponsioen et al., 2004).

Although the Epac1-camps and Epac2-camps sensor show different affinities with cAMP they both give high FRET responses and were used to investigate the dynamics of cAMP after different first messenger stimulation in different cells. Furthermore, the creation of a transgenic reporter mouse line expressing Epac1-camps has opened up new horizons to simulate a native *in vivo* environment for the investigation of effects of different ligands (Calebiro et al., 2009).

Yet another set of Epac-based cAMP biosensors named indicator of cAMP using Epac (ICUE) biosensors, which use CFP and Citrine have been reported (Di Pilato et al., 2004).

Furthermore, recently different Epac-based cAMP biosensors designated to different microdomains have been successfully used to study compartmentation of cAMP in distinct cell regions. For example, Epac-based cAMP biosensors targeted to the plasma membrane (pm Epac) (Perera et al., 2015), Epac-based cAMP biosensors linked to Phospholamban (PLN Epac) (Sprenger et al., 2015), and Epac based cAMP biosensors near to ryanodine receptors (Epace1-JNC) (Berisha et al., 2019) have been effectively deployed to visualize dynamics of cAMP in different domains of cardiomyocytes.

1.4.4.3 FRET Applications

FRET is a fantastic technique that can be used in combination with other advanced visualizing techniques as confocal and scanning ion conductance microscopy (SCIM). A long list of scientific reports has been generated by applying the FRET technique: Structure and conformation of proteins (Johnson et al., 2005): spatial distribution and assembly of proteins (Watson et al., 1995), receptor/ligand interactions (Berger et al., 1994), immunoassays (Khanna et al., 1980), structure and conformation of nucleic acids (Clegg et al., 1994), real-time PCR assays and single nucleotide polymorphism (SNP) detection (Lee et al., 1999; Myakishev et al., 2006), nucleic acid hybridization (Parkhurst et al., 1995), distribution and transport of lipids (Nichols et al., 1983), membrane fusion assays (Uster, 1993) and indicators for cyclic AMP (Nikolaev et al., 2006).

1.5 Mission statement

Second messenger cAMP regulates genomic, proteomic, and electrophysiological effects of first messengers (like PKA and Ca^{2+}) and other signaling molecules in cardiomyocytes. The aim of the investigation described in this thesis was to study the dynamics of cAMP after β_1-ARs stimulation by NE, the natural ligand of these receptors in hiPSC-CMs. Furthermore, it was the desire of the described project to map the PDE activity profile in hiPSC-CMs under basal conditions as well as the impact of PDE enzymes on NE-induced cAMP. Further auxiliary endpoints of the presented work were to find out if there would be differences in the above parameters when focusing on two different domains (cytosolic and sarcolemma) of hiPSC-CMs, by using two different Epac-based cAMP FRET sensors which are expressed in these cellular compartments. Therefore hiPSC-CMs were isolated from ML and EHT to compare the dynamics of NE-induced cAMP alone, as well as in the presence of inhibition of different PDE enzymes. The ultimate ambition of evaluating the dynamics of cAMP was to determine the level of maturation of hiPSC-CMs and to characterize factors, which could be revised in future to make hiPSC-CMs as similar as to native adult cardiomyocytes as possible.

2. Materials and Methods

2.1 Materials

All chemicals, devices, softwares and consumable materials for this study are as follow.

2.1.1 Culture media

All media, solutions, and buffers used for generation, culture, transduction, and experimentation of hiPSC-CMs were prepared under the highest possible sterile conditions.

Table 2.1: FTDA-Medium

Substances	Concentration	Made by
DMEM/F12 without glutamine		Gibco, Thermo Scientific, Waltham, MA, USA
Lipid mix	1:1000 v/v	Sigma, St. Louis, MO, USA
Penicillin/Streptomycin	0.5% v/v	Gibco, Thermo Scientific, Waltham, MA, USA
Transferrin	5 mg/l	Sigma, St. Louis, MO, USA
TGFβ1	0.5 ng/ml	PeproTech, Hamburg, Germany
Sodium selenite	5 µg/l	Sigma, St. Louis, MO, USA
Human serum albumin	0.1% v/v	Biological Industries, Cromwell, CT, USA
bFGF	30 ng/ml	PeproTech, Hamburg, Germany
Dorsomorphin	50 nM	Tocris, Bristol, UK
Activin A	2.5 ng/ml	R&D Systems, Minneapolis, MN, USA
Human recombinant insulin	5 mg/l	Sigma, St. Louis, MO, USA
L-glutamine	2 mM	Gibco, Thermo Scientific, Waltham, MA, USA

This sterile filtered medium was prepared according to a recent protocol (Mannhardt et al., 2016), kept at 4 °C and bFGF was added to the medium just before use.

Table 2.2: Medium used for Embryoid body formation

Substances	Concentration	Made by
FTDA-medium		Prepared in the lab, UKE, Hamburg, Germany
Polyvinyl alcohol	4 mg/ml in 1 X PBS	Sigma, St. Louis, MO, USA
Y-27632	10 µM	Biaffin, Kassel, Germany

Table 2.3: Medium used for mesoderm induction

Substances	Concentration	Made by
RPMI 1640 (medium)		Gibco, Thermo Scientific, Waltham, MA, USA
Y-27632	10 µM	Biaffin, Kassel, Germany
Penicillin/Streptomycin	0.5%	Gibco, Thermo Scientific, Waltham, MA, USA
Lipid mix	1:1000 v/v	Sigma, St. Louis, MO, USA
Humane serum albumin	0.05% v/v	Biological Industries, Cromwell, CT, USA
Phosphoascorbate	250 µM	Sigma, St. Louis, MO, USA
Transferrin	5 mg/l	Sigma, St. Louis, MO, USA
Sodium selenite	5 µg/l	Sigma, St. Louis, MO, USA
HEPES (pH 7.4)	10 mM	Roth, Karlsruhe, Germany
bFGF	5 ng/ml	PeproTech, Hamburg, Germany
Polyvinyl alcohol	4 mg/ml	Sigma, St. Louis, MO, USA
BMP-4	10 ng/ml	R&D Systems, Minneapolis, MN, USA
Activin-A	3 ng/ml	R&D Systems, Minneapolis, MN, USA

Table 2.4: Washing medium for mesoderm induction

Substances	Concentration	Made by
RPMI 1640		Gibco, Thermo Scientific, Waltham, MA, USA
Polyvinyl alcohol	4 mg/ml	Sigma, St. Louis, MO, USA
Penicillin/Streptomycin	0.5% v/v	Gibco, Thermo Scientific, Waltham, MA, USA
HEPES (pH 7.4)	10 mM	Roth, Karlsruhe, Germany

Table 2.5: Washing medium for cardiac specification

Substances	Concentration	Made by
RPMI 1640		Gibco, Thermo Scientific, Waltham, MA, USA
Penicillin/Streptomycin	0.5% v/v	Gibco, Thermo Scientific, Waltham, MA, USA
HEPES (pH 7.4)	10 mM	Roth, Karlsruhe, Germany

Table 2.6: Cardiac specification medium I

Substances	Concentration	Made by
RPMI 1640		Gibco, Thermo Scientific, Waltham, MA, USA
Y-27632	1 µM	Biaffin, Kassel, Germany
Penicillin/Streptomycin	0.5%	Gibco, Thermo Scientific, Waltham, MA, USA
Lipidmix	1:1000 v/v	Sigma, St. Louis, MO, USA
Transferrin	5 mg/l	Sigma, St. Louis, MO, USA
Sodium selenite	5 µg/l	Sigma, St. Louis, MO, USA
Wnt-Inhibitor DS-I-7/ XAV939	100 nM/1µM	Von Dr. Dennis Schade, Dortmund, Germany
HEPES (pH 7.4)	10 mM	Roth, Karlsruhe, Germany
Humane serum albumin	0.05% v/v	Biological Industries, Cromwell, CT, USA
Phosphoascorbat	250 µM	Sigma, St. Louis, MO, USA

Table 2.7: Cardiac specification medium II

Substances	Concentration	Made by
RPMI 1640		Gibco, Thermo Scientific, Waltham, MA, USA
Y-27632	1 µM	Biaffin, Kassel, Germany
Penicillin/Streptomycin	0.5%	Gibco, Thermo Scientific, Waltham, MA, USA
1-Thioglycerol	500 µM	Sigma, St. Louis, MO, USA
B27 with insulin	2% (v/v)	Gibco, Thermo Scientific, Waltham, MA, USA
HEPES (pH 7.4)	10 mM	Roth, Karlsruhe, Germany
Wnt-Inhibitor DS-I-7or XAV939	100 nM or 1 µM	Von Dr. Dennis Schade, Dortmund, Germany

Table 2.8: Cardiac specification medium III

Substances	Concentration	Made by
RPMI 1640		Gibco, Thermo Scientific, Waltham, MA, USA
Y-27632	1 µM	Biaffin, Kassel, Germany
Penicillin/Streptomycin	0.5%	Gibco, Thermo Scientific, Waltham, MA, USA
1-Thioglycerol	500 µM	Sigma, St. Louis, MO, USA
B27 with insulin	2% (v/v)	Gibco, Thermo Scientific, Waltham, MA, USA
HEPES (pH 7.4)	10 mM	Roth, Karlsruhe, Germany

Table 2.9: EHT casting medium

Substances	Concentration	Made by
DMEM		Biochrom, Berlin, Germany
L-glutamine	2 mM	Gibco, Thermo Scientific, Waltham, MA, USA
Penicillin/Streptomycin	0.5%	Gibco, Thermo Scientific, Waltham, MA, USA
Fetal calf serum (FCS), heat-inactivated	10% (v/v)	Gibco, Thermo Scientific, Waltham, MA, USA

Table 2.10: EHT culture medium

Substances	Concentration	Made by
DMEM		Biochrom, Berlin, Germany
Aprotinin	33 µg/ml	Sigma, St. Louis, MO, USA
Penicillin/Streptomycin	1%	Gibco, Thermo Scientific, Waltham, MA, USA
Fetal calf serum (FCS), heat-inactivated	10% (v/v)	Gibco, Thermo Scientific, Waltham, MA, USA
Human recombinant insulin	10 µg/l	Sigma, St. Louis, MO, USA

Table 2.11: Stopping buffer for enzymatic isolation of CMs

Substances	Concentration	Made by
DMEM		Biochrom, Berlin, Germany
Penicillin/Streptomycin	1%	Gibco, Thermo Scientific, Waltham, MA, USA
Fetal calf serum (FCS), heat-inactivated	10% (v/v)	Gibco, Thermo Scientific, Waltham, MA, USA

2.1.2 Buffer for FRET Microscopy

Table 2.12: FRET buffer

Substances	Concentration	Made by
NaCl	144 mM	JT Baker, 7647-14-5
KCl	5.4 mM	Merck, 1.04936
$MgCl_2$-$7H_2O$	1 mM	Fuka, 63063
$CaCl_2$	1 mM	Merck, 2382
HEPES	10 mM	Roth, 9105.4

2.1.3 Reagents/Solutions

Table 2.13: Recipes for reagents

Reagents/ Solutions	Compositions
Agarose for casting of EHT	2% (w/v) agarose dissolved in 300 ml 1xPBS autoclaved and stored at 60 °C
Aprotinin	33 mg/ml aprotinin dissolved in sterile water 250 µl aliquots stored at -20 °C up to one year
Stopping buffer solution	DMEM+10% fetal calf serum +1% Pen/Strep
Dissociation buffer	HBSS without **Ca^{2+}**/magnesium collagenase II, 200 units/mL 1 mM HEPES 10 µM Y-27632 30 µM BTS Sterile filtered (0.2 µm)
EDTA	0.5 mM EDTA in 1x PBS stored at 4 °C
Polyvinyl alcohol (50x)	20 g of polyvinyl alcohol dissolved in 100 mL of aqua dest stored at 4 °C up to one year
Phosphoascorbate, 250 mM	1 g Phosphoascorbate in 12.4 ml PBS
Pluronic F-127 solution	Pluronic F-127 dissolved in 1x PBS to a concentration of 1% (w/v), filter sterilized (0.2 µm filter) and stored at 4 °C for up to 1 year.
Gelatin 0.1%	Take 0.5 g galantine (500 ml) and pour it into DPBS under hood Keep it in incubator for 1 hr. Filter it under hood.
Collagenase II	HBSS w/o Mg^{2+}/Ca^{2+}, Gibco, 14175-053 and 1 mM HEPES pH 7.4
Thrombin	100 U/ml thrombin dissolved in 60% (v/v) 1xPBS and 40% (v/v) sterile water. Stored at -20 °C for max. 1 year.
Transferrin–selenium	100 mg transferrin dissolved in 2 ml sodium selenite (382 µM).Stored at -80 °C up to six months
10x DMEM	Solve 134 mg 10x DMEM powder in 5 mlv of water for injection, filter with 0.22µm filter and stored in well-closed container at 4°C.
HEPES Stock Solution	1M HEPES dissolved in 1xPBS and adjusted pH to 7.4 with potassium hydroxide. Filter sterilized (0.2µm filter) and stored at 4 °C for max. 1 year.

2.1.4 Consumables

Table 2.14: Consumables

Consumable	Manufacturer, Item Number
6 Well Plate	Falcon, #351146
96 Well Plates	Thermo Fisher Scientific, #167008
Microscope Cover Glasses 25mm	Assistent, #41001125
Serological Pipette 10mL	Sarstedt, #86.1254.001
Serological Pipette 2mL	Sarstedt, #86.1252.001
Serological Pipette 25mL	Sarstedt, #86.1255.001
Serological Pipette 5mL	Sarstedt, #86.1253.001
Serological Pipette 50mL	Sarstedt, #86.1256.001
Tube 15mL	Sarstedt, #62.554.002
Tube 50mL	Sarstedt, #62.574.004
Quality Pipette Tips 1000 µL	Sarstedt, #70.762.100
U-40 Insulin 30Gx1/X	Braun, #9161309V
U-40 Insulin Omni_x Solo	Braun, #9161309V
500 mL Vacuum Filtration "rapid"-Filtermax	TPP, 99500
Cell culture flask T175	Sarstedt, 83.3911.002
Cell culture flask T80	Nunc, 178905
Cell culture plate 12/ 24	Nunc
Neubauer counting chamber	Karl-Hecht KG
Pipette tips	Sarstedt
Silicone rack	EHT Technologies, C0001
Spinner flasks 500 / 1000 mL	Integra Biosciences, 182101 / 182051
Teflon Spacer	EHT Technologies, C0002
Aspiration pipette 2 mL	Sarstedt, 86.1252.011

2.1.5 Software

Table 2.15: Software

Software	Version	Manufacturer
Excel	Professional Plus 2013	Microsoft
GraphPad	Prism 6.01	GraphPad
ImageJ	1.44n9	National Institutes of Health
Mendeley Desktop	1.15.2	Mendeley
Micro-Manager	1.4.5	Open Imaging
PowerPoint	Professional Plus 2013	Microsoft
Word	Professional Plus 2013	Microsoft

2.1.6 Chemicals

Table 2.16: Chemicals

Products	Manufacturer
Accutase cell dissociation reagent	Sigma-Aldrich, A6964
Activin A	R&D Systems, 338-AC
Agarose	Invitrogen, 15510-027
Aprotinin	Sigma-Aldrich, A1153
bFGF	PeproTech, 100-18B
B27 plus insulin	Gibco, 17504-044
$CaCl_2$ x $2H_2O$	Merck, 2382
Collagenase II	Worthington, LS004176
DMEM	Biochrom, F0415
DMEM/F12	Gibco, 21331-046
DMSO	Sigma-Aldrich, D4540
Dorsomorphin	Tocris, 3093

2. Materials and Methods

DPBS	Gibco, 14040-133
EDTA	Roth, 8043.2
Ethanol, absolute	Chemsolute, 2246.1000
Fetal calf serum	Biochrom, S0615
Fibrinogen	Sigma-Aldrich, F8630
Gelatin	Sigma-Aldrich, G1890
Geltrex	Gibco, A1413302
HBSS minus Ca2+/Mg2+	Gibco, 14175-053
HEPES	Roth, 9105.4
Human serum albumin	Biological Industries, 05-720-1B
Human recombinant insulin	Sigma-Aldrich, I9278
L-glutamine	Gibco, 25030-081
Lipidmix	Sigma-Aldrich, L5146
Matrigel basement membrane matrix	Corning, 354234
Matrigel growth factor reduced (GFR) basement membrane matrix	Corning, 354230
Methanol	J. Baker, 8045
$MgCl_2$	Fuka, 63063
Penicillin/streptomycin	Gibco, 15140
Phosphoascorbate(2-Phospho ascorbic acid trisodium salt)	Sigma-Aldrich, 49752
Pluronic F-127	Sigma-Aldrich, P2443
Polyvinyl alcohol (PVA)	Sigma-Aldrich, P8136
Potassium chloride (KCl)	Merck, 1.04936
Potassium di-hydrogen phosphate (KH_2PO_4)	Merck, 104873
RPMI 1640	Gibco, 21875
Selenium	Sigma, S5261
Sodium chloride (NaCl)	JT Baker, 7647-14-5

Sodium di-hydrogen phosphate mono-hydrate (NaH_2PO_4 x H_2O)	Merck, 6346
Sodium hydrogen carbonate ($NaHCO_3$)	Merck, 106329
TGFß1	Peprotech, 100-21
Thrombin	Sigma-Aldrich, T7513; Biopur, BP11-10-1104
Transferrin	Sigma-Aldrich, T8158
Trypan blue	Biochrom, L 6323
XAV-939	Tocris, 3748

2.1.7 Devices

Table 2.17: Devices

Devices	Manufacturer
LED pE-100 440 nm	CoolLED
Beam splitter DV2	Photometrics
Centrifuge Fresco 17	Thermo Fisher Scientific
Class II Biological Safety Cabinet	Labgard
CO_2 Incubator	Sanyo
Freezer Comfort	Liebherr
Fridge Comfort	Liebherr
Water Bath	Julabo
Cell culture incubator	Binder
Cell culture incubators S2020 1.8, HERA cell 240 & 150i	Thermo Fischer Scientific
Centrifuges 5415 R & 5810 R	Eppendorf
Centrifuge J-6B	Beckmann
Centrifuges Rotanta/RP & Universal 30 RF	Hettich
Pipettes 10 / 100 / 1000 µL	Eppendorf
Precision advanced scale	Ohaus

2.2 Methodology

2.2.1 Human-induced pluripotent stem cells (hiPSCs) culture

2.2.1.1 Generation of human-induced pluripotent stem cells (hiPSCs)

HiPSCs were generated by engineered heart tissue group of Institute of Experimental Pharmacology and Toxicology, UKE, Hamburg. Dr. Umber Saleem and Dr. Pierre Bobin kindly facilitated this whole study by providing hiPSCs and hiPSC-CMs. An in-house protocol (Breckwoldt et al., 2017) was used to generate undifferentiated hiPSCs from three cell lines C-25, ERC-01 and ERC-18. This protocol was chosen because it was the most feasible approach and already established in our lab. In detail, fibroblasts were obtained from a skin biopsy from a healthy donor. Every donor had given informed consent. These fibroblasts were reprogrammed into undifferentiated hiPSCs at the Institute of Experimental Pharmacology and Toxicology, UKE, Hamburg by utilizing the Sendai virus-based cyto tune kit (Life Technologies, USA). Expansion of the undifferentiated hiPSCs was executed in the Y-27632 (10 µM) containing FTDA medium (Table 2.1) and this batch of undifferentiated hiPSCs was cultured in T80 flasks. T80 flasks were coated with Geltrex (1:200 in DMEM, 1 ml/10 cm^2). These Geltrex coated T80 flasks were then incubated for a week at conditions stated as 37 °C, 5% CO_2, 21% O_2, and 90% humidity. During incubation, hiPSCs were fed every day with pre-warmed FTDA (2 ml/10 cm^2) till cells achieved the desired 80% confluency. Standard hiPSCs passaging was carried out with Accutase (Sigma-Aldrich A6964). Briefly, undifferentiated hiPSCs were incubated with Rho-kinase inhibitor Y-27632 (10 µM) after 2 times washing with warmed (37 °C) Phosphate-Buffered Saline (PBS). Then undifferentiated hiPSCs were detached from Geltrex-coated T80 cell culture flasks by lowering Ca^{2+} with 1 ml of EDTA /10 cm^2 growth surface. The detached clusters of cells were subjected to karyotyping and mycoplasma testing.

2.2.1.2 Differentiation of hiPSC-CMs

Dr. Umber Saleem and Dr. Pierre Bobin differentiated hiPSC-CMs for this study. In order to achieve high-quality differentiation of hiPSCs into cardiomyocytes, a well-established protocol was followed for differentiation of undifferentiated hiPSCs into cardiomyocytes (Breckwoldt et al., 2017). Step by step differentiation, as fully illustrated in (Fig.11), was executed. Cells were washed with PBS. The single cell suspension was achieved by trituration with 10 ml pipette in embryoid body (EB) formation media (Table 2.2). Cells were counted by using trypan blue dye in a Neubauer chamber. Undifferentiated hiPSCs were transferred into spinner flasks (500 ml) and incubated in EB formation media (Table 2.2)

The volume of EB formation media was adjusted in such a way that 100 ml of media contains 30 million cells. The formation of the EB was facilitated by the stirring with a rotor at a speed of 40 rpm and incubated at 37 °C, 5% CO_2 and 5% O_2 for the night.

The next day this suspension was divided into two portions: 50 ml were separated into a falcon tube and the rest was poured into T175 flasks. These T175 flasks were put on specially designed v-shaped racks and incubated for a maximum of 20 minutes, while the EBs in the falcon tube were washed once with the respective medium (Table 2.4). Their volume was measured and from this measurement the total volume of EBs was estimated (Breckwoldt et al., 2017). All EBs from the falcon tube and from T175 flasks were put together and were washed with washing medium (Table 2.4).

EBs were resuspended in mesoderm induction medium (Table 2.3). Two types of flasks, T75 and T175, were used and these were coated with Pluronic F-127 (1 ml/10 cm^2). The volume of EBs and mesodermal induction medium was adapted according to the flask used i.e. 50-100 µl EBs with 20 ml of medium and 150-250 µl of EBs with 40 ml of medium for T75 and T175 flasks respectively. The EBs were cultured using the mesodermal induction medium (Table 2.3) for three days under conditions at 37 °C, 5% O_2, 5% CO_2, and 90% humidity. Half of the volume of the mesodermal induction medium was regularly replaced by fresh mesodermal induction medium every day.

After 3 days 90% of mesodermal induction medium was removed and EBs were washed with 20 ml of washing medium (Table 2.5). After sedimentation, 90% of washing medium was removed and 5 ml of cardiac induction medium I (Table 2.6) was used. Then the volume was estimated again before further differentiation of hiPSC into cardiomyocytes. For this EBs were poured into two types of flasks,T75 and T175, which were coated with Pluronic F-127 (1 ml/10 cm^2). The volume of EBs and cardiac induction medium I was adapted according to the flask used i.e. 80-100 µl EBs with 20 ml of medium and 200-250 µl of EBs with 46 ml of medium for T75 and T175 flasks respectively.

For the first day these flasks containing EBs of undifferentiated hiPSCs in cardiac induction medium I (Table 2.6) were incubated at conditions 37 °C, 5% O_2, 5% CO_2, and 90% humidity and every day half of the cardiac induction medium I was exchanged with fresh cardiac induction medium I for the next two days. Following this, cardiac induction medium I was completely replaced by cardiac induction medium II (Table 2.7) and incubated for four days. Again, half of the cardiac induction medium II was exchanged with fresh cardiac induction medium II every day.

Finally, the whole cardiac induction medium II was exchanged to cardiac induction medium III (Table 2.8) and was incubated for the next 3 days while exchanging half of the medium every day. Through this process, EBs of undifferentiated hiPSCs were converted into spontaneously beating embryoid bodies after 9-11 days of sequential exposure to three different culture media. On the17th day, spontaneously beating EBs were exposed to collagenase II (Worthington, LS004176; 200 U/ml) solution for 3.5 hours at 37°C for enzymatical dissociation of EBs to a single cardiac cells.

Cardiac differentiation efficacy was quality controlled by flow cytometry. For this purpose hiPSC-CMs were labelled with anti-cardio-troponin (cTnT) antibody.

2.2.1.3 Storage of hiPSC-CMs

Dissociated hiPSC-CMs from EBs were transferred into freezing solution containing-cryovials. The freezing solution was comprised of 10% fetal calf serum (FCS) and DMSO (Breckwoldt et al., 2017). Dissociated hiPSC-CMs were gradually cooled to -80 °C for 1 day by utilizing cryopreservation equipment Asymptote EF600M (Grant Instruments). After cooling the hiPSC-CMs were transferred to -150 °C storage facility for long-time.

2.2.2 Generation of Monolayer (ML) and Engineered heart Tissue (EHT)

Dr. Umber Saleem and Dr. Pierre Bobin kindly facilitated the casting of differentiated hiPSC-CMs and cultured in two formats:conventional 2D ML and 3D EHT. Frozen hiPSC-CMs in cryovials were thawed in a water-bath and were then transferred into a centrifuge tube. RPMI 1640 medium containing 1% penicillin/streptomycin was poured drop by drop into the centrifuge tube containing the hiPSC-CMs with utmost care as the pouring of the medium can damage hiPSC-CMs by osmotic stress.

2.2.2.1 Monolayer (ML)

For the ML format black-sided 96 well-plates were used, which were coated with 0.1% gelatin solution in sterile BPS. These gelatin-coated plates were incubated for 45 minutes before cardiomyocytes were poured in each well. 20,000 cells per each well were plated and 200 µl of Dulbecco's Modified Eagle Medium (DMEM) was added and the plates were incubated till the formation of a ML. The medium was changed every Monday, Wednesday, and Friday.

2.2.2.2 Casting of EHT

Dr. Umber Saleem and Dr. Pierre Bobin casted EHT for this study. EHT from hiPSC-CMs was generated according to the protocol as reported recently (Mannhardt et al., 2017). This three-phase protocol requires high qualitative and quantitative precision. In the first phase of generation of EHTs, 1.6 ml of 2% agarose was poured into each well of a 24 well-plate. Teflon spacers were placed immediately to generate a mold. As the agarose took 10-15 minutes for solidification at room temperature, this time was used for the preparation of the master mix (Table 2.18), which contains all required components including hiPSC-CMs for EHT generation.

The volume of the master mix depends upon numbers of EHTs to be generated. For this project $1x10^6$ hiPSC-CMs per EHT were used to get spontaneously beating EHT. Teflon spacers were replaced by Polydimethylsiloxane (PDMS) racks after the conversion of translucent agarose into opaque. In the second phase, thrombin (3 µl) was added into each well containing 100 µl master mix. This 24 well-plate, containing PDMS racks with master mix, was incubated at 37 °C, 40% O_2, 7% CO_2 at 90% humidity for 1.5-2 hours. Then 200-500 µl of medium was added in each well and the plate was shaken gently 5 to 10 times to and fro. Afterwards, the plate was again incubated for 10-15 minutes. Then all PDMS racks containing EHT were transferred into a new plate containing 1.5 ml of culture medium in each well and were incubated further at 37 °C, 40% O_2, 7% CO_2 and 90% humidity. The culture medium (Table 2.10) was replaced every Monday, Wednesday and Friday. Typically, EHT starts spontaneously beating after 7 days of culture. Cardiomyocytes were isolated from EHTs after 21 days of culture.

2.3 Isolation of Cardiomyocytes from EHT and ML tissues

Single hiPSC-CM was dissociated from ML and EHT from different cell lines by an already established protocol in our lab (Uzun et al., 2016). In detail, MLs or EHTs were fed with culture medium for at least 21 days. Afterwards, MLs or EHTs were washed with 1.5 ml PBS (37°C) for three times for 10 minutes each time. Then, 1.5 ml of collagenase type II (Worthington, LS004176; 200 U/ml) was poured into each well-containing ML or EHT. Then these ML or EHT containing well-plates were incubated at 37 °C, 40% O_2, 7% CO_2 and 90% humidity.
A trituration plan for tissues in collagenase type II solution was strictly followed to get the highest possible number of cardiomyocytes from each tissue.

ML tissue in collagenase type II was triturated after 1 and 2 hours while EHT in collagenase type II was triturated after 1 hour and 3 hours. Isolation of cardiomyocytes took 5 hours for EHTs and 3 hours for ML tissues. When a sufficient number of isolated cardiomyocytes had dissociated from the wells, a stop buffer containing FCS was used to stop further enzymatic digestion (Table 2.11). The suspension containing cardiomyocytes, collagenase type II, and stop buffer was centrifuged at 800 rpm for 10 minutes. After careful decantation of supernatant, the pellet containing cells were taken into culture medium at 37 °C (Table 2.10). It is known that hiPSC-derived cardiomyocytes turn into a round oval shape (Fig. 12) after enzymatic dissociation. The number of cells were counted by using trypan blue dye in a Neubauer chamber. About 60-65% hiPSC-CMs could be isolated after enzymatic digestion of an EHT.

Table 2.18: Computation of volume of constituents of master-mix recipe per one EHT

Components	**Volume**
hiPSC-CMs	1.1x 10^6 cells
EHT casting medium	86.9 µl
2xDMEM	6.2 µl
10% Matrigel	11 µl
0.1% Y-27632	0.11 µl
Fibrinogen	2.8 µl
Thrombin	3.34 µl

The volume of constituents can be expanded according to the number of projected EHTs to be formed.

2. Materials and Methods

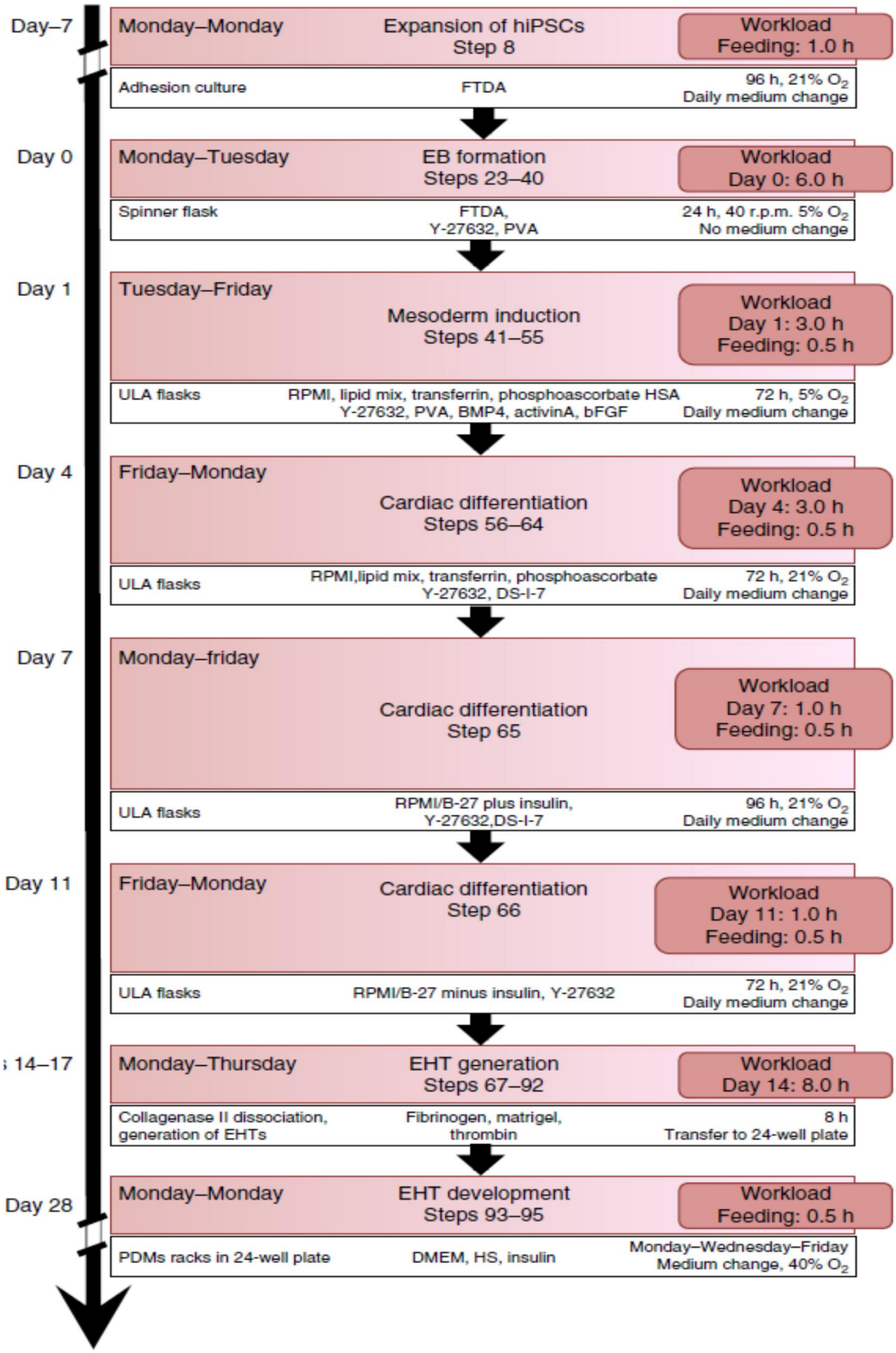

Figure 11: Workflow of the cardiac differentiation protocol
Every step is labelled with time point, culture medium, and medium composition (taken from Breckwoldt et al., 2017).

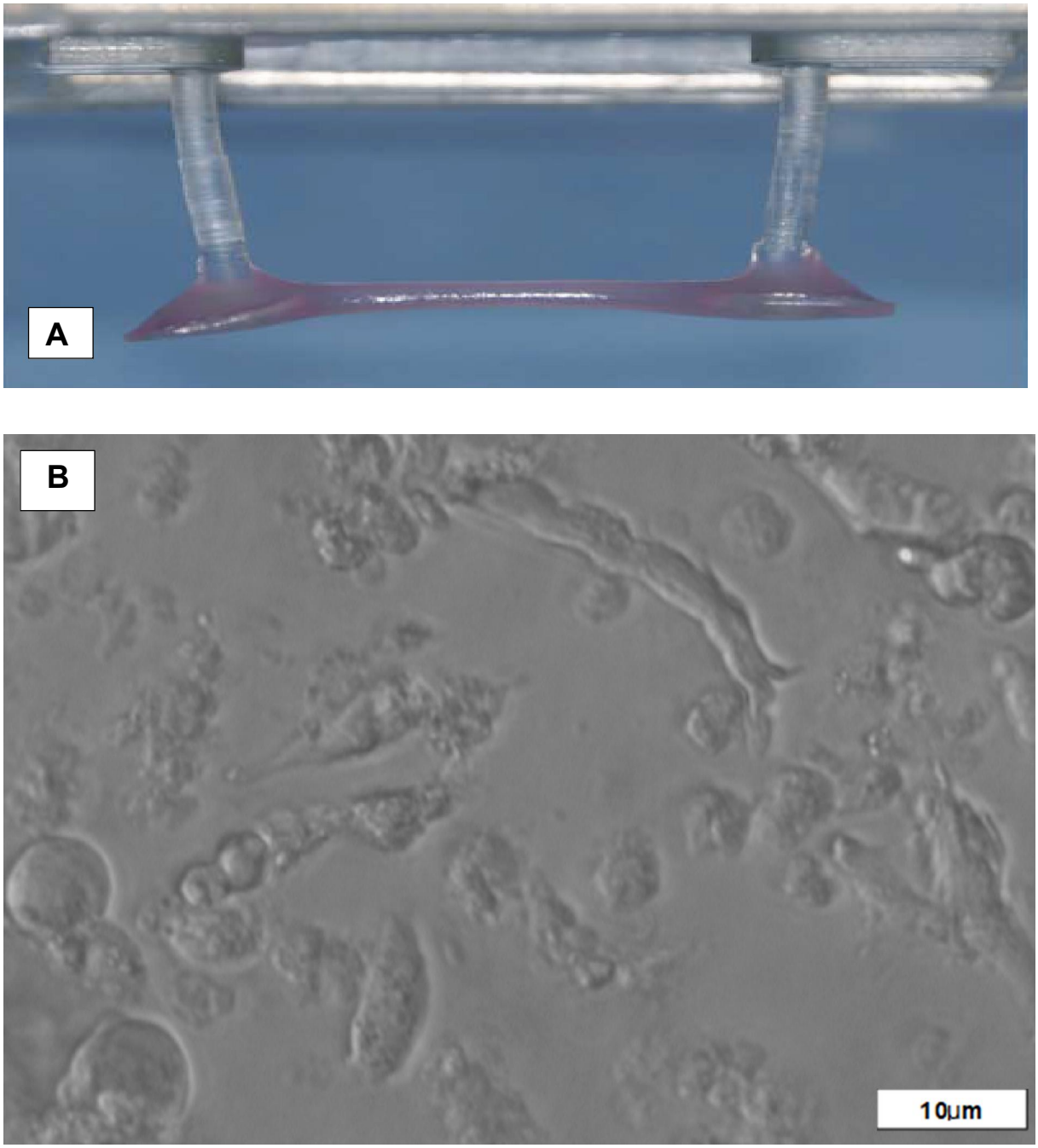

Figure 12: EHT and freshly isolated hiPSC-derived cardiomyocytes
An EHT on a silicone post before exposure to enzymatic degradation (**A).** HiPSC-derived cardiomyocytes three hours after isolation from EHT by using collagenase type II protocol Most of the cells become oval-shaped and few cells rod-shaped **(B)**.

2.4 Transduction of hiPSC-CMs with FRET sensors

It was the aim of the study to measure real-time cAMP in living intact hiPSC-CMs by using FRET. This approach requires the expression of FRET sensors in hiPSC-CMs, which react to a change in intracellular concentration of cAMP. Adenovirus and adeno-associated viruses are established and effective tools to express biosensors in cardiomyocytes isolated for adult heart tissue (Mironov et. al., 2009). We used the same approach for the transduction of hiPSC-CMs. Freshly isolated hiPSC-CMs were plated in two ways. Initially, 25 mm diameter glass coverslips were used. First coverslips were coated with a 0.1% gelatin solution for at least 45 minutes. Every coverslip was loaded with 1.5 µl of cell suspension containing hiPSC-CMs. Cells were transduced with adenovirus-encoding an Epac-based FRET biosensor to measure cAMP. However, it was problematic to transfer coverslips into the recording chamber during experiments. Sometimes coverslip were broken during shifting them from the well-plate to the FRET measurement chamber and often leakage of fluid from the chamber occurred and produced artefacts. Therefore, another approach was developed. The new approach was to use 29 mm diameter glass dishes with a 10 mm bottom well (Lot# 150906, Cellvis, China) that served as a recording chamber afterwards. The alternative chambers helped to avoid complications by transferring coverslips into the recording chamber. The central parts of the glass dishes were coated with a 0.1% gelatin solution for at least 45 minutes. Consecutively, every dish was loaded with 1.5 µl of cell suspension containing hiPSC-CMs.

Cells were transduction with adenovirus-encoding Epac-based FRET biosensor (Fig. 13) to measure cAMP globally in the cytosol (E1-camps) or in the L-type Ca^{2+} channel domain (pm-Epac1). The two different adenovirus-encoding biosensors were provided by Prof. Viacheslav Nikolaev from the Institute of Experimental Cardiovascular Research, UKE Hamburg. The volume of adenovirus-encoding biosensor solution was calculated by using an established protocol:

Number of cells = A
Desired Multiplicity of infection (MOI) = B
Plaque forming unit (pfu) needed = A x B
Required volume of virus = pfu needed/ pfu actual/ml

The required volume of adenovirus containing solution was mixed with culture medium and poured into the wells or dishes containing cells. These well-plates or dishes were incubated for at least 48 hours to allow for proper transduction. Both biosensors gave smooth and uniform expression throughout the cytosol and sarcolemmal domain with MOI=100 pfu/cell and MOI=50 pfu/cell respectively (Fig. 14).

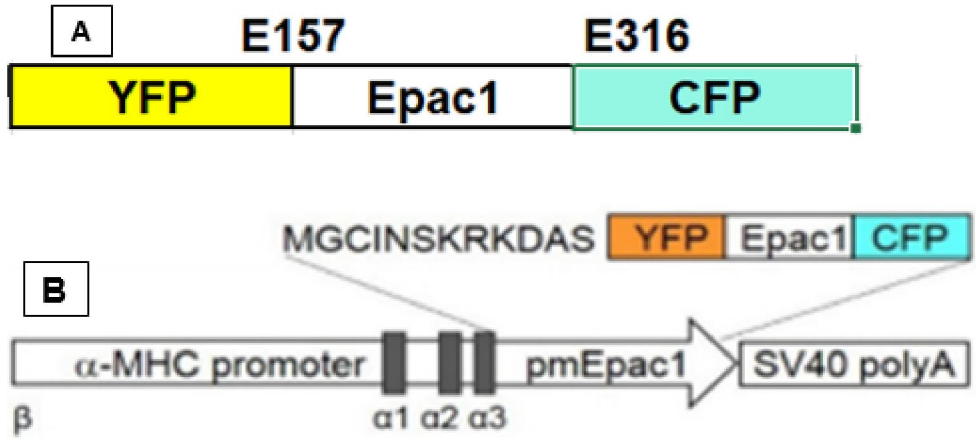

Figure 13: Construct of Epac1 based biosensors
A. Schematic representation of the construct of E1-camps FRET biosensor which includes two fluorophores, Yellow Fluorescent Protein (YFP) and Cyan Fluorescent Protein (CFP) and the EPAC cAMP binding domain (EPAC1). **B.** pm-Epac FRET biosensor used by Perera et al., 2015.

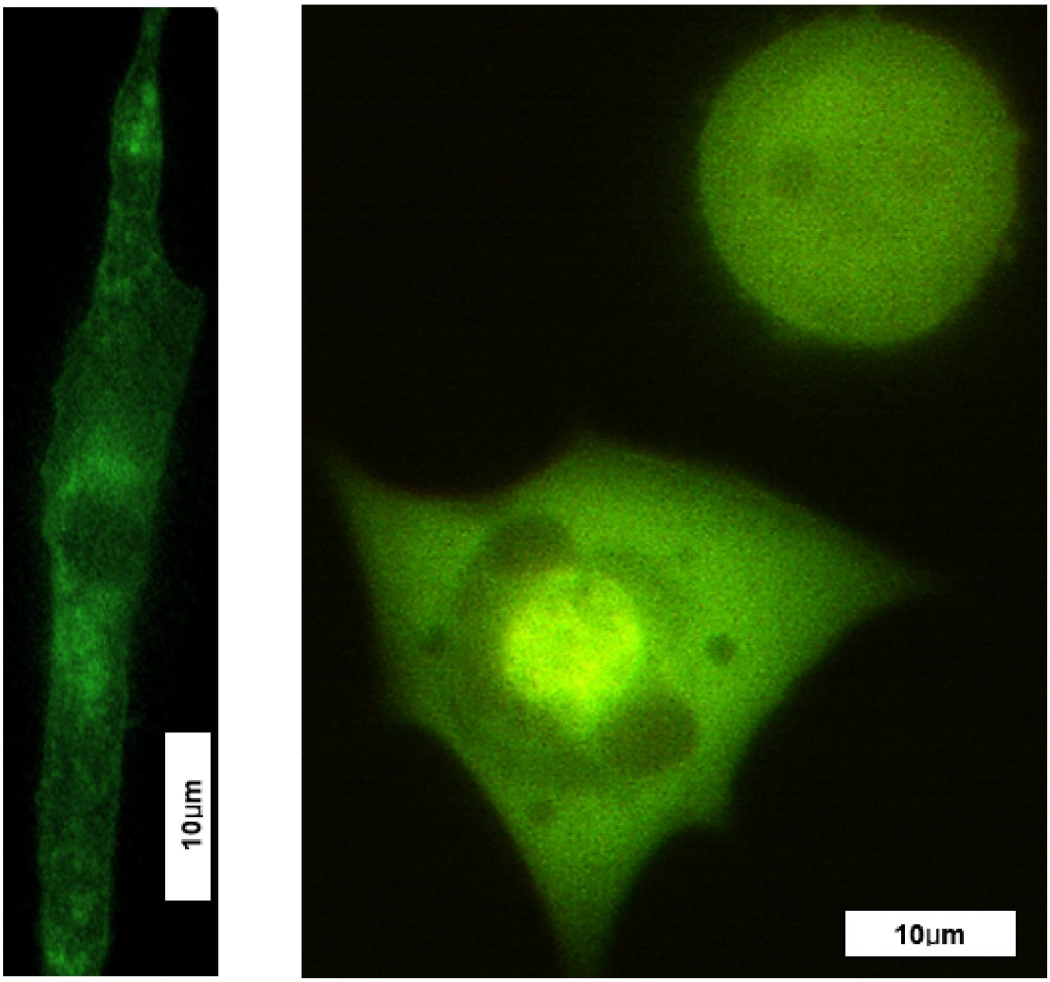

Figure 14: Expression of FRET-based biosensor in isolated hiPSC-derived cardiomyocytes
On the left image is an isolated hiPSC-derived cardiomyocyte transduced with adenovirus-encoding pm-Epac1 biosensor (sarcolemma) while on the right image there are isolated hiPSC-derived cardiomyocytes transduced with adenovirus-encoding E1-camps biosensor (global) after 48 hours of transduction (MOI=100 for global and MOI=50 for sarcolemma).

2.5. FRET microscopy

2.5.1 Components of FRET microscope assembly

This following FRET set up (Fig. 15) with its components was used to record changes in real-time cAMP levels after exposing the transduced hiPSC-CMs to different agents. The used agents increase cAMP levels either by generating cAMP or inhibiting cAMP degradation by phosphodiesterase enzymes.

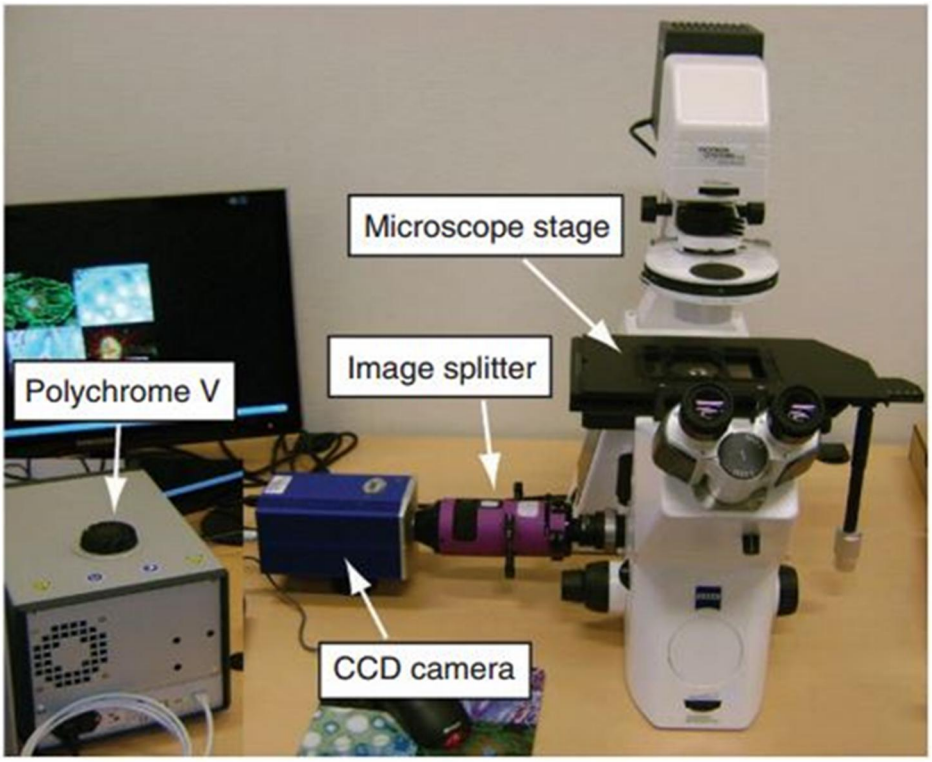

Figure 15: FRET Microscope

FRET measurement assembly at the Institute of Experimental Cardiovascular Research, University Medical Center Eppendorf, Hamburg, Germany. Its vital components are: beam splitter, cool LED, and Complementary Metal-Oxide Semiconductor (CMOS) camera.

2.5.2 FRET experimental procedure

Glass coverslips or dishes containing transduced cells and the virus-containing culture medium were washed with FRET buffer (Table 2.12) before any experiment. Coverslips were transferred into a microscopy cell chamber or culture medium was sucked from glass-bottom dishes and dishes were put directly on the microscope stage.

Every chamber or dish was filled with 400 µL of FRET buffer. For FRET experiments, an inverted microscope (Leica DMI3000 B, Germany) which possesses an oil immersion objective with 63X magnification was used.

Not every hiPSC-CM showed sufficient expression of the sensor. For experimentation cells with uniform exposure of biosensor were therefore carefully selected (Fig.14). Both white as well as fluorescent lights were applied to select cells. The exposure time and intensity of the cool-LED used to excite fluorescence were finely tuned to avoid artefacts and to get a good signal to noise ratio of the cell.

The cool-LED single-wavelength light-emitting diode was used to excite cells at 440 nm. The emitted light of the sample, which was received by the microscope, was split into individual donor and acceptor channels by a beam-splitter (D480/30 m and D535/40 m emission filters (Photometrics)) and then transmitted to Complementary Metal-Oxide Semiconductor (CMOS) camera, which recorded the light signals from both channels. CFP and YFP emission channels were recorded and stored by the software “micro-manger 1.4” on a computer and images were taken every 5 seconds. Cells were exposed to 400 µL of desired test compound solution after having reached a stable FRET baseline (run-in phase). Later on, for quantification of the change in intracellular cAMP level, the FRET ratio (averaged YFP intensity/averaged CFP intensity) was determined by using ImageJ, GraphPad prism, and Excel software (Sprenger JU et al., 2013).

2.6 Drugs for Cell Stimulation

2.6.1 Norepinephrine

Norepinephrine is a naturally occurring catecholamine with a higher affinity to β_1-AR than to β_2-AR. Norepinephrine hydrochloride with a molecular weight of 205.64 atomic mass unit (a.m.u), CAS No.329-56-6 from Sigma-Aldrich (Fig.16) was used for the experiments described herein. A stock solution of 100 mM concentration was prepared in 0.1 M HCl and 10 nM, 100 nM, 1 µM, 10 µM, and 100 µM final concentrations were used in experiments.

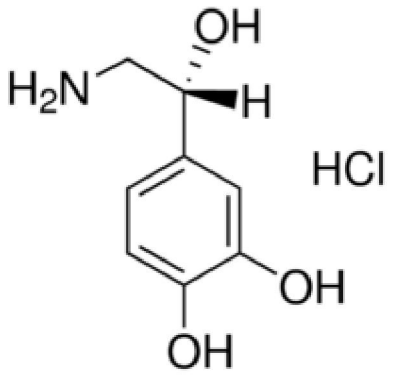

Figure 16: Chemical structure of norepinephrine

2.6.2 Forskolin

Forskolin is a direct adenylyl cyclase activator, which generates cAMP. Forskolin 10 mg with a molecular weight of 410.51 a.m.u, Batch No.3A/200408, and chemical structure as shown in the (Fig. 17) was purchased from Tocris.

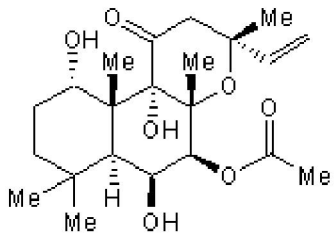

Figure 17: Chemical structure of forskolin

A stock solution of 10 mM concentration in DMSO was prepared and stored at -20 °C. It was diluted in FRET buffer to obtain a 10 µM concentration for experiments.

2.6.3 ICI-118,551

ICI-118,551 is a β_2-AR inhibitor, which binds to the β_2 subtype with at least 100 times greater affinity than β_1 or β_3, the two other known subtypes of the β-AR-(Bilski et al., 1983). ICI-118,551 has a molecular weight of 313.86 a.m.u., CAS No.72795-01-6, the chemical structure shown in the (Fig. 18) and was purchased from Sigma-Aldrich.

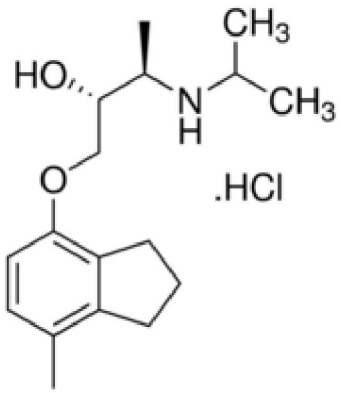

Figure 18: Chemical structure of ICI-118,551

A 10 mM stock solution of ICI-118,551 was prepared in distilled water and it was used in 50 nM final concentration for experiments.

2.6.4 BAY 60-7550

BAY 60-7550 is a selective inhibitor of PDE2, a PDE that degrades both cGMP and cAMP. We bought 1 mg of BAY 60-7550 with molecular weight 476.6 a.m.u. CAS number 439083-90-6, and chemical structure as shown in the (Fig. 19). A stock solution of 100 µm BAY 60-7550 in DMSO was stored at -20 ◦C. It was diluted in FRET buffer to 100 nm concentration for experiments (Mehel et al., 2013).

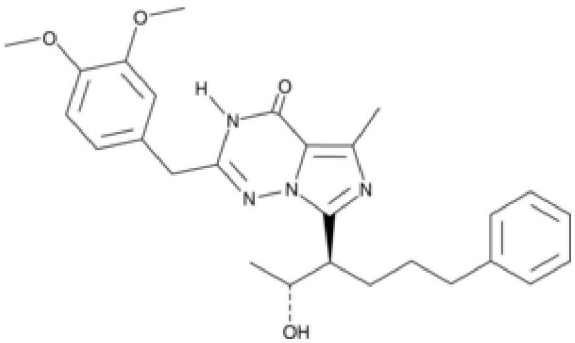

Figure 19: Chemical structure of BAY 60-7550

2.6.5 Cilostamide

Cilostamide inhibits degradation of both cAMP and cGMP. Cilostamide is chemically known as N-cyclohexyl-N-methyl-4- (1, 2-dihydro-2-oxo-6-quinolyloxy) –butyramide, as shown in the (Fig. 20), is a relatively selective inhibitor of PDE 3.

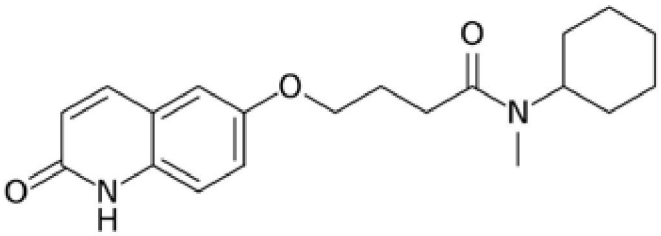

Figure 20: Chemical structure of cilostamide

Cilostamide 5mg was purchased from Sigma-Aldrich with molecular weight 342.43 a.m.u. A stock solution of 600 µM in DMSO was stored and was diluted with FRET buffer at a concentration of 300 nM for experiments. 300 nM of cilostamide were used as test concentration as it showed selective inhibition of PDE3 (Fig. 21).

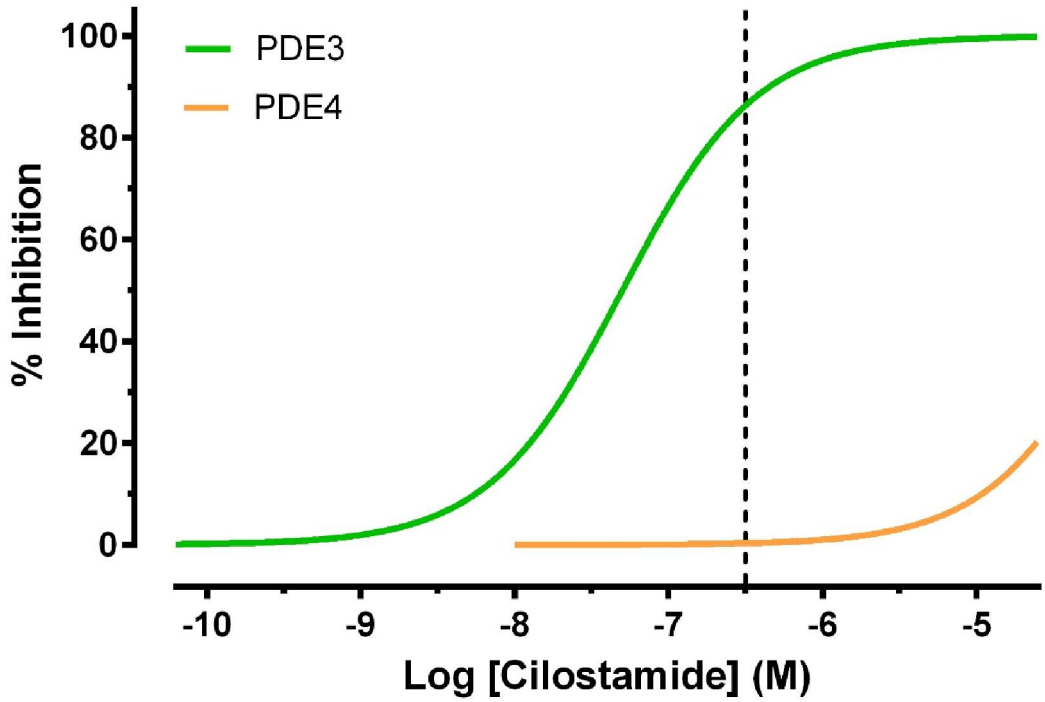

Figure 21: Percentage inhibition of PDE 3 and PDE 4 by cilostamide

The calculated CRC of cilostamide for PDE3 and PDE4 based on published IC_{50} values (Vargas et al., 2006) assuming a Hill slope = 1.

2.6.6 Rolipram

There are different pharmacological agents to inhibit PDE4. We have used rolipram a selective inhibitor of cAMP phosphodiesterase PDE4. Rolipram with the chemical name 4-(3-(Cyclopentyloxy)-4-methoxyphenyl) pyrrolidin-2-one is shown as chemical structure in (Fig. 22). Rolipram has been used as a selective inhibitor of PDE4 in many studies and in many species i.e. in guinea- pig (Bethke et al., 1992) and in human myocardium (Reeves et al., 1987).

We purchased rolipram 10 mg from Tocris with molecular a weight of. 275.35 a.m.u. and Batch No. 18B/230355.The stock solution (1 mM) was prepared in DMSO and stored at -20 °C. For experiments rolipram at a concentration of 10 µM was used, from which nearly complete inhibition of PDE4 without relevant inhibition of PDE3 can be expected (Fig. 23).

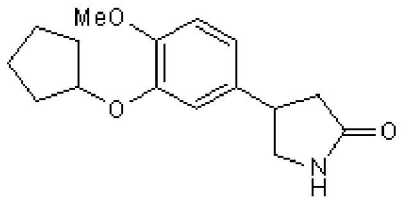

Figure 22: Chemical structure of rolipram

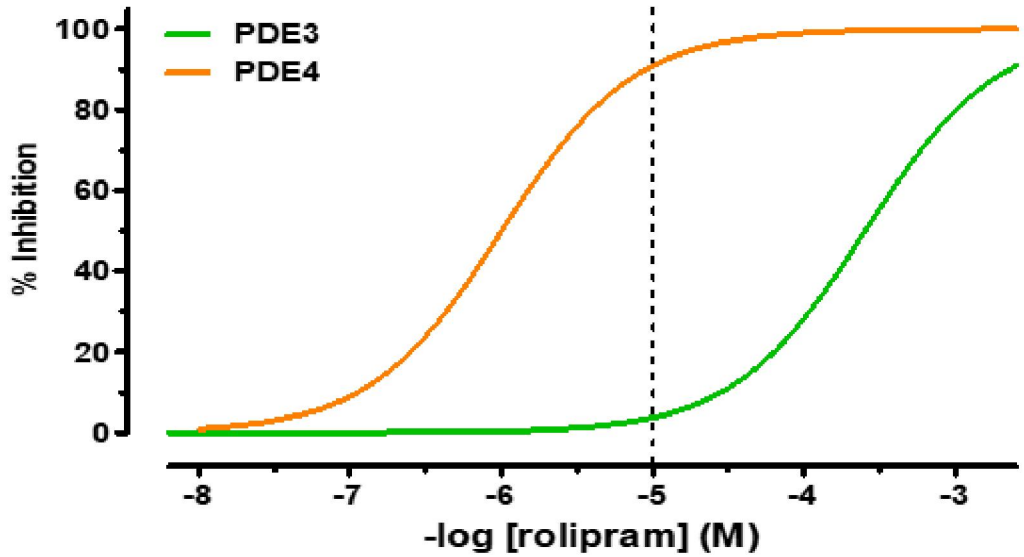

Figure 23: Percentage inhibition of PDE 3 and PDE 4 by rolipram

The calculated CRC of rolipram for PDE3 and PDE4 based on published IC_{50} values (Vargas et al., 2006) assuming a Hill slope = 1.

2.6.7 Tadalafil

Tadalafil is a potent and selective inhibitor of PDE5 (IC_{50} values for PDE5 is 9.4 nM) but at much higher concentration (1 µM) it also blocks PDE11 as shown in the graph (Fig. 24). However, even at such high concentrations PDE1, PDE3 and PDE5 are almost not affected. Tadalafil with molecular weight of 389.4 a.m.u. Cat. No. 6311, and chemical structure as shown in (Fig. 20) was bought from Tocris.

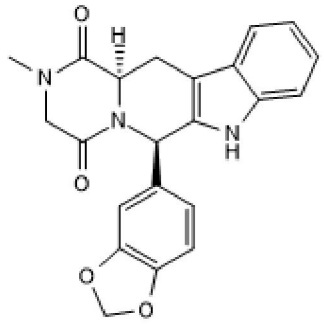

Figure 24: Chemical structure of tadalafil

Tadalafil powder was dissolved in DMSO and stored at 1 mM stock solution concentration. The stock solution was diluted in FRET buffer to 1 µM concentration for experiments.

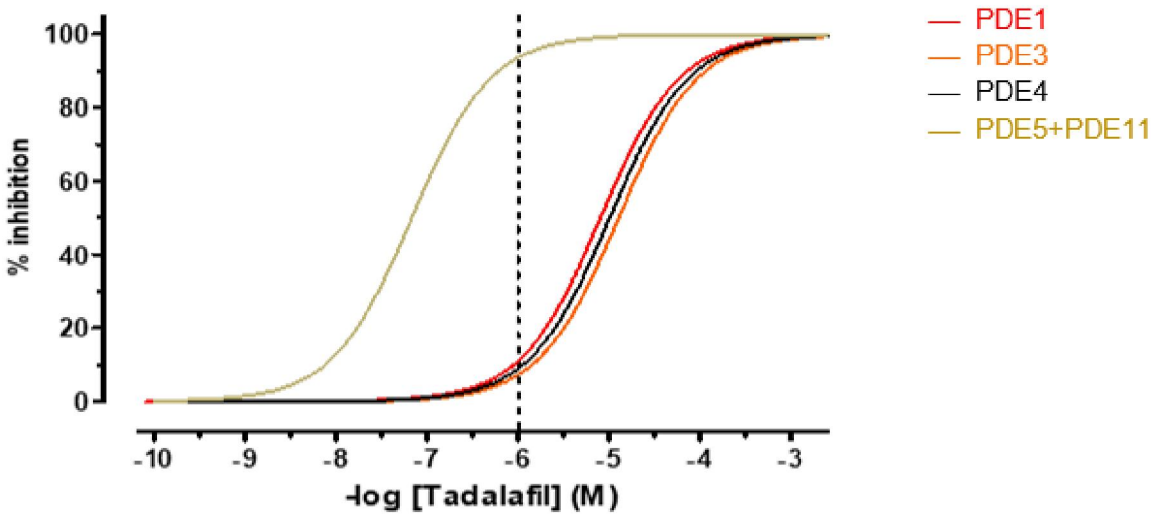

Figure 25: Percentage inhibition of PDE 1, PDE3, PDE 4 and PDE 11 by tadalafil

The calculated CRC of tadalafil for PDE1, PDE3 and PDE4, and PDE11 is based on published IC_{50} values (Bischoff, 2004) assuming a Hill slope = 1. A 10% inhibition of PDE4; and PDE1 with almost 100% inhibition of PDE11 is predicted from published data for the percentage of inhibition of PDEs by tadalafil (1µM).

2.7 Statistical analysis

Values are expressed as Mean±SEM. Statistical significance was evaluated using a Student's t-test for two groups and ANOVA was used for comparison of multiple effects. Differences were considered statistically significant when $p < 0.05$. Statistical analyses of the results were conducted with GraphPad Prism software 6.0. Bar graphs and scatterplots were used for data representation.

3. Results

The prime focus of the present study was the investigation of hiPSC-CMs from a cell line (C-25) cultured in both ML and EHT formats in regard to their cAMP signaling profile. Consecutively, hiPSC-CMs from cell line C-25 were both cultured in ML and EHT formats and transduced with two biosensors: E1-camps (global) and pm-Epac1 (sarcolemmal). In total 397 hiPSC-CMs from 134 EHTs and 244 hiPSC-CMs from 70 ML tissues were isolated and transduced with the global biosensor. In comparison, a total of 66 hiPSC-CMs from 20 EHTs and 82 hiPSC-CMs from 10 ML tissues were isolated and transduced with the sarcolemmal biosensor. In five preparations sufficient transduction was not achieved (most probably this happened because an inadequate MOI of adenovirus-encoding Epac based FRET biosensor was used). As comparators hiPSC-CMs from two more cell lines i.e. ERC-01, and ERC-18 cultured in EHT format were used. It is important to note that hiPSC-CMs from the ERC-01 and ERC-18 cell lines were only cultured in EHT format and were only transduced with the global biosensor. In total 49 hiPSC-CMs from 8 EHTs from cell line ERC-18 and 42 hiPSC-CMs from 6 EHTs from cell line ERC-01 were used.

3.1. Cell line C-25

3.1.1 Effects of norepinephrine on cAMP in hiPSC-CMs (C-25) transduced with global biosensor

3.1.1.1 Effects of NE on cAMP in hiPSC-CMs from C-25 cultured in ML format

To measure the effects of NE on cAMP in hiPSC-CMs from ML (C-25) we determined complete CRCs as follows: In the first set of experiments, cells were exposed to cumulatively increasing concentrations of NE starting from 10 nM up to 10 µM. A representative FRET ratio response curve is given in (Fig. 26 A). Every cell produced a change in FRET signals when exposed to NE (Fig. 26 B). However, the lowest concentration of NE used (10 nM) gave very small effects in some cells and was ineffective in many cells. A clear effect was always seen with a concentration of ≥ 100 nM NE.

In the next set of experiments, the exposure time of cells to NE was reduced to avoid desensitization of β-ARs, since one of the main goals of the study was to measure effects of PDE-inhibition not only under basal conditions, but also when β-ARs are stimulated by NE. Consecutively concentrations most relevant for quantification of NE effects were chosen with maximum effect size (E_{max}) and potency (expressed as the concentration needed to give half maximum effects (EC_{50}).

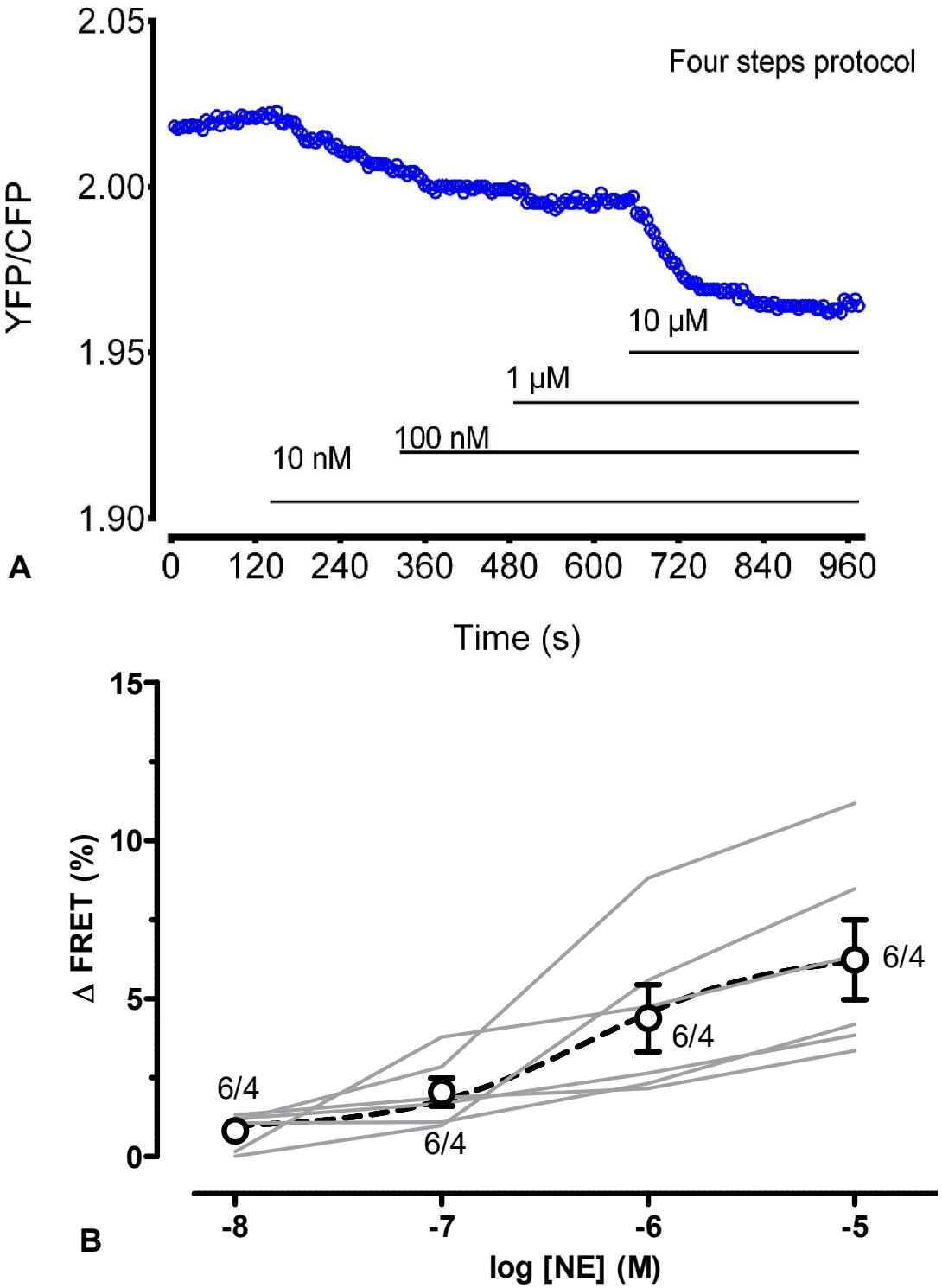

Figure 26: Effect of NE on FRET in hiPSC-CMs from C-25 cultured in ML format
Typical representative time course of FRET change (ΔFRET) in an isolated hiPSC-CM from C-25, cultured in ML format, exposed to cumulatively increasing concentrations of NE. concentrations are indicated by bars **(A)**. Increase in ΔFRET (%) in individual hiPSC-CMs from C-25 cultured in ML format exposed to cumulatively increasing concentrations of NE. Every line indicates a single cell experiment. A sigmoidal curve was fitted to calculate mean values±SEM, estimated EC_{50} was 520±0.4 nM and E_{max} was 6.4±1.1% over basal **(B)**.

Therefore we exposed cells to a concentration near to the expected EC_{50} and to a concentration sufficiently high enough to evoke maximum effects. Effects of threshold concentrations (10 nM) were taken from the pilot experiments which had been performed with the lowest concentration.

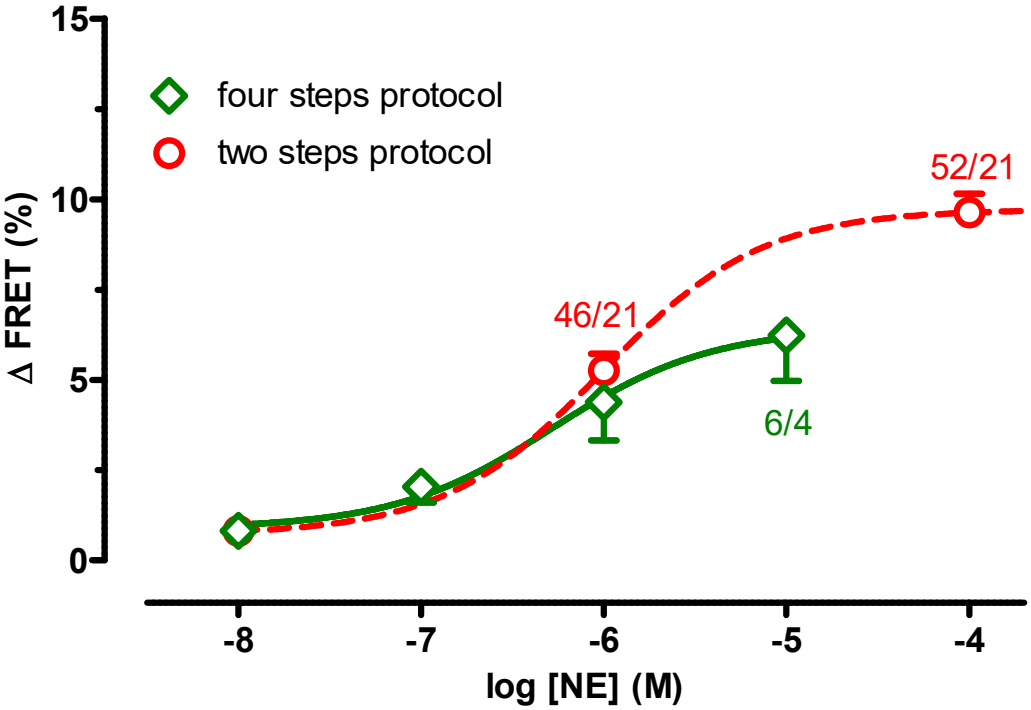

Figure 27: Effect of different exposure modes on potency and efficacy of NE to increase *Δ*FRET (%) in hiPSC-CMs from C-25, cultured in ML format

Mean values±SEM for an increase in ΔFRET ratio in cells exposed to four cumulatively increasing concentrations of NE (four-steps protocol) and for cells exposed to only two cumulatively increasing concentrations of NE (two-steps protocol). n/N indicates the number of cells/preparations.

The mode of exposure i.e. four-steps protocol vs. two-steps protocol may affect both E_{max} and EC_{50} of NE in hiPSC-CMs from C-25 cultured in ML format (Fig. 27). There was a tendency to higher E_{max} but smaller potency for NE when the two-step protocol was used (expressed as –$logEC_{50}$) as the E_{max} 9.7±0.2 vs. 6.4±0.5% and -$LogEC_{50}$ 6.1±0.1 vs. 6.3±0.2 M measured. However, this difference was not statistically significant (p=0.07). In summary, if the effects of a threshold concentration of NE are known, two concentrations of NE may be sufficient to get a rough estimate for NE potency and efficacy.

3.1.1.2 Effects of NE on cAMP in hiPSC-CMs from C-25 cultured in EHT format

It has recently been shown that hiPSC-CMs cultured in EHT format have a much higher increase in $I_{Ca,L}$ by NE than hiPSC-CMs cultured in ML format (Ismaili et al., 2020, Uzun et al., 2016). Therefore, we wanted to investigate whether hiPSC-CMs cultured in EHT format generate more cAMP than hiPSC-CMs cultured in ML format. Again complete CRC for NE in hiPSC-CMs from C-25 cultured in EHT format was determined. For that purpose, we exposed cells to a pair of two concentrations of NE (1 nM and 100 µM, 10 nM and 1 µM, and 100 nM and 10 µM). Please note that a large number of data for 1 µM and 100 µM NE comes from control experiments when the effect of NE in the presence of different PDE-inhibitors was measured. There was a tendency to higher sensitivity of EHT vs ML depicted in (Fig.28) (-logEC_{50}: 6.2±0.1 vs 6.0±0.1 M, p=0.16) but E_{max} was significantly larger (12.1±0.3 vs 9.7±0.5%, P<0.05, extra sum of squares of F-test).

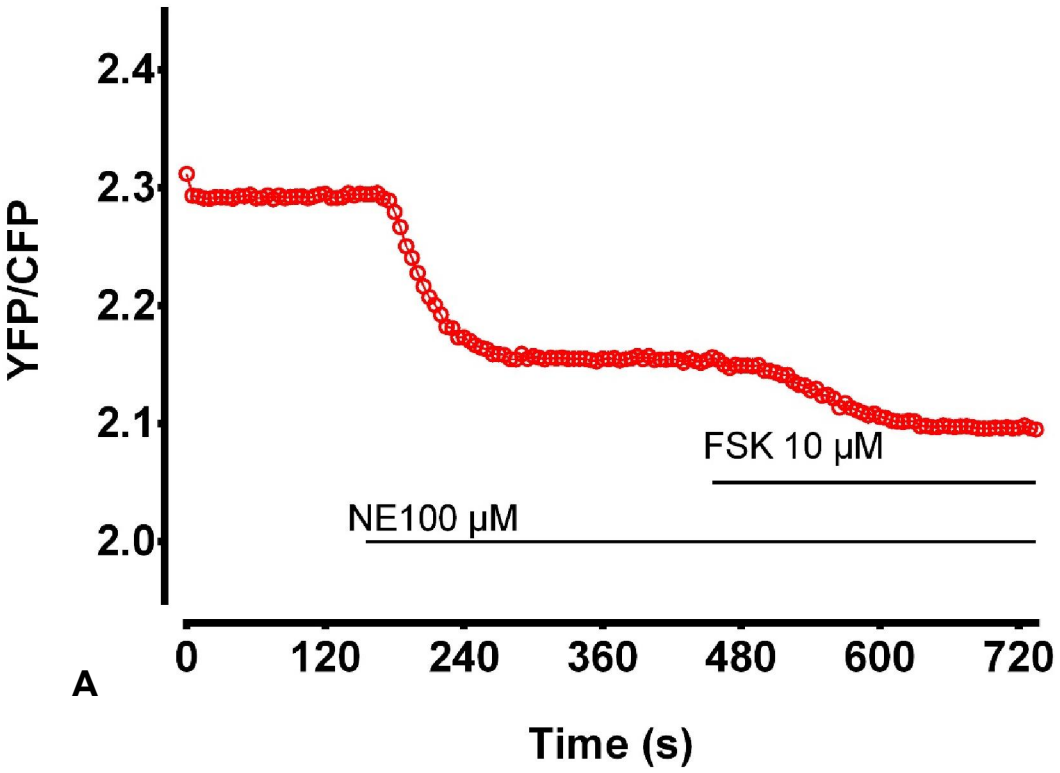

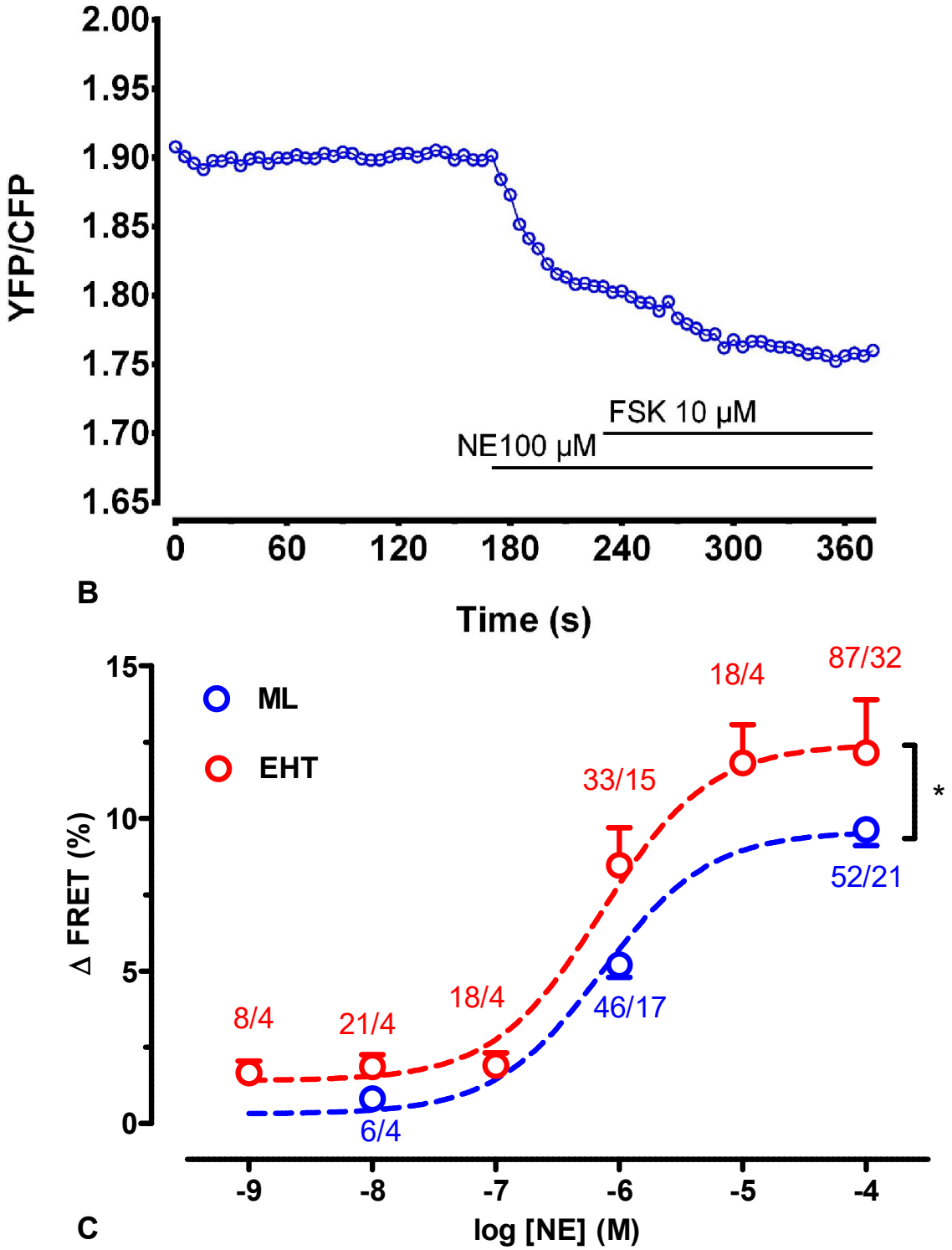

Figure 28: Effect of culture conditions on NE-evoked cAMP in hiPSC-CMs from C-25, cultured in ML and EHT format

Typical representative time and response course of FRET change in an isolated hiPSC-CM from C-25, cultured in EHT format (**A**) and an isolated hiPSC-CMS from C-25, cultured in ML format (**B**). Mean values±SEM for cAMP increase stimulated by NE in C-25-EHT(**C**). For comparison data for C-25 ML are taken from Fig.27.

3.1.1.3 Measurement of AC activity independent and dependent from GPCRs stimulation

FSK can activate AC directly and is frequently used in pharmacology to investigate cAMP/PKA signaling independent from GPCRs, which gives a maximum increase in cAMP (Insel and Ostrom 2003). In order to investigate whether β_1-ARs stimulation (100 µM NE) can completely activate AC, we measured effects of FSK alone and in the presence of NE (100 µM) in hiPSC-CMs from C-25, cultured in EHT format. FSK (10 µM) increased the ΔFRET ratio significantly. Surprisingly, effects were smaller than with 100 µM NE. On the other hand, adding FSK on top of NE increased FRET to the same extent as in the absence of NE. The analysis of these experiments is illustrated in Fig.29.

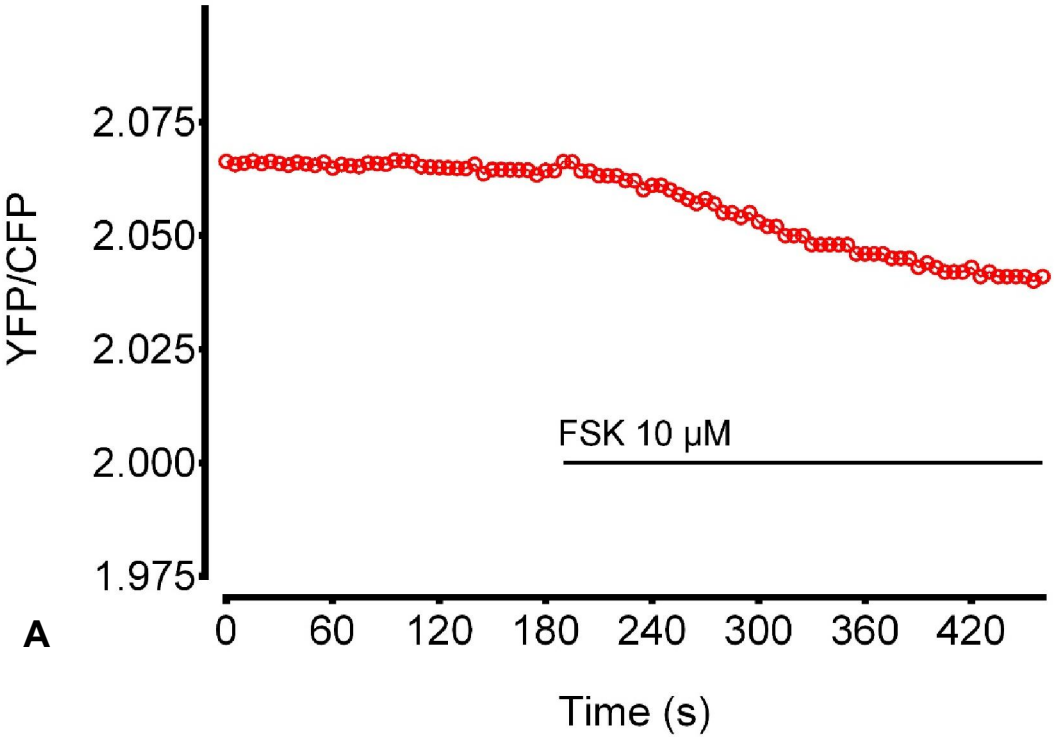

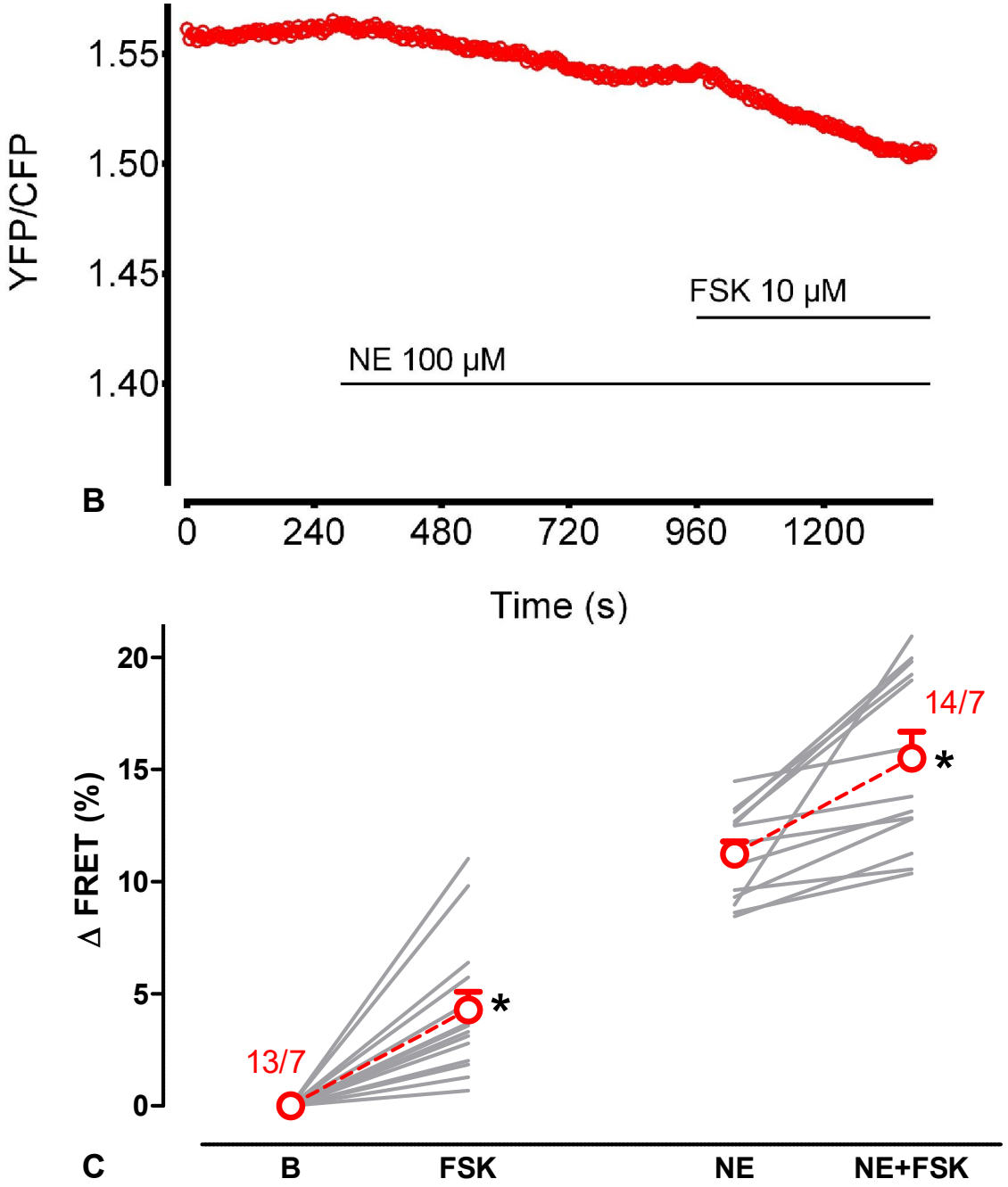

Figure 29: Effect of FSK, alone and in presence of NE on cAMP in isolated hiPSC-CMs cultured in EHT format (C-25)

Representative time and response course of FRET change in an isolated hiPSC-CM, C-25 cell line cultured in EHT, after exposure to FSK (10 µM) alone **(A).** Representative Time course of FRET change in an isolated hiPSC-CM, C-25 cell line cultured in EHT, after exposure to FSK (10 µM) in the presence of NE (100 µM) **(B)**. Mean values±SEM for cAMP increase in individual hiPSC-CM exposed to FSK (10 µM) alone and in the presence of NE (100 µM). Every line indicates a single cell experiment. * indicates $P < 0.05$ vs. basal and pretreated with NE (100 µM) **(C)**.

3.1.1.4 Effect of PDEs on NE-evoked cAMP in hiPSC-CMs (C-25)

In both ML (C-25) and EHT (C-25) the increase in $I_{Ca,L}$ through addition of rolipram (PDE4 inhibitor) is larger than through addition of cilostamide (PDE3 inhibitor) (Ismaili et al., 2019). In ML (C-25) NE effects on $I_{Ca,L}$ were very small, however they could be increased by inhibition of PDE4 but not by inhibition of PDE3 (Ismaili et al., 2019). The same observation holds true regarding force (Saleem et al., 2020). Therefore we investigated whether effects of inhibition of PDE3 or PDE4 on NE-evoked $I_{Ca,L}$ can be explained by the effects of inhibition of PDE3 or PDE4 on NE-evoked cAMP. For this purpose, the effects of two concentrations of NE on cAMP in the presence and absence of inhibitors of PDE3 or PDE4 were measured. First, the results for ML (C-25) are shown in the following paragraph.

3.1.1.5 Effects of PDE3 inhibition on cAMP in hiPSC-CMs cultured in ML format (C-25)

HiPSC-CMs were first exposed to 300 nM cilostamide and then in the continuous presence of cilostamide to two concentrations of NE (1 µM and 100 µM, cumulatively). Cilostamide alone increased the cAMP FRET ratio by 3±0.2%. Responses to NE (both at 1 µM and 100 µM) were additive to the cAMP response to cilostamide, giving the impression that the concentration response-curve for NE was shifted horizontally (Fig.30). Accordingly, E_{max} for 100 µM NE was significantly increased by cilostamide as compared to 100µM NE alone (12.7±0.5% vs 9.2±0.7% NE (100 µM) alone).

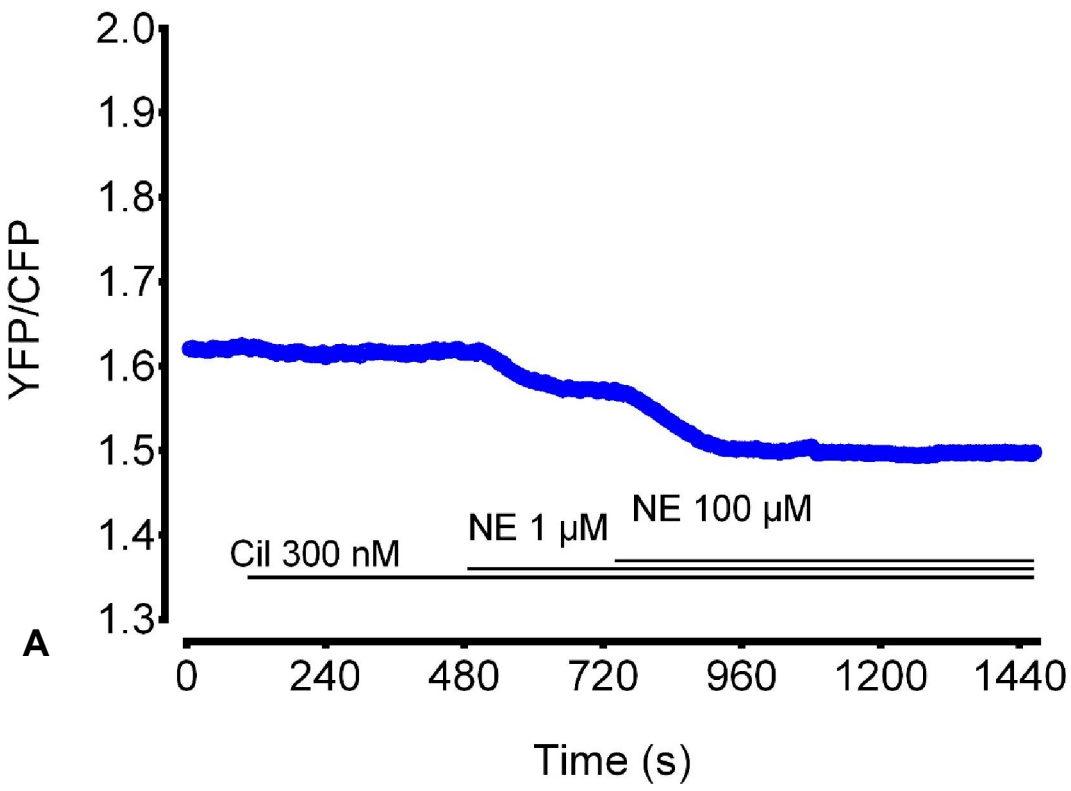

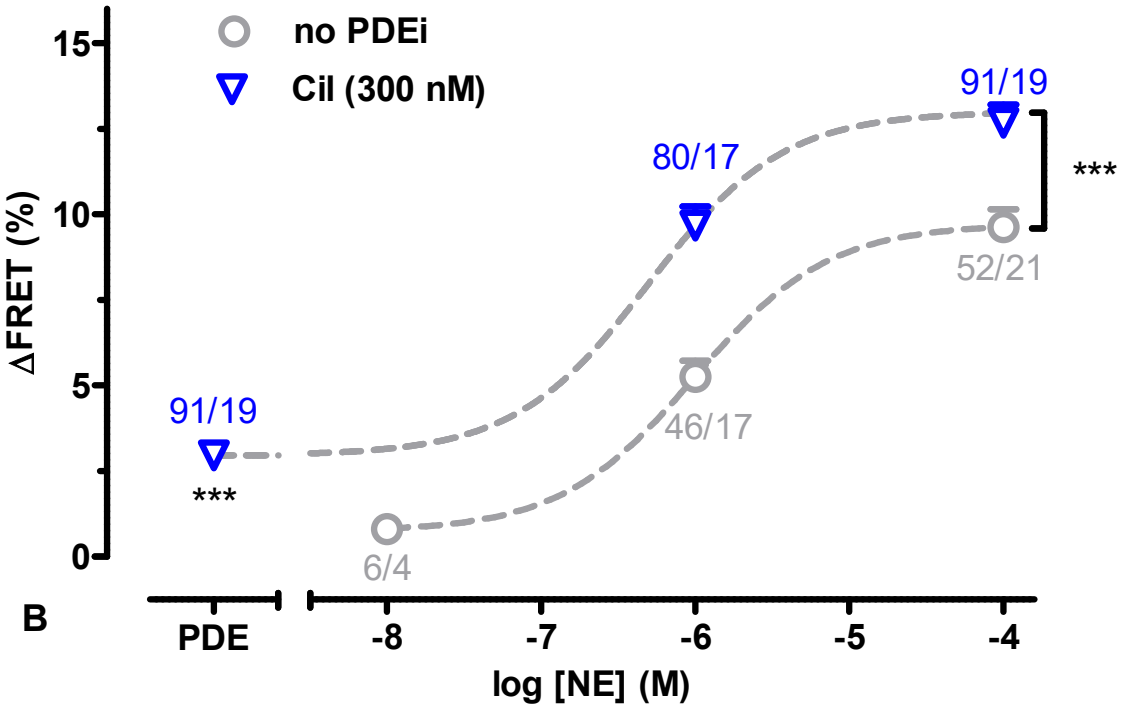

Figure 30: Effect of selective inhibition of PDE3 by cilostamide on basal cAMP and NE-induced cAMP in hiPSC-CMs cultured in ML format (C-25)
Time course of the FRET signal indicating a change in global cAMP after cilostamide (300 nM) and NE (near EC_{50} and E_{max}) addition in the presence of cilostamide (300 nM) in hiPSC-CMs C-25 cultured in ML format **(A).** Mean values±SEM of ΔFRET (%) increase by NE (1 µM and 100 µM) in the presence of cilostamide in hiPSC-CMs cultured in ML format vs treated with cilostamide alone. ** indicates P < 0.01 vs. pretreated with cilostamide. Data for control experiments have been taken from Fig.27 **(B)**.

3.1.1.6 Effects of inhibition of PDE4 on cAMP in hiPSC-CMs cultured in ML format C-25

To measure the effect of PDE4 on cAMP in hiPSC-CMs cultured in ML format (C-25) we used the same protocol as for PDE3 but treated cells with 10 µM rolipram. The effect size of 10 µM rolipram on basal cAMP was almost equal compared to the effect of 300 nM cilostamide (3.4±0.2% vs 3±0.2%). However, ΔFRET ratio response by 100 µM NE was larger in the presence of rolipram than in the presence of cilostamide (15.7±0.8% vs 12.7±0.5%). These results indicate that inhibition of PDE4 and PDE3 has similar control on basal cAMP in hiPSC-CMs from C-25 cultured in ML format but PDE4 predominantly regulates cAMP generated by β_1-ARs stimulation (Fig. 31).

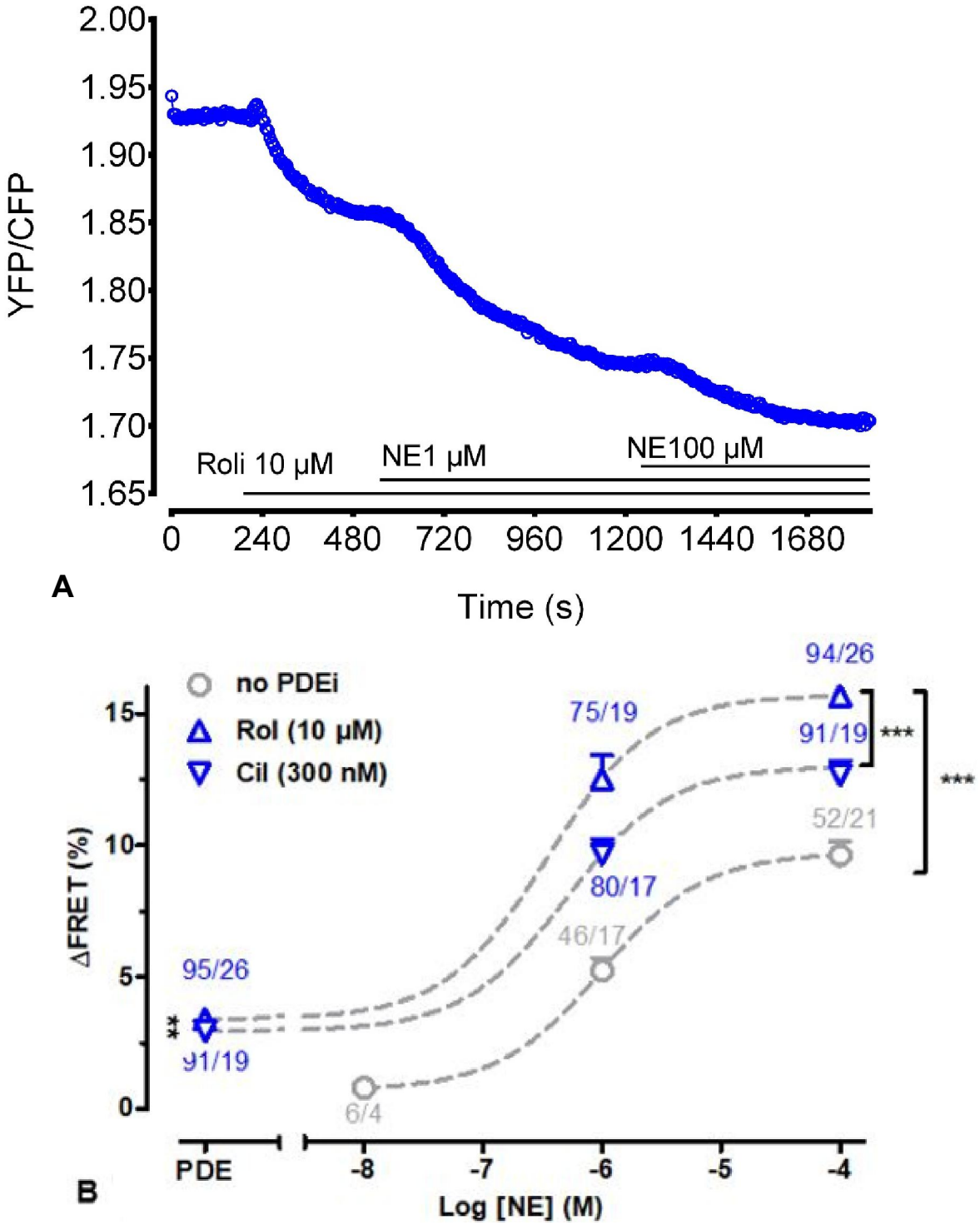

Figure 31: Effect of selective inhibition of PDE4 by rolipram on basal cAMP and NE-induced cAMP in hiPSC-CMs cultured in ML format (C-25)

Time and response course of the FRET signal indicating a change in global cAMP after rolipram (10 µM) and NE (near EC_{50} and E_{max}) in the presence of rolipram (10 µM) in hiPSC-CMs cultured in ML format **(A).**Mean values±SEM of ΔFRET (%) increase by NE (1 µM and 100 µM) in hiPSC-CM pretreated with rolipram.** indicates $P < 0.01$ vs treated with rolipram. Data for control and in the presence of cilostamide have been taken from Fig.27 and Fig.30 respectively **(B)**.

3.1.1.7 Effects of inhibition of PDE4 on cAMP in hiPSC-CMs cultured in EHT format (C-25)

Inhibition of PDE4 by rolipram (10 µM) in the absence of NE also increased ΔFRET ratio in hiPSC-CMs from C-25 cultured in EHT format, as seen before in ML (C-25). The effect size of PDE4 Inhibition on basal cAMP (4.2±0.4%) in EHT format was clearly larger than ML Format (3.4±0.2%). But surprisingly the FRET responses to NE (1 µM and 100 µM) in the presence of rolipram (10 µM) were not affected in hiPSC-CMS from EHT. In contrast to the findings of ML, there was no augmentation of the effects of 100 µM NE by inhibition of PDE4 (Fig.32).

3.1.1.8 Effects of inhibition of PDE3 on cAMP in hiPSC-CMs cultured in EHT format (C-25)

In contrast to ML (C-25) inhibition of PDE3 by cilostamide (300 nM) increased ΔFRET ratio (%) by a smaller magnitude in the absence of NE (1.6±0.2 vs 3±0.2%). Furthermore, the presence of cilostamide appeared to suppress FRET responses to NE (both at 1 µM and 100 µM). Results are compared in (Fig.33 B) as an effect size of 100 µM NE (9.2±0.7 vs 12.1±0.3%) in the presence of cilostamide vs in the absence of cilostamide.

3.1.1.9 Effects of inhibition of PDE2 on cAMP in hiPSC-CMs cultured in EHT format (C-25)

The suppression of NE responses by inhibition of PDE3 was unexpected and suggested the activation of hydrolytic activity of other PDEs. PDE3 is a dual substrate PDE, which hydrolyzes both cAMP and cGMP. Therefore cGMP is expected to increase by inhibition of PDE3 and could activate cGMP-regulated PDEs. One of these cGMP-activated PDEs is PDE2. Therefore, we measured the impact of PDE2 on NE-induced cAMP in the presence of cilostamide (Fig.34). Like cilostamide, the PDE2 inhibitor Bay 60-7550 alone had a very small effect on ΔFRET (1.5±0.3%), but both agents give simultaneously increased ΔFRET (%) to a comparable extent that of rolipram (3.2±0.5%). Effects of 100 µM NE in the presence of cilostamide were definitely not changed by Bay 60-7550 (8±1.0%).

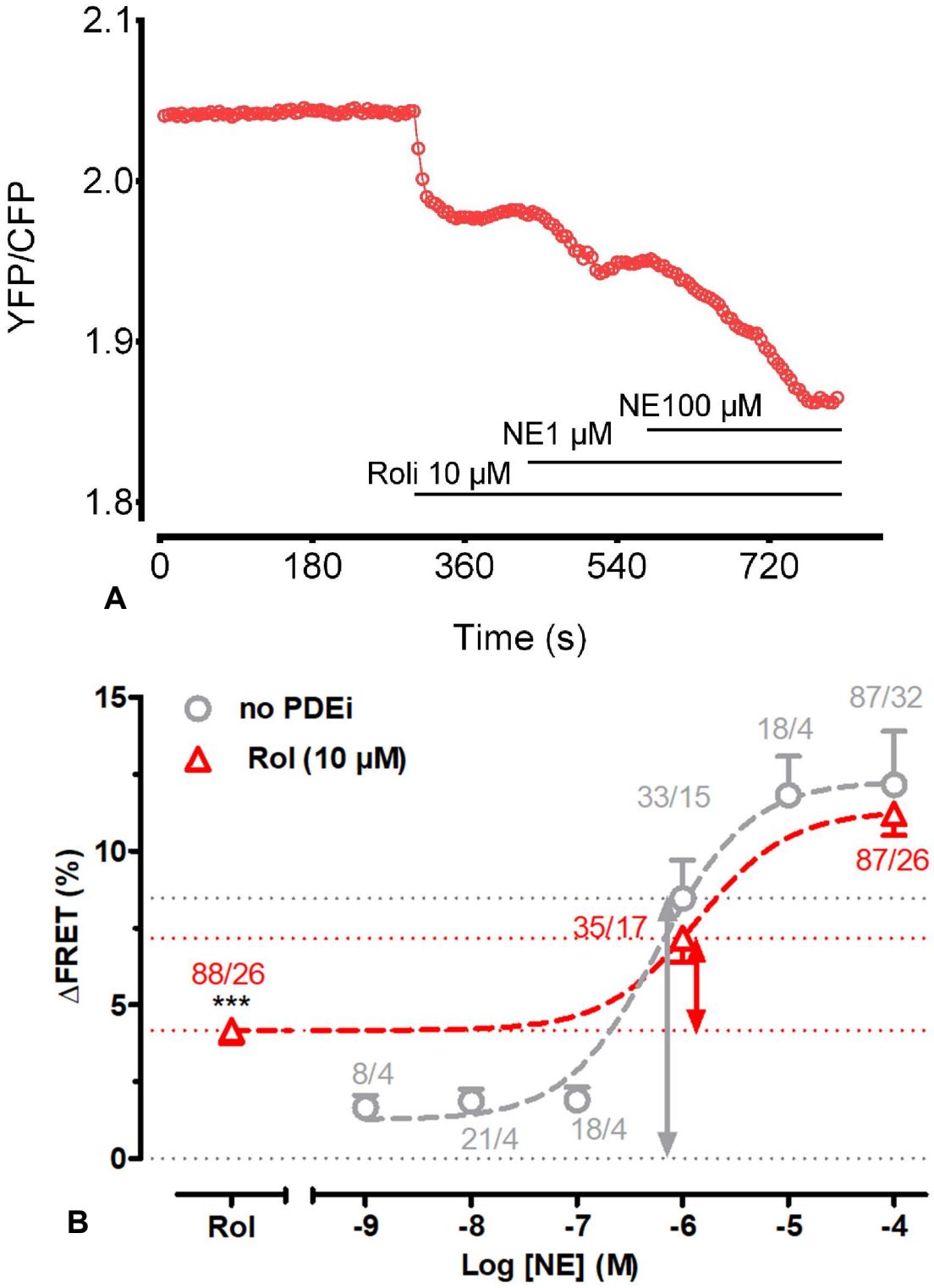

Figure 32: Impact of selective inhibition of PDE4 by rolipram on basal cAMP and NE-induced cAMP in hiPSC-CMs cultured in EHT format (C-25)

Time and response course of FRET signal indicating a change in global cAMP after rolipram (10 µM) and NE (near EC_{50} and E_{max}) in the presence of rolipram (10 µM) in hiPSC-CMs cultured in EHT format **(A).** Mean values±SEM of FRET increase by NE (1 µM and 100 µM) in hiPSC- CMs treated with rolipram. *** indicates P < 0.001 vs only rolipram **(B)**. Data for control experiments was taken from Fig.28.

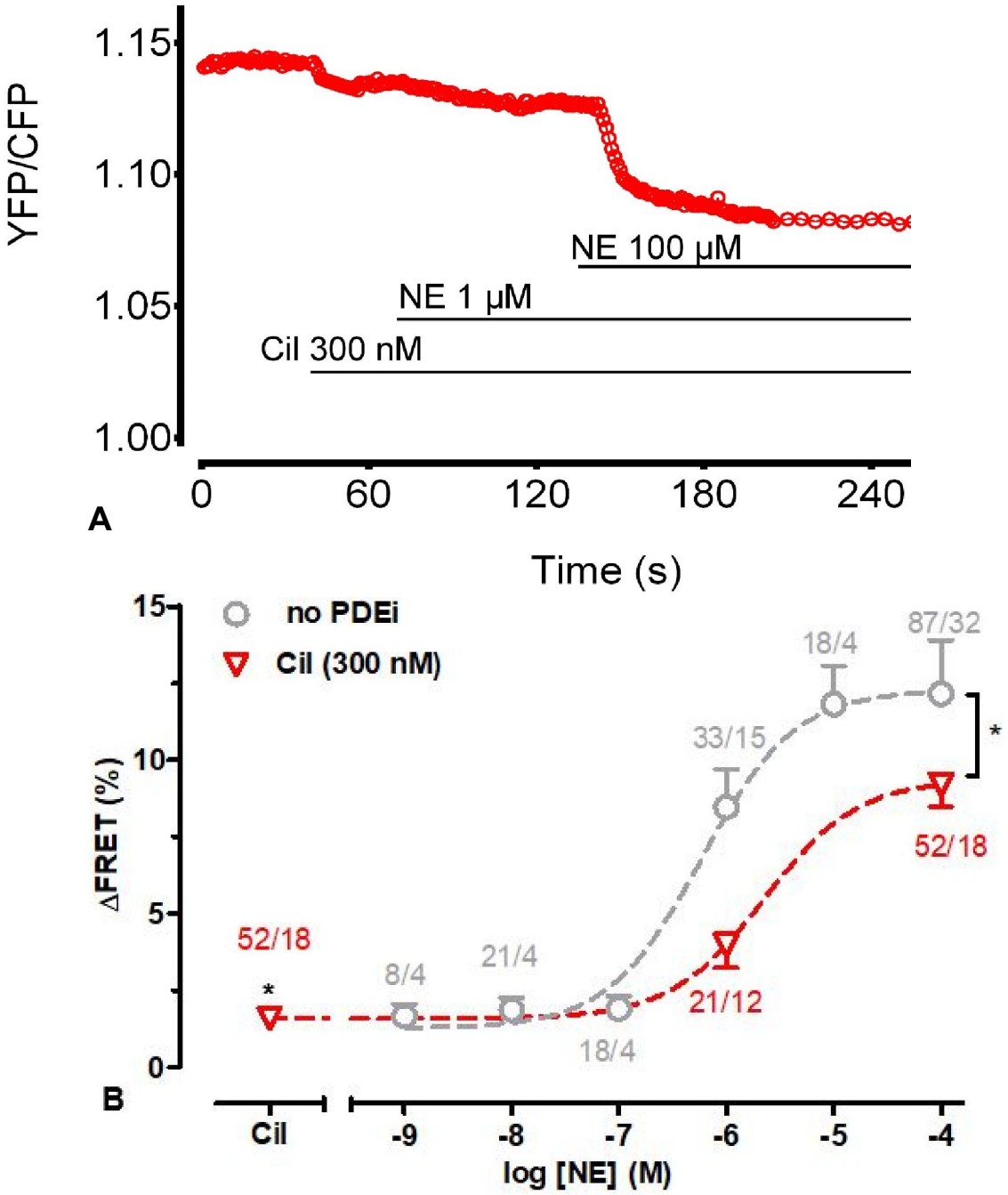

Figure 33: Effect of selective inhibition of PDE3 by cilostamide on basal and NE-activated cAMP in hiPSC-CMs cultured in EHT format

Time and response course of the FRET signal indicating a change in global cAMP after cilostamide (300 nM) and NE (near EC_{50} and E_{max}) in the presence of cilostamide (300 nM) in hiPSC-CMs cultured in EHT format **(A)**.Mean values±SEM of FRET change by NE (1 µM and 100 µM) in hiPSC-CMs pretreated with cilostamide on cAMP in hiPSC-CMs vs cilostamide alone. * indicates $P < 0.05$ vs treated with cilostamide. Data of control experiments have been taken from Fig.28 **(B).**

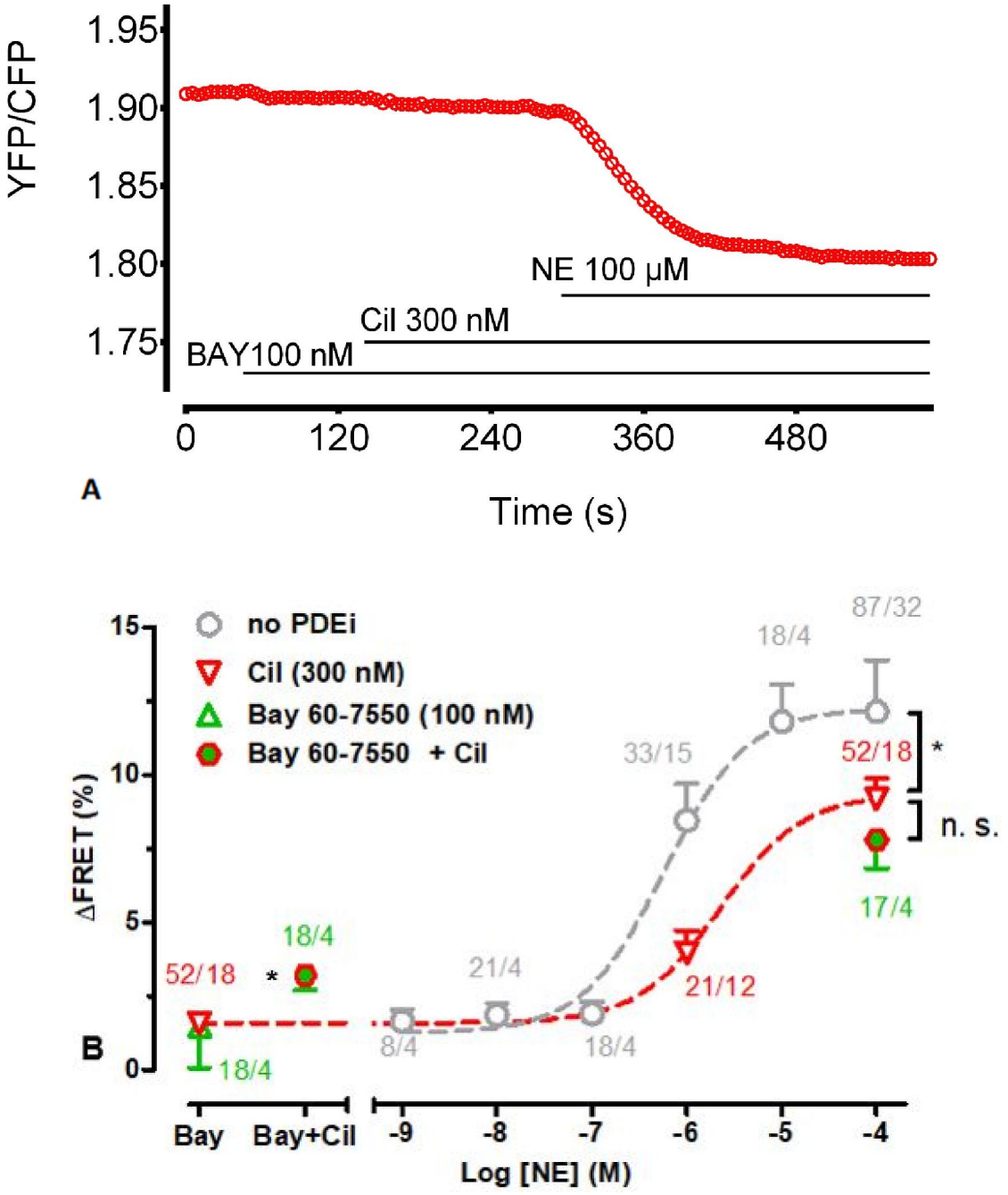

Figure 34: Impact of concomitant inhibition of PDE2 and PDE3 on cAMP evoked by NE
Time and response course of change in FRET ratio indicating a change in global cAMP after Bay 60-7550 (100 nM), cilostamide (300 nM) and NE (100 µM) in the presence of Bay (100nM) and cilostamide (300nM) in hiPSC-CMs cultured in EHT format **(A).** Mean±SEM of ΔFRET change evoked by inhibition of PDE2 alone (Bay 60-7550), by inhibition of PDE2 and PDE3 (Bay+Cil) and NE in the presence the concomitant inhibition of PDE2 and PDE3 with green colour. Data for control experiments and for inhibition of PDE3 are taken from Fig. 28 and Fig.33 respectively. * indicates $p<0.05$ vs. effects by NE (100 µM) without cilostamide **(B)**.

3.1.1.10 Effects of inhibition of PDE11 on cAMP in hiPSC-CMs from cell line C-25 cultured in EHT format

The suppressed NE-induced ΔFRET ratio (%) in the presence of cilostamide cannot be explained by PDE2 activity (Fig.34). To investigate whether other cGMP-activated PDEs could be involved in the suppression of NE-induced ΔFRET ratio (%) by cilostamide, we tried to inhibit PDE11. Selective inhibitors of PDE11 are not available. Therefore we used very high concentrations of tadalafil (1 µM) a compound often used to inhibit PDE5 (Fig.35). Different groups have reported selectivity of tadalafil for PDE5 over PDE11 such as 5 fold (Gbekor et al., 2002) and 6.7 fold (Saenz et al., 2002). Like Bay 60-7550, tadalafil alone did not have significant effect on ΔFRET (1.4±0.3%), but tadalafil (1 µM), when given simultaneously with cilostamide, increased ΔFRET (%) to the same extent as rolipram (4.3±0.7%). Interestingly, the effect of 100 µM NE in the presence of cilostamide was no longer suppressed in the presence of (1µM) tadalafil (12.1±1.8 vs 12.1±0.3% control).

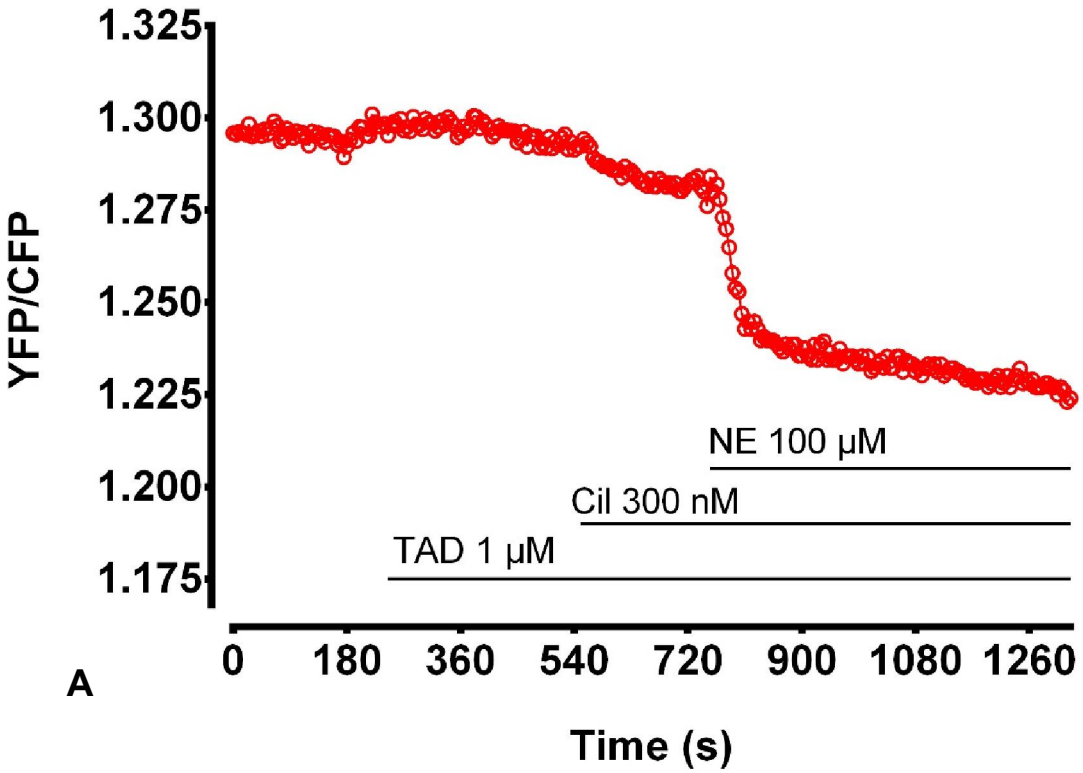

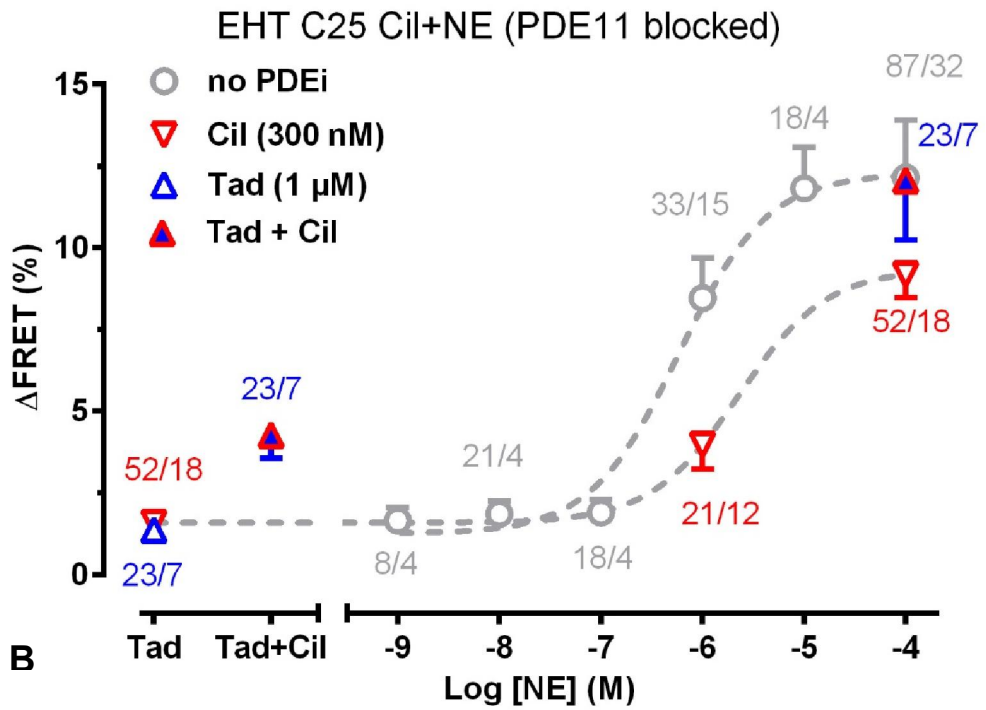

Figure 35: Impact of concomitant inhibition of PDE11 and PDE3 on FRET increased by NE
Time and response course of change in FRET ratio indicating a change in global cAMP after tadalafil (1 µM), cilostamide (300 nM) and NE (100 µM) in the presence of tadalafil (1µM) and cilostamide (300nM) in hiPSC-CMs cultured in EHT format **(A).** Mean±SEM of ΔFRET change evoked by inhibition of PDE11 alone (tadalafil), by inhibition of PDE11 and PDE3 (Tad+Cil) and NE in the presence of the concomitant inhibition of PDE11 and PDE3. Data for control experiments and inhibition of PDE3 are taken from Fig.28 and Fig.33 respectively. * indicates $p<0.05$ vs. effects by NE (100 µM) without cilostamide **(B)**.

This result suggests that cilostamide has suppressed NE-evoked increase in ΔFRET by the activation of PDE11 consequently. Hence, it appears that activation of PDE11 by cGMP generated by inhibition of PDE3 leads to the suppression of NE-evoked cAMP by PDE11. If this observation holds true, then the effect of inhibition of PDE11 on NE-induced ΔFRET should be larger in the presence than in the absence of cilostamide. To verify this hypothesis the effects of tadalafil on the NE-evoked increase in ΔFRET (%) in cells pretreated with cilostamide as well as in the absence of cilostamide were measured. Cells were randomly assigned to the two aforementioned treatment conditions (cilostamide and controls). Mean values were calculated for every experimental day, allowing paired statistics and increasing statistical power. By using this paired approach, we could confirm the suppression of the NE effect on cAMP levels by cilostamide (Fig.36 A).

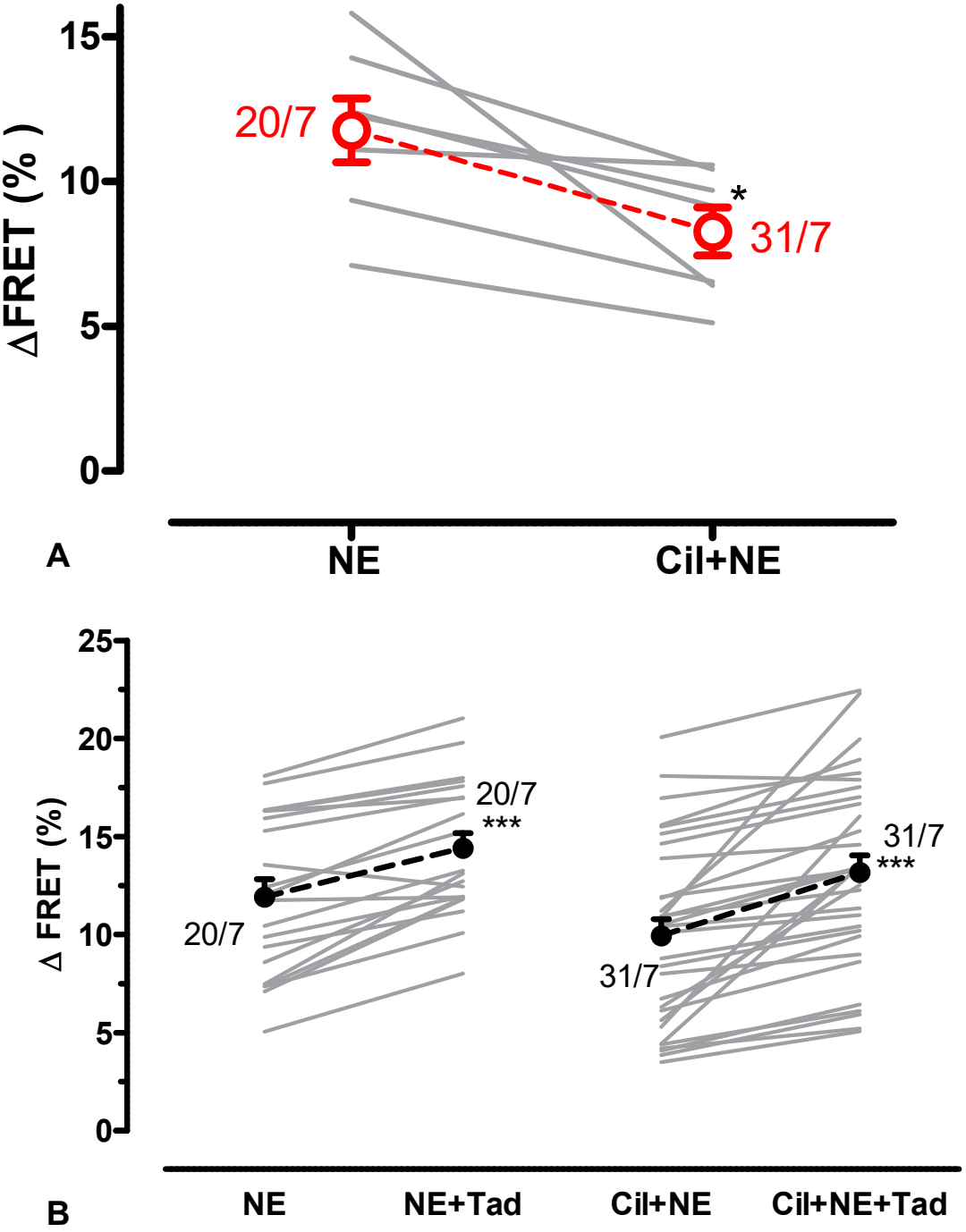

Figure 36: Comparison of effects on hiPSC-CMs, paired (Cil+NE vs. NE) or as Tad effect on Cil+NE vs. NE alone

Mean values±SEM for cAMP increase in individual hiPSC-CMs exposed to NE (100 µM) alone and in the presence of cilostamide (300 nM). Every line indicates a single cell. * indicates $P < 0.05$ vs. NE (100 µM) and with NE (100 µM) in the presence of cilostamide (300 nM (**A**). Mean values±SEM for cAMP increase in individual hiPSC-CMs exposed to NE (100 µM) + cilostamide (300 nM) and tadalafil (1 µM) in the presence of Cil+NE. Every line indicates a single cell. *** indicates $P < 0.001$ vs. NE (100 µM) and with NE (100 µM) in the presence of cilostamide (300 nM (**B**).

We found suppression of NE-induced cAMP by cilostamide could be overcome when tadalafil (1 µM) was given on top of NE in the presence of cilostamide. The resulting ΔFRET ratio signals were quite similar as pretreatment with tadalafil was able to completely reverse the suppression of NE-induced cAMP by cilostamide. However, the ΔFRET generated by tadalafil on top of NE was not larger in cells pre-treated with cilostamide compared to cells not treated with cilostamide (Fig.36 B). The findings of this new set of experiments argued against the contribution of PDE11 to the suppression of NE-induced ΔFRET (%) in the presence of cilostamide.

3.1.2 Effects of NE on cAMP in hiPSC-CMs (C-25) transduced with a sarcolemmal biosensor

The results with the global cAMP biosensor, indicate that a smaller cAMP increase by maximum concentrations of NE (100 µM) can be expected in isolated hiPSC-CMs from ML in comparison to hiPSC-CMs from the EHT format. It is known that cAMP is highly compartmentalized and concentrated close to its effectors rather than globally. Local rather than global cAMP is relevant for many of its physiological effects. The activation of individual effectors is hard to measure, since they act in a concerted manner. For the presented work recently obtained through Ca^{2+} channel measurements in C-25 (both from ML and EHT) served as reference. Therefore, we have used a cAMP sensor that is preferentially expressed in the sarcolemma and should monitor cAMP relevant for Ca^{2+} channels. Cells could be robustly transduced with the sarcolemmal (SL) biosensor (compare section methods). All cells expressing the SL sensor showed a clear increase in the ΔFRET ratio when exposed to NE. Surprisingly, the amount of increase in the ΔFRET ratio (%) measured by the SL sensor was not different between ML and EHT for both NE and FSK on top of NE. As Fig.37 describes the average increase in ΔFRET ratio (%) by 100 µM NE in hiPSC-CMs cultured in ML was 9.3±0.7% while in hiPSC-CMs cultured in EHT format it was 10.1±0.9%).

3.1.2.1 Effects of inhibition of PDE3 and PDE4 on cAMP in hiPSC-CMs, (C-25) cultured in ML format, transduced with SL biosensor

In ML the inhibition of PDE3 or PDE4 increased both global cAMP and cAMP in the SL compartment. Inhibition of PDE3 increased global basal cAMP more than basal cAMP in the SL compartment. (3±0.2 vs 1.7±0.3 %) while inhibition of PDE4 increased cAMP in the SL compartment more than global basal cAMP (4.2±0.4 vs 3.4±0.2).

The effect size for inhibition of PDE4 alone was 20% larger in the SL region near to LTCC than in global cAMP measurements, but a significantly smaller effect size was seen with inhibition of PDE3 in the SL compartment than in the global compartment. It is clear in both compartments that a basal cloud of cAMP is predominantly regulated by PDE4 in hiPSC-CMs cultured in the ML format (C-25).

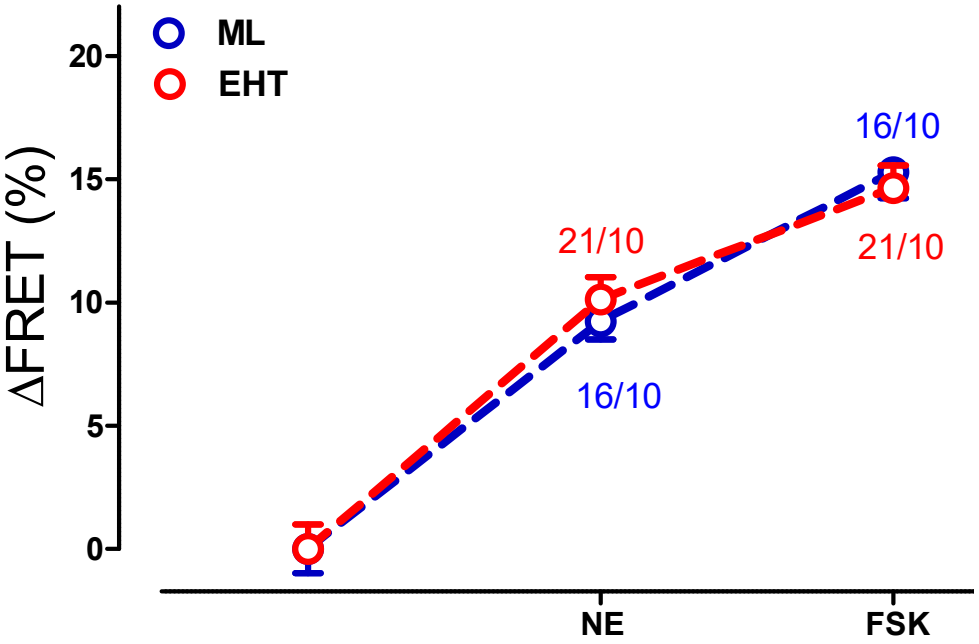

Figure 37: Effect of NE on cAMP in the SL compartment in isolated hiPSC-CMs cultured in ML format and EHT format
Mean values±SEM for cAMP increase in individual EHT (C-25) hiPSC-CM and ML (C-25) hiPSC-CM exposed to NE (100 µM) alone and FSK (10 µM) in the presence of NE (100 µM).

Next, the effect of inhibition of PDE3 and PDE4 on cAMP evoked by NE (100 µM) in hiPSC-CMs transduced with the SL biosensor was measured (Fig. 38). The measurement was performed in the same manner as the measurement in hiPSC-CMs transduced with the global biosensor. The FRET ratio response was larger in the concomitant presence of rolipram and NE vs. NE alone in both the global and SL compartment (globally; 15.7±0.8 vs 9.6±0.5% and SL; 11.5±0.5 vs 9.2±0.7%). While in the presence of cilostamide NE-induced cAMP was increased in global (12.7±0.5 vs 9.6±0.5%) but not SL compartment (8.2±0 7.vs 9.2±0.7%).

3.1.2.2 Effects of inhibition of PDE3 and PDE4 on cAMP in hiPSC-CMs, (C-25) cultured in EHT format, transduced with the SL biosensor

In hiPSC-CMs isolated from EHT, inhibition of PDE3 or PDE4 increased both global cAMP and cAMP in the SL compartment (Fig. 39).

Inhibition of PDE3 was found to increase basal cAMP (2.6±0.6 vs 1.6±0.2%) more strongly in cells with the SL vs the global biosensor and PDE4 inhibition increased basal cAMP (4.7±0.5 vs 4.2±0.4%) in cells with the SL vs the global biosensor.

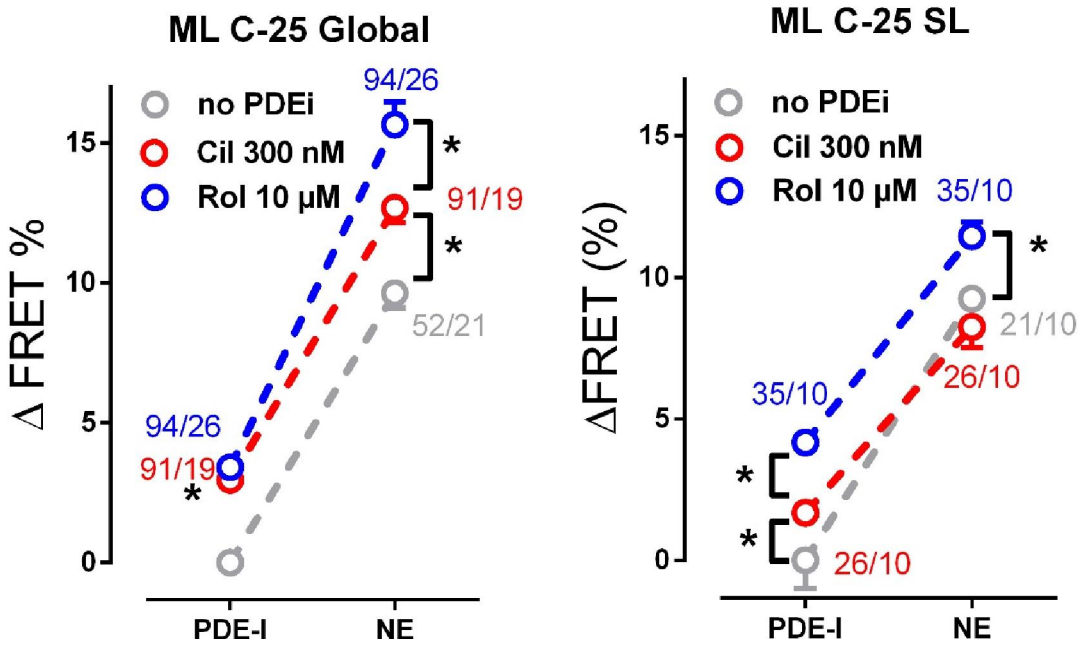

Figure 38: Effects of inhibition of PDE3 or PDE4 on NE-induced cAMP in an isolated hiPSC-CM (cultured in ML format) expressing global and SL biosensor
Mean values±SEM of FRET change by NE (100 µM) alone in hiPSC-CMs and NE (100 µM) in the presence of cilostamide (300 nM) or rolipram (10 µM) in hiPSC-CMs. * indicates P < 0.05 vs. pre-treatment with cilostamide or rolipram.

The effect size for PDE inhibition in the SL compartment alone was significantly smaller for cilostamide vs. rolipram (2.7±0.6 vs 4.7±0.5%), which also holds true in the global compartment. Again this finding confirms dominance of PDE4 vs PDE3 to regulate the basal level of cAMP in hiPSC-CMs (C-25) cultured in EHT format.

Next, the effect of inhibition of PDE3 and PDE4 on cAMP evoked by NE (100 µM) in isolated hiPSC-CMs transduced with the SL biosensor was measured in the same manner in isolated hiPSC-CMs transduced with the global biosensor. The cAMP increase during the concomitant presence of rolipram and NE vs. NE alone was almost not affected when measured in the global compartment but was larger in SL compartment (globally; 11.2±0.7 vs 12.1±0.3% and SL; 13.9±0.7 vs 10.1±0.7%). While ΔFRET ratio in the presence of cilostamide and NE was suppressed compared to NE alone in both the global (9.2±0.7 vs 12.1±0.3%) and in the SL compartment (9.0±0.7 vs 10.1±0.9%).

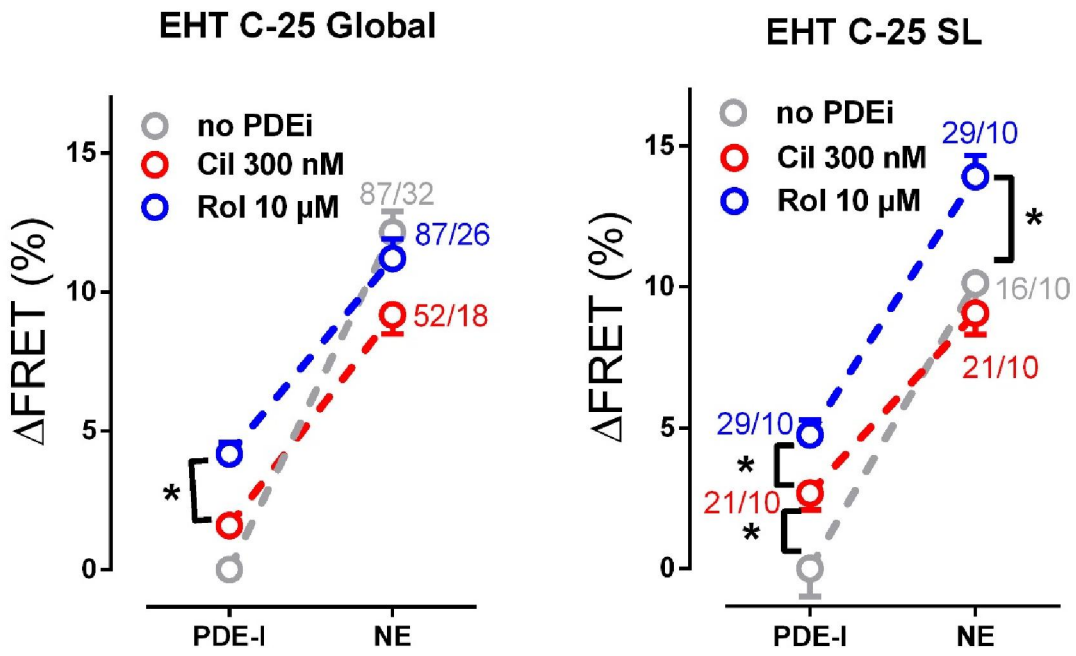

Figure 39: Effects of Inhibition of PDE3 or PDE4 on NE-induced cAMP in an isolated hiPSC-CMs (cultured in EHT format) expressing global and sarcolemmal biosensor
Mean values±SEM of FRET change by NE (100 µM) alone in hiPSC-CM and NE (100 µM) in the presence of cilostamide (300 nM) or rolipram (10 µM) in hiPSC-CMs. * indicates $P < 0.05$ vs. pretreated with cilostamide or rolipram.

3.2 Other cell lines (ERC-01 and ERC-18)

3.2.1 Comparison of effects of NE on cAMP in hiPSC-CMs from different cell lines (C-25; ERC-01; ERC-18) transduced by global biosensor

Next, we investigated hiPSC-CMs from two other cell lines both cultured in EHT format. Both cell lines were generated in the house. HiPSC were obtained from two people who are healthy controls and were used within the ERC project performed at the UKE Hamburg Eppendorf, for comparison. As seen before in the C-25 cell line every hiPSC-CM showed a clear increase in ΔFRET upon exposure to 100 µM NE (Fig. 40). The magnitude of the increase was not different in ERC-18 vs. C-25 (12.6±0.4 vs 12.1±0.3%), but significantly smaller in ERC-01 (9.2±0.8 vs 12.1±0.3%).

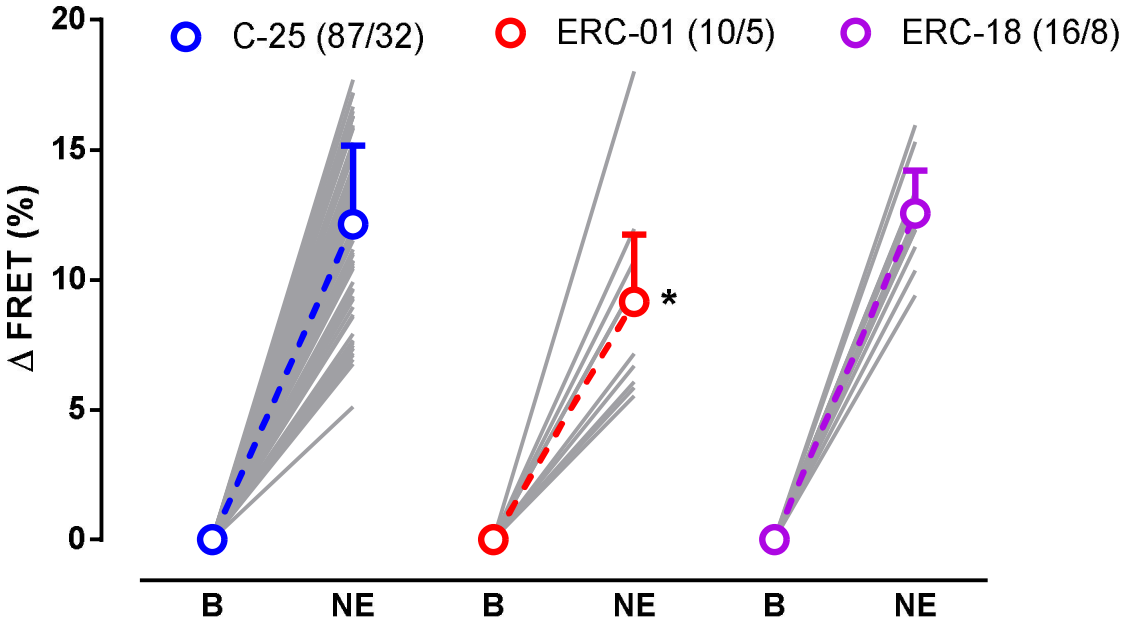

Figure 40: Effects of NE on cAMP increase in isolated hiPSC-CMs from three cell lines cultured in EHT format expressing a global cAMP sensor

Mean values±SEM for cAMP increases in isolated hiPSC-CMs exposed to NE (100 µM). Every line indicates a single cell in an individual experiment.

3.2.2 Comparison of effects of inhibition of PDE3 and PDE4 on global cAMP in hiPSC-CMs from different cell lines(C-25; ERC-01; ERC-18)

As seen from the previous experiments in C-25 (1.6±0.2 vs 4.2±0.4%), hiPSC-CMs cultured in EHT format from ERC-01 (0.9±0.3 vs 4.8±0.6%) and ERC-18 (2.5±0.6 vs 4.6±0.6%) showed smaller effects on basal cAMP with inhibition of PDE3 than inhibition of PDE4.

In strong contrast to C-25 (9.2±0.7 vs 12.1±0.3%), inhibition of PDE3 did not suppress cAMP response to NE in both ERC-01 (10.9±0.8 vs 9.2±0.8%) and ERC-18 (16.7±1.1 vs 12.6±0.4%). In all three cell lines the increase in cAMP FRET response was larger in the presence of rolipram and NE compared to NE alone.

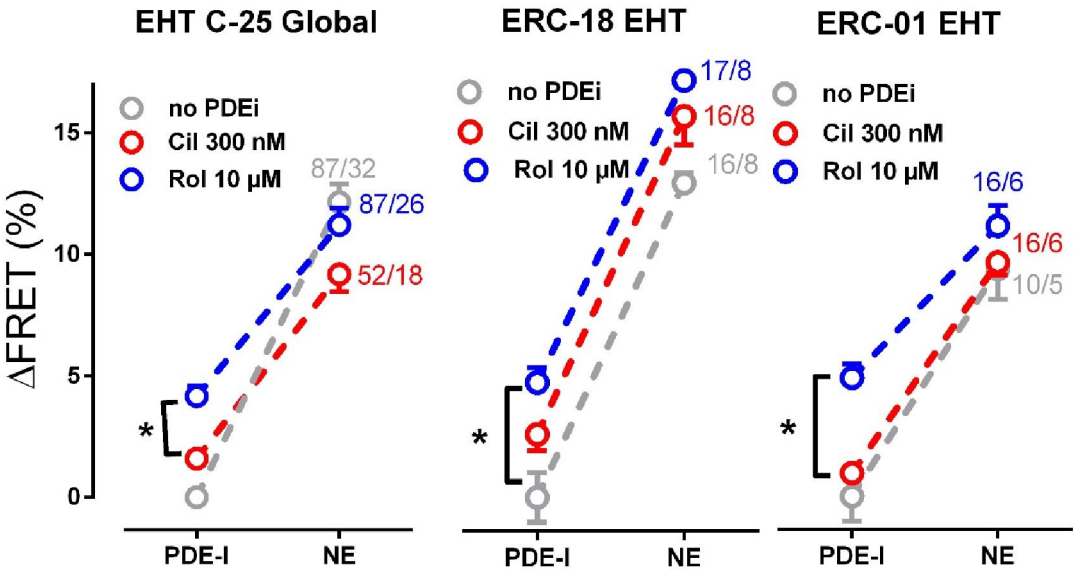

Figure 41: Effects of Inhibition of PDE3 or PDE4 on NE-induced cAMP in isolated hiPSC-CMs from three cell lines (cultured in EHT format) expressing a global cAMP sensor
Mean values±SEM of FRET change by NE (100 µM) alone in hiPSC-CMs and NE (100 µM) in the presence of cilostamide (300 nM) or rolipram (10 µM) in hiPSC-CMs. * indicates $P < 0.05$ vs. pretreated with cilostamide or rolipram.

3.3 Relationship between FSK and NE-induced cAMP in the presence or absence of Inhibition of PDE3 or PDE4 on isolated hiPSC-CM from three cell lines expressing a global cAMP biosensor

Physiologically AC is stimulated by activation of membrane receptors. FSK is frequently used to activate AC directly (Seamon et al., 1981; Dessauer et al., 2017; Jurevičius and Fischmeister., 1996). In Fig. 29 we have seen that FSK alone evokes smaller cAMP increase than β-AR stimulation with NE (100 µM).

To investigate whether the small increases of cAMP by NE stimulation are due to incomplete activation of AC, FSK was added on top of 100 µM NE in most experiments. If NE activates AC only weakly in individual cells one would expect larger increases of cAMP by adding FSK on top of NE in these cells.

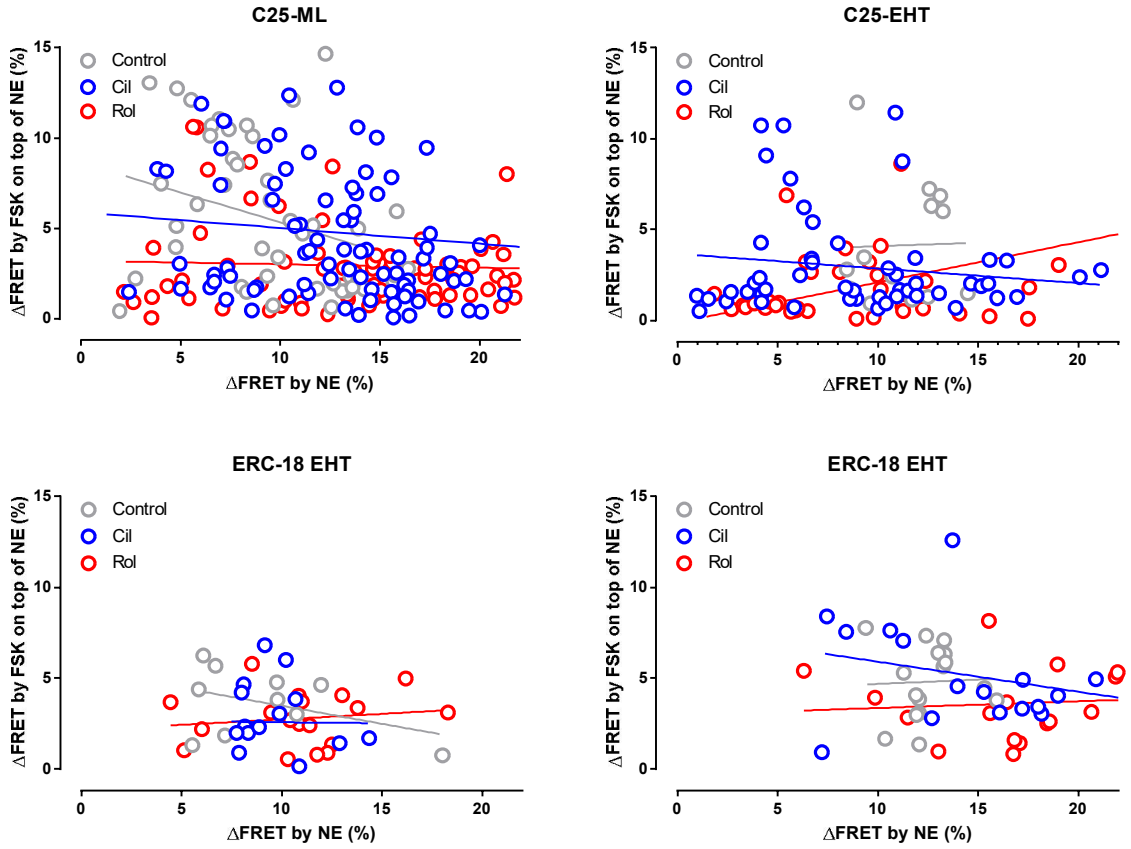

Figure 42: Relationship between cAMP induced by NE alone and cAMP induced by FSK and NE-induced in presence or absence of inhibition of PDE3 or PDE4 on isolated hiPSC-CMs from three cell lines expressing a global cAMP biosensor
Mean values±SEM of FRET change by NE (100 µM) alone in hiPSC-CM, NE (100 µM) in the presence of cilostamide (300 nM) or rolipram (10 µM) in hiPSC-CM and FSK on the top of NE alone and NE in the presence of PDE3/PDE4 inhibition

Therefore we have plotted cAMP increases by NE vs. FSK (FSK-NE) in individual cells. All cells showed a further increase in FRET after FSK was given on top of NE. However, in all three cell lines the effect size of FSK did not depend on the effect size of NE neither in the absence nor in the presence of inhibitors of PDE3 or PDE4, arguing against the assumption that the NE effect is restricted by a limited activation of AC by β-AR in hiPSC-CMs.

4. Discussion

4.1 Potency of catecholamines to increase ΔFRET ratio, $I_{Ca,L}$ and force

There are only a few published reports about the regulation of cAMP by catecholamines in hiPSC-CMs. From the study of Wu et al., 2015 it can be concluded that a single high concentration of the catecholamine ISO (1 µM) can increase the cAMP FRET response significantly in hiPSC-CMs. In another study, several, high concentrations of ISO (100 nM up to 1 mM) were employed to study the regulation of cAMP in hiPSC-CMs from another cell line (Borchert et al., 2017). From these experiments, one can extrapolate the potency of ISO to increase ΔFRET ratio in hiPSC-CMs from other cell lines. The lowest concentration used that gave almost maximal FRET responses in hiPSC-CMs from a healthy donor was 100 nM ISO. There was a non-significant trend of larger FRET responses with concentrations of ISO higher than 100 nM in the Borchert et al. experiments. In general, a 30 times higher potency of ISO vs. NE at β_1-ARs has to be expected as was established by another research group (Hoffmann et al., 2004). Apart from this, we have to expect that in our experiments 50 nM ICI-118,551 shifted the concentration-response curve at β_1-ARs by about 0.3 log units to the right (Pecha et al., 2015). So, it should be noted that the net difference between ISO in the absence of any antagonist vs. NE in the presence of 50 nM ICI-188, 551 should be around two log units. For this reason, 100 nM ISO should be equipotent to 10 µM NE in the presence of ICI-118, 551. In our experiments, 10 µM NE (in the presence of 50 nM ICI-118, 551) gave almost maximal FRET responses (Fig.28 and Fig.43). The comparison of cAMP FRET data presented in this thesis to the above-mentioned data (Wu et al., 2015; Borchert et al., 2017) critically depends upon the assumption that the trend of lower FRET responses with 100 nM NE compared to 1 µM NE can be interpreted as a concentration-dependent difference. No further FRET data on the cAMP increase upon β_1-AR stimulation in hiPSC-CMs are available.

$I_{Ca,L}$ is one of the many targets regulated by cAMP. As was shown in the past, using the same cell line and EHT format used in this thesis, NE increased $I_{Ca,L}$ substantially in isolated hiPSC-CMs (Uzun et al., 2016). A complete concentration response curve could be constructed for these hiPSC-CMs (Uzun et al., 2016), which allows for a direct comparison of the potency of NE to increase ΔFRET ratio and to increase $I_{Ca,L}$. The EC_{50} for both effects were in the range of 1 µM (Fig.43). Potency of NE to increase ΔFRET (cAMP) tends to be slightly higher than the potency to increase $I_{Ca,L}$. However, the difference did not reach statistical significance. No further data on the potency of agonists at the β_1-ARs to increase $I_{Ca,L}$ in hiPSC-CMs are available.

4. Discussion

Together with the stimulation of $I_{Ca,L}$, the inotropic response seen in hiPSC-CMs may result from activation of several partners in electro-mechanical coupling. The -logEC_{50} value for the positive inotropic effect of ISO in EHTs (cell line C-25) was 8.5 (Saleem et al., 2020).

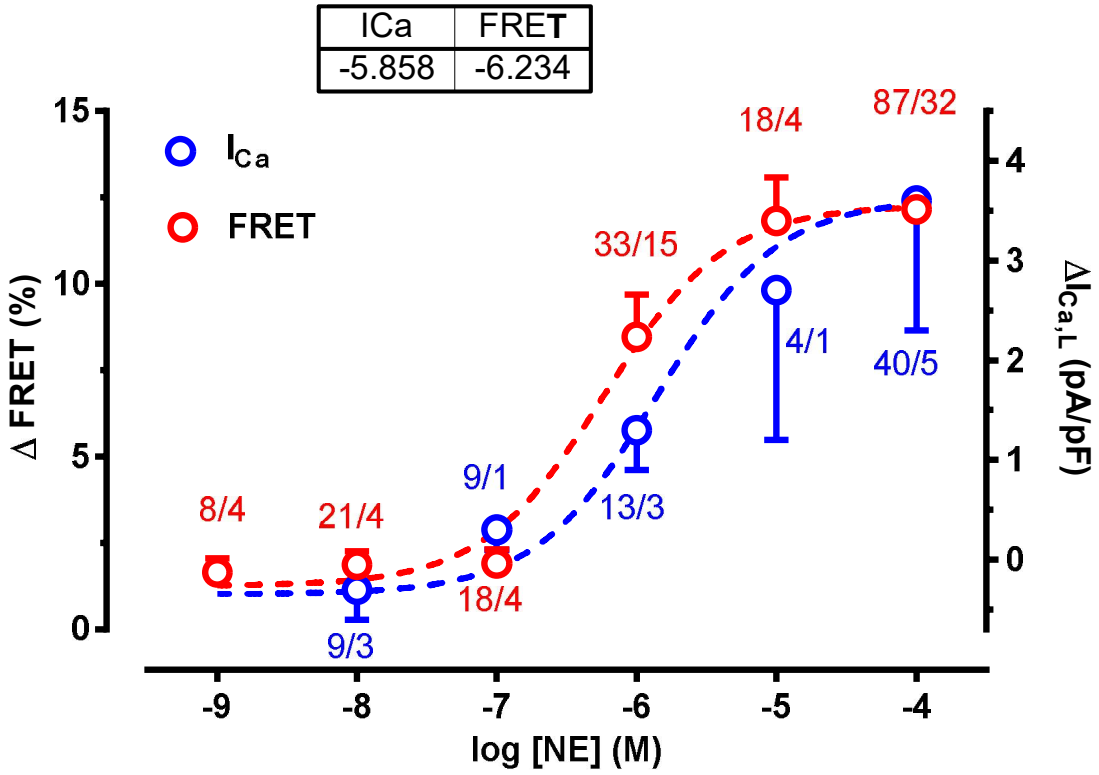

Figure 43: Concentration-response curves for NE on cAMP and $I_{Ca,L}$ in isolated hiPSC-CMs cultured in EHT format
Mean values±SEM of FRET change and on increase in $I_{Ca,L}$ by different concentrations of NE in isolated hiPSC-CMs. Data for FRET are taken from Fig.28, while for $I_{Ca,L}$ from Uzun et al, 2016.

In the study of Borchert et al., 2017 the potency of ISO to increase force in isometric contracting 3D constructs of hiPSC-CMs was 6 nM (–logEC_{50} = 8.2 M). Again we have to account for a two log unit shift when comparing this data to our experimental conditions, predicting an -logEC_{50} for NE to increase force. The resulting -logEC_{50} of ~-6.5 M is close to our results obtained with FRET (6.2 M measured).

In summary, the stimulation of β_1-ARs increases cAMP, $I_{Ca,L}$ and contractility with almost the same sensitivity. This finding is in strong contrast to adult cardiac tissue. As sensitivity to increase force compared to $I_{Ca,L}$ is more than 10 fold higher in human atrial tissue (–logEC_{50} = 7.06±0.03 M vs 5.79±0.15 M) (Christ et al., 2014) and in rat ventricular tissue (–logEC_{50} = 6.88±0.02 M vs 5.95±0.15 M) (Christ et al., 2009). No sensitivity data for cAMP measured as FRET response in human atrial CMs and rat ventricular tissue are available. However, in mice NE potency to increase cAMP measured by FRET is 10 fold lower compared to its inotropic potency (Nikolaev et al., 2006). Therefore the same potency to increase inotropy and cAMP or $I_{Ca,L}$ and force are somewhat unexpected from adult heart tissue.

4.2 Comparing maximum effects of NE on FRET and $I_{Ca,L}$

We saw differences in the maximum effects of NE to increase the cAMP ΔFRET ratio in hiPSC-CMs from EHT from different cell lines (Fig.40). This difference in maximum effects of NE to increase the cAMP ΔFRET ratio was also found between hiPSC-CMs isolated from ML and EHT format (Fig.28). For instance, effect sizes of NE (100µM) on the cAMP ΔFRET ratio in isolated hiPSC-CMs (cell line C-25) cultured in ML format and in isolated hiPSC-CMs cultured in EHT (ERC-01) are smaller than in any isolated hiPSC-CM cultured in EHT format (C-25 and ERC-18). However, the increase in $I_{Ca,L}$ in isolated hiPSC-CMs (cell line C-25) cultured in ML format was clearly smaller than what could have been expected from the increase in cAMP ΔFRET (Fig.44). From this finding we have to expect a less efficient activation of $I_{Ca,L}$ by NE-induced cAMP in isolated hiPSC-CMs (cell line C-25) cultured in ML format. It is not to be expected that the small increase in $I_{Ca,L}$ by NE in isolated hiPSC-CMs (cell line C-25) cultured in ML format is due to a diminished responsiveness of Ca^{2+}-channels to cAMP. This assumption derives from the observation that serotonin known for its lower capacity to stimulate AC evokes robust increases in $I_{Ca,L}$ in C-25 ML (Uzun et al., 2016). Therefore, we have to assume that Ca^{2+}-channels react properly in response to cAMP in isolated hiPSC-CMs (cell line C-25) cultured in ML format. Therefore, the unexpectedly low $I_{Ca,L}$ response would suggest an impairment of cAMP propagation in a distinct compartment relevant for the regulation of Ca^{2+}-channels.

4.3 “Unexpected” small effects of direct AC activation (FSK) on cAMP

In pharmacology, FSK is frequently used to activate AC independent from GPCRs. Many researchers have used 10 µM FSK for this purpose (Christ et al., 2014; Sprenger et al., 2016; Müller et al., 2001; Gao et al., 1997; Akita et al., 1994; Osaka and Joyner,1992; Dunkern and Hatzelmann, 2007). However, in hiPSC-CMs the effect of 10 µM FSK on FRET is clearly smaller as compared to 100 µM NE (Fig.29). Our results are in line with Ca^{2+} current measurements in isolated hiPSC-CMs (cell line C-25) cultured in EHT format, where FSK only tended to increase $I_{Ca,L}$. This is in contrast to human atrial CM where increases in $I_{Ca,L}$ by 100 µM NE and 10 µM FSK are not different in size (Christ et al., 2014). More importantly from the latter study, presenting complete concentration-response curves, it can be concluded that 10 µM FSK is sufficient to evoke maximum responses.

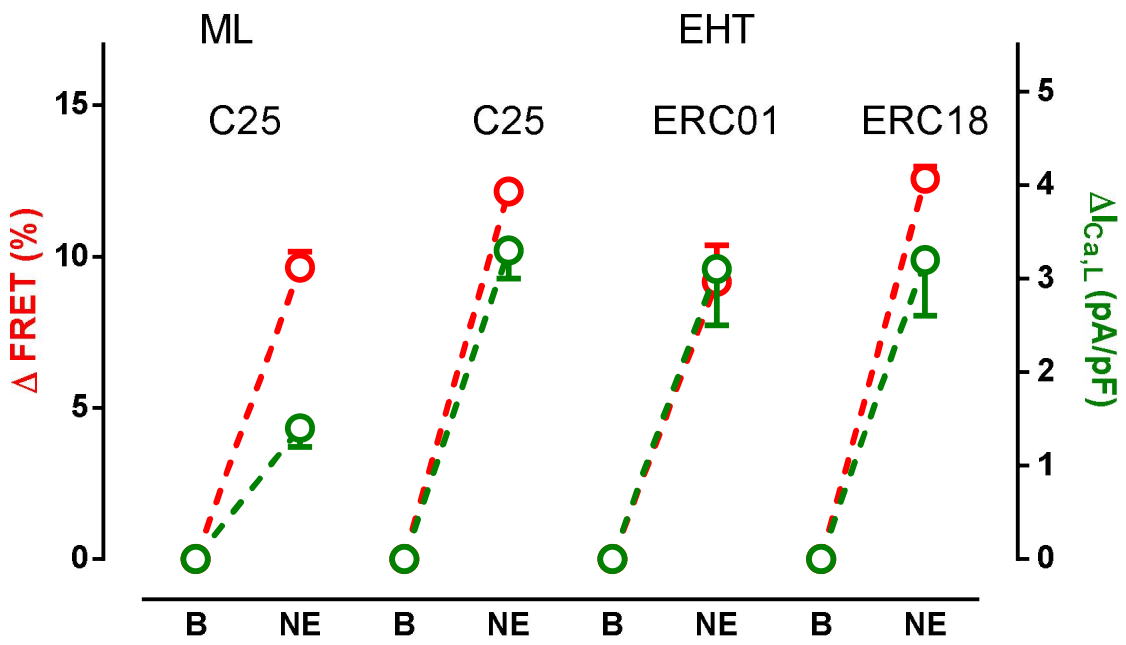

Figure 44: Comparison of responses of NE on cAMP ΔFRET and $I_{Ca,L}$ in isolated hiPSC-CMs from different cell lines

Mean values±SEM of effects of 100 µM NE on ΔFRET in % and on the increase in $I_{Ca,L}$ in isolated hiPSC-CMs from different cell lines. Green colour represents $I_{Ca,L}$ while red colour represents FRET data. Data for $I_{Ca,L}$ for cell line C-25 have been taken from (Ismaili et al., 2020) while data for cell lines ERC-01 and ERC18 are unpublished from our lab. Data for FRET are taken from Fig.28 and Fig. 40.

in β_1-AR signaling in cardiomyocytes, (Dessauer et al., 2017). Therefore, 10 µM should activate AC5 to ~33% of the maximum response (Fig.45), which is perfectly in line with our findings on cAMP ΔFRET and $I_{Ca,L}$. No data about the effects of FSK on cAMP ΔFRET in adult human cardiomyocytes exist. Probably, in hiPSC-CMs maximal activation of AC is needed to activate Ca^{2+}-channels completely, whereas in adult human CM even submaximal activation of AC is sufficient. In line with this assumption, similar magnitudes of cAMP were generated by 100 nM ISO alone or 10 µM FSK in isolated ventricular cardiomyocytes from adult transgenic mice expressing the Epac1-camps FRET sensor (Perera et al., 2017).

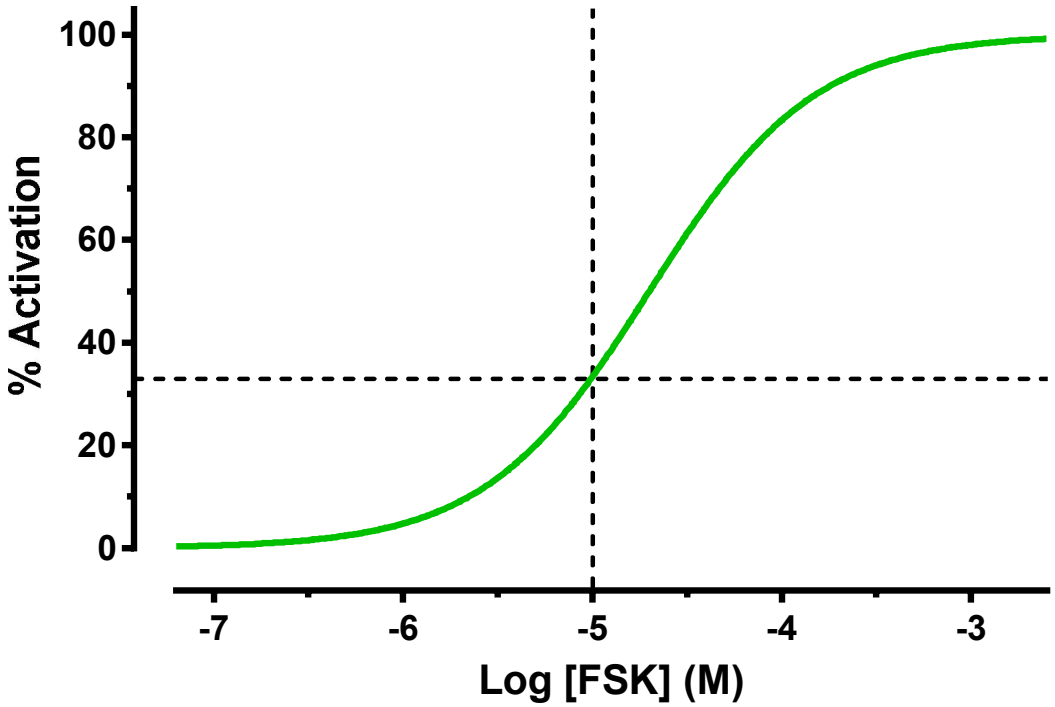

Figure 45: Model concentration-response curve (CRC) of FSK on the activation of AC5
Different concentrations of FSK and their corresponding effect on %age activation of AC5 adapted from Dessauer et al., 2017.

4.4 Regulation of basal cAMP by different PDE isoforms

Compartmentalized pools of cAMP are built up by distinct spatial expression patterns of PDEs. Therefore the impact of different PDEs to regulate ΔFRET ratio and $I_{Ca,L}$ will be discussed in the following paragraphs, as PDE activity is vital for adult human cardiomyocytes and differences in the regulation of both basal cAMP and $I_{Ca,L}$ in hiPSC-CMs need to be comparable for hiPSC-CMs to become a valid toxicological screening tool or implantable.

4.4.1 PDE2

We found a small but significant increase in cAMP ΔFRET by inhibition of PDE2 with Bay 60-7550 (100 nM) in isolated hiPSC-CMs cultured in EHT format (C-25; Fig.34). Interestingly, the effect size was as small as by PDE3 inhibition with 300 nM cilostamide. These findings are perfectly in line with data from Wu et al., 2015, who also found a small increase in cAMP after inhibition with the same PDE2 inhibitor Bay 60-7550 (also 100 nM) in hiPSC-CMs from another cell line expressing a global biosensor. Moreover, the observed increase in cAMP ΔFRET by Bay 60-7550 (100 nM) was not significantly smaller than with milrinone (10 µM) used to block PDE3 (Wu et al., 2015).

It should be noted that the group of Wu et al. used a different biosensor to measure cAMP by FRET (AKAR3). Unfortunately, there is no data available to compare the effect of PDE2-inhibition on cAMP measured by FRET in human cardiomyocytes.

However, different groups have published contrasting effects of PDE2 inhibition on ΔFRET ratio in cardiomyocytes of different species. For example, the small increase in cAMP by PDE2 inhibitor can be explained by keeping in mind that PDE2 contributes less than 5% of total cAMP hydrolytic activity by PDEs in adult rat cardiomyocytes (Rochais et al., 2006). Similarly, treatment with EHNA (10 µM), a selective PDE2 inhibitor, produced a small increase in ΔFRET ratio in unstimulated neonatal rat cardiac ventriculocytes expressing a genetically-encoded FRET biosensor for cAMP (Mongillo et al., 2006). In contrast, 50 nM Bay 60-7550 produced no effect on basal FRET ratio in isolated adult ventricular rat myocytes transduced with modified versions of the cytosolic FRET-based sensor Epac1-camps RI_epac (soluble fraction) and RII_epac (particulate fraction) (Fields, 2013). Then again, EHNA (10 µM) increased ΔFRET ratio significantly in the soluble fraction of non-stimulated neonatal rat cardiac ventricular cardiomyocytes (Di Benedetto et al., 2008).

$I_{Ca,L}$ was slightly increased by inhibition of PDE2 by Bay-60-7550 (100 nM) in isolated hiPSC-CMs from C-25 cultured in ML and EHT formats, but not in in human right atrium (RA) (Ismaili, 2020).

In summary, inhibition of PDE2 increases both FRET and $I_{Ca,L}$ in hiPSC-CMs. Effects are very small and may indicate marginal contribution to the regulation of both basal cAMP and basal $I_{Ca,L}$ in hiPSC-CMs.

4.4.2 PDE3

In our study, inhibition of PDE3 by 300 nM cilostamide increases ΔFRET ratio not only in isolated hiPSC-CMs from cell line C-25 cultured in ML format, but also in isolated hiPSC-CMs cultured in EHT format from all three different hiPSC-CM cell lines (C-25, ERC-01, and ERC-18, Fig.41). Correspondingly, inhibition of PDE3 also increases $I_{Ca,L}$ in all isolated hiPSC-CMs cultured in EHT format from three different cell lines (C-25, ERC-01, and ERC-18, Fig.46). This finding is in line with work in human RA (Molina et al., 2012). Notably, the increase in ΔFRET ratio with PDE3 inhibition in isolated hiPSC-CMs from cell line C-25 cultured in ML format amounts to about 30% of the maximum NE effect, while effect size is clearly smaller in isolated hiPSC-CMs cultured in EHT format from C-25, ERC-01 and ERC-18 cell lines.

4. Discussion

Interestingly, the accompanying increase in $I_{Ca,L}$ is not different in size between isolated hiPSC-CMs from cell line C-25 cultured in ML format and EHT format, suggesting a larger contribution to global cAMP and a similar contribution to cAMP relevant for $I_{Ca,L}$ regulation in isolated hiPSC-CMs from ML compared to isolated hiPSC-CMs from EHT format (Fig.46).

In adult rat cardiomyocytes, PDE3 contributes 31% of total cAMP hydrolytic activity by PDEs (Rochais et al., 2006). The same holds true for neonatal rat cardiomyocytes, where PDE3 contributes almost 30% of total cAMP hydrolytic activity by PDEs (Mongillo et al., 2004). In spite of significant regulation of total cAMP hydrolytic activity by PDE3, the effect of PDE3 on basal cAMP and $I_{Ca,L}$ is not homogenous in cardiomyocytes from different species. Inhibition of PDE3 by cilostamide (1 µM) produced a clear but transient effect on ΔFRET ratio in resting neonatal rat ventricular cardiomyocytes expressing a PKA-based biosensor (Mongillo et al., 2004). However, in another study, even higher concentrations of cilostamide (10 µM) produced very little effect on basal cAMP in particulate as well as in a soluble fractions of neonatal rat cardiac ventricular cardiomyocytes (Benedetto et al., 2008). In strong contrast, cilostamide (10 µM) was without any effect on basal the cAMP FRET ratio in isolated adult ventricular rat myocytes transduced with modified versions of the cytosolic FRET-based sensor Epac1-camps RI_epac (soluble fraction) and RII_epac (particulate fraction) (Fields, 2013).

Application of cilostamide (300nM) did not increase basal $I_{Ca,L}$ in rat ventricular myocytes (Christ et al., 2009). In contrast, 100 µM of pimobendan (another PDE3 inhibitor) stimulated $I_{Ca,L}$ in a highly significant way in isolated human RA cardiomyocytes (Kajimoto et al., 1997). In line with this early study basal $I_{Ca,L}$ was more predominantly regulated by cilostamide than rolipram in adult human atrial myocytes obtained from patients with sinus rhythm as well as in patients suffering from permanent atrial fibrillation (Berk et al., 2016).

Generally speaking, PDE3 regulates basal cAMP concentrations in cardiomyocytes from human as well as from different animals, but the degree of contribution is somewhat different. Application of milrinone (10 µM) produced significant ($p<0.001$) inotropic responses in both human right atrial and human left ventricular myocardium (Cremers et al., 2003).

Only cilostamide (300 nM) potentiated the positive inotropic response of NE in human atrial trabeculae from non-failing heart while rolipram failed to do so (Christ et al 2006).

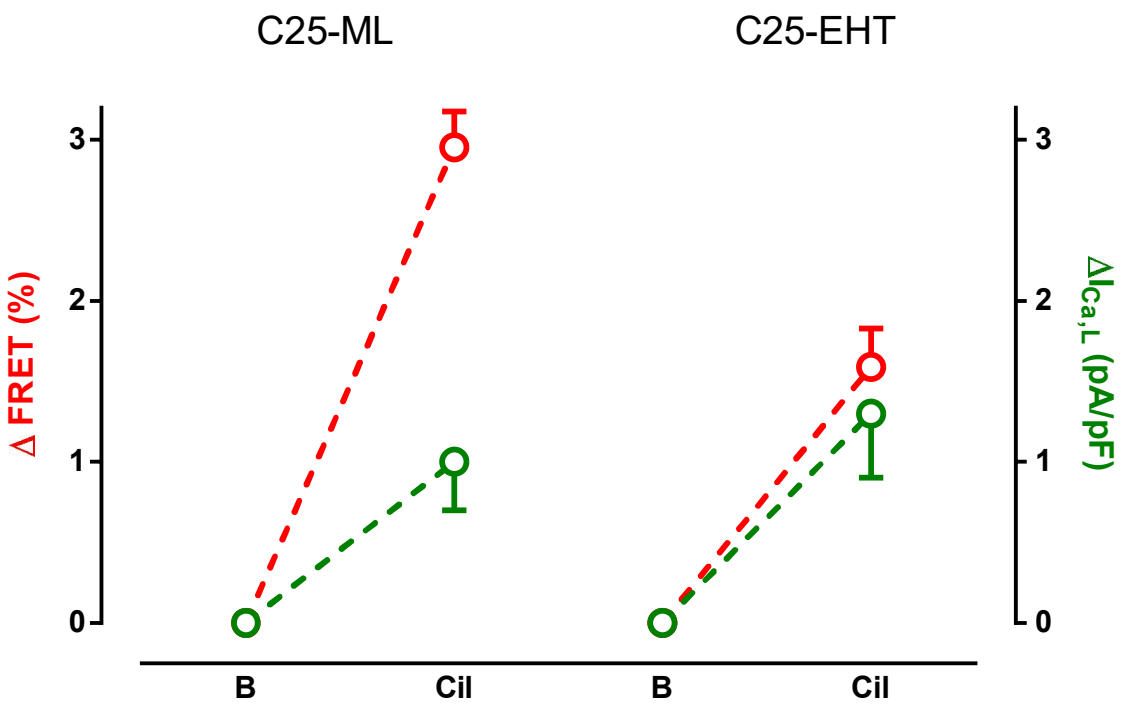

Figure 46: Comparison of effects of cilostamide (300nM) on $I_{Ca,L}$ and ΔFRET
Mean values±SEM of effects of 300nM cilostamide on ΔFRET (%) and on $I_{Ca,L}$ in isolated hiPSC-CMs (cell line C-25) cultured in both ML and EHT formats. Green colour represents $I_{Ca,L}$ while red colour represents FRET data. Data for $I_{Ca,L}$ for cell line C-25 have been taken from (Ismaili et al., 2020) while data for FRET are taken from Fig.30 and Fig.33.

4.4.3 Concomitant inhibition of PDE2 and PDE3

PDE3 inhibition by cilostamide suppressed NE-induced cAMP in isolated hiPSC-CMs cultured in EHT format from cell line C-25. Therefore, we assumed that sparing of cGMP from hydrolytic degradation, due to inhibition of PDE3, has possibly activated PDE2. Therefore we decided to repeat the set of PDE3 inhibition experiments in the presence of Bay 60-7550 (PDE2 inhibitor). In isolated hiPSC-CMs cultured in EHT format from cell line C-25 both selective inhibition of PDE2 (Bay 60-7550; 100 nM) and PDE3 (cilostamide; 300 nM) increased FRET by about 1.5±0.33% and 1.6±0.23% respectively. Effects were additive when PDE2 and PDE3 were simultaneously inhibited (3.21±0.5%), arguing that PDE3-block-evoked cGMP may activate PDE2 in a relevant manner (Fig.34).

4.4.4 PDE4

Inhibition of PDE4 by 10 µM rolipram increased basal cAMP to a larger extent than inhibition of PDE3 by 300nM cilostamide in isolated hiPSC-CMs both in ML and EHT culturing conditions (Fig.31-34). This finding is in strong contrast to human RA where inhibition of PDE3 (1 µM cilostamide) had a larger effect than inhibition of PDE4 (10 µM Ro 20-1724) on ΔFRET ratio (Molina et al., 2012). The effects of inhibition of PDE4 on cAMP are clearly smaller than (100 µM) NE-induced cAMP in both culturing conditions i.e. ML and EHT. However, effects of inhibition of PDE4 on $I_{Ca,L}$ are as large as of (100 µM) NE in isolated hiPSC-CMs cultured in EHT format (cell line C-25) or even larger than (100 µM) NE in isolated hiPSC-CMs cultured in ML format (cell line C-25) (Ismaili, 2020). For $I_{Ca,L}$ in human RA results are conflicting showing a small increase vs. no effect (Molina et al., 2012, Berk et al., 2016).

The situation is also variable in mice, and rat, where PDE4 contributes more strongly to basal cAMP regulation than PDE3. These results are hand in hand with biochemical studies. In adult rat cardiomyocytes PDE4 contributes 38% of total cAMP hydrolytic activity by PDEs (Rochais et al., 2006). Furthermore, in neonatal rat cardiomyocytes, PDE4 contributes even more than 60% of total cAMP hydrolytic to total PDE activity (Mongillo et al., 2004). In addition, inhibition of PDE4 by rolipram (1 µM) produced a significant effect on ΔFRET ratio in resting neonatal rat ventricular cardiomyocytes expressing a PKA based biosensor and surprisingly the effect of rolipram was even greater than effects by the non-specific inhibition of PDEs by 100 µM IBMX (11.5±0.9% vs 9±1.2%) (Mongillo et al., 2004). Similarly, rolipram (10 µM) produced a significantly stronger effect on basal cAMP in the particulate fraction as compared to the soluble fraction of neonatal rat cardiac ventriculocytes (Benedetto et al., 2008).

Yet there are many studies in different species, which postulate indecisiveness of predominance of PDE4 over PDE3 regarding the regulation of both basal cAMP and $I_{Ca,L}$. For example, rolipram (10 µM) produced no effect on basal FRET ratio in isolated adult ventricular rat myocytes transduced with modified versions of the cytosolic FRET-based sensor Epac1-camps RI_epac (soluble fraction) and RII_epac (particulate fraction) (Fields, 2013).

In a similar manner the application of rolipram (1 µM) in the presence of ICI-118,551 (50 nM) or CGP-20712A (300 nM) only tends to increase basal $I_{Ca,L}$ in rat ventricular myocytes (Christ et al., 2009).

Likewise, inhibition of PDE4 with the inhibitor Ro 20-1724 (10 µM) exhibited no effect on basal $I_{Ca,L}$ in adult rat ventricular cardiomyocytes (Rochais et al., 2006). In another study, even 100 µM of rolipram did not stimulate $I_{Ca,L}$ in a significant way in isolated human right atrial cardiomyocytes, but it produced a significant increase in $I_{Ca,L}$ in the presence of PDE3 inhibition in isolated human right atrial cardiomyocytes in another study (Kajimoto et al., 1997). The same author reported that concurrent inhibition of PDE3 and PDE4 produced a much larger increase in $I_{Ca,L}$ in isolated rabbit atrial cardiomyocytes. Our findings in hiPSC-CMs illustrate a dominant role of PDE4 over PDE3 in general and a larger impact of PDE4 on cAMP compartments relevant for $I_{Ca,L}$ than on global cAMP.

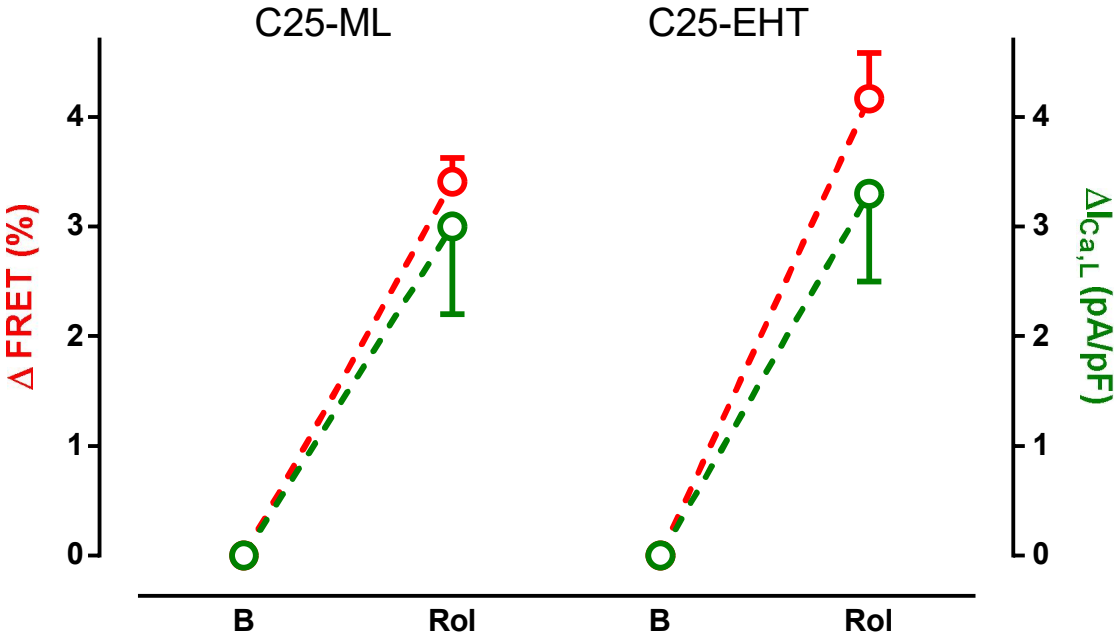

Figure 47: Comparison of effects of rolipram (10µM) on $I_{Ca,L}$ and ΔFRET
Mean values±SEM of effects of 10 µM rolipram on ΔFRET (%) and on $I_{Ca,L}$ (in Δ) in isolated hiPSC-CMs (C-25) cultured in both ML and EHT formats. Green colour represents $I_{Ca,L}$ while red colour represents FRET data. Data for $I_{Ca,L}$ for cell line C-25 have been taken from (Ismaili et al., 2020) while data for FRET are taken from Fig.31 and Fig.32.

4.4.5 PDE5

PDE5 may play a precarious role in cardiac diseases as it hydrolyses cGMP which is hypothesized to blunt cardiac hypertrophy and negative remodelling in heart failure. Yet its role and expression in cardiomyocytes is highly debatable (Degen et al., 2015). We used 1 µM tadalafil (selective PDE5 inhibitor) in order to elaborate on a potential contribution of PDE11 on cGMP degradation in hiPSC-CMs. From this concentration, we should expect complete inhibition of PDE5 and more than 90% of PDE11 as well. However, even such a high concentration of tadalafil showed no effect on basal ΔFRET ratio in isolated hiPSC-CMs cultured in EHT format (cell line C-25 Fig.35).

This finding can be interpreted as follows: both PDE11 and PDE5 do not contribute to the regulation of basal cAMP in hiPSC-CMs cultured in EHT format. Theoretically, PDE5 can play a vital role in the crosstalk between cGMP and cAMP in cardiomyocytes as the accumulation of cGMP could both activate and inhibit cAMP hydrolysis. Firstly, the effects of PDE5 on cAMP depend upon how much cGMP is hydrolyzed by PDE5. Inhibition of PDE5 in murine hearts and cardiomyocytes increased basal protein kinase G (PKG-1) activity by 10% (Takimoto et al., 2005). Moreover, inhibition of PDE5A with sildenafil (EC_{50} 44±29 nM/l) versus placebo produced no effects on basal contractility of unstimulated cardiomyocytes in healthy volunteers (Borlaug et al., 2005). While in another study inhibition of PDE5 with sildenafil (1 µM) increased cGMP production measured by FRET in cultured rat neonatal myocytes transduced with the cygnet-2 biosensor (Stangherlin et al., 2011). Yet the application of a wide range of sildenafil (0.0001–10 µM) failed to produce significant inotropic responses in both human right atrial and left ventricular myocardium (Cremers et al., 2003). Similarly, concomitant use of ISO (0.1 µM) and sildenafil (10 µM) enhanced the force of contraction insignificantly in both human right atrial and left ventricular myocardium (Cremers et al., 2003). Pretreatment with sildenafil (1µM) decreased 10 µM ISO-induced cAMP generation in neonatal mice cardiomyocytes expressing the ICUE3 sensor. Furthermore, this decrease of ISO-induced cAMP in the presence of sildenafil was augmented by cilostamide (10 µM) but suppressed by EHNA (10 µM) (Isidori et al., 2015).

4.5 Regulation of NE-activated cAMP and $I_{Ca,L}$ by different PDE isoforms

In isolated hiPSC-CMs cultured in EHT, the increase in the basal cAMP ΔFRET ratio is larger by inhibition of PDE4 than by inhibition of PDE3. The same holds true for $I_{Ca,L}$ (Ismaili, 2020). Inhibition of PDE4 increased maximum NE effects on ΔFRET ratio in ML more than by inhibition of PDE3. In ML $I_{Ca,L}$ responses to NE were drastically increased by inhibition of PDE4 but remained unaltered by inhibition of PDE3. In EHT tissues, from the three different cell lines, results are slightly different in size, but there is a clear tendency of larger effects through the inhibition of PDE4 compared to inhibition of PDE3.

4.5.1 Lack of potentiation of NE-induced increase in ΔFRET ratio by inhibition of PDE3 and PDE4

Inhibition of cAMP hydrolyzing PDEs should increase the potency of stimulation of β-ARs via an agonist, typically measured as a leftward shift of the CRC for catecholamines. Obviously, this seems not to be true for the ΔFRET ratio increased by NE in hiPSC-CMs both in ML and EHT format. This is an unsuspected finding. It should be noted that in EHT (C-25) the CRC for the positive inotropic effect isoprenaline was shifted by inhibition of PDE4 (Saleem et al., 2020).

Since there are no data about NE-evoked FRET signals in hiPSC-CMs and human CMs it remains unclear whether this unsuspected lack of potentiation of submaximal NE effects on FRET reflects a peculiarity of hiPSC-CMs or if the concentration-dependent increase in global cAMP is not regulated by PDE3 and PDE4. As was observed in the experiments described in this thesis, global cAMP does not relate to the classic leftward shift of the CRC for catecholamine-induced positive inotropy.

4.5.2 Increases in NE-induced ΔFRET by PDE-inhibition in ML but not in EHT

Effects of PDE4 inhibition in isolated hiPSC-CMs, on the maximum effect size of NE-induced cAMP, were dissimilar in different culturing conditions, namely ML vs EHT. Inhibition of PDE4 increased the maximum effect size of NE on cAMP ΔFRET by 66% in isolated hiPSC-CMs cultured in ML format from cell line C-25 but remained unaltered in EHT (C-25). In line with our results in EHT, Molina et al.,2012 reported that in human atrial cardiomyocytes the effect of 100 nM ISO on FRET was not further augmented by inhibition of PDE3 (1 µM cilostamide) or by inhibition of PDE4 (10 µM Ro 20-1724). Furthermore, the maximum effect size of NE (100 µM) on cAMP was not increased even under the concomitant inhibition of both PDE3 and PDE4 in adult human atrial cardiomyocytes expressing a cytosolic biosensor (Dolce, 2020). In contrast, inhibition of PDE4 augmented β_1-AR effects on cAMP in cardiomyocytes in other species. For example, in mice 100 nM isoprenaline (EC_{50} 10 nM for NE to increase cAMP in this species) effects on cAMP were drastically increased in the presence of inhibition of PDE4 in early cAMP FRET papers using a different FRET (HCN2-camps) sensor in CMs (Nikolaev et al., 2006). The lack of potentiation of NE-induced cAMP in the presence of PDE-inhibition in EHT vs. ML indicates a regulation of catecholamine effects by PDEs that is closer to the situation in human cardiomyocytes compared to mice.

Differential regulation of catecholamine effects on cAMP increases as well as on $I_{Ca,L}$ by isozymes of PDEs in different species has been documented. For example, effects of stimulation of β-ARs on cAMP by ISO (5 µM) plus ICI-188, 551(1 µM) and ISO (5 µM) plus CGP-20712A (1 µM) respectively were significantly potentiated by PDE4 inhibition with Ro 20-1724 (Ro; 10 µM) but remained unaffected by inhibition of PDE3 with cilostamide (1 µM) in adult rat ventricular myocytes (ARVMs) expressing nucleotide-gated (CNG) channels as cAMP biosensors (Rochais et al., 2006).

In a similar manner, inhibition of PDE4 with Ro 20-1724 (Ro; 10 µM) and inhibition of PDE3 with cilostamide (1 µM) exhibited no effect on basal $I_{Ca,L}$ but effects of ISO (1 nM) plus ICI-188, 551(1 µM) were significantly potentiated in the presence of Ro 20-1724 (Ro 10 µM). However, there was only an observable trend to increased potentiation by addition of cilostamide (1 µM) in adult rat ventricular myocytes (Rochais et al., 2006).

In another set of experiments by a different group, both PDE3 and PDE4 regulated (5 nM) NE-evoked increase in ΔFRET ratio, but 10% inhibition of PDE4 activity by rolipram (25 nM) augmented the (5 nM) NE-evoked increase in ΔFRET ratio significantly larger (9±2% vs 2%) as compared to cilostamide (3.6±1.3% vs 2%) in neonatal rat ventricular cardiomyocytes expressing a PKA based biosensor (Mongillo et al., 2004).

Similar consequences on ΔFRET ratio in the soluble fraction and the particulate fraction of isolated adult ventricular rat myocytes after exposure to ISO (100 nM) in the presence of cilostamide (10 μM) or rolipram (10 μM) effect have been reported (Fields, 2013). PDE4 is a major regulator of cytosolic ISO-induced cAMP, as inhibition of PDE4 with rolipram (10 μM) increased 100 nM ISO-induced cAMP more strongly, than inhibition of PDE3 with cilostamide (10 μM) in isolated adult rat ventricular cardiomyocytes expressing the cytosolic Epac1 camps biosensor (Bastug-Özel et al., 2019). Inhibition of PDE4 with rolipram (10 μM) significantly affects ISO-induced accumulation of cAMP measured by radioimmunoassays and ISO-induced phosphorylation of contractile proteins, i.e. PLB and TnI, as shown in adult β_2-KO mouse ventricular myocytes and neonatal β_2-KO mouse ventricular myocytes. (De Arcangelis et al, 2008). In contrast, inhibition of PDE3 with cilostamide (10 μM) did not affect ISO-induced accumulation of cAMP measured by radioimmunoassay and ISO-induced contraction (as deduced from phosphorylation of contractile proteins i.e. PLB and TnI as read-out) in adult β_2-KO ventricular myocytes and neonatal β_2-KO ventricular myocytes from mice (De Arcangelis et al, 2008).

Differential regulation of catecholamine effects on cAMP as well as on $I_{Ca,L}$ by different isozymes of PDEs may be interpreted as a result of compartmentation. ISO (10 nM) in the presence of selective PDE4B knock-out produced smaller effects in isolated neonatal mice cardiomyocytes, expressing cytosolic EPAC2 sensor, as compared to cardiomyocytes, expressing sarcolemmal pmEPAC2 biosensor (Mika et al., 2014).

Differential regulation of catecholamine effects on cAMP as well as on $I_{Ca,L}$ by isozymes of PDEs may also vary, depending on whether CMs are neonatal or adult. For example, in adult rabbit ventricular myocytes, PDE3 inhibition, in the presence of 0.1 μM ISO, produced 70% additional effects on $I_{Ca,L}$ vs only a small additional increase in $I_{Ca,L.}$ by PDE4 inhibition. In contrast to this, PDE4 inhibition, in the presence of 0.1 μM ISO, produced 80% additional effects on $I_{Ca,L}$ vs only a small additional increase in $I_{Ca,L.}$ by PDE3 inhibition in neonatal rabbit ventricular myocytes (Akita et al., 1994).

The application of cilostamide (300nM) in the presence of ICI-118, 551 (50nM) potentiated NE (1 µM) induced $I_{Ca,L}$ significantly ($p<0.05$) as compared to 1 µM rolipram ($p<0.01$) in rat ventricular myocytes (Christ et al., 2009). Also, inotropic effects of NE in rat ventricular papillary muscles were potentiated by PDE4 inhibition, but not by PDE3 inhibition (Christ et al., 2009). PDE4 inhibition with rolipram (1 µM) insignificantly reshaped inotropic effects of NE in the presence of ICI-118, 551 (50 nM) on human atrial trabeculae from non-failing hearts. In disease this appears to differ, as PDE3 inhibition with cilostamide (300nM) potentiated the inotropic effects of NE significantly in the presence of ICI-118, 551 (50 nM) on human atrial trabeculae from non-failing hearts (Christ et al., 2006).

From our experiments in hiPSC-CM, we can conclude that PDE4 is the dominant isoform hydrolyzing NE-induced cAMP in these cells (Fig.31 and Fig.32). The same holds true when ISO-induced inotropy was measured, as rolipram but not cilostamide shifted the concentration-response curve to the left. (Saleem et al., 2020). This finding is in strong contrast to adult human cardiac tissue and was discussed in detail before (Eschenhagen, 2013). The dominance of PDE4 over PDE3 in hiPSC-CMs may represent a limitation of hiPSC-CMs when used for drug screening or disease modelling.

4.5.3 Suppression of NE-induced cAMP in the presence of PDE3 in EHT (C-25)

The suppression of maximum effects on NE-induced ΔFRET ratio by inhibition of PDE3 in isolated hiPSC-CMs cultured in EHT (C-25) was completely unexpected. However, attenuation of β-ARs stimulated effects by cross-talk between cGMP and cAMP is not a new phenomenon and we hypothesized that it can explain this observation in hiPSC-CMs.

Our initial results were confirmed in a second set of experiments, where individual cells were treated with cilostamide or without cilostamide in an alternating fashion in order to minimize effects by differences in experimental conditions (culture time, batch number). In addition, results on ΔFRET ratio goes hand in hand with $I_{Ca,L}$ data from (Ismaili, 2020).

Therefore, we are confident that inhibition of PDE3 in isolated hiPSC-CMs from cell line (C-25 EHT) in fact suppresses NE-induced cAMP as well as $I_{Ca,L}$. One attractive hypothesis is the activation of a cAMP-hydrolyzing PDEs by sparing of cGMP from degradation due to inhibition of PDE3. Such a cross-talk could be mediated via PDE2 or PDE11. The low micromolar concentration of cGMP can enhance the cAMP hydrolytic activity of PDE2 by a factor of 4 (Michie et al., 1996). Numerous reports have been published to discuss cross-talk between cGMP and cAMP. Activation of PDE2 by inhibition of PDE3 was shown for human atrial CMs before (Rosmatiritza et al., 2014).

4. Discussion

Interestingly, it has been reported that several nitric oxide (NO) donors did not affect basal $I_{Ca,L}$ in rat ventricular myocytes whereas 100 µM of 2-(N, N-diethylamino)-diazenolate-2-oxide (DEANO, another NO donor) inhibited $I_{Ca,L}$ stimulated either by ISO (1-10 nM) or IBMX (10-80 µM) in rat ventricular myocytes (Abi-Gerges et al., 2001). The authors investigated possible reasons for the anti-adrenergic effects of DEANO and reported that the effects are cGMP-dependent, and involve the activation of PKG and the regulation of a pertussis toxin-sensitive G protein. Moreover, PDE2 has been found as a causative agent in the reduction of the cAMP level after β-ARs stimulation in rabbit atrioventricular nodal cells (Han et al 1996). NE (5 nM) in the presence of EHNA (10 µM) resulted in highly significant increases in ΔFRET ratio as compared to NE (5 nM) in the absence of EHNA (10 µM) in neonatal rat cardiac ventricular myocytes expressing a genetically-encoded FRET biosensor for cAMP (Mongillo et al., 2006). The same author has reported similar results in mice under an identical experimental protocol. Sodium nitroprusside (10 µM), a NO donor, reduced 1 µM NE-induced cAMP by almost 50% in neonatal rat cardiac ventriculocytes expressing a genetically-encoded FRET biosensor for cAMP. Interestingly, in the absence of NE sodium nitroprusside (10 µM) produced no effect on the cAMP levels of neonatal rat cardiac ventriculocytes expressing a genetically-encoded FRET biosensor for cAMP (Mongillo et al., 2006). The author has declared that the involvement of β_3-ARs may be the possible reason for reduction of NE-evoked cAMP in the presence of cGMP. β-AR overstimulation and their desensitization in heart failure was supposed to be the hidden reason behind the up-regulation of PDE2 (Mehel et al., 2013). In an in-vivo study, exposure to the PDE2 inhibitor Bay 60-7550 (3mg/kg) totally restored the positive inotropic and chronotropic response to β-ARs stimulation by ISO in mice chronically treated with ISO (30 mg/kg/d for 7 days) (Vettel et al., 2016).

Debilitating effects of ISO (30nM) on cAMP, in isolated cardiomyocytes from the ventricle of a transgenic mouse infected with an adenovirus expressing the FRET-based cAMP probe Epac-SH^{187}, has been reported (Vettel et al., 2016).

PDE 2 overexpression in transgenic mice substantially reduced the β-AR–induced (ISO 30 nM) increase in $I_{Ca,L}$ by 35% in WT vs 8% in PDE 2-transgenic animals (Vettel et al., 2016).

This aforementioned discrepancy was solved by PDE2 inhibition by 100 nM Bay 60-7550. Interestingly, 50 nM Bay 60-7550 significantly potentiated the ISO (100 nM) effect on FRET ratio in the soluble fraction as well as in the particulate fraction of isolated adult ventricular rat myocytes (Fields, 2013).

4. Discussion

C-natriuretic peptide (CNP)-induced cGMP can reduce the cAMP-PDE activity of PDE3 and increase the cAMP-PDE activity of PDE2 in a concentration-dependent manner in rat cardiomyocyte homogenates in a similar way in cells from sham treated and heart failure animals (Meier et al., 2015). PDE2 inhibition with Bay 60-7550 (100 nM) increased cAMP by about 20% after application of rolipram (10 µM) + ISO (100 nM) + ICI-181,551 (50 nM) in both cytosolic and sarcolemmal micro-domains in isolated adult mice cardiomyocytes expressing both Epac1 camps (cytosolic) and pmEpac1 (sarcolemmal) biosensors (Perera et al., 2015).
There are several selective inhibitors of PDE2 available. One of them is Bay-60-7550. From our results with this compound, it seems clear that PDE2 is not involved in the suppression of NE effects in the presence of cilostamide. PDE11 is another candidate to mediate cGMP/cAMP cross-talk. PDE11 is expressed in several tissues including heart as discussed in the introduction. But no functional data about PDE11 in cardiomyocytes has been published yet. There are no selective inhibitors of PDE11 available. Tadalafil, a potent inhibitor of PDE5, also blocks PDE11 at much higher concentrations (see methods section). Therefore we have used 1 µM of tadalafil to block PDE11. Pretreatment with tadalafil (1 µM) reversed the suppression of NE (100 µM)-induced ΔFRET ratio in the presence of cilostamide. Tadalafil given on top of NE in the presence of cilostamide increased the ΔFRET ratio even further. However, the increase in ΔFRET ratio by tadalafil on top of NE is not significantly larger in the presence vs in the absence of cilostamide, arguing against relevant activation of PDE11 by cilostamide-induced cGMP. The increase in ΔFRET ratio by tadalafil could result from inhibition of other PDEs.
The selectivity of tadalafil at 1 µM over the most important PDE isoform (PDE4) is limited and we have to expect that the concentration we used blocks ~10% of PDE4-activity (see methods section). The mechanism of how cilostamide suppresses NE-induced cAMP in isolated hiPSC-CMs cultured in EHT (C-25) remains at present unclear. One possibility is that the off-target effects of cilostamide may play a role. It should be noted that the NE-induced ΔFRET ratio is not suppressed by cilostamide in isolated hiPSC-CMs cultured in EHT format from other cell lines than C25 (ERC-01 and ERC-18).

Therefore, we assume that the suppression of NE-induced cAMP by inhibition of PDE3 seems to be a peculiarity of C-25. Probably the C-25 cell line has a higher susceptibility for mutation during culture, since we recently demonstrated aberrant expression patterns for ion channels in EHTs (C-25) (Horváth et al., 2020). It could also be that EHT (C-25) expresses other yet unidentified PDE isoforms. In conclusion, it seems necessary to characterize any hiPSC-CMs cell line separately before its utilization in drug screening and disease modelling.

4.5.4 Effects of PDE-inhibition on ΔFRET and $I_{Ca,L}$ in hiPSC-CMs vs. adult human CMs

To summarize effects of PDE-inhibition on ΔFRET and $I_{Ca,L}$ in hiPSC-CMs we have plotted FRET and $I_{Ca,L}$ responses to inhibitors of PDE3 and PDE4, NE and both to the inhibitor and NE for hiPSC-CMs from ML and EHT (C-25).

In RA data points for the increase in ΔFRET and $I_{Ca,L}$ by the four different interventions overlap to a single line. Effects of maximum activation of β_1-AR stimulation cannot be increased further by the inhibition of PDE3 or PDE4 (Fig.48).

4.6 Sarcolemmal sensor (SL)

The sensor, we used to measure FRET in the SL compartment, is expressed in the close vicinity of Ca^{2+}-channels (Perera et al., 2015). Furthermore, this biosensor exhibits a different expression pattern than the biosensor used to measure global FRET (Fig.14). Therefore FRET should facilitate the detection of cAMP relevant for activation of $I_{Ca,L.}$ In order to prove that an SL sensor is superior in detecting localized cAMP, which is relevant for $I_{Ca,L}$. FRET signals measured with SL sensor should more closely resemble functional effects on $I_{Ca,L}$ than global FRET.

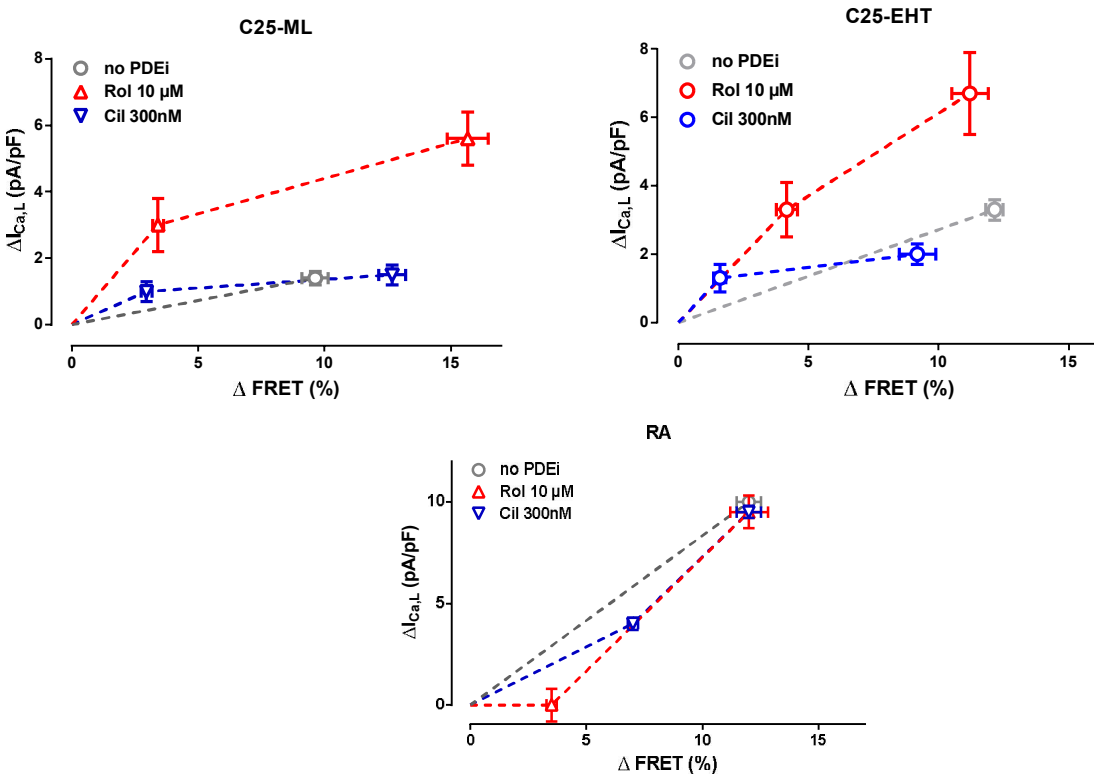

Figure 48: Comparison of effects of PDE3 or PDE4 inhibition on 100µM NE-induced ΔFRET (in %) and $I_{Ca,L}$

Mean values±SEM of effects of 100µM NE on ΔFRET (in %) and on $I_{Ca,L}$ by in the absence PDEi or presence of 10µM rolipram or 300 nM cilostamide (first symbol) in isolated hiPSC-CMs (C-25) cultured in both ML and EHT formats and human right atrial tissue. $I_{Ca,L}$ data are taken from (Ismaili et al. 2020) while FRET data of RA are taken from Molina et al., 2012 (which used ISO instead of NE).

4.6.1 NE-induced cAMP in ML and EHT

Although the smaller increase in $I_{Ca,L}$ by NE in hiPSC-CMs ML vs. EHT format (C-25) is reflected in the global FRET signals in hiPSC-CMs ML vs. EHT format (C-25) yet FRET signals in close proximity of the Ca^{2+}-channels must be measured to obtain exact insights.

Although the increase in sarcolemmal cAMP after exposure of hiPSC-CMs (C-25) to NE (100 µM) was almost 10% higher in EHT than ML format (ML =9.2±0.7% vs. EHT =10.1±0.9%), this larger effect size in cAMP was far smaller than the difference in effect size of $I_{Ca,L}$ in EHT vs. ML (Fig.49). This finding suggests that the sarcolemmal sensor also detects NE-evoked cAMP not relevant for the activation of $I_{Ca,L}$.

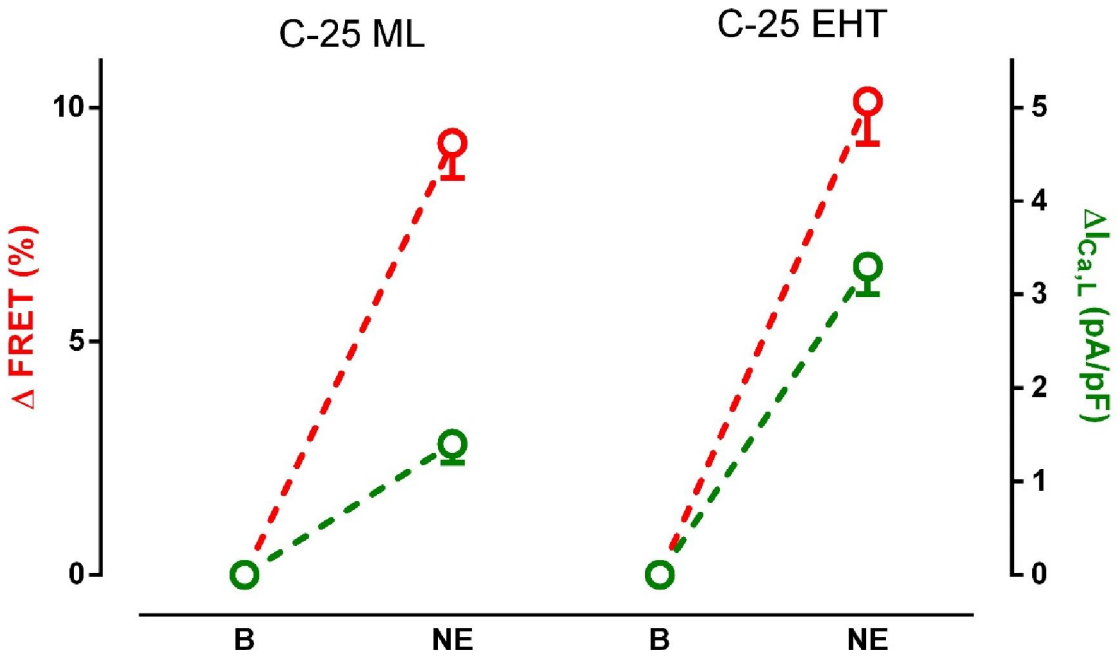

Figure 49: Comparison of the response of NE on cAMP and $I_{Ca,L}$ in isolated hiPSC-CMs transduced with SL biosensor

Mean values±SEM of effects of 100 µM NE on ΔFRET (in %) and on $I_{Ca,L}$ in isolated hiPSC-CMs transduced with SL biosensor. Green colour represents $I_{Ca,L}$ while red colour represents FRET data. Data for $I_{Ca,L}$ for cell line C-25 have been taken from (Ismaili et al., 2020) while data for FRET are taken from Fig.37.

4.6.2 Effects of PDE-inhibition on basal cAMP and on NE-induced cAMP in ML and EHT hiPSC-CMs

In hiPSC-CMs (C-25) cultured in ML format, inhibition of PDE3 or inhibition of PDE4 increased basal global ΔFRET ratio almost to the same extent (Fig.31), while the increase in basal $I_{Ca,L}$ was clearly smaller with inhibition of PDE3 than with PDE4 inhibition. The smaller increase in basal $I_{Ca,L}$ by inhibition of PDE3 than by inhibition of PDE4 can be nicely explained by the effects of PDE3 /PDE4 on basal sarcolemmal cAMP (1.7±0.3% vs 4.2±0.4%), suggesting that the SL sensor measures cAMP relevant for $I_{Ca,L}$ more accurately when cAMP is increased by PDE inhibition (Fig.50 and Fig.51).

The same holds true for NE-evoked cAMP in the presence of PDE3/PDE4 inhibition. The NE-induced increase in $I_{Ca,L}$ in the presence of cilostamide (PDE3-inhibition) was not larger than for NE alone in isolated hiPSC-CMs from ML tissue (C-25), which can be explained when looking at FRET signals from the SL but not the global camp FRET sensor. The larger NE-induced increase in $I_{Ca,L}$ in the presence of rolipram vs. NE alone is reflected by both global and SL FRET signals.

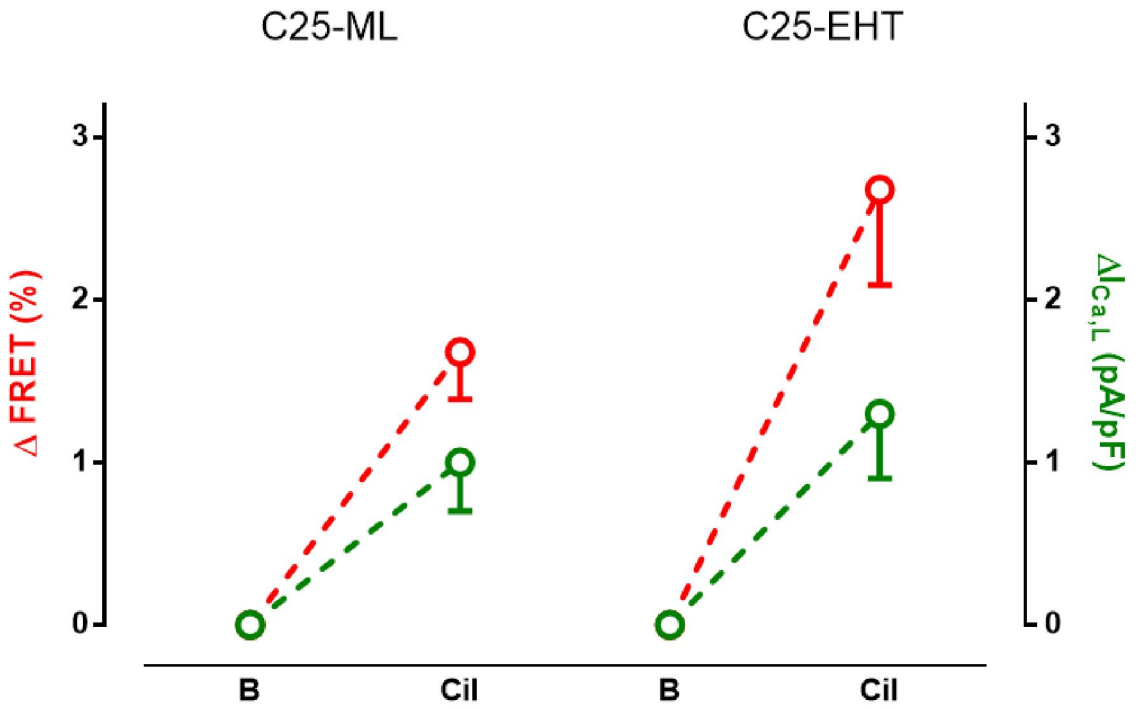

Figure 50: Comparison of effects of cilostamide (300nM) on $I_{Ca,L}$ and change in FRET
Mean values±SEM of effects of 300nM cilostamide on ΔFRET in (%) and on $I_{Ca,L}$ in isolated hiPSC-CM (cell line C-25) cultured in both ML and EHT formats**.** Green colour represents $I_{Ca,L}$ while red colour represents FRET data. Data for $I_{Ca,L}$ for cell line C-25 have been taken from (Ismaili et al., 2020) while data for FRET are taken from Fig.38 and Fig.39

In hiPSC-CMs (C-25) cultured in EHT format inhibition of PDE3 evokes consistently smaller effects than with inhibition of PDE4 in all three experimental designs (global FRET, SL FRET and $I_{Ca,L}$) as explained by (Fig.50 and Fig.51). Similar findings about the predominance of PDE4 over PDE3 have been reported in isolated adult mice cardiomyocytes. As for instance, PDE3 inhibition with cilostamide (10 μM) increases about 50% cAMP produced by rolipram (10 μM) under similar experimental conditions in both cytosolic and sarcolemmal micro-domains in isolated adult mice cardiomyocytes expressing both Epac1 camps (cytosolic) and pmEpac1 (Sarcolemmal) biosensors (Perera et al., 2015).
Effects of NE on $I_{Ca,L}$ in the presence of cilostamide were suppressed (2±0.4 vs 3.3±0.3) which holds perfectly true when observing the global ΔFRET ratio (9.2±0.7 vs 12.1±0.3%) in hiPSC-CMs (C-25) cultured in EHT format. Although effects of NE on the ΔFRET ratio in the presence of cilostamide in SL compartment were suppressed (9.1±0.7 vs 10.1±0.9%) their magnitude was far less when compared to suppression of $I_{Ca,L}$.

Simultaneously, larger effect sizes of NE in the presence of rolipram on $I_{Ca,L}$ (6.1±1.1 vs 3.3±0.3) were nicely reflected by ΔFRET ratio (13.9±0.8 vs 10.1±0.9%) in the SL compartment but not in the cytosolic compartment (11.2±0.7 vs 12.1±v 0.3%).

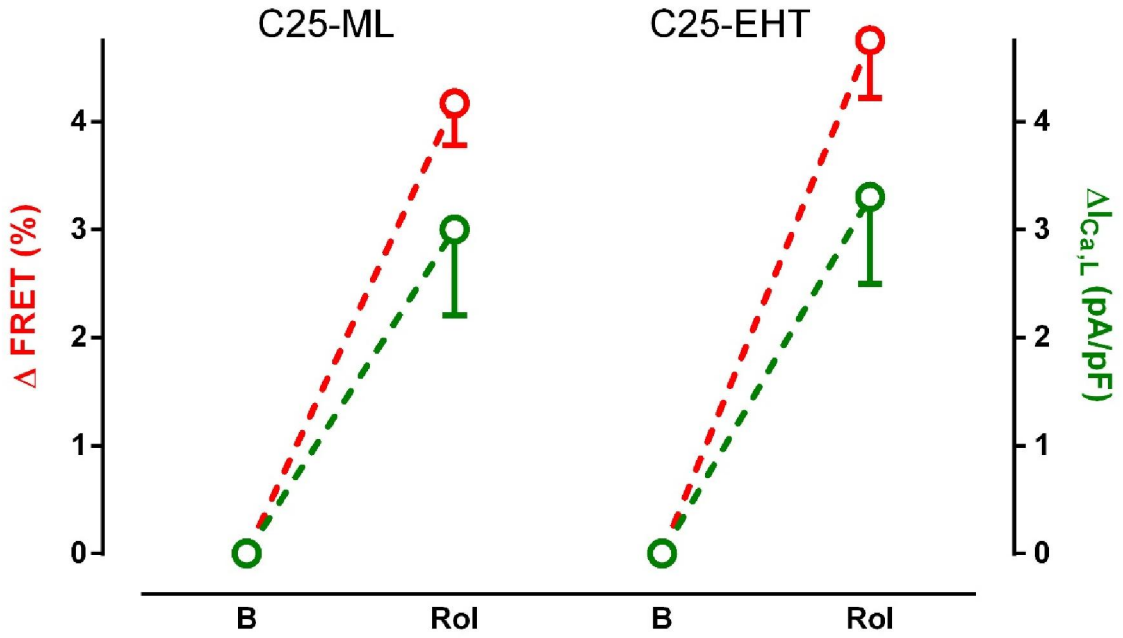

Figure 51: Comparison of effects of rolipram (10µM) on $I_{Ca,L}$ and change in FRET
Mean values±SEM of effects of 10µM rolipram on ΔFRET (in %) and on I_{Ca} (expressed as Δ) in isolated hiPSC-CM (C-25) cultured in both ML and EHT formats. Green colour represents $I_{Ca,L}$ while red colour represents FRET data. Data for $I_{Ca,L}$ for cell line C-25 have been taken from (Ismaili et al., 2020) while data for FRET are taken from Fig.38 and Fig.39.

In summary, results with NE alone do not support the idea that the SL sensor measures cAMP relevant for activation of $I_{Ca,L}$ more accurately than the global sensor. In the case of basal PDE-inhibition as well as when looking at the effect of PDE-inhibition on NE-induced cAMP, the ΔFRET ratio in SL compartments reflects $I_{Ca,L}$ activation better than global FRET in ML.
Results with NE alone in EHT corresponding to all three experimental designs (global ΔFRET, SL ΔFRET and $I_{Ca,L}$) are divergent. In the case of basal PDE-inhibition as well as when looking at the effect of PDE-inhibition on NE-induced cAMP, ΔFRET ratio in the SL compartment reflects $I_{Ca,L}$ activation better than global FRET measurements. Obviously, the ability of the SL sensor to detect cAMP relevant for the activation of I_{Ca} depends on the mode of cAMP increase (activation of AC by NE vs. inhibition of PDE) and the difference in maturation (ML vs. EHT).

5. Conclusion and future perspectives

Isolated hiPSC-CMs from both ML and EHT tissues can be transduced with cAMP-based FRET biosensors designed to study the dynamics of cAMP by using FRET in both global and sarcolemmal compartments. It is clearly demonstrated that hiPSC-CMs after transduction respond to different regulators of cAMP. HiPSC-CMs are sensitive to NE and the potency of NE to increase ΔFRET and $I_{Ca,L}$ is almost similar. The maximal increase in ΔFRET by NE (100 µM) is larger in hiPSC-CMs from EHT than ML when measured by the global biosensor but no difference can be seen with the SL biosensor. PDE4 is the predominant isoform among PDEs to regulate the basal global level of cAMP and basal $I_{Ca,L}$ in hiPSC-CMs. Predominance of PDE4 to regulate basal global cAMP is a consistent finding in isolated hiPSC-CMs from EHT of two other cell hiPSC-CM lines (ERC-01 and ERC-18). Effects of stimulation by NE on cAMP are potentiated by both PDE3 inhibition as well as by PDE4 inhibition in isolated hiPSC-CMs from ML tissues (C-25) with larger determinable effects by PDE4 than by PDE3 inhibition.

In contrast, β_1-AR effects on cAMP are neither increased by PDE4 inhibition nor by PDE3 inhibition in hiPSC-CMs from EHT tissues from the C-25 cell line.

In hiPSC-CMs isolated from EHT tissue (C-25), inhibition of PDE3 produced divergent and inconclusive effects on NE-induced cAMP. It is quite unexpected that cilostamide tends to suppress the effect of NE on cAMP. However it should be noted that this suppression of NE-induced cAMP by cilostamide is a peculiar feature of hiPSC-CMs isolated from EHT tissue from cell line C-25 as it is not found in hiPSC-CMs isolated from EHT tissues of other cell lines (EC-01 and ERC-18). It was also not found in hiPSC-CMs isolated from ML tissues of the same cell line (C-25).

This suppression of NE-induced cAMP by inhibition of PDE3 is a highly concerning finding in and of itself that is also puzzling because it appears to be unrelated to cGMP-activated PDEs.

The small effect of NE on $I_{Ca,L}$ observed in ML is not paralleled by a small effect on cAMP measured with the SL biosensor. This finding suggest that the SL biosensor does not necessarily indicate cAMP pools relevant for $I_{Ca,L}$-activation in ML.

Predominance of PDE4 to regulate both $I_{Ca,L}$ and cAMP is a relevant limitation when hiPSC-CMs are used as a pharmacological model to study PDEs in human heart. Further work is needed to clarify whether predominance of PDE4 is a sign for immaturity and can be overcome by different culture methods. Spatially expressed biosensors have to be checked for relevance before being used to study local control of cAMP in hiPSC-CMs.

6. Bibliography

Abassi, Y. A., Xi, B., Li, N., Ouyang, W., Seiler, A., Watzele, M., Kettenhofen, R., Bohlen, H., Ehlich, A., Kolossov, E., Wang, X., & Xu, X. (2012). Dynamic monitoring of beating periodicity of stem cell-derived cardiomyocytes as a predictive tool for preclinical safety assessment. *British Journal of Pharmacology*, *165*(5), 1424–1441. https://doi.org/10.1111/j.1476-5381.2011.01623.x

Abi-Gerges, A., Richter, W., Lefebvre, F., Mateo, P., Varin, A., Heymes, C., Samuel, J. L., Lugnier, C., Conti, M., Fischmeister, R., & Vandecasteele, G. (2009). Decreased expression and activity of cAMP phosphodiesterases in cardiac hypertrophy and its impact on β-Adrenergic cAMP signals. Circulation Research, 105(8), 784–792. https://doi.org/10.1161/CIRCRESAHA.109.197947;

Abi-Gerges, N., Fischmeister, R., & Méry, P.-F. (2001). G protein-mediated inhibitory effect of a nitric oxide donor on the L-type Ca 2+ current in rat ventricular myocytes. The Journal of Physiology, 531(1), 117–130. https://doi.org/10.1111/j.1469-7793.2001.0117j.x

Adams, S. R., Harootunian, A. T., Buechler, Y. J., Taylor, S. S., & Tsien, R. Y. (1991). Fluorescence ratio imaging of cyclic AMP in single cells. Nature, 349(6311), 694–697. https://doi.org/10.1038/349694a0

AHLQUIST, R. P. (1948). A study of the adrenotropic receptors. The American Journal of Physiology, 153(3), 586–600. https://doi.org/10.1152/ajplegacy.1948.153.3.586

Ahmad, F., Murata, T., Shimizu, K., Degerman, E., Maurice, D., & Manganiello, V. (2015). Cyclic nucleotide phosphodiesterases: Important signaling modulators and therapeutic targets. Oral Diseases, 21(1), e25–e50. https://doi.org/10.1111/odi.12275

Akita, T., Joyner, R. W., Lu, C., Kumar, R., & Hartzell, H. C. (1994). Developmental changes in modulation of calcium currents of rabbit ventricular cells by phosphodiesterase inhibitors. Circulation, 90(1), 469–478. https://doi.org/10.1161/01.CIR.90.1.469

Albini, A., Pennesi, G., Donatelli, F., Cammarota, R., De Flora, S., & Noonan, D. M. (2010). Cardiotoxicity of anticancer drugs: The need for cardio-oncology and cardio-oncological prevention. *Journal of the National Cancer Institute*, *102*(1), 14–25. https://doi.org/10.1093/jnci/djp440

Alessandra Moretti, P. D., Milena Bellin, P. D., Andrea Welling, P. D., Christian Billy Jung, M. S., Jason T. Lam, P. D., Lorenz Bott-Flügel, M. D., Tatjana Dorn, P. D., Alexander Goedel, M. D., Christian Höhnke, M. D., Franz Hofmann, M. D., Melchior Seyfarth, M. D., Daniel Sinnecker, M. D., Albert Schömig, M. D., & Karl-Ludwig Laugwitz, M. D. (2010). Patient-Specific Induced Pluripotent Stem-Cell Models for Long-QT Syndrome Alessandra. New England Journal of Medicine, 307–319. https://doi.org/10.1056/NEJMoa1203165

Alig, J., Marger, L., Mesirca, P., Ehmke, H., Mangoni, M. E., & Isbrandt, D. (2009). Control of heart rate by cAMP sensitivity of HCN channels. Proceedings of the National Academy of Sciences of the United States of America, 106(29), 12189–12194. https://doi.org/10.1073/pnas.0810332106

Allen, M. D., & Zhang, J. (2006). Subcellular dynamics of protein kinase A activity visualized by FRET-based reporters. Biochemical and Biophysical Research Communications, 348(2), 716–721. https://doi.org/10.1016/j.bbrc.2006.07.136

6. Bibliography

Antoni, F. A. (2000). Molecular diversity of cyclic AMP signalling. Frontiers in Neuroendocrinology, 21(2), 103–132. https://doi.org/10.1006/frne.1999.0193

Austin, M. A., Hutter, C. M., Zimmern, R. L., & Humpries, S. E. (2004). Familial hypercholesterolemia and coronary heart disease: A HuGE association review. American Journal of Epidemiology, 160(5), 421–429. https://doi.org/10.1093/aje/kwh237

Balfour, J. A. B., & Wiseman, L. R. (1999). Moxifloxacin. Drugs, 57(3), 363–373. https://doi.org/10.2165/00003495-199957030-00007

Bass, A., Kinter, L., & Williams, P. (2004). Origins, practices and future of safety pharmacology. Journal of Pharmacological and Toxicological Methods, 49(3), 145–151. https://doi.org/10.1016/j.vascn.2004.02.007

Bastug-özel, Z., Wright, P. T., Kraft, A. E., Pavlovic, D., Howie, J., Froese, A., Fuller, W., Gorelik, J., Shattock, M. J., & Nikolaev, V. O. (2018). Heart failure leads to altered b 2 - adrenoceptor / cAMP dynamics in the sarcolemmal phospholemman / Na , K ATPase microdomain. August. https://doi.org/10.1093/cvr/cvy221/5079901

Baxendale, R. W., & Fraser, L. R. (2005). Mammalian sperm phosphodiesterases and their involvement in receptor-mediated cell signaling important for capacitation. Molecular Reproduction and Development, 71(4), 495–508. https://doi.org/10.1002/mrd.20265

Bean, B. (1989). Classes Of Calcium Channels In Vertebrate Cells. Annual Review of Physiology, 51(1), 367–384. https://doi.org/10.1146/annurev.physiol.51.1.367

Beavo, J. A., & Reifsnyder, D. H. (1990). Primary sequence of cyclic nucleotide phosphodiesterase isozymes and the design of selective inhibitors. Trends in Pharmacological Sciences, 11(4), 150–155. https://doi.org/10.1016/0165-6147(90)90066-H

Belmonte, S. L., & Blaxall, B. C. (2011). G protein coupled receptor kinases as therapeutic targets in cardiovascular disease. Circulation Research, 109(3), 309–319. https://doi.org/10.1161/CIRCRESAHA.110.231233

Benitah, J. P., Alvarez, J. L., & Gómez, A. M. (2010). L-type Ca2+ current in ventricular cardiomyocytes. Journal of Molecular and Cellular Cardiology, 48(1), 26–36. https://doi.org/10.1016/j.yjmcc.2009.07.026

Benjamin, E. J., Blaha, M. J., Chiuve, S. E., Cushman, M., Das, S. R., Deo, R., De Ferranti, S. D., Floyd, J., Fornage, M., Gillespie, C., Isasi, C. R., Jim'nez, M. C., Jordan, L. C., Judd, S. E., Lackland, D., Lichtman, J. H., Lisabeth, L., Liu, S., Longenecker, C. T., … Muntner, P. (2017). Heart Disease and Stroke Statistics'2017 Update: A Report from the American Heart Association. In Circulation (Vol. 135, Issue 10). https://doi.org/10.1161/CIR.0000000000000485

Benjamin, E. J., Muntner, P., Alonso, A., Bittencourt, M. S., Callaway, C. W., Carson, A. P., Chamberlain, A. M., Chang, A. R., Cheng, S., Das, S. R., Delling, F. N., Djousse, L., Elkind, M. S. V., Ferguson, J. F., Fornage, M., Jordan, L. C., Khan, S. S., Kissela, B. M., Knutson, K. L., … Virani, S. S. (2019). Heart Disease and Stroke Statistics-2019 Update: A Report From the American Heart Association. In Circulation (Vol. 139, Issue 10). https://doi.org/10.1161/CIR.0000000000000659

6. Bibliography

Berger, W., Prinz, H., Striessnig, J., Kang, H. C., Haugland, R., & Glossmann, H. (1994). Complex Molecular Mechanism for Dihydropyridine Binding to L-Type Ca2+-Channels As Revealed by Fluorescence Resonance Energy Transfer. Biochemistry, 33(39), 11875–11883. https://doi.org/10.1021/bi00205a025

Berisha, F., Götz, K. R., Wegener, J. W., Jungen, C., Kraft, A. E., Warnke, S., Lindner, D., Westermann, D., Blankenberg, S., Meyer, C., Hasenfuß, G., Lehnart, S. E., & Nikolaev, V. O. (2019). Direct monitoring of cAMP at the cardiac ryanodine receptor using a novel targeted fluorescence biosensor mouse. https://doi.org/doi.org/10.1101/623934

Berisha, F., & Nikolaev, V. O. (2017). Cyclic nucleotide imaging and cardiovascular disease. Pharmacology and Therapeutics, 175, 107–115. https://doi.org/10.1016/j.pharmthera.2017.02.038

Berk, E., Christ, T., Schwarz, S., Ravens, U., Knaut, M., & Kaumann, A. J. (2016). In permanent atrial fibrillation, PDE3 reduces force responses to 5-HT, but PDE3 and PDE4 do not cause the blunting of atrial arrhythmias. British Journal of Pharmacology, 2478–2489. https://doi.org/10.1111/bph.13525

Bers, D. M. (2008). Calcium Cycling and Signaling in Cardiac Myocytes. Annual Review of Physiology, 70(1), 23–49. https://doi.org/10.1146/annurev.physiol.70.113006.100455

Bers, D. M., & Perez-Reyes, E. (1999). Ca channels in cardiac myocytes: Structure and function in Ca influx and intracellular Ca release. Cardiovascular Research, 42(2), 339–360. https://doi.org/10.1016/S0008-6363(99)00038-3

Bethke, T., Meyer, W., Schmitz, W., Scholz, H., Stein, B., Thomas, K., & Wenzlaff, H. (1992). Phosphodiesterase inhibition in ventricular cardiomyocytes from guinea-pig hearts. British Journal of Pharmacology, 107(1), 127–133. https://doi.org/10.1111/j.1476-5381.1992.tb14474.x

Bischoff, E. (2004). Potency, selectivity, and consequences of nonselectivity of PDE inhibition. International Journal of Impotence Research, 16(SUPPL. 1), 0–3. https://doi.org/10.1038/sj.ijir.3901208

Bolego, C. (2002). Smoking and gender. *Cardiovascular Research*, *53*(3), 568–576. https://doi.org/10.1016/S0008-6363(01)00520-X

Borchert, T., Hübscher, D., Guessoum, C. I., Lam, T. D. D., Ghadri, J. R., Schellinger, I. N., Tiburcy, M., Liaw, N. Y., Li, Y., Haas, J., Sossalla, S., Huber, M. A., Cyganek, L., Jacobshagen, C., Dressel, R., Raaz, U., Nikolaev, V. O., Guan, K., Thiele, H., … Streckfuss-Bömeke, K. (2017). Catecholamine-Dependent β-Adrenergic Signaling in a Pluripotent Stem Cell Model of Takotsubo Cardiomyopathy. Journal of the American College of Cardiology, 70(8), 975–991. https://doi.org/10.1016/j.jacc.2017.06.061

Borlaug, B. A., Melenovsky, V., Marhin, T., Fitzgerald, P., & Kass, D. A. (2005). Sildenafil inhibits β-adrenergic-stimulated cardiac contractility in humans. Circulation, 112(17), 2642–2649. https://doi.org/10.1161/CIRCULATIONAHA.105.540500

Börner, S., Schwede, F., Schlipp, A., Berisha, F., Calebiro, D., Lohse, M. J., & Nikolaev, V. O. (2011). FRET measurements of intracellular cAMP concentrations and cAMP analog permeability in intact cells. *Nature Protocols*, *6*(4), 427–438. https://doi.org/10.1038/nprot.2010.198

6. Bibliography

Breckwoldt, K., Letuffe-Brenière, D., Mannhardt, I., Schulze, T., Ulmer, B., Werner, T., Benzin, A., Klampe, B., Reinsch, M. C., Laufer, S., Shibamiya, A., Prondzynski, M., Mearini, G., Schade, D., Fuchs, S., Neuber, C., Krämer, E., Saleem, U., Schulze, M. L., Hansen, A. (2017). Differentiation of cardiomyocytes and generation of human engineered heart tissue. Nature Protocols, 12(6), 1177–1197. https://doi.org/10.1038/nprot.2017.033

Bristow, M. R., Ginsburg, R., Umans, V., Fowler, M., Minobe, W., Rasmussen, R., Zera, P., Menlove, R., Shah, P., & Jamieson, S. (1986). β1- and β2-adrenergic-receptor subpopulations in nonfailing and failing human ventricular myocardium: Coupling of both receptor subtypes to muscle contraction and selective β1-receptor down-regulation in heart failure. Circulation Research, 59(3), 297–309. https://doi.org/10.1161/01.RES.59.3.297

Brodde, O. -E. (1994). Adrenoceptors and their signal transduction mechanisms. Journal of Autonomic Pharmacology, 14(1), 3–4. https://doi.org/10.1111/j.1474-8673.1994.tb00581.x

Brodde, O. E., & Michel, M. C. (1999). Adrenergic and muscarinic receptors in the human heart. Pharmacological Reviews, 51(4), 651–690.

Calebiro, D., Nikolaev, V. O., Gagliani, M. C., De Filippis, T., Dees, C., Tacchetti, C., Persani, L., & Lohse, M. J. (2009). Persistent cAMP-signals triggered by internalized G-protein-coupled receptors. PLoS Biology, 7(8). https://doi.org/10.1371/journal.pbio.1000172

Castro, L. R. V., Schittl, J., & Fischmeister, R. (2010). Feedback control through cGMP-dependent protein kinase contributes to differential regulation and compartmentation of cGMP in rat cardiac myocytes. Circulation Research, 107(10), 1232–1240. https://doi.org/10.1161/CIRCRESAHA.110.226712

Castro, L. R. V., Verde, I., Cooper, D. M. F., & Fischmeister, R. (2006). Cyclic guanosine monophosphate compartmentation in rat cardiac myocytes. Circulation, 113(18), 2221–2228. https://doi.org/10.1161/CIRCULATIONAHA.105.599241

Catterall, W. A. (2014). Voltage-Gated Sodium Channels and Electrical Excitability of the Heart. In Cardiac Electrophysiology: From Cell to Bedside: Sixth Edition (Sixth Edit). Elsevier Inc. https://doi.org/10.1016/B978-1-4557-2856-5.00001-7

Catterall, W. a. (2000). Structure and Regulation of Voltage-Gated Ca 2+ Channels. Annual Review of Cell and Developmental Biology, 16(1), 521–555. https://doi.org/10.1146/annurev.cellbio.16.1.521

Cazzola, M., Matera, M. G., & Donner, C. F. (2005). Inhaled ??2-Adrenoceptor Agonists. *Drugs*, *65*(12), 1595–1610.

https://doi.org/10.2165/00003495-200565120-00001

Champagne, S., Coste, E., Peyrière, H., Nigond, J., Mania, E., Pons, M., Hillaire-Buys, D., Balmes, P., Blayac, J.-P., & Davy, J.-M. (1999). Chronic Constrictive Pericarditis Induced by Long-Term Bromocriptine Therapy: Report of Two Cases. *Annals of Pharmacotherapy*, *33*(10), 1050–1054.

https://doi.org/10.1345/aph.18461

Chao, C. L., Chen, W. J., Chen, M. F., & Lee, Y. T. (1996). Torsade de pointes in a patient using usual dose of beta agonist therapy. *International Journal of Cardiology*, *57*(3), 295–296. https://doi.org/10.1016/S0167-5273(96)02831-8

6. Bibliography

Chen, J., Levin, L. R., & Buck, J. (2012). Role of soluble adenylyl cyclase in the heart. American Journal of Physiology - Heart and Circulatory Physiology, 302(3), 538–543. https://doi.org/10.1152/ajpheart.00701.2011

Christ, T., Engel, A., Ravens, U., & Kaumann, A. J. (2006). Cilostamide potentiates more the positive inotropic effects of (-)-adrenaline through β2-adrenoceptors than the effects of (-)-noradrenaline through β1-adrenoceptors in human atrial myocardium. Naunyn-Schmiedeberg's Archives of Pharmacology, 374(3), 249–253. https://doi.org/10.1007/s00210-006-0119-5

Christ, Torsten, Galindo-Tovar, A., Thoms, M., Ravens, U., & Kaumann, A. J. (2009). Inotropy and L-type Ca 2+ current, activated by β 1- and β 2-adrenoceptors, are differently controlled by phosphodiesterases 3 and 4 in rat heart. British Journal of Pharmacology, 156(1), 62–83. https://doi.org/10.1111/j.1476-5381.2008.00015.x

Christ, Torsten, Rozmaritsa, N., Engel, A., Berk, E., Knaut, M., Metzner, K., Canteras, M., Ravens, U., & Kaumann, A. (2014). Arrhythmias, elicited by catecholamines and serotonin, vanish in human chronic atrial fibrillation. Proceedings of the National Academy of Sciences, 111(30), 11193–11198. https://doi.org/10.1073/pnas.1324132111

Clegg, R. M., Murchie, A. I., & Lilley, D. M. (1994). The solution structure of the four-way DNA junction at low-salt conditions: a fluorescence resonance energy transfer analysis. Biophysical Journal, 66(1), 99–109. https://doi.org/10.1016/S0006-3495(94)80765-9

Colan, S. D., Liberthson, R. R., Cahen, L., Shannon, D. C., & Kelly, D. H. (1984). Incidence and significance of primary abnormalities of cardiac rhythm in infants at high risk for sudden infant death syndrome. Pediatric Cardiology, 5(4), 267–271. https://doi.org/10.1007/BF02424971

Colatsky, T., Fermini, B., Gintant, G., Pierson, J. B., Sager, P., Sekino, Y., Strauss, D. G., & Stockbridge, N. (2016). The Comprehensive in Vitro Proarrhythmia Assay (CiPA) initiative — Update on progress. Journal of Pharmacological and Toxicological Methods, 81, 15–20. https://doi.org/10.1016/j.vascn.2016.06.002

Connolly, H. M., Crary, J. L., McGoon, M. D., Hensrud, D. D., Edwards, B. S., Edwards, W. D., & Schaff, H. V. (1997). Valvular Heart Disease Associated with Fenfluramine–Phentermine. *New England Journal of Medicine*, *337*(9), 581–588. https://doi.org/10.1056/NEJM199708283370901

Corbin, J. D., Turko, I. V., Beasley, A., & Francis, S. H. (2000). Phosphorylation of phosphodiesterase-5 by cyclic nucleotide-dependent protein kinase alters its catalytic and allosteric cGMP-binding activities. European Journal of Biochemistry, 267(9), 2760–2767. https://doi.org/10.1046/j.1432-1327.2000.01297.x

Cordula M. Wolf and Charles I. Berul. (2008). Molecular mechanisms of inherited cardiomyopathies. Physiological Reviews, 82(4), 945–980. https://doi.org/10.1152/physrev.00012.2002

Coulter, D. M., Bate, A., Meyboom, R. H. B., Lindquist, M., & Edwards, I. R. (2001). Antipsychotic drugs and heart muscle disorder in international pharmacovigilance: Data mining study. *British Medical Journal*, *322*(7296), 1207–1209. https://doi.org/10.1136/bmj.322.7296.1207

6. Bibliography

Craven, K. B., & Zagotta, W. N. (2006). CNG AND HCN CHANNELS: Two Peas, One Pod. Annual Review of Physiology, 68(1), 375–401. https://doi.org/10.1146/annurev.physiol.68.040104.134728

Cremers, B., Scheler, M., Maack, C., Wendler, O., Schäfers, H. J., Südkamp, M., & Böhm, M. (2003). Effects of sildenafil (Viagra) on human myocardial contractility, in vitro arrhythmias, and tension of internal mammaria arteries and saphenous veins. Journal of Cardiovascular Pharmacology, 41(5), 734–743. https://doi.org/10.1097/00005344-200305000-00010

Curto, M., Girardi, N., Lionetto, L., Ciavarella, G. M., Ferracuti, S., & Baldessarini, R. J. (2016). Systematic Review of Clozapine Cardiotoxicity. Current Psychiatry Reports, 18(7). https://doi.org/10.1007/s11920-016-0704-3

De Arcangelis, V., Soto, D., & Xiang, Y. (2008). Phosphodiesterase 4 and phosphatase 2A differentially regulate cAMP/protein kinase A signaling for cardiac myocyte contraction under stimulation of β1 adrenergic receptor. Molecular Pharmacology, 74(5), 1453–1462. https://doi.org/10.1124/mol.108.049718

De Ponti, F., Poluzzi, E., & Montanaro, N. (2001). Organising evidence on QT prolongation and occurrence of Torsades de Pointes with non-antiarrhythmic drugs: A call for consensus. European Journal of Clinical Pharmacology, 57(3), 185–209. https://doi.org/10.1007/s002280100290

De Rooij, J., Zwartkruis, F. J. T., Verheijen, M. H. G., Cool, R. H., Nijman, S. M. B., Wittinghofer, A., & Bos, J. L. (1998). Epac is a Rap1 guanine-nucleotide-exchange factor directly activated by cyclic AMP. Nature, 396(6710), 474–477. https://doi.org/10.1038/24884

Degen, C. V., Bishu, K., Zakeri, R., Ogut, O., Redfield, M. M., & Brozovich, F. V. (2015). The Emperor's New Clothes: PDE5 and the Heart. PLOS ONE, 10(3), e0118664. https://doi.org/10.1371/journal.pone.0118664

Dessauer, C. W., Watts, V. J., Ostrom, R. S., Conti, M., Dove, S., & Seifert, R. (2017). International union of basic and clinical pharmacology. CI. structures and small molecule modulators of mammalian adenylyl cyclases. Pharmacological Reviews, 69(2), 96–139. https://doi.org/10.1124/pr.116.013078

Di Benedetto, G., Zoccarato, A., Lissandron, V., Terrin, A., Li, X., Houslay, M. D., Baillie, G. S., & Zaccolo, M. (2008). Protein kinase A type i and type II define distinct intracellular signaling compartments. Circulation Research, 103(8), 836–844. https://doi.org/10.1161/CIRCRESAHA.108.174813

Ding, B., Abe, J. I., Wei, H., Huang, Q., Walsh, R. A., Molina, C. A., Zhao, A., Sadoshima, J., Blaxall, B. C., Berk, B. C., & Yan, C. (2005). Functional role of phosphodiesterase 3 in cardiomyocyte apoptosis: Implication in heart failure. Circulation, 111(19), 2469–2476. https://doi.org/10.1161/01.CIR.0000165128.39715.87

DiPilato, L. M., Cheng, X., & Zhang, J. (2004). Fluorescent indicators of cAMP and Epac activation reveal differential dynamics of cAMP signaling within discrete subcellular compartments. Proceedings of the National Academy of Sciences of the United States of America, 101(47), 16513–16518. https://doi.org/10.1073/pnas.0405973101

Dunkern, T. R., & Hatzelmann, A. (2007). Characterization of inhibitors of phosphodiesterase 1C on a human cellular system. FEBS Journal, 274(18), 4812–4824. https://doi.org/10.1111/j.1742-4658.2007.06001.x

6. Bibliography

Eisner, D. A., Caldwell, J. L., Kistamás, K., & Trafford, A. W. (2017). Calcium and Excitation-Contraction Coupling in the Heart. Circulation Research, 121(2), 181–195. https://doi.org/10.1161/CIRCRESAHA.117.310230

El-Armouche, A., & Eschenhagen, T. (2009). β-Adrenergic stimulation and myocardial function in the failing heart. Heart Failure Reviews, 14(4), 225–241. https://doi.org/10.1007/s10741-008-9132-8

Eschenhagen, T. (2013). PDE4 in the human heart - Major player or little helper? British Journal of Pharmacology, 169(3), 524–527. https://doi.org/10.1111/bph.12168

Fabiato, A., & Fabiato, F. (1975). Contractions induced by a calcium-triggered release of calcium from the sarcoplasmic reticulum of single skinned cardiac cells. The Journal of Physiology, 249(3), 469–495. https://doi.org/10.1113/jphysiol.1975.sp011026

Faria J, , Barbosa J1, 2, 3§, Moreira R1, Queirós O1, Carvalho F2, D.-O. R. (2016). COMPARATIVE PHARMACOLOGY AND TOXICOLOGY OF TRAMADOL AND TAPENTADOL. International Journal of Laboratory Hematology, 38(1), 42–49. https://doi.org/10.1002/ejp.1196

Fawcett, L., Baxendale, R., Stacey, P., McGrouther, C., Harrow, I., Soderling, S., Hetman, J., Beavo, J. A., & Phillips, S. C. (2000). Molecular cloning and characterization of a distinct human phosphodiesterase gene family: PDE11A. Proceedings of the National Academy of Sciences of the United States of America, 97(7), 3702–3707. https://doi.org/10.1073/pnas.97.7.3702

Ferdinandy, P., Baczkó, I., Bencsik, P., Giricz, Z., Görbe, A., Pacher, P., Varga, Z. V., Varró, A., & Schulz, R. (2019). Definition of hidden drug cardiotoxicity: Paradigm change in cardiac safety testing and its clinical implications. European Heart Journal, 40(22), 1771-1777C. https://doi.org/10.1093/eurheartj/ehy365

Ferguson, R. (2013). Towards the Synthesis of Novel Photoactivatable Fluorescent Probes for Use in Super-Resolution Microscopy Robert Ferguson submitted for the degree of Master of Research Heriot Watt University, School of Engineering and Physical Sciences. September 2013.https://www.researchgate.net/publication/320870943_Towards_the_Synthesis_of_Novel_Photoactivatable_Fluorescent_Probes_for_Use_in_Super-Resolution_Microscopy

Fermini, B., Coyne, K. P., & Coyne, S. T. (2018). Challenges in designing and executing clinical trials in a dish studies. Journal of Pharmacological and Toxicological Methods, 94, 73–82. https://doi.org/10.1016/j.vascn.2018.09.002

Fields, L. A. (2013). (2013). Local cAMP signalling and phosphodiesterase activity in an in vitro model of cardiac hypertrophy. http://theses.gla.ac.uk/4755

Fisher, P. W., Salloum, F., Das, A., Hyder, H., & Kukreja, R. C. (2005). Phosphodiesterase-5 inhibition with sildenafil attenuates cardiomyocyte apoptosis and left ventricular dysfunction in a chronic model of doxorubicin cardiotoxicity. Circulation, 111(13), 1601–1610. https://doi.org/10.1161/01.CIR.0000160359.49478.C2

Force, T., & Kolaja, K. L. (2011). Cardiotoxicity of kinase inhibitors: The prediction and translation of preclinical models to clinical outcomes. *Nature Reviews Drug Discovery*, *10*(2), 111–126.https://doi.org/10.1038/nrd3252

6. Bibliography

Francis, G. S. (2008). The contemporary use of digoxin for the treatment of heart failure. Circulation. Heart Failure, 1(3), 208–209. https://doi.org/10.1161/CIRCHEARTFAILURE.108.806646

Francis, S. H., Bessay, E. P., Kotera, J., Grimes, K. A., Liu, L., Joseph Thompson, W., & Corbin, J. D. (2002). Phosphorylation of isolated human phosphodiesterase-5 regulatory domain induces an apparent conformational change and increases cGMP binding affinity. Journal of Biological Chemistry, 277(49), 47581–47587. https://doi.org/10.1074/jbc.M206088200

Francis, S. H., & Houslay, M. D. (2006). Cyclic Nucleotide Phosphodiesterases in Health and Disease. In Cyclic Nucleotide Phosphodiesterases in Health and Disease. https://doi.org/10.1201/9781420020847

Frolov, R. V., Ignatova, I. I., & Singh, S. (2011). Inhibition of herg potassium channels by celecoxib and its mechanism. PLoS ONE, 6(10), 1–7. https://doi.org/10.1371/journal.pone.0026344

Galindo-Tovar, A., Vargas, M. L., Escudero, E., & Kaumann, A. J. (2009). Ontogenic changes of the control by phosphodiesterase-3 and -4 of 5-HT responses in porcine heart and relevance to human atrial 5-HT 4 receptors. British Journal of Pharmacology, 156(2), 237–249. https://doi.org/10.1111/j.1476-5381.2008.00023.x

Galindo-Tovar, A., Vargas, M. L., & Kaumann, A. J. (2018). Phosphodiesterase PDE2 activity, increased by isoprenaline, does not reduce β-adrenoceptor-mediated chronotropic and inotropic effects in rat heart. Naunyn-Schmiedeberg's Archives of Pharmacology, 391(6), 571–585. https://doi.org/10.1007/s00210-018-1480-x

Gao, T., Yatani, A., Dell'Acqua, M. L., Sako, H., Green, S. A., Dascal, N., Scott, J. D., & Hosey, M. M. (1997). cAMP-dependent regulation of cardiac L-type Ca2+ channels requires membrane targeting of PKA and phosphorylation of channel subunits. Neuron, 19(1), 185–196. https://doi.org/10.1016/S0896-6273(00)80358-X

Gauthier, C., Tavernier, G., Charpentier, F., Langin, D., & Le Marec, H. (1996). Functional beta3-adrenoceptor in the human heart. Journal of Clinical Investigation, 98(2), 556–562. https://doi.org/10.1172/JCI118823

Giordano, D., De Stefano, M. E., Citro, G., Modica, A., & Giorgi, M. (2001). Expression of cGMP-binding cGMP-specific phosphodiesterase (PDE5) in mouse tissues and cell lines using an antibody against the enzyme amino-terminal domain. Biochimica et Biophysica Acta - Molecular Cell Research, 1539(1–2), 16–27. https://doi.org/10.1016/S0167-4889(01)00086-6

Goaillard, J. M., Vincent, P., & Fischmeister, R. (2001). Simultaneous measurements of intracellular cAMP and L-type Ca2+ current in single frog ventricular myocytes. Journal of Physiology, 530(1), 79–91. https://doi.org/10.1111/j.1469-7793.2001.0079m.x

Goldstein, R. E., Boccuzzi, S. J., Cruess, D., Nattel, S., Friday, K., Lenkei, S., Nattel, S., & Rubison, M. (1991). Diltiazem increases late-onset congestive heart failure in postinfarction patients with early reduction in ejection fraction. *Circulation*, *83*(1), 52–60. https://doi.org/10.1161/01.CIR.83.1.52

6. Bibliography

Guellich, A., Mehel, H., & Fischmeister, R. (2014). Cyclic AMP synthesis and hydrolysis in the normal and failing heart. Pflugers Archiv European Journal of Physiology, 466(6), 1163–1175. https://doi.org/10.1007/s00424-014-1515-1

Hagiwara, N., & Kameyama, M. (1988). Nobuhisa hagiwara, hiroshi. Journal of Physiology, 395, 233–253. https://physoc.onlinelibrary.wiley.com/doi/abs/10.1113/jphysiol.1988.sp016916

Hambleton, R., Krall, J., Tikishvili, E., Honeggar, M., Ahmad, F., Manganiello, V. C., & Movsesian, M. A. (2005). Isoforms of cyclic nucleotide phosphodiesterase PDE3 and their contribution to cAMP hydrolytic activity in subcellular fractions of human myocardium. Journal of Biological Chemistry, 280(47), 39168–39174. https://doi.org/10.1074/jbc.M506760200

Han, J., Kim, E., Lee, S. H., Yoo, S., Ho, W. K., & Earm, Y. E. (1998). cGMP facilitates calcium current via cGMP-dependent protein kinase in isolated rabbit ventricular myocytes. Pflugers Archiv European Journal of Physiology, 435(3), 388–393. https://doi.org/10.1007/s004240050528

Hanoune, J., & Defer, N. (2001). REGULATION AND ROLE OF ADENYLYL CYCLASE ISOFORMS. Annual Review of Pharmacology and Toxicology, 41(1), 145–174. https://doi.org/10.1146/annurev.pharmtox.41.1.145

Hetman, J. M., Robas, N., Baxendale, R., Fidock, M., Phillips, S. C., Soderling, S. H., & Beavo, J. A. (2000). Cloning and characterization of two splice variants of human phosphodiesterase 11A. Proceedings of the National Academy of Sciences of the United States of America, 97(23), 12891–12895. https://doi.org/10.1073/pnas.200355397

Heubach, J. F., Rau, T., Eschenhagen, T., Ravens, U., & Kaumann, A. J. (2002). Physiological antagonism between ventricular β1-adrenoceptors and α1-adrenoceptors but no evidence for β2- and β3-adrenoceptor function in murine heart. British Journal of Pharmacology, 136(2), 217–229. https://doi.org/10.1038/sj.bjp.0704700

Himmel, H. M., Bussek, A., Hoffmann, M., Beckmann, R., Lohmann, H., Schmidt, M., & Wettwer, E. (2012). Field and action potential recordings in heart slices: Correlation with established in vitro and in vivo models. British Journal of Pharmacology, 166(1), 276–296. https://doi.org/10.1111/j.1476-5381.2011.01775.x

Hirano, Y., Fozzard, H. A., & January, C. T. (1989). Characteristics of L- and T-type Ca2+ currents in canine cardiac Purkinje fibers. American Journal of Physiology - Heart and Circulatory Physiology, 256(5). https://doi.org/10.1152/ajpheart.1989.256.5.h1478

Hirt, M. N., Sörensen, N. A., Bartholdt, L. M., Boeddinghaus, J., Schaaf, S., Eder, A., Vollert, I., Stöhr, A., Schulze, T., Witten, A., Stoll, M., Hansen, A., & Eschenhagen, T. (2012). Increased afterload induces pathological cardiac hypertrophy: A new in vitro model. Basic Research in Cardiology, 107(6). https://doi.org/10.1007/s00395-012-0307-z

Hoffmann, C., Leitz, M. R., Oberdorf-Maass, S., Lohse, M. J., & Klotz, K.-N. (2004). Comparative pharmacology of human β-adrenergic receptor subtypes-characterization of stably transfected receptors in CHO cells. Naunyn-Schmiedeberg's Archives of Pharmacology, 369(2), 151–159. https://doi.org/10.1007/s00210-003-0860-y

Honda, M., Kiyokawa, J., Tabo, M., & Inoue, T. (2011). Electrophysiological characterization of cardiomyocytes derived from human induced pluripotent stem cells. Journal of Pharmacological Sciences, 117(3), 149–159. https://doi.org/10.1254/jphs.11038FP

6. Bibliography

Honig, P. K., Wortham, D. C., Zamani, K., Conner, D. P., Mullin, J. C., & Cantilena, L. R. (1993). Terfenadine-Ketoconazole Interaction: Pharmacokinetic and Electrocardiographic Consequences. *JAMA: The Journal of the American Medical Association*, *269*(12), 1513–1518. https://doi.org/10.1001/jama.1993.03500120051025

Horváth, A., Christ, T., Koivumäki, J. T., Prondzynski, M., Zech, A. T. L., Spohn, M., Saleem, U., Mannhardt, I., Ulmer, B., Girdauskas, E., Meyer, C., Hansen, A., Eschenhagen, T., & Lemoine, M. D. (2020). Case Report on: Very Early Afterdepolarizations in HiPSC-Cardiomyocytes—An Artifact by Big Conductance Calcium Activated Potassium Current (Ibk,Ca). Cells, 9(1), 253. https://doi.org/10.3390/cells9010253

Houslay, M. D., & Adams, D. R. (2003). PDE4 cAMP phosphodiesterases: Modular enzymes that orchestrate signalling cross-talk, desensitization and compartmentalization. Biochemical Journal, 370(1), 1–18. https://doi.org/10.1042/BJ20021698

Hove-Madsen, L., Mery, P. F., Jurevicius, J., Skeberdis, A. V., & Fischmeister, R. (1996). Regulation of myocardial calcium channels by cyclic AMP metabolism. Basic Research in Cardiology, Supplement, 91(2), 1–8. https://doi.org/10.1007/bf00795355

Insel, P. A., & Ostrom, R. S. (2003). Forskolin as a tool for examining adenylyl cyclase expression, regulation, and G protein signaling. Cellular and Molecular Neurobiology, 23(3), 305–314. https://doi.org/10.1023/A:1023684503883

Isenberg, G. (1982). Ca entry and contraction as studied in isolated bovine ventricular myocytes. Zeitschrift Fur Naturforschung - Section C Journal of Biosciences, 37(5–6), 502–512. https://doi.org/10.1515/znc-1982-5-623

Ishikawa, N., Imamura, T., Nakajima, K., Yamaga, J., Yuchi, H., Ootsuka, M., Inatsu, H., Aoki, T., & Eto, T. (2001). Acute pericarditis associated with 5-aminosalicylic acid (5-ASA) treatment for severe active ulcerative colitis. *Internal Medicine*, *40*(9), 901–904. https://doi.org/10.2169/internalmedicine.40.901

Isidori, A. M., Cornacchione, M., Barbagallo, F., Di Grazia, A., Barrios, F., Fassina, L., Monaco, L., Giannetta, E., Gianfrilli, D., Garofalo, S., Zhang, X., Chen, X., Xiang, Y. K., Lenzi, A., Pellegrini, M., & Naro, F. (2015). Inhibition of type 5 phosphodiesterase counteracts β2-adrenergic signalling in beating cardiomyocytes. Cardiovascular Research, 106(3), 408–420. https://doi.org/10.1093/cvr/cvv123

Ismaili, D., Geelhoed, B., & Christ, T. (2020). Ca2+ currents in cardiomyocytes: How to improve interpretation of patch clamp data? Progress in Biophysics and Molecular Biology, xxxx. https://doi.org/10.1016/j.pbiomolbio.2020.05.003

Johnson, A. E. (2005). Fluorescence approaches for determining protein conformations, interactions and mechanisms at membranes. Traffic, 6(12), 1078–1092. https://doi.org/10.1111/j.1600-0854.2005.00340.x

Johnson, W. B., Katugampola, S., Able, S., Napier, C., & Harding, S. E. (2012). Profiling of cAMP and cGMP phosphodiesterases in isolated ventricular cardiomyocytes from human hearts: Comparison with rat and guinea pig. Life Sciences, 90(9–10), 328–336. https://doi.org/10.1016/j.lfs.2011.11.016

Kajimoto, K., Hagiwara, N., Kasanuki, H., & Hosoda, S. (1997). Contribution of phosphodiesterase isozymes to the regulation of the L-type calcium current in human cardiac myocytes. British Journal of Pharmacology, 121(8), 1549–1556. https://doi.org/10.1038/sj.bjp.0701297

6. Bibliography

Kameyama, M., Hescheler, J., Hofmann, F., & Trautwein, W. (1986). Modulation of Ca current during the phosphorylation cycle in the guinea pig heart. Pflügers Archiv European Journal of Physiology, 407(2), 123–128. https://doi.org/10.1007/BF00580662

Kamp, T. J., & Hell, J. W. (2000). Regulation of cardiac L-type calcium channels by protein kinase A and protein kinase C. Circulation Research, 87(12), 1095–1102. https://doi.org/10.1161/01.RES.87.12.1095

Karakikes, I., Ameen, M., Termglinchan, V., & Wu, J. C. (2015). Human Induced Pluripotent Stem Cell-Derived Cardiomyocytes: Insights into Molecular, Cellular, and Functional Phenotypes. Circulation Research, 117(1), 80–88. https://doi.org/10.1161/CIRCRESAHA.117.305365

Kathleen Dracup, DNSc; Sharon McKinley, RN, PhD; Lynn V. Doering, RN, DNSc; Barbara Riegel, RN, DNSc; Hendrika Meischke, PhD; Debra K. Moser, RN, DNSc; Michele Pelter, RN, PhD; Beverly Carlson, RN, MS; Leanne Aitken, RN, PhD; Andrea Marshall, RN, MS; Rebe, P., & Background: (2008). Acute coronary syndrome. Surgical Critical Care Therapy: A Clinically Oriented Practical Approach, 168(10), 1049–1054. https://doi.org/10.1007/978-3-319-71712-8_10

Kaumann, A. J., & Molenaar, P. (1997). Modulation of human cardiac function through 4 β-adrenoceptor populations. Naunyn-Schmiedeberg's Archives of Pharmacology, 355(6), 667–681. https://doi.org/10.1007/PL00004999

Kerin, N. Z., & Somberg, J. (1994). Proarrhythmia: Definition, risk factors, causes, treatment, and controversies. *American Heart Journal*, *128*(3), 575–585. https://doi.org/10.1016/0002-8703(94)90634-3

Khanna, P. L., & Ullman, E. F. (1980). 4′,5′-dimethoxy-6-carboxyfluorescein: A novel dipole-dipole coupled fluorescence energy transfer acceptor useful for fluorescence immunoassays. Analytical Biochemistry, 108(1), 156–161. https://doi.org/10.1016/0003-2697(80)90706-X

Kincaid, R. L., Stith-Coleman, I. E., & Vaughan, M. (1985). Proteolytic activation of calmodulin-dependent cyclic nucleotide phosphodiesterase. Journal of Biological Chemistry, 260(15), 9009–9015. https://www.jbc.org/content/260/15/9009.full.pdf

Kobrinsky, E., Tiwari, S., Maltsev, V. A., Harry, J. B., Lakatta, E., Abernethy, D. R., & Soldatov, N. M. (2005). Differential role of the α1C subunit tails in regulation of the Cav1.2 channel by membrane potential, β subunits, and Ca2+ ions. Journal of Biological Chemistry, 280(13), 12474–12485. https://doi.org/10.1074/jbc.M412140200

Kotera, J., Fujishige, K., Imai, Y., Kawai, E., Michibata, H., Akatsuka, H., Yanaka, N., & Omori, K. (1999). Genomic origin and transcriptional regulation of two variants of cGMP- binding cGMP-specific phosphodiesterases. European Journal of Biochemistry, 262(3), 866–872. https://doi.org/10.1046/j.1432-1327.1999.00450.x

Kristóf, A., Husti, Z., Koncz, I., Kohajda, Z., Szél, T., Juhász, V., Biliczki, P., Jost, N., Baczkó, I., Papp, J. G., Varró, A., & Virág, L. (2012). Diclofenac Prolongs Repolarization in Ventricular Muscle with Impaired Repolarization Reserve. PLoS ONE, 7(12), 1–9. https://doi.org/10.1371/journal.pone.0053255

Laflamme, M. A., & Murry, C. E. (2011). Heart regeneration. Nature, 473(7347), 326–335. https://doi.org/10.1038/nature10147

Landis, I. K. and J., & The. (2004). Can the pharmaceutical industry reduce attrition rates?Architectural Record, 3(3), 711–715. https://doi.org/10.1038/news070604-1

6. Bibliography

Laverty, H. G., Benson, C., Cartwright, E. J., Cross, M. J., Garland, C., Hammond, T., Holloway, C., McMahon, N., Milligan, J., Park, B. K., Pirmohamed, M., Pollard, C., Radford, J., Roome, N., Sager, P., Singh, S., Suter, T., Suter, W., Trafford, A., … Valentin, J. P. (2011). How can we improve our understanding of cardiovascular safety liabilities to develop safer medicines? *British Journal of Pharmacology*, *163*(4), 675–693. https://doi.org/10.1111/j.1476-5381.2011.01255.x

Lee, L. G., Livak, K. J., Mullah, B., Graham, R. J., Vinayak, R. S., & Woudenberg, T. M. (1999). Seven-color, homogeneous detection of six PCR products. BioTechniques, 27(2), 342–349. https://doi.org/10.2144/99272rr01

Lee, S. Y., Kim, Y. J., Kim, K. T., Choe, H., & Jo, S. H. (2006). Blockade of HERG human K + channels and I (Kr) of guinea-pig cardiomyocytes by the antipsychotic drug clozapine. British Journal of Pharmacology, 148(4), 499–509. https://doi.org/10.1038/sj.bjp.0706744

Lehnart, S. E., Wehrens, X. H. T., Reiken, S., Warrier, S., Belevych, A. E., Harvey, R. D., Richter, W., Jin, S. L. C., Conti, M., & Marks, A. R. (2005). Phosphodiesterase 4D deficiency in the ryanodine-receptor complex promotes heart failure and arrhythmias. Cell, 123(1), 25–35. https://doi.org/10.1016/j.cell.2005.07.030

Lemme, M., Ulmer, B. M., Lemoine, M. D., Zech, A. T. L., Flenner, F., Ravens, U., Reichenspurner, H., Rol-Garcia, M., Smith, G., Hansen, A., Christ, T., & Eschenhagen, T. (2018). Atrial-like Engineered Heart Tissue: An In Vitro Model of the Human Atrium. Stem Cell Reports, 11(6), 1378–1390. https://doi.org/10.1016/j.stemcr.2018.10.008

Leroy, J., Abi-Gerges, A., Nikolaev, V. O., Richter, W., Lechêne, P., Mazet, J. L., Conti, M., Fischmeister, R., & Vandecasteele, G. (2008). Spatiotemporal dynamics of β-adrenergic cAMP signals and L-type Ca2+ channel regulation in adult rat ventricular myocytes: Role of phosphodiesterases. Circulation Research, 102(9), 1091–1100. https://doi.org/10.1161/CIRCRESAHA.107.167817

Leroy, J., Richter, W., Mika, D., Castro, L. R. V., Abi-Gerges, A., Xie, M., Scheitrum, C., Lefebvre, F., Schittl, J., Mateo, P., Westenbroek, R., Catterall, W. A., Charpentier, F., Conti, M., Fischmeister, R., & Vandecasteele, G. (2011). Phosphodiesterase 4B in the cardiac L-type Ca2+ channel complex regulates Ca2+ current and protects against ventricular arrhythmias in mice. Journal of Clinical Investigation, 121(7), 2651–2661. https://doi.org/10.1172/JCI44747

Lezoualc'H, F., Fazal, L., Laudette, M., & Conte, C. (2016). Cyclic AMP sensor EPAC proteins and their role in cardiovascular function and disease. Circulation Research, 118(5), 881–897. https://doi.org/10.1161/CIRCRESAHA.115.306529

Libretto, S. E. (1994). A review of the toxicology of salbutamol (albuterol). *Archives of Toxicology*, *68*(4), 213–216. https://doi.org/10.1007/s002040050059

Lindegger, N., & Niggli, E. (2005). Paradoxical SR Ca2+ release in guinea-pig cardiac myocytes after β-adrenergic stimulation revealed by two-photon photolysis of caged Ca2+. Journal of Physiology, 565(3), 801–813. https://doi.org/10.1113/jphysiol.2005.084376

Lohse, M. J., Engelhardt, S., & Eschenhagen, T. (2003). What Is the Role of β-Adrenergic Signaling in Heart Failure? Circulation Research, 93(10), 896–906. https://doi.org/10.1161/01.RES.0000102042.83024.CA

6. Bibliography

Loughney, K., Martins, T. J., Harris, E. A. S., Sadhu, K., Hicks, J. B., Sonnenburg, W. K., Beavo, J. A., & Ferguson, K. (1996). Isolation and characterization of cDNAs corresponding to two human calcium, calmodulin-regulated, 3′,5′-cyclic nucleotide phosphodiesterase. Journal of Biological Chemistry, 271(2), 796–806. https://doi.org/10.1074/jbc.271.2.796

Lu, H. R., Mariën, R., Saels, A., & De Clerck, F. (2001). Species plays an important role in drug-induced prolongation of action potential duration and early afterdepolarizations in isolated Purkinje fibers. Journal of Cardiovascular Electrophysiology, 12(1), 93–102. https://doi.org/10.1046/j.1540-8167.2001.00093.x

Lu, Z., Xu, X., Hu, X., Lee, S., Traverse, J. H., Zhu, G., Fassett, J., Tao, Y., Zhang, P., Remedios, C. Dos, Pritzker, M., Hall, J. L., Garry, D. J., & Chen, Y. (2010). Oxidative stress regulates left ventricular PDE5 expression in the failing heart. Circulation, 121(13), 1474–1483. https://doi.org/10.1161/CIRCULATIONAHA.109.906818

Lugnier, C., Schoeffter, P., Le Bec, A., Strouthou, E., & Stoclet, J. C. (1986). Selective inhibition of cyclic nucleotide phosphodiesterases of human, bovine and rat aorta. Biochemical Pharmacology, 35(10), 1743–1751. https://doi.org/10.1016/0006-2952(86)90333-3

Lukyanenko, Y. O., Younes, A., Lyashkov, A. E., Tarasov, K. V., Riordon, D. R., Lee, J., Sirenko, S. G., Kobrinsky, E., Ziman, B., Tarasova, Y. S., Juhaszova, M., Sollott, S. J., Graham, D. R., & Lakatta, E. G. (2016). Ca2 +/calmodulin-activated phosphodiesterase 1A is highly expressed in rabbit cardiac sinoatrial nodal cells and regulates pacemaker function. Journal of Molecular and Cellular Cardiology, 98, 73–82. https://doi.org/10.1016/j.yjmcc.2016.06.064

Lymperopoulos, A., Rengo, G., & Koch, W. J. (2013). Adrenergic nervous system in heart failure: Pathophysiology and therapy. Circulation Research, 113(6), 739–753. https://doi.org/10.1161/CIRCRESAHA.113.300308

MacDonald, J. S., & Robertson, R. T. (2009). Toxicity testing in the 21st century: A view from the pharmaceutical industry. Toxicological Sciences, 110(1), 40–46. https://doi.org/10.1093/toxsci/kfp088

Mannhardt, I., Breckwoldt, K., Letuffe-Brenière, D., Schaaf, S., Schulz, H., Neuber, C., Benzin, A., Werner, T., Eder, A., Schulze, T., Klampe, B., Christ, T., Hirt, M. N., Huebner, N., Moretti, A., Eschenhagen, T., & Hansen, A. (2016). Human Engineered Heart Tissue: Analysis of Contractile Force. Stem Cell Reports, 7(1), 29–42. https://doi.org/10.1016/j.stemcr.2016.04.011

Marchese, A., George, S. R., Kolakowski, L. F., Lynch, K. R., & O'Dowd, B. F. (1999). Novel GPCRs and their endogenous ligands: Expanding the boundaries of physiology and pharmacology. Trends in Pharmacological Sciences, 20(9), 370–375. https://doi.org/10.1016/S0165-6147(99)01366-8

Marcu, I. C., Illaste, A., Heuking, P., Jaconi, M. E., & Ullrich, N. D. (2015). Functional Characterization and Comparison of Intercellular Communication in Stem Cell-Derived Cardiomyocytes. STEM CELLS, 33(7), 2208–2218. https://doi.org/10.1002/stem.2009

Marquardt, K., & Albertson, T. E. (2001). Treatment of hydroxychloroquine overdose. *American Journal of Emergency Medicine*, *19*(5), 420–424. https://doi.org/10.1053/ajem.2001.25774

6. Bibliography

Martinez, S. E., Beavo, J. A., & Hol, W. G. J. (2002). GAF domains: two-billion-year-old molecular switches that bind cyclic nucleotides. Molecular Interventions, 2(5), 317–323. https://doi.org/10.1124/mi.2.5.317

Massion, P. B., & Balligand, J.-L. (2003). Modulation of cardiac contraction, relaxation and rate by the endothelial nitric oxide synthase (eNOS): lessons from genetically modified mice. The Journal of Physiology, 546(1), 63–75. https://doi.org/10.1113/jphysiol.2002.025973

Maurice, D. H., Ke, H., Ahmad, F., Wang, Y., Chung, J., & Manganiello, V. C. (2014). Advances in targeting cyclic nucleotide phosphodiesterases. Nature Reviews Drug Discovery, 13(4), 290–314. https://doi.org/10.1038/nrd4228

Maw, G. N., Allerton, C. M. N., Gbekor, E., & Million, W. A. (2003). Design, synthesis and biological activity of β-carboline-based type-5 phosphodiesterase inhibitors. Bioorganic and Medicinal Chemistry Letters, 13(8), 1425–1428. https://doi.org/10.1016/S0960-894X(03)00159-8

Meacci, E., Taira, M., Moos, M., Smith, C. J., Movsesian, M. A., Degerman, E., Belfrage, P., & Manganiello, V. (1992). Molecular cloning and expression of human myocardial cGMP-inhibited cAMP phosphodiesterase. Proceedings of the National Academy of Sciences of the United States of America, 89(9), 3721–3725. https://doi.org/10.1073/pnas.89.9.3721

Mehel, H., Emons, J., Vettel, C., Wittköpper, K., Seppelt, D., Dewenter, M., Lutz, S., Sossalla, S., Maier, L. S., Lechêne, P., Leroy, J., Lefebvre, F., Varin, A., Eschenhagen, T., Nattel, S., Dobrev, D., Zimmermann, W. H., Nikolaev, V. O., Vandecasteele, G., … El-Armouche, A. (2013). Phosphodiesterase-2 is up-regulated in human failing hearts and blunts β-adrenergic responses in cardiomyocytes. Journal of the American College of Cardiology, 62(17), 1596–1606. https://doi.org/10.1016/j.jacc.2013.05.057

Meier, S., Andressen, K. W., Aronsen, J. M., Sjaastad, I., Skomedal, T., Osnes, J.-B., Qvigstad, E., Levy, F. O., & Moltzau, L. R. (2015). Enhancement of cAMP-mediated inotropic responses by CNP is regulated differently by PDE2 in normal and failing hearts. BMC Pharmacology and Toxicology, 16(S1), 6511. https://doi.org/10.1186/2050-6511-16-s1-a66

Melanie Nichols, Nick Townsend, P. S. and M. R. (2012). European cardiovascular disease statistics. In E. S. of C. Susanne Løgstrup, European Heart Network, and Sophie O'Kelly (Ed.), European Heart Network and European Society of Cardiology (2012th ed.). http://www.herzstiftung.ch/uploads/media/European_cardiovascular_disease_statistics_2008.pdf

Mellor, H. R., Bell, A. R., Valentin, J. P., & Roberts, R. R. A. (2011). Cardiotoxicity associated with targeting kinase pathways in cancer. *Toxicological Sciences*, *120*(1), 14–32. https://doi.org/10.1093/toxsci/kfq378

Michie, A. M., Lobban, M., Müller, T., Harnett, M. M., & Houslay, M. D. (1996). Rapid regulation of PDE-2 and PDE-4 cyclic AMP phosphodiesterase activity following ligation of the T cell antigen receptor on thymocytes: Analysis using the selective inhibitors erythro-9-(2-hydroxy-3-nonyl)-adenine (EHNA) and rolipram. Cellular Signalling, 8(2), 97–110. https://doi.org/10.1016/0898-6568(95)02032-2

6. Bibliography

Mika, D., Bobin, P., Pomérance, M., Lechêne, P., Westenbroek, R. E., Catterall, W. A., Vandecasteele, G., Leroy, J., & Fischmeister, R. (2013). Differential regulation of cardiac excitation-contraction coupling by cAMP phosphodiesterase subtypes. Cardiovascular Research, 100(2), 336–346. https://doi.org/10.1093/cvr/cvt193

Mika, D., Richter, W., Westenbroek, R. E., Catterall, W. A., & Conti, M. (2014). PDE4B mediates local feedback regulation of β1-adrenergic cAMP signaling in a sarcolemmal compartment of cardiac myocytes. Journal of Cell Science, 127(5), 1033–1042. https://doi.org/10.1242/jcs.140251

Miller, C. L., Oikawa, M., Cai, Y., Wojtovich, A. P., Nagel, D. J., Xu, X., Xu, H., Florio, V., Rybalkin, S. D., Beavo, J. A., Chen, Y. F., Li, J. D., Blaxall, B. C., Abe, J. I., & Yan, C. (2009). Role of Ca2+/calmodulin-stimulated cyclic nucleotide phosphodiesterase 1 in mediating cardiomyocyte hypertrophy. Circulation Research, 105(10), 956–964. https://doi.org/10.1161/CIRCRESAHA.109.198515

Miller, E. M., & Hinton, R. B. (2014). A pediatric approach to family history of cardiovascular disease. diagnosis, risk assessment, and management. Pediatric Clinics of North America, 61(1), 187–205. https://doi.org/10.1016/j.pcl.2013.09.018

Mironov, S. L., Skorova, E., Taschenberger, G., Hartelt, N., Nikolaev, V. O., Lohse, M. J., & Kügler, S. (2009). Imaging cytoplasmic cAMP in mouse brainstem neurons. BMC Neuroscience, 10, 1–11. https://doi.org/10.1186/1471-2202-10-29

Mishra, S. K., & Hermsmeyer, K. (1994). Selective inhibition of T-type Ca2+ channels by Ro 40-5967. Circulation Research, 75(1), 144–148. https://doi.org/10.1161/01.res.75.1.144

Mitcheson, J. S., Hancox, J. C., & Levi, A. J. (1998). Cultured adult cardiac myocytes: Future applications, culture methods, morphological and electrophysiological properties. Cardiovascular Research, 39(2), 280–300. https://doi.org/10.1016/S0008-6363(98)00128-X

Molina, C. E., Leroy, J., Richter, W., Xie, M., Scheitrum, C., Lee, I. O., Maack, C., Rucker-Martin, C., Donzeau-Gouge, P., Verde, I., Llach, A., Hove-Madsen, L., Conti, M., Vandecasteele, G., & Fischmeister, R. (2012). Cyclic adenosine monophosphate phosphodiesterase type 4 protects against atrial arrhythmias. Journal of the American College of Cardiology, 59(24), 2182–2190. https://doi.org/10.1016/j.jacc.2012.01.060

Mongillo, M., McSorley, T., Evellin, S., Sood, A., Lissandron, V., Terrin, A., Huston, E., Hannawacker, A., Lohse, M. J., Pozzan, T., Houslay, M. D., & Zaccolo, M. (2004). Fluorescence resonance energy transfer-based analysis of cAMP dynamics in live neonatal rat cardiac myocytes reveals distinct functions of compartmentalized phosphodiesterases. Circulation Research, 95(1), 67–75. https://doi.org/10.1161/01.RES.0000134629.84732.11

Mongillo, M., Tocchetti, C. G., Terrin, A., Lissandron, V., Cheung, Y. F., Dostmann, W. R., Pozzan, T., Kass, D. A., Paolocci, N., Houslay, M. D., & Zaccolo, M. (2006). Compartmentalized phosphodiesterase-2 activity blunts β-adrenergic cardiac inotropy via an NO/cGMP-dependent pathway. Circulation Research, 98(2), 226–234. https://doi.org/10.1161/01.RES.0000200178.34179.93

Movsesian, M., Stehlik, J., Vandeput, F., & Bristow, M. R. (2009). Phosphodiesterase inhibition in heart failure. Heart Failure Reviews, 14(4), 255–263. https://doi.org/10.1007/s10741-008-9130-x

6. Bibliography

Murphy, C. A., & Dargie, H. J. (2007). Drug-Induced Cardiovascular Disorders. *Drug Safety*, *30*(9), 783–804. https://doi.org/10.2165/00002018-200730090-00005

Myagmar, B. E., Flynn, J. M., Cowley, P. M., Swigart, P. M., Montgomery, M. D., Thai, K., Nair, D., Gupta, R., Deng, D. X., Hosoda, C., Melov, S., Baker, A. J., & Simpson, P. C. (2017). Adrenergic receptors in individual ventricular myocytes: the beta-1 and alpha-1B are in all cells, the alpha-1A is in a subpopulation, and the beta-2 and beta-3 are mostly absent. In Circulation Research (Vol. 120, Issue 7). https://doi.org/10.1161/CIRCRESAHA.117.310520

Myakishev, M. V., Khripin, Y., Hu, S., & Hamer, D. H. (2001). High-throughput SNP genotyping by allele-specific PCR with universal energy-transfer-labeled primers. Genome Research, 11(1), 163–169. https://doi.org/10.1101/gr.157901

Nagel, D. J., Aizawa, T., Jeon, K. I., Liu, W., Mohan, A., Wei, H., Miano, J. M., Florio, V. A., Gao, P., Korshunov, V. A., Berk, B. C., & Yan, C. (2006). Role of nuclear Ca2+/calmodulin-stimulated phosphodiesterase 1A in vascular smooth muscle cell growth and survival. Circulation Research, 98(6), 777–784. https://doi.org/10.1161/01.RES.0000215576.27615.fd

Nagendran, J., Archer, S. L., Soliman, D., Gurtu, V., Moudgil, R., Haromy, A., St. Aubin, C., Webster, L., Rebeyka, I. M., Ross, D. B., Light, P. E., Dyck, J. R. B., & Michelakis, E. D. (2007). Phosphodiesterase type 5 is highly expressed in the hypertrophied human right ventricle, and acute inhibition of phosphodiesterase type 5 improves contractility. Circulation, 116(3), 238–248. https://doi.org/10.1161/CIRCULATIONAHA.106.655266

Nichols, J. W., & Pagano, R. E. (1983). Resonance energy transfer assay of protein-mediated lipid transfer between vesicles. Journal of Biological Chemistry, 258(9), 5368–5371. https://www.jbc.org/content/258/9/5368.full.pdf

NICOLE DEFER, MARTIN BEST-BELPOMME, A. J. H. (2000). Invited Review. FrAmerican Journal of Physiology, 279, F400–F416. https://doi.org/10.1080/10715760410001727858

Nikolaev, V. O., Bünemann, M., Hein, L., Hannawacker, A., & Lohse, M. J. (2004). Novel single chain cAMP sensors for receptor-induced signal propagation. Journal of Biological Chemistry, 279(36), 37215–37218. https://doi.org/10.1074/jbc.C400302200

Nikolaev, V. O., & Lohse, M. J. (2006). Monitoring of cAMP synthesis and degradation in living cells. Physiology, 21(2), 86–92. https://doi.org/10.1152/physiol.00057.2005

Nilius, B., Hess, P., Lansman, J. B., & Tsien, R. W. (1985). A novel type of cardiac calcium channel in ventricular cells. Nature, 316(6027), 443–446. https://doi.org/10.1038/316443a0

Nuss, H. B., & Houser, S. R. (1993). T-type Ca2+ current is expressed in hypertrophied adult feline left ventricular myocytes. Circulation Research, 73(4), 777–782. https://doi.org/10.1161/01.RES.73.4.777

Onakpoya, I. J., Heneghan, C. J., & Aronson, J. K. (2016). Post-marketing withdrawal of 462 medicinal products because of adverse drug reactions: A systematic review of the world literature. BMC Medicine, 14(1), 1–11. https://doi.org/10.1186/s12916-016-0553-2

Orkand, R. K., & Niedergerke, R. (1964). Heart Action Potential: Dependence on External Calcium and Sodium Ions. Science, 146(3648), 1176–1177. https://doi.org/10.1126/science.146.3648.1176

6. Bibliography

Parkhurst, K. M., & Parkhurst, L. J. (1995). Kinetic Studies by Fluorescence Resonance Energy Transfer Employing a Double-Labeled Oligonucleotide: Hybridization to the Oligonucleotide Complement and to Single-Stranded DNA. Biochemistry, 34(1), 285–292. https://doi.org/10.1021/bi00001a035

Pecha, S., Flenner, F., Söhren, K. D., Lorenz, K., Eschenhagen, T., & Christ, T. (2015). β1Adrenoceptor antagonistic effects of the supposedly selective β2adrenoceptor antagonist ICI 118,551 on the positive inotropic effect of adrenaline in murine hearts. Pharmacology Research and Perspectives, 3(5), 1–8. https://doi.org/10.1002/prp2.168

Perera, R. K., Fischer, T. H., Wagner, M., Dewenter, M., Bork, N. I., Maier, L. S., Conti, M., Wess, J., & El-armouche, A. (2017). Atropine augments cardiac contractility by inhibiting cAMP- specific phosphodiesterase type 4. August, 1–8. https://doi.org/10.1038/s41598-017-15632-x

Perera, R. K., Sprenger, J. U., Steinbrecher, J. H., Hübscher, D., Lehnart, S. E., Abesser, M., Schuh, K., El-Armouche, A., & Nikolaev, V. O. (2015). Microdomain switch of cGMP-regulated phosphodiesterases leads to ANP-induced augmentation of β-adrenoceptor-stimulated contractility in early cardiac hypertrophy. Circulation Research, 116(8), 1304–1311. https://doi.org/10.1161/CIRCRESAHA.116.306082

Pollard, C. E., Abi Gerges, N., Bridgland-Taylor, M. H., Easter, A., Hammond, T. G., & Valentin, J. P. (2010). An introduction to QT interval prolongation and non-clinical approaches to assessing and reducing risk. *British Journal of Pharmacology*, *159*(1), 12–21. https://doi.org/10.1111/j.1476-5381.2009.00207.x

Ponsioen, B., Zhao, J., Riedl, J., Zwartkruis, F., van der Krogt, G., Zaccolo, M., Moolenaar, W. H., Bos, J. L., & Jalink, K. (2004). Detecting cAMP-induced Epac activation by fluorescence resonance energy transfer: Epac as a novel cAMP indicator. EMBO Reports, 5(12), 1176–1180. https://doi.org/10.1038/sj.embor.7400290

Post, S. R., Hammond, H. K., & Insel, P. A. (1999). B-Adrenergic Receptors and Receptor Signaling in Heart Failure. Annual Review of Pharmacology and Toxicology, 39(1), 343–360. https://doi.org/10.1146/annurev.pharmtox.39.1.343

Rall, T. W., & Sutherland, E. W. (1958). Formation of a cyclic by tissue. The Journal Of Biological Chemistry, Vol. 232(2), 1065-1076. https://www.jbc.org/content/232/2/1065.long

RAMZI OCKAILI,* FADI SALLOUM,* JOHN HAWKINS, A. R. C. K. (2002). special communication. 283, 1263–1269. https://doi.org/10.1152/ajpheart.00324.2002.

Redfern, W. S., Carlsson, L., Davis, A. S., Lynch, W. G., MacKenzie, I., Palethorpe, S., Siegl, P. K. S., Strang, I., Sullivan, A. T., Wallis, R., Camm, A. J., & Hammond, T. G. (2003). Relationships between preclinical cardiac electrophysiology, clinical QT interval prolongation and torsade de pointes for a broad range of drugs: Evidence for a provisional safety margin in drug development. Cardiovascular Research, 58(1), 32–45. https://doi.org/10.1016/S0008-6363(02)00846-5

Reeves, M. L., Leigh, B. K., & England, P. J. (1987). The identification of a new cyclic nucleotide phosphodiesterase activity in human and guinea-pig cardiac ventricle. Implications for the mechanism of action of selective phosphodiesterase inhibitors. Biochemical Journal, 241(2), 535–541. https://doi.org/10.1042/bj2410535

6. Bibliography

Remme, C. A., Wilde, A. A. M., & Bezzina, C. R. (2008). Cardiac Sodium Channel Overlap Syndromes: Different Faces of SCN5A Mutations. Trends in Cardiovascular Medicine, 18(3), 78–87. https://doi.org/10.1016/j.tcm.2008.01.002

Reuter, H. (1966). Strom-Spannungsbeziehungen yon Purkinje-Fasern bei versehiedenen extracellul/iren Calcium-Konzentrationen und unter Adrenalineinwirkung. PPflüger's Archiv Für Die Gesamte Physiologie Des Menschen Und Der Tiere, 287(4), 357–367. https://doi.org/10.1007/BF00363250

Rich, T. C., Tse, T. E., Rohan, J. G., Schaack, J., & Karpen, J. W. (2001). In vivo assessment of local phosphodiesterase activity using tailored cyclic nucleotide-gated channels as cAMP sensors. Journal of General Physiology, 118(1), 63–77. https://doi.org/10.1085/jgp.118.1.63

Richter, W., Jin, S. L. C., & Conti, M. (2005). Splice variants of the cyclic nucleotide phosphodiesterase PDE4D are differentially expressed and regulated in rat tissue. Biochemical Journal, 388(3), 803–811. https://doi.org/10.1042/BJ20050030

Riegler, J., Tiburcy, M., Ebert, A., Tzatzalos, E., Raaz, U., Abilez, O. J., Shen, Q., Kooreman, N. G., Neofytou, E., Chen, V. C., Wang, M., Meyer, T., Tsao, P. S., Connolly, A. J., Couture, L. A., Gold, J. D., Zimmermann, W. H., & Wu, J. C. (2015). Human engineered heart muscles engraft and survive long term in a rodent myocardial infarction model. Circulation Research, 117(8), 720–730. https://doi.org/10.1161/CIRCRESAHA.115.306985

Ringer, S. (1883). A further Contribution regarding the influence of the different Constituents of the Blood on the Contraction of the Heart. The Journal of Physiology, 4(1), 29–42. https://doi.org/10.1113/jphysiol.1883.sp000120

Rochais, F., Abi-Gerges, A., Horner, K., Lefebvre, F., Cooper, D. M. F., Conti, M., Fischmeister, R., & Vandecasteele, G. (2006). A specific pattern of phosphodiesterases controls the cAMP signals generated by different Gs-coupled receptors in adult rat ventricular myocytes. Circulation Research, 98(8), 1081–1088. https://doi.org/10.1161/01.RES.0000218493.09370.8e

Rockman, H. A., Koch, W. J., & Lefkowitz, R. J. (2002). Seven-transmembrane-spanning receptors and heart function. Nature, 415(6868), 206–212. https://doi.org/10.1038/415206a

Rodolphe Fischmeister" and H. Criss Hartzell. (1991). CYCLIC AMP PHOSPHODIESTERASES AND Ca 2+ CURRENT REGULATION IN CARDIAC CELLS. 48(c), 2365–2376. https://doi.org/doi: 10.1016/0024-3205(91)90369-m

Rozmaritsa, N., Christ, T., Van Wagoner, D. R., Haase, H., Stasch, J. P., Matschke, K., & Ravens, U. (2014). Attenuated response of L-type calcium current to nitric oxide in atrial fibrillation. Cardiovascular Research, 101(3), 533–542. https://doi.org/10.1093/cvr/cvt334

Rubin, R. L. (2005). Drug-induced lupus. *Toxicology*, *209*(2), 135–147. https://doi.org/10.1016/j.tox.2004.12.025

Rybalkin, S. D., Yan, C., Bornfeldt, K. E., & Beavo, J. A. (2003). Cyclic GMP phosphodiesterases and regulation of smooth muscle function. Circulation Research, 93(4), 280–291. https://doi.org/10.1161/01.RES.0000087541.15600.2B

Sáenz de Tejada, I. (2002). Molecular mechanisms for the regulation of penile smooth muscle contractility. International Journal of Impotence Research, 14, S6–S10. https://doi.org/10.1038/sj.ijir.3900790

6. Bibliography

Saleem, U., Ismaili, D., Mannhardt, I., Pinnschmidt, H., Schulze, T., Christ, T., Eschenhagen, T., & Hansen, A. (2020). Regulation of ICa,L and force by PDEs in human-induced pluripotent stem cell-derived cardiomyocytes. British Journal of Pharmacology, 177(13), 3036–3045. https://doi.org/10.1111/bph.15032

Saleem, U., Mannhardt, I., Braren, I., Denning, C., Eschenhagen, T., & Hansen, A. (2020). Force and Calcium Transients Analysis in Human Engineered Heart Tissues Reveals Positive Force-Frequency Relation at Physiological Frequency. Stem Cell Reports, 14(2), 312–324. https://doi.org/10.1016/j.stemcr.2019.12.011

Schimmel, K. J. M., Richel, D. J., van den Brink, R. B. A., & Guchelaar, H. J. (2004). Cardiotoxicity of cytotoxic drugs. *Cancer Treatment Reviews*, *30*(2), 181–191. https://doi.org/10.1016/j.ctrv.2003.07.003

Seisenberger, C., Specht, V., Welling, A., Platzer, J., Pfeifer, A., Kühbandner, S., Striessnig, J., Klugbauer, N., Feil, R., & Hofmann, F. (2000). Functional embryonic cardiomyocytes after disruption of the L-type α1C (Cav1.2) calcium channel gene in the mouse. Journal of Biological Chemistry, 275(50), 39193–39199. https://doi.org/10.1074/jbc.M006467200

Shan, X., Quaile, M. P., Monk, J. K., French, B., Cappola, T. P., & Margulies, K. B. (2012). Differential expression of pde5 in failing and nonfailing human myocardium. Circulation: Heart Failure, 5(1), 79–86. https://doi.org/10.1161/CIRCHEARTFAILURE.111.961706

Shimizu-Albergine, M., Rybalkin, S. D., Rybalkina, I. G., Feil, R., Wolfsgruber, W., Hofmann, F., & Beavo, J. A. (2003). Individual cerebellar Purkinje cells express different cGMP phosphodiesterases (PDEs): In vivo phosphorylation of cGMP-specific PDE (PDE5) as an indicator of cGMP-dependent protein kinase (PKG) activation. Journal of Neuroscience, 23(16), 6452–6459. https://doi.org/10.1523/jneurosci.23-16-06452.2003

Singer, D., Biel, M., Lotan, I., Flockerzi, V., Hofmann, F., & Dascal, N. (1991). The roles of the subunits in the function of the calcium channel. Science, 253(5027), 1553–1557. https://doi.org/10.1126/science.1716787

Soderling, S. H., & Beavo, J. A. (2000). Regulation of cAMP and cGMP signaling: New phosphodiesterases and new functions. Current Opinion in Cell Biology, 12(2), 174–179. https://doi.org/10.1016/S0955-0674(99)00073-3

Song, L., Wang, S., Xiao, R., Spurgeon, H., G, E., Lakatta, E. G., & Cheng, H. (2001). Release During Excitation-Contraction Coupling in Cardiac Myocytes. Circulation Research. https://doi.org/10.1161/hh0801.090461

Sonnenburg, W. K., Seger, D., & Beavo, J. A. (1993). Molecular cloning of a cDNA encoding the “61-kDa” calmodulin-stimulated cyclic nucleotide phosphodiesterase. Tissue-specific expression of structurally related isoforms. Journal of Biological Chemistry, 268(1), 645–652. https://www.jbc.org/content/268/1/645.full.pdf

Sprenger, J. U., & Nikolaev, V. O. (2013). Biophysical techniques for detection of cAMP and cGMP in living cells. International Journal of Molecular Sciences, 14(4), 8025–8046. https://doi.org/10.3390/ijms14048025

6. Bibliography

Sprenger, J. U., Perera, R. K., Steinbrecher, J. H., Lehnart, S. E., Maier, L. S., Hasenfuss, G., & Nikolaev, V. O. (2015). In vivo model with targeted cAMP biosensor reveals changes in receptor-microdomain communication in cardiac disease. Nature Communications, 6, 1–11. https://doi.org/10.1038/ncomms7965

Stangherlin, A., Gesellchen, F., Zoccarato, A., Terrin, A., Fields, L. A., Berrera, M., Surdo, N. C., Craig, M. A., Smith, G., Hamilton, G., & Zaccolo, M. (2011). CGMP signals modulate camp levels in a compartment-specific manner to regulate catecholamine-dependent signaling in cardiac myocytes. Circulation Research, 108(8), 929–939. https://doi.org/10.1161/CIRCRESAHA.110.230698

Stephenson, D. T., Coskran, T. M., Wilhelms, M. B., Adamowicz, W. O., O'Donnell, M. M., Muravnick, K. B., Menniti, F. S., Kleiman, R. J., & Morton, D. (2009). Immunohistochemical localization of phosphodiesterase 2A in multiple mammalian species. Journal of Histochemistry and Cytochemistry, 57(10), 933–949. https://doi.org/10.1369/jhc.2009.953471

Stoetzer, C., Voelker, M., Doll, T., Heineke, J., Wegner, F., & Leffler, A. (2017). Cardiotoxic Antiemetics Metoclopramide and Domperidone Block Cardiac Voltage-Gated Na+ Channels. Anesthesia and Analgesia, 124(1), 52–60. https://doi.org/10.1213/ANE.0000000000001673

Sugioka, M., Ito, M., Masuoka, H., Ichikawa, K., Konishi, T., Tanaka, T., & Nakano, T. (1994). Identification and characterization of isoenzymes of cyclic nucleotide phosphodiesterase in human kidney and heart, and the effects of new cardiotonic agents on these isoenzymes. Naunyn-Schmiedeberg's Archives of Pharmacology, 350(3), 284–293. https://doi.org/10.1007/BF00175034

Takahashi, K., & Yamanaka, S. (2006). Induction of Pluripotent Stem Cells from Mouse Embryonic and Adult Fibroblast Cultures by Defined Factors. Cell, 126(4), 663–676. https://doi.org/10.1016/j.cell.2006.07.024

Takeda, N., Kyozuka, K., & Deguchi, R. (2006). Increase in intracellular cAMP is a prerequisite signal for initiation of physiological oocyte meiotic maturation in the hydrozoan Cytaeis uchidae. Developmental Biology, 298(1), 248–258. https://doi.org/10.1016/j.ydbio.2006.06.03

Takimoto, E., Champion, H. C., Belardi, D., Moslehi, J., Mongillo, M., Mergia, E., Montrose, D. C., Isoda, T., Aufiero, K., Zaccolo, M., Dostmann, W. R., Smith, C. J., & Kass, D. A. (2005). cGMP catabolism by phosphodiesterase 5A regulates cardiac adrenergic stimulation by NOS3-dependent mechanism. Circulation Research, 96(1), 100–109. https://doi.org/10.1161/01.RES.0000152262.22968.72

Thomas, M. K., Francis, S. H., & Corbin, J. D. (1990). Characterization of a purified bovine lung cGMP-binding cGMP phosphodiesterase. Journal of Biological Chemistry, 265(25), 14964–14970. https://www.jbc.org/content/265/25/14964.full.pdf

Timothy J. Martins, Marc C. Mumby+, and J. A. B. (1982). Purification and characterization of a cyclic GMP-stimulated cyclic nucleotide phosphodiesterase from the cytosol of human platelets. The Journal of Biological Chemistry, 257(4), 1973–1979. https://www.jbc.org/content/257/4/1973.long

Townsend, M., & MacIver, D. H. (2004). Constrictive pericarditis and pleuropulmonary fibrosis secondary to cabergoline treatment for Parkinson's disease. *Heart (British Cardiac Society)*, *90*(8), 1–2. https://doi.org/10.1136/hrt.2004.036236

6. Bibliography

Townsend, N., Wilson, L., Bhatnagar, P., Wickramasinghe, K., Rayner, M., & Nichols, M. (2016). Cardiovascular disease in Europe: Epidemiological update 2016. European Heart Journal, 37(42), 3232–3245. https://doi.org/10.1093/eurheartj/ehw334

Tsien, R. W., Hess, P., McCleskey, E. W., & Rosenberg, R. L. (1987). Calcium channels: mechanisms of selectivity, permeation, and block. Annual Review of Biophysics and Biophysical Chemistry, 16, 265–290. https://doi.org/10.1146/annurev.bb.16.060187.001405

Uster, P. S. (1993). [19] In situ resonance energy transfer microscopy: Monitoring membrane fusion in living cells (Vol. 171, Issue 1986, pp. 239–246). https://doi.org/10.1016/0076-6879(93)21021-Y

Uzun, A. U., Mannhardt, I., Breckwoldt, K., Horvï¿½th, A., Johannsen, S. S., Hansen, A., Eschenhagen, T., & Christ, T. (2016). Ca2+-currents in human induced pluripotent stem cell-derived cardiomyocytes effects of two different culture conditions. Frontiers in Pharmacology, 7(SEP). https://doi.org/10.3389/fphar.2016.00300

Van Der Linde, D., Konings, E. E. M., Slager, M. A., Witsenburg, M., Helbing, W. A., Takkenberg, J. J. M., & Roos-Hesselink, J. W. (2011). Birth prevalence of congenital heart disease worldwide: A systematic review and meta-analysis. Journal of the American College of Cardiology, 58(21), 2241–2247. https://doi.org/10.1016/j.jacc.2011.08.025

Vandecasteele, G., Verde, I., Rücker-Martin, C., Donzeau-Gouge, P., & Fischmeister, R. (2001). Cyclic GMP regulation of the L-type Ca 2+ channel current in human atrial myocytes. Journal of Physiology, 533(2), 329–340. https://doi.org/10.1111/j.1469-7793.2001.0329a.x

Vandeput, F., Wolda, S. L., Krall, J., Hambleton, R., Uher, L., McCaw, K. N., Radwanski, P. B., Florio, V., & Movsesian, M. A. (2007). Cyclic nucleotide phosphodiesterase PDE1C1 in human cardiac myocytes. Journal of Biological Chemistry, 282(45), 32749–32757. https://doi.org/10.1074/jbc.M703173200

Vargas, M. L., Hernandez, J., & Kaumann, A. J. (2006). Phosphodiesterase PDE3 blunts the positive inotropic and cyclic AMP enhancing effects of CGP-12177 but not of noradrenaline in rat ventricle. British Journal of Pharmacology, 147(2), 158–163. https://doi.org/10.1038/sj.bjp.0706498

Verde, I., Vandecasteele, G., Lezoualc'h, F., & Fischmeister, R. (1999). Characterization of the cyclic nucleotide phosphodiesterase subtypes involved in the regulation of the L-type Ca2+ current in rat ventricular myocytes. British Journal of Pharmacology, 127(1), 65–74. https://doi.org/10.1038/sj.bjp.0702506

Veronesi, G., Gianfagna, F., Giampaoli, S., Chambless, L. E., Mancia, G., Cesana, G., & Ferrario, M. M. (2014). Improving long-term prediction of first cardiovascular event: The contribution of family history of coronary heart disease and social status. Preventive Medicine, 64, 75–80. https://doi.org/10.1016/j.ypmed.2014.04.007

Vettel, C., Lämmle, S., Ewens, S., Cervirgen, C., Emons, J., Ongherth, A., Dewenter, M., Lindner, D., Westermann, D., Nikolaev, V. O., Lutz, S., Zimmermann, W. H., & El-Armouche, A. (2014). PDE2-mediated cAMP hydrolysis accelerates cardiac fibroblast to myofibroblast conversion and is antagonized by exogenous activation of cGMP signaling pathways. American Journal of Physiology - Heart and Circulatory Physiology, 306(8), 1246–1252. https://doi.org/10.1152/ajpheart.00852.2013

6. Bibliography

Vettel, Christiane, Lindner, M., Dewenter, M., Lorenz, K., Schanbacher, C., Riedel, M., Lämmle, S., Meinecke, S., Mason, F. E., Sossalla, S., Geerts, A., Hoffmann, M., Wunder, F., Brunner, F. J., Wieland, T., Mehel, H., Karam, S., Lechêne, P., Leroy, J., … El-Armouche, A. (2017). Phosphodiesterase 2 Protects Against Catecholamine-Induced Arrhythmia and Preserves Contractile Function after Myocardial Infarction. Circulation Research, 120(1), 120–132. https://doi.org/10.1161/CIRCRESAHA.116.310069

Warrier, S., Belevych, A. E., Ruse, M., Eckert, R. L., Zaccolo, M., Pozzan, T., & Harvey, R. D. (2005). β-adrenergic- and muscarinic receptor-induced changes in cAMP activity in adult cardiac myocytes detected with FRET-based biosensor. American Journal of Physiology - Cell Physiology, 289(2 58-2), 455–461. https://doi.org/10.1152/ajpcell.00058.2005

Watanabe, H., Koopmann, T. T., Le Scouarnec, S., Yang, T., Ingram, C. R., Schott, J. J., Demolombe, S., Probst, V., Anselme, F., Escande, D., Wiesfeld, A. C. P., Pfeufer, A., Kääb, S., Wichmann, H. E., Hasdemir, C., Aizawa, Y., Wilde, A. A. M., Roden, D. M., & Bezzina, C. R. (2008). Sodium channel β1 subunit mutations associated with Brugada syndrome and cardiac conduction disease in humans. Journal of Clinical Investigation, 118(6), 2260–2268. https://doi.org/10.1172/JCI33891

Watanabe, H., Yang, T., Stroud, D. M., Lowe, J. S., Harris, L., Atack, T. C., Wang, D. W., Hipkens, S. B., Leake, B., Hall, L., Kupershmidt, S., Chopra, N., Magnuson, M. A., Tanabe, N., Knollmann, B. C., George, A. L., & Roden, D. M. (2011). Striking in vivo phenotype of a disease-associated human scn5a mutation producing minimal changes in vitro. Circulation, 124(9), 1001–1011. https://doi.org/10.1161/CIRCULATIONAHA.110.987248

Watson, B. S., Hazlett, T. L., Eccleston, J. F., Davis, C., Jameson, D. M., & Johnson, A. E. (1995). Macromolecular Arrangement in the Aminoacyl-tRNA•Elongation Factor Tu•GTP Ternary Complex. A Fluorescence Energy Transfer Study. Biochemistry, 34(24), 7904–7912. https://doi.org/10.1021/bi00024a015

Wechsler, J., Choi, Y. H., Krall, J., Ahmad, F., Manganiello, V. C., & Movsesian, M. A. (2002). Isoforms of cyclic nucleotide phosphodiesterase PDE3A in cardiac myocytes. Journal of Biological Chemistry, 277(41), 38072–38078. https://doi.org/10.1074/jbc.M203647200

Weeks, J. L., Zoraghi, R., Beasley, A., Sekhar, K. R., Francis, S. H., & Corbin, J. D. (2005). High biochemical selectivity of tadalafil, sildenafil and vardenafil for human phosphodiesterase 5A1 (PDE5) over PDE11A4 suggests the absence of PDE11A4 cross-reaction in patients. International Journal of Impotence Research, 17(1), 5–9. https://doi.org/10.1038/sj.ijir.3901283

Wehmeier, P. M., Heiser, P., & Remschmidt, H. (2005). Myocarditis, pericarditis and cardiomyopathy in patients treated with clozapine. *Journal of Clinical Pharmacy and Therapeutics*, *30*(1), 91–96. https://doi.org/10.1111/j.1365-2710.2004.00616_1.x

WEILONG, YUAN AND DONALD, & Bers, D. M. (1994). Ca-dependent facilitation of cardiac Ca current A A is due to Ca-calmodulin-dependent protein kinase. American Physiological Society, 26(2), H982–H993. https://doi.org/10.1017/CBO9781107415324.004

Weinberger, F., Breckwoldt, K., Pecha, S., Kelly, A., Geertz, B., Starbatty, J., Yorgan, T., Cheng, K. H., Lessmann, K., Stolen, T., Marielle, S. C., Smith, G., Reichenspurner, H., Hansen, A., & Eschenhagen, T. (2016). Cardiac repair in Guinea pigs with human engineered heart tissue from induced pluripotent stem cells. Science Translational Medicine, 8(363), 1–13. https://doi.org/10.1126/scitranslmed.aaf8781

6. Bibliography

Weishaar, R. E., Kobylarz-Singer, D. C., Steffen, R. P., & Kaplan, H. R. (1987). Subclasses of cyclic AMP-specific phosphodiesterase in left ventricular muscle and their involvement in regulating myocardial contractility. Circulation Research, 61(4), 539–547. https://doi.org/10.1161/01.RES.61.4.539

Weishaar, Ronald E., Burrows, S. D., Kobylarz, D. C., Quade, M. M., & Evans, D. B. (1986). Multiple molecular forms of cyclic nucleotide phosphodiesterase in cardiac and smooth muscle and in platelets. Isolation, characterization, and effects of various reference phosphodiesterase inhibitors and cardiotonic agents. Biochemical Pharmacology, 35(5), 787–800. https://doi.org/10.1016/0006-2952(86)90247-9

Williams, C. (2004). cAMP detection methods in HTS: Selecting the best from the rest. Nature Reviews Drug Discovery, 3(2), 125–135. https://doi.org/10.1038/nrd1306

Wu, A. Y., Tang, X. B., Martinez, S. E., Ikeda, K., & Beavo, J. A. (2004). Molecular determinants for cyclic nucleotide binding to the regulatory domains of phosphodiesterase 2A. Journal of Biological Chemistry, 279(36), 37928–37938. https://doi.org/10.1074/jbc.M404287200

Wu, H., Lee, J., Vincent, L. G., Wang, Q., Gu, M., Lan, F., Churko, J. M., Sallam, K. I., Matsa, E., Sharma, A., Gold, J. D., Engler, A. J., Xiang, Y. K., Bers, D. M., & Wu, J. C. (2015). Epigenetic Regulation of Phosphodiesterases 2A and 3A Underlies Compromised β-Adrenergic Signaling in an iPSC Model of Dilated Cardiomyopathy. Cell Stem Cell, 17(1), 89–100. https://doi.org/10.1016/j.stem.2015.04.020

Xu, X., Bishop, E. E., Kennedy, S. M., Simpson, S. A., & Pechacek, T. F. (2015). Annual healthcare spending attributable to cigarette smoking: An update. American Journal of Preventive Medicine, 48(3), 326–333. https://doi.org/10.1016/j.amepre.2014.10.012

Yan, C., Zhao, A. Z., Bentley, J. K., Loughney, K., Ferguson, K., & Beavo, J. A. (1995). Molecular cloning and characterization of a calmodulin-dependent phosphodiesterase enriched in olfactory sensory neurons. Proceedings of the National Academy of Sciences of the United States of America, 92(21), 9677–9681. https://doi.org/10.1073/pnas.92.21.9677

Yau, K. W. (1994). Cyclic nucleotide-gated channels: An expanding new family of ion channels. Proceedings of the National Academy of Sciences of the United States of America, 91(9), 3481–3483. https://doi.org/10.1073/pnas.91.9.3481

Yu, J., Vodyanik, M. A., Smuga-Otto, K., Antosiewicz-Bourget, J., Frane, J. L., Tian, S., Nie, J., Jonsdottir, G. A., Ruotti, V., Stewart, R., Slukvin, I. I., & Thomson, J. A. (2007). Induced pluripotent stem cell lines derived from human somatic cells. Science, 318(5858), 1917–1920. https://doi.org/10.1126/science.1151526

Yuasa, K., Kotera, J., Fujishige, K., Michibata, H., Sasaki, T., & Omori, K. (2000). Isolation and characterization of two novel phosphodiesterase PDE11a variants showing unique structure and tissue-specific expression. Journal of Biological Chemistry, 275(40), 31469–31479. https://doi.org/10.1074/jbc.M003041200

Yuasa, Keizo, Ohgaru, T., Asahina, M., & Omori, K. (2001). Identification of rat cyclic nucleotide phosphodiesterase 11A (PDE11A): Comparison of rat and human PDE11A splicing variants. European Journal of Biochemistry, 268(16), 4440–4448. https://doi.org/10.1046/j.1432-1327.2001.02366.x

6. Bibliography

Zaccolo, M. (2006). Phosphodiesterases and compartmentalized cAMP signalling in the heart. European Journal of Cell Biology, 85(7), 693–697. https://doi.org/10.1016/j.ejcb.2006.01.002

Zaccolo, M., De Giorgi, F., Cho, C. Y., Feng, L., Knapp, T., Negulescu, P. A., Taylor, S. S., Tsien, R. Y., & Pozzan, T. (2000). A genetically encoded, flourescent indicator for cyclic AMP in living cells. Nature Cell Biology, 2(1), 25–29. https://doi.org/10.1038/71345

Zaccolo, M., & Pozzan, T. (2002). Discrete microdomains with high concentration of cAMP in stimulated rat neonatal cardiac myocytes. Science, 295(5560), 1711–1715. https://doi.org/10.1126/science.1069982

Zanettini, R., Antonini, A., Gatto, G., Gentile, R., Tesei, S., & Pezzoli, G. (2007). Valvular Heart Disease and the Use of Dopamine Agonists for Parkinson's Disease. *New England Journal of Medicine*, *356*(1), 39–46. https://doi.org/10.1056/NEJMoa054830

Zhang, M., Koitabashi, N., Nagayama, T., Rambaran, R., Feng, N., Takimoto, E., Koenke, T., O'Rourke, B., Champion, H. C., Crow, M. T., & Kass, D. A. (2008). Expression, activity, and pro-hypertrophic effects of PDE5A in cardiac myocytes. Cellular Signalling, 20(12), 2231–2236. https://doi.org/10.1016/j.cellsig.2008.08.012

Zhang, J., Wilson, G. F., Soerens, A. G., Koonce, C. H., Yu, J., Palecek, S. P., Thomson, J. A., & Kamp, T. J. (2009). Functional cardiomyocytes derived from human induced pluripotent stem cells. Circulation Research, 104(4). https://doi.org/10.1161/CIRCRESAHA.108.192237

Zhang, M., Takimoto, E., Hsu, S., Lee, D. I., Nagayama, T., Danner, T., Koitabashi, N., Barth, A. S., Bedja, D., Gabrielson, K. L., Wang, Y., & Kass, D. A. (2010). Myocardial remodeling is controlled by myocyte-targeted gene regulation of phosphodiesterase type 5. Journal of the American College of Cardiology, 56(24), 2021–2030. https://doi.org/10.1016/j.jacc.2010.08.612

Zhu, W., Petrashevskaya, N., Ren, S., Zhao, A., Chakir, K., Gao, E., Chuprun, J. K., Wang, Y., Talan, M., Dorn, G. W., Lakatta, E. G., Koch, W. J., Feldman, A. M., & Xiao, R. P. (2012). Gi-biased β2AR signaling links GRK2 upregulation to heart failure. Circulation Research, 110(2), 265–274. https://doi.org/10.1161/CIRCRESAHA.111.253260

Zoraghi, R., Bessay, E. P., Corbin, J. D., & Francis, S. H. (2005). Structural and functional features in human PDE5A1 regulatory domain that provide for allosteric cGMP binding, dimerization, and regulation. Journal of Biological Chemistry, 280(12), 12051–12063. https://doi.org/10.1074/jbc.M413611200

7. Supplements

7.1 List of figures

7. Supplements

7. Supplements

7.2 Acronyms

A	
α-AR	Alpha -adrenergic receptor
AC	Adenylyl cyclase
AF	Atrial fibrillation
AHA/ACC/HRS	American Heart Association/American College of Cardiology/Heart Rhythm Society
AKAP	A-kinase anchoring proteins
AP	Action potential
APD	Action potential duration
Aqua dest	Aqua destillata (distilled water)
AT1	angiotensin receptors
ATP	Adenosine triphosphate
B	
β1-AR	Beta 1-adrenergic receptor
β2-AR	Beta 2-adrenergic receptor
bFGF	Basic fibroblast growth factor

7. Supplements

BMP-4	Bone-morphogenetic protein 4
BTS	N-Benzyl-p-Toluenesulfonamide
C	
°C	Degree Celsius
cAMP	Cyclic adenosine monophosphate
CaMKII	Ca2+ /calmodulin-dependent protein kinase II
cDNA	Complementary DNA
CFP	Cyan fluorescent protein
CHD	coronary heart disease
CHD	congenital heart diseases
CHO	Chinese hamster ovary
Cil	Cilostamide
CICR	Calcium-induced calcium release
cGMP	3'-5'-cyclic Guanosine Monophosphate
CMOS	Complementary Metal-Oxide-Semiconductor
CNBD	Cyclic Nucleotide-Binding Domain

7. Supplements

CNG	Cyclic Nucleotide-Gated Ion Channels
cm^2	Square centimeter
CRC	Concentration response curve Ctrl
CTiD	Clinical Trials in a Dish
Ctrl	Control
CVDs	Cardiovascular diseases
D	
DAG	diacylglycerol
DCM	Dilated cardiomyopathy
DMEM	Dulbecco's Modified Eagle Medium
DMSO	Dimethyl sulfoxide
E	
EAD	Early after depolarization
EB	Embryoid body
ECC	Excitation-contraction coupling
ECF	extracellular fluid

7. Supplements

ECFP	Enhanced cyan fluorescent protein
EC_{-50}	Effective concentration 50%
ECM	Extracellular matrix
EDTA	Ethylenediaminetetraacetic acid
EHT	Engineered heart tissue
ELISA	Enzyme-Linked Immunosorbent Assay
EPAC	Exchange Proteins Activated by cAMP
Epi	Epinephrine
EPR	Prostaglandin Receptor
ERP	Effective refractory period
ESC	Embryonic stem cell
ET	Endothelin
et al.	Et alii (and others)
F	
FBS	Fetal bovine serum
FACS	Fluorescence-activated cell sorting

7. Supplements

FCS	Fetal calf serum
FGF-2	Fibroblast growth factor-2
FRET	Förster resonance energy transfer or fluorescence resonance energy transfer
FSK	Forskolin
FTDA	bFGF, TGFβ1, dorsomorphin and activin A-based hiPSC culture medium
G	
GF	Growth factor
GPCR	G-proteins coupled receptor
Gs	Stimulatory G-protein
Gi	Inhibitory G-protein
H	
H	Hour
HF	Heart Failure
HBSS	Hanks' Balanced Salt Solution
HCN4	Potassium/sodium hyperpolarization-activated cyclic nucleotide-gated channel 4
HEK	human embryonic kidney

7. Supplements

HEPES	4-(2-hydroxyethyl)-1-piperazineethanesulfonic acid
hESC	Human embryonic stem cell
hERG	Human ether a-go-go-related gene
hiPSC	Human induced pluripotent stem cell
hiPSC-CMs	Human induced pluripotent stem cell derived cardiomyocytes
hPSC	Human pluripotent stem cell
Hz	Hertz
I	
IBMX	3-isobutyl-1-methylxanthine
ICaL	Calcium L-type current
ICUE1	indicator of cAMP using Epac 1
If	Pacemaker current
IHD	Ischemic heart disease
I_{Na}	Na^+ current
I_{NCX}	Sodium-calcium exchanger current
IP3	inositol trisphosphate

7. Supplements

iPSC	Induced pluripotent stem cell
ISO	Isoprenaline
Iti	Transient inward current
K	
Klf4	Kruppel-like factor 4
L	
LA	Left atrium
LTCC	Voltage-dependent L-type Ca^{2+} channel
LED	Light emitting diode
LV	Left ventricle
M	
M2	muscarinic receptors
mA	Milliampere
µg	Microgram
µl	Microliter
µm	Micrometre

7. Supplements

µM	Micromolar
MEM	Minimum essential medium
mg	Milligram
min	Minutes
MI	myocardial infarction
ML	Monolayer
ml	Milliliter
mm	Millimeter
MOI	Multiplicity of infection
mRNA	Messenger RNA
N	
n	Number of experiments
N	Number of tissues used
NCX	Sodium-calcium exchanger
NE	Norepinephrine

7. Supplements

NFH	Non failing heart
NKA	Na+, K+-ATPase
nm	Nanometer
ns	Not significant
O	
Oct4	Octamer-binding transcription factor 4
P	
PBS	Phosphate-buffered saline
PCR	Polymerase chain reaction
PDE	Phosphodiesterase
PDEi	PDE inhibitor
PDMS	Polydimethylsiloxane
PGE1	prostaglandins E1
pH	-log10 hydrogen ion activity
PIP2	phosphatidylinositol 4, 5-bisphosphate
PKA	Protein kinase A

7. Supplements

PKC	Protein Kinase C
PLB	Phospholamban
PLC	Phospholipase C
Pm	plasma membrane
R	
RA	Right atrium
RHD	rheumatic heart diseases
RIAs	radioimmunoassays
rpm	Round per minute
Rol	Rolipram
RPMI	Roswell Park Memorial Institute
RyR2	Ryanodine receptor 2
S	
SEM	Standard error of the mean
SERCA2a	Sarcoplasmic-endoplasmic reticulum calcium ATPase 2a
SNS	Sympathetic Nervous System

7. Supplements

Sox2	Sex determining region Y-box 2
SR	Sarcoplasmic reticulum
T	
TGFβ1	Transforming growth factor-β1
TnI	Troponin I
TnT	Troponin T
TnC	Troponin C
TMC	Time matched control
TTCC	Voltage-dependent T-type calcium channel
U	
UKE	University Medical Center Hamburg Eppendorf
USA	United states of America
V	
v/v	Volume/volume
vs	versus
VTE	venous thromboembolism

7. Supplements

Y	
YFP	Yellow fluorescent protein
X	
x	times

7.3 List of GHS Hazard and Precautionary Statements (H-codes)

Code	Phrase
H200	Unstable explosive
H201	Explosive; mass explosion hazard
H202	Explosive; severe projection hazard
H203	Explosive; fire, blast or projection hazard
H204	Fire or projection hazard
H205	May mass explode in fire
H206	Fire, blast or projection hazard: increased risk of explosion if desensitizing agent is reduced
H207	Fire or projection hazard: increased risk of explosion if desensitizing agent is reduced
H208	Fire hazard: increased risk of explosion if desensitizing agent is reduced
H220	Extremely flammable gas
H221	Flammable gas
H222	Extremely flammable aerosol
H223	Flammable aerosol
H224	Extremely flammable liquid and vapour

7. Supplements

H225	Highly flammable liquid and vapour
H226	Flammable liquid and vapour
H227	Combustible liquid
H228	Flammable solid
H229	Pressurized container: may burst if heated
H230	May react explosively even in the absence of air
H231	May react explosively even in the absence of air at elevated pressure and/or temperature
H232	May ignite spontaneously if exposed to air
H240	Heating may cause an explosion
H241	Heating may cause a fire or explosion
H242	Heating may cause a fire
H250	Catches fire spontaneously if exposed to air
H251	Self-heating; may catch fire
H252	Self-heating in large quantities; may catch fire
H260	In contact with water releases flammable gases which may ignite spontaneously
H261	In contact with water releases flammable gas
H270	May cause or intensify fire; oxidizer
H271	May cause fire or explosion; strong oxidizer
H272	May intensify fire; oxidizer
H280	Contains gas under pressure; may explode if heated
H281	Contains refrigerated gas; may cause cryogenic burns or injury
H290	May be corrosive to metals
H311	Toxic in contact with skin
H312	Harmful in contact with skin

H313	May be harmful in contact with skin
H314	Causes severe skin burns and eye damage
H315	Causes skin irritation
H316	Causes mild skin irritation
H317	May cause an allergic skin reaction
H318	Causes serious eye damage
H319	Causes serious eye irritation
H320	Causes eye irritation
H330	Fatal if inhaled
H331	Toxic if inhaled
H332	Harmful if inhaled
H333	May be harmful if inhaled
H334	May cause allergy or asthma symptoms or breathing difficulties if inhaled
H335	May cause respiratory irritation
H336	May cause drowsiness or dizziness
H340	May cause genetic defects
H341	Suspected of causing genetic defects
H350	May cause cancer
H351	Suspected of causing cancer
H360	May damage fertility or the unborn child
H361	Suspected of damaging fertility or the unborn child
H361d	Suspected of damaging the unborn child
H361e	May damage the unborn child
H361f	Suspected of damaging fertility

7. Supplements

H361g	May damage fertility
H362	May cause harm to breast-fed children
H370	Causes damage to organs
H371	May cause damage to organs
H372	Causes damage to organs through prolonged or repeated exposure
H373	May cause damage to organs through prolonged or repeated exposure
H300+H310	Fatal if swallowed or in contact with skin
H300+H330	Fatal if swallowed or if inhaled
H310+H330	Fatal in contact with skin or if inhaled
H300+H310+H330	Fatal if swallowed, in contact with skin or if inhaled
H301+H311	Toxic if swallowed or in contact with skin
H301+H331	Toxic if swallowed or if inhaled
H311+H331	Toxic in contact with skin or if inhaled
H301+H311+H331	Toxic if swallowed, in contact with skin or if inhaled
H302+H312	Harmful if swallowed or in contact with skin
H302+H332	Harmful if swallowed or if inhaled
H312+H332	Harmful in contact with skin or if inhaled
H302+H312+H332	Harmful if swallowed, in contact with skin or if inhaled
H303+H313	May be harmful if swallowed or in contact with skin
H303+H333	May be harmful if swallowed or if inhaled
H313+H333	May be harmful in contact with skin or if inhaled
H303+H313+H333	May be harmful if swallowed, in contact with skin or if inhaled
H315+H320	Causes skin and eye irritation
H400	Very toxic to aquatic life

H401	Toxic to aquatic life
H402	Harmful to aquatic life
H410	Very toxic to aquatic life with long-lasting effects
H411	Toxic to aquatic life with long-lasting effects
H412	Harmful to aquatic life with long-lasting effects
H413	May cause long-lasting harmful effects to aquatic life
H420	Harms public health and the environment by destroying ozone in the upper atmosphere
H433	Harmful to terrestrial vertebrates

7.4 GHS hazard. P-codes

Code	Phrase
P101	If medical advice is needed, have product container or label at hand
P102	Keep out of reach of children
P103	Read label before use
P201	Obtain special instructions before use
P202	Do not handle until all safety precautions have been read and understood
P210	Keep away from heat, hot surfaces, sparks, open flames and other ignition sources. No smoking
P211	Do not spray on an open flame or other ignition source
P220	Keep/Store away from clothing/…/combustible materials
P221	Take any precaution to avoid mixing with combustibles
P222	Do not allow contact with air
P223	Do not allow contact with water
P230	Keep wetted with …

7. Supplements

P231	Handle under inert gas
P232	Protect from moisture
P233	Keep container tightly closed
P234	Keep only in original container
P235	Keep cool
P240	Ground/bond container and receiving equipment
P241	Use explosion-proof electrical/ventilating/lighting/…/equipment
P242	Use only non-sparking tools
P243	Take precautionary measures against static discharge
P244	Keep valves and fittings free from oil and grease
P250	Do not subject to grinding/shock/…/friction
P251	Do not pierce or burn, even after use
P260	Do not breathe dust/fumes/gas/mist/vapours/spray
P261	Avoid breathing dust/fumes/gas/mist/vapours/spray
P262	Do not get in eyes, on skin, or on clothing
P263	Avoid contact during pregnancy/while nursing
P264	Wash … thoroughly after handling
P270	Do not eat, drink or smoke when using this product
P271	Use only outdoors or in a well-ventilated area
P272	Contaminated work clothing should not be allowed out of the workplace
P273	Avoid release to the environment
P280	Wear protective gloves/protective clothing/eye protection/face protection
P282	Wear cold insulating gloves/face shield/eye protection
P283	Wear fire/flame resistant/retardant clothing

7. Supplements

P284	[In case of inadequate ventilation] wear respiratory protection
P301	IF SWALLOWED
P302	IF ON SKIN
P303	IF ON SKIN (or Hair)
P304	IF INHALED
P305	IF IN EYES
P306	IF ON CLOTHING
P308	If exposed or concerned
P310	Immediately call a POISON CENTER/doctor/…
P311	Call a POISON CENTER/ doctor/…
P312	Call a POISON CENTER/ doctor/…/if you feel unwell
P313	Get medical advice/attention
P314	Get medical advice/attention if you feel unwell
P315	Get immediate medical advice/attention
P320	Specific treatment is urgent (see … on this label)
P321	Specific treatment (see … on this label)
P330	Rinse mouth
P331	Do NOT induce vomiting
P332	If skin irritation occurs:
P333	If skin irritation or a rash occurs:
P334	Immerse in cool water/wrap in wet bandages
P335	Brush off loose particles from skin
P336	Thaw frosted parts with lukewarm water. Do not rub affected areas
P337	If eye irritation persists:

7. Supplements

P338	Remove contact lenses if present and easy to do. Continue rinsing.
P340	Remove person to fresh air and keep comfortable for breathing.
P342	If experiencing respiratory symptoms:
P351	Rinse cautiously with water for several minutes
P352	Wash with plenty of water/…
P353	Rinse skin with water/shower
P360	Rinse immediately contaminated clothing and skin with plenty of water
P361	Take off immediately all contaminated clothing
P362	Take off contaminated clothing
P363	Wash contaminated clothing before reuse
P364	And wash it before reuse
P370	In case of fire:
P371	In case of major fire and large quantities:
P372	Explosion risk in case of fire
P373	DO NOT fight fire when fire reaches explosives
P374	Fight fire with normal precautions from a reasonable distance
P375	Fight fire remotely due to the risk of explosion
P376	Stop leak if safe to do so
P377	Leaking gas fire – do not extinguish unless leak can be stopped safely
P378	Use … to extinguish
P380	Evacuate area
P381	Eliminate all ignition sources if safe to do so
P391	Collect spillage
P301+310	IF SWALLOWED: Immediately call a POISON CENTER/doctor/…

7. Supplements

P301+312	IF SWALLOWED: Call a POISON CENTER/doctor/…/if you feel unwell
P301+330+331	IF SWALLOWED: Rinse mouth. Do NOT induce vomiting
P302+334	IF ON SKIN: Immerse in cool water/wrap in wet bandages
P302+352	IF ON SKIN: Wash with plenty of water/…
P303+361+353	IF ON SKIN (or hair): Take off immediately all contaminated clothing. Rinse skin with water/ shower
P304+312	IF INHALED: Call a POISON CENTER or doctor/physician if you feel unwell
P304+340	IF INHALED: Remove person to fresh air and keep comfortable for breathing
P305+351+338	IF IN EYES: Rinse cautiously with water for several minutes. Remove contact lenses if present and easy to do – continue rinsing
P306+360	IF ON CLOTHING: Rinse immediately contaminated clothing and skin with plenty of water before removing clothes
P308+311	If exposed or concerned: Call a POISON CENTER/ doctor/…
P308+313	If exposed: Call a POISON CENTER or doctor/physician
P332+313	If skin irritation occurs: Get medical advice/attention
P333+313	If skin irritation or a rash occurs: Get medical advice/attention
P335+334	Brush off loose particles from skin. Immerse in cool water/wrap in wet bandages
P337+313	If eye irritation persists get medical advice/attention
P342+311	If experiencing respiratory symptoms: Call a POISON CENTER/doctor/…
P361+364	Take off immediately all contaminated clothing and wash it before reuse
P362+364	Take off contaminated clothing and wash it before reuse
P370+376	In case of fire: Stop leak if safe to do so
P370+378	In case of fire: Use … to extinguish
P370+380	In case of fire: Evacuate area
P370+380+375	In case of fire: Evacuate area. Fight fire remotely due to the risk of explosion
P371+380+375	In case of major fire and large quantities: Evacuate area. Fight fire remotely due to the risk of explosion
P401	Store …

7. Supplements

P402	Store in a dry place
P403	Store in a well-ventilated place
P404	Store in a closed container
P405	Store locked up
P406	Store in a corrosive resistant/… container with a resistant inner liner
P407	Maintain air gap between stacks/pallets
P410	Protect from sunlight
P411	Store at temperatures not exceeding … °C/… °F
P412	Do not expose to temperatures exceeding 50 °C/122 °F
P413	Store bulk masses greater than … kg/… lbs at temperatures not exceeding … °C/… °F
P420	Store away from other materials
P422	Store contents under …
P402+404	Store in a dry place. Store in a closed container
P403+233	Store in a well-ventilated place. Keep container tightly closed
P403+235	Store in a well-ventilated place. Keep cool
P410+403	Protect from sunlight. Store in a well-ventilated place
P410+412	Protect from sunlight. Do not expose to temperatures exceeding 50 °C/122 °F
P411+235	Store at temperatures not exceeding … °C/… °F. Keep cool
P501	Dispose of contents/container to …
P502	Refer to manufacturer/supplier for information on recovery/recycling

8. Summary

Although the impact of cardiovascular diseases on human life has been declining yet there are still many open questions. These need to be answered in the field of cardiovascular diseases. These questions focus on the (I).pathophysiology of several lethal cardiovascular diseases (II) the scrutiny of available drug screening models for their safe use in human beings and (III) the potential creation of human cardiovascular tissue for the repair of the heart. Human-induced pluripotent stem cell-derived cardiomyocytes (hiPSC-CMs) can be a bag full of solutions for all hindrances and shortcomings in the research field of cardiovascular diseases. But before they can be utilized, hiPSC-CMs must closely resemble adult cardiomyocytes on a genomic, anatomical, electrophysiological and physiological level. β_1-ARs are a key regulator of ECC in the heart. Calcium channels in hiPSC-CMs respond to β_1-AR signaling, however the effect size depends upon culture conditions with smaller effects having been observed in conventional 2D than in 3D culture constructs. Since in adult heart β_1-AR-mediated effects are spatially and temporally controlled by different PDEs, it was the aim of the presented study to investigate whether smaller effects of NE in ML relate to a different impact of PDEs on β_1-AR-dependent cAMP.

Suitable generation and propagation of cAMP to its effectors like the L-type calcium channels produces a wide range of physiological and pathophysiological activities in cardiomyocytes. So the study of dynamics of cAMP and its impact on $I_{Ca,\,L}$ can be vital parameters to judge the resemblance between hiPSC-CMs and adult cardiomyocytes.

We used hiPSC-CMs produced in our lab and cast them into ML and EHT formats. After 21 days continuous feeding with culture medium we isolated hiPSC-CMs from ML and EHT by using an established protocol (Uzun et al., 2016). These hiPSC-CMs were used to measure $I_{Ca,\,L}$ by patch clamp technique and cAMP by FRET. Effects of inhibition of different PDEs on the basal level of I_{Ca} and cAMP as well as on NE-induced $I_{Ca,\,L}$ and cAMP were investigational parameters of this study.

HiPSC-CMs show proper sensitivity to β_1-adrenergic receptor stimulation with respect to $I_{Ca,\,L}$ and cAMP in MI construct (Fig 52 A). PDE4 is the dominant regulator of basal $I_{Ca,\,L}$ and cAMP levels in hiPSC-CMs, which is in contrast to adult human atrial cardiomyocytes (Molina et al., 2012; Christ et al., 2006). Furthermore, PDE4 is the major phosphodiesterase which regulates NE-induced $I_{Ca,\,L}$ and cAMP in hiPSC-CMs isolated from ML tissue (Fig 52 A).

8. Summary

NE-induced $I_{Ca,\,L}$ was augmented by the inhibition of PDE4 in isolated hiPSC-CMs from EHTs, while results of NE-induced cAMP in the absence of PDE4 in isolated hiPSC-CMs from EHTs were not conclusive (Fig.52 B).

Contribution of PDE3 to define NE-induced $I_{Ca,\,L}$ and cAMP in hiPSC-CMs from EHT (C-25) was divergent (Fig.52 B). In all three experimental designs ($I_{Ca,\,L,}$ global FRET and SL FRET) effects of NE on $I_{Ca,\,L}$ and cAMP were suppressed in the presence of cilostamide. We studied contributions of other PDEs to this discrepancy, until we realized that these results may be a peculiarity of a single cell line, namely C-25, as we do not find this in hiPSC-CMs from other cell lines

HiPSC-CMs from both ML and EHT respond to NE with an increase in cAMP, but the maximum effect size is smaller in ML than EHT, whereas the sensitivity is not changed.

As in human adult atrial CMs basal cAMP can be increased by inhibition of PDE3 and PDE4. While the impact of PDE3 on cAMP in adult human atrial CMs is clearly larger than with PDE4, the contribution of PDE4 in hiPSC-CMs is at least as large as with PDE3 (ML) or even larger than with PDE3 (EHT).

The maximum effect size of NE is not regulated by PDE3 and PDE4 in adult human atrial CMs. In stark contrast, inhibition of either PDE3 or PDE4 can increase the maximum effect size of NE in ML but not EHT. The latter finding could indicate a more mature regulation of β_1-AR-mediated cAMP signals in hiPSC-CMs from EHT.

Regulation of maximum effects of NE by PDE3 and PDE4 is a strong disadvantage in ML. On the other hand maximum effects of NE not sensitive to PDE4 inhibition in EHT resemble the situation in adult human atrial CMs. Suppression of maximum effects of NE in the presence of PDE3 inhibition as observed in just one cell line serves as a precautionary note to always profile hiPSC-CMs from different origins. Stringent investigational exploration of different cell lines is required, before they are used to make generalized statements about the utilization of hiPSC-CMs as a model for scientific study of cardiovascular diseases and their treatments.

8. Summary

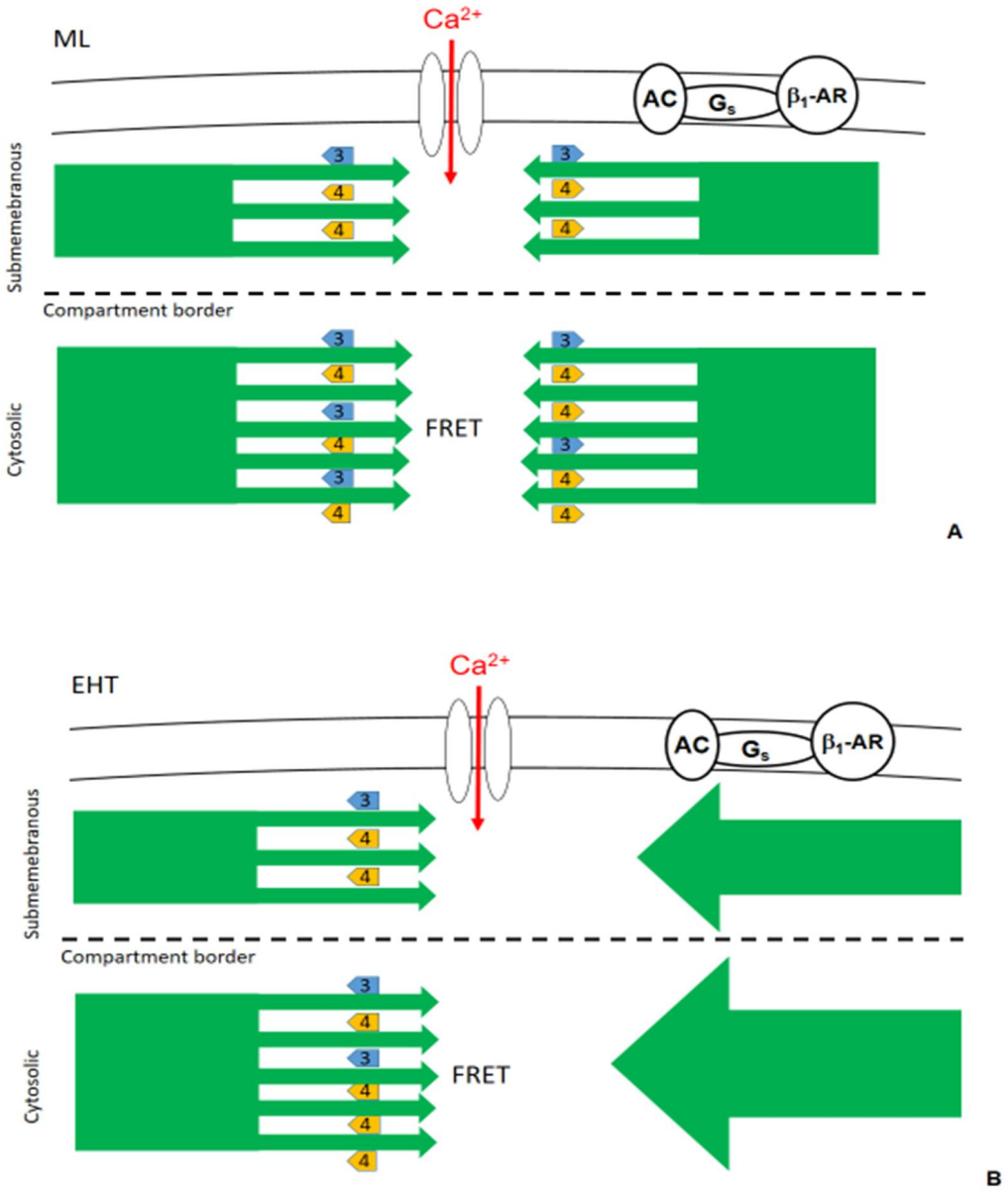

Figure 52: Proposed scheme of cAMP regulation in isolated hiPSC-CMs from EHT or ML tissues

In ML (**A**): Both basal and maximum NE-stimulated cAMP is regulated by PDE3 and PDE4 in the compartment relevant for $I_{Ca,L}$ and in the global compartment. Effects of PDE4 are larger than effects of PDE3 except basal cAMP in the global compartment. In EHT (**B**): In the compartment relevant for $I_{Ca,L}$ regulation and in the global compartment only basal cAMP is regulated by PDE3 and PDE4. Effects of PDE4 are larger than effects of PDE3. Maximum NE-stimulated cAMP is no longer restricted by PDE3 or PDE4.

9. Zusammenfassung

Obwohl der Einfluss kardiovaskulärer Erkrankungen auf das menschliche Leben abnehmend ist, gibt es immer noch ungeklärte Fragen im Bereich der kardiovaskulären Forschung, welche beantwortet werden müssen. Diese Fragen fokussieren sich auf die (I) Pathophysiologie verschiedener letaler kardiovaskulärer Erkrankungen, (II) die Suche nach verfügbaren Medikamenten-Screening Modellen für die sichere Anwendung von Medikamenten am Menschen und (III) die potenzielle Herstellung von humanem kardiovaskulärem Gewebe für die Reparatur des Herzmuskelgewebes. Myokardzellen auf der Basis von humanen induzierten pluripotenten Stammzellen (hiPSC-CMs) könnten eine Fülle von Lösungen für jegliche Hindernisse und Unzulänglichkeiten in der Erforschung kardiovaskulärer Erkrankungen darstellen. Aber vor ihrer Anwendung müssen hiPSC-CMs in ihrer Genetik, Anatomie, physiologischen sowie elektrophysiologischen Eigenschaften adulter Myokardzellen angeglichen werden. β_1-AR nehmen eine Schlüsselrolle in der Regulation der elektromechanischen Kopplung im Herzen ein. Zwar sprechen Calciumkanäle in hiPSC-CMs auf ein β_1-AR-Signalling an, jedoch ist ihre Effektgröße abhängig von ihren Kulturbedingungen. So ist ein geringerer Effekt in konventionellen 2D verglichen mit 3D Kulturbedingungen zu verzeichnen. β_1-AR-vermittelte Effekte in adulten Herzen werden räumlich und zeitlich durch verschiedene PDE's reguliert. Das Ziel der vorliegenden Arbeit war es zu untersuchen, ob die geringeren Effekte von NE in ML durch die unterschiedlichen Einflüsse von PDEs auf β_1-AR abhängige cAMP erklärbar sind.

Eine adäquate Generierung und Vervielfachung von cAMP für seine Effektoren wie die L-Typ Calcium-Kanäle entfachen zahlreiche physiologische und pathophysiologische Vorgänge in Myokardzellen. Somit stellen die Untersuchung der Dynamik von cAMP und seine Auswirkung auf $I_{Ca,\,L}$ entscheidende Parameter für die Beurteilung der Ähnlichkeit zwischen hiPSC-CMs und adulten humanen Myokardzellen dar.

In unserem Labor hergestellte hiPSC-CMs wandelten wir in ML- und EHT-Konstrukte um. Nach 21 Tagen kontinuierlicher Ernährung mit Kulturmedium isolierten wir hiPSC-CMs anhand eines etablierten Protokolls (Uzun et al., 2016). Diese hiPSC-CMs wurden für die Messung des $I_{Ca,\,L}$ durch Patch-Clamp-Technik und für die Bestimmung von cAMP durch FRET verwendet. Die Effekte der Hemmung verschiedener PDEs auf den basalen $I_{Ca,\,L}$ und cAMP sowie den NE-induzierten $I_{Ca,\,L}$ und cAMP waren Untersuchungsparameter dieser Studie.

HiPSC-CMs zeigen eine entsprechende Empfindlichkeit gegenüber β_1-adrenerger Rezeptorstimulation in Bezug auf $I_{Ca,\,L}$ und cAMP (Fig. 52 A). PDE4 stellt den wichtigsten Regulator des basalen $I_{Ca,\,L}$ und des cAMP-Spiegels in hiPSC-CMs dar, wodurch diese sich von adulten humanen Vorhofmyokardzellen unterscheiden (Molina et al., 2012; Christ et al., 2006). Darüber hinaus ist PDE4 die vorrangige Phosphodiesterase, welche den NE-induzierten $I_{Ca,\,L}$ und den cAMP-Spiegel aus ML Gewebe isolierten hiPSC-CMs reguliert (Fig. 52A).

Der NE-induzierte $I_{Ca,\,L}$ wurde durch die Hemmung der PDE4 in isolierten hiPSC-CMs aus EHT's verstärkt, während die Ergebnisse des NE-induzierten cAMP-Spiegels in Abwesenheit von PDE4 in isolierten hiPSC-CMs aus EHT's nicht eindeutig waren (Fig. 52 B).

Die Ergebnisse der Versuche mit EHT (C-25) sind divergent bezüglich des Beitrags von PDE3 für die Bedeutung des NE-induzierten $I_{Ca,\,L}$ und cAMP in hiPSC-CMs (Fig. 52 B). In allen drei Studiendesigns ($I_{Ca,\,L}$, global FRET und SL FRET) waren die Effekte von NE auf $I_{Ca,\,L}$ und cAMP in Anwesenheit von Cilostamid supprimiert. Wir untersuchten die Bedeutung anderer PDEs bezüglich dieser Diskrepanz, bis wir realisierten, dass diese Ergebnisse wahrscheinlich

eine Besonderheit einer einzigen Zelllinie, nämlich von C-25, darstellen. Diese Besonderheit fanden wir nicht in hiPSC-CMs anderer Zelllinien.

HiPSC-CMs sowohl von ML als auch von EHT reagieren auf NE mit einem Anstieg von cAMP. Dabei ist die maximale Effektgröße kleiner in ML verglichen mit EHT, wohingegen die Empfindlichkeit sich nicht unterscheidet.

In humanen adulten Vorhofmyokardzellen kann der basale cAMP-Spiegel durch die Hemmung von PDE3 und PDE4 gesteigert werden. Während der Einfluss von PDE3 auf cAMP in adulten humanen Vorhofmyokardzellen deutlich größer ist als von PDE4, so ist der Beitrag von PDE4 in hiPSC-CMs mindestens so groß wie PDE3 (ML) oder sogar größer als mit PDE3 (EHT).

Die maximale Effektgröße von NE wird nicht durch PDE3 und PDE4 in adulten humanen Vorhofmyokardzellen reguliert. Im Kontrast dazu führt eine Hemmung von PDE3 oder PDE4 zu einer Steigerung der maximalen Effektgröße von NE in ML, hingegen nicht beim EHT. Letzteres könnte auf eine ausgereiftere Regulation von β_1-AR-vermittelten cAMP Signalen in hiPSC-CMs aus dem EHT hinweisen.

Die Regulation des maximalen Effektes von NE durch PDE3 und PDE4 ist ein starker Nachteil im ML. Auf der anderen Seite spiegelt das Nichtansprechen der PDE4-Hemmung auf den maximalen Effekt von NE im EHT die Situation in adulten humanen Vorhofmyokardzellen wieder. Die Suppression der maximalen Effekte von NE in Anwesenheit der PDE3-Hemmung, so wie sie nur in einer Zelllinie beobachtet wurde, lehrt uns, die hiPSC-CMs stets nach ihrem Ursprung zu charakterisieren. Allgemeine Aussagen über die Nutzung von hiPSC-CMs als Modell für wissenschaftliche Studien im Bereich kardiovaskulärer Erkrankungen und ihrer Behandlungen setzen eine vorherige präzise wissenschaftliche Untersuchung der verschiedenen Zelllinien voraus.

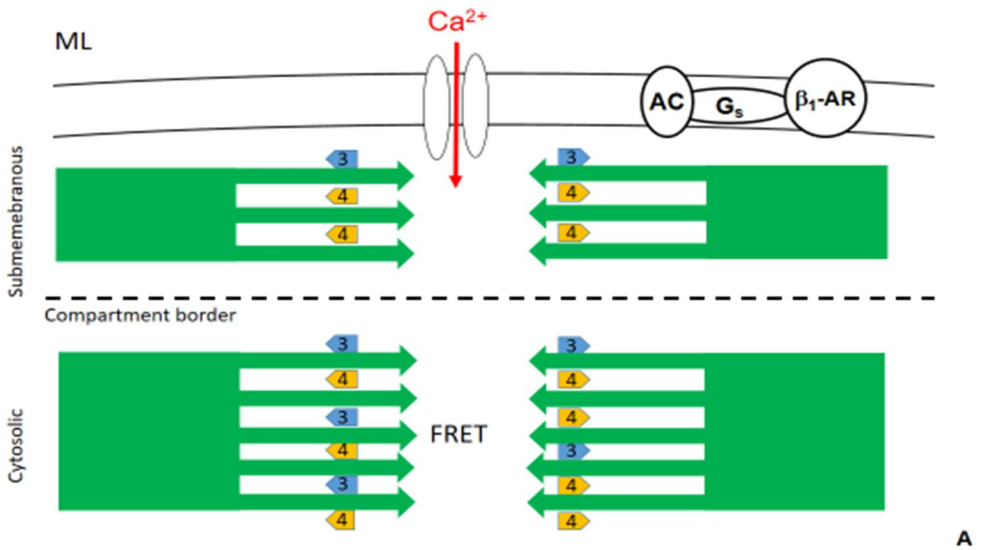

A

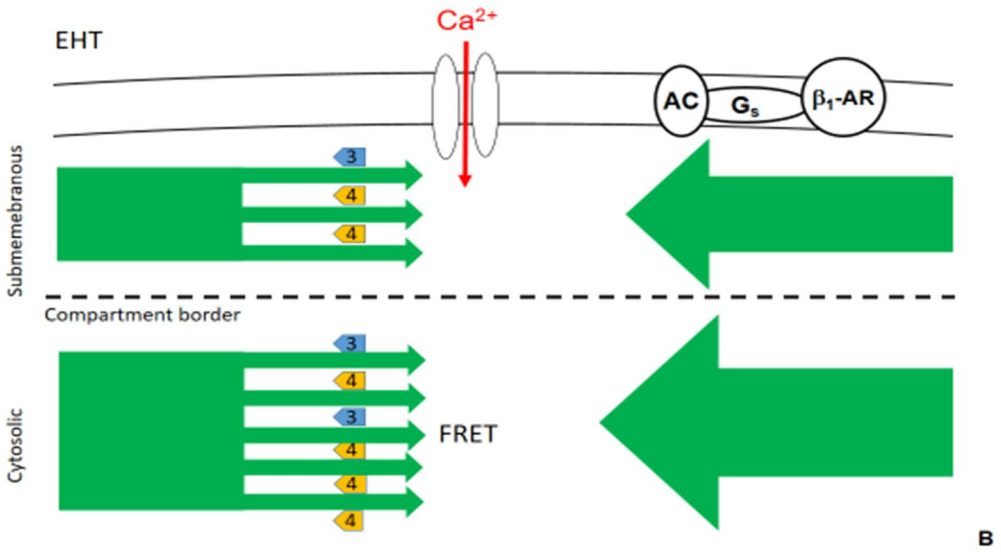

Abbildung 52: Vorgeschlagenes Schema der cAMP Regulation in isolierten hiPSC-CMs aus EHT oder ML Gewebe

Bei ML (**A**): Sowohl der basale als auch der maximale NE-induzierte cAMP-Spiegel wird durch PDE3 und PDE4 im für $I_{Ca,\ L}$ relevanten Kompartiment und im globalen Kompartiment reguliert. Die Effekte von PDE4 sind größer als die Effekte von PDE3 mit Ausnahme des basalen cAMP im globalen Kompartiment. Beim EHT (**B**): Im Kompartiment relevant für die $I_{Ca,\ L}$ -Regulation und im globale Kompartiment wird nur der basale cAMP-Spiegel durch PDE3 und PDE4 reguliert. Die Effekte von PDE4 sind größer als die Effekte von PDE3. Der maximale NE-induzierte cAMP-Spiegel ist nicht mehr eingeschränkt durch PDE3 oder PDE4.

10. Acknowledgments

Life is beautiful not only philosophically but also practically as it is highly dynamic. In one moment you are up and the next moment you are down. You have your facilitators as well as competitors in these unpredictable moments, which will make these moments unforgettable. You will take facilitators as your team and competitors as opponents but at the end both will be on your side as the ultimate goal of life is to make you self-sufficient and confident.

I would like to thank both facilitators and competitors for their role in the past 4 years of my life. I would like to especially mention names of those facilitators, which are no longer in this world but who will always remain with me. First of them is My Father **Muhammad Nawaz**, who became even closer to me after His death. Second my Romanian friend Tibi who loved me as my brother: I will never forget you.

I would like to mention sacrifice and courage of **My Mother** to face all problems and allow me to return back to complete my work.

I would like to convey my warm gratitude to my wife **Azra Batool** and my daughters i.e. **Mashal Zahra and Mehrab Zahra** who shared all the unpredictable moments of my life. I was used to face life but they were not and they proved that they are brave enough to even support me.

I want to appreciate **Umber Saleem, Pierre Bobin and Marta Lemme** for providing me ML and EHT tissues which required strenuous work to be produced. My whole research owes to their countless support as it is not hidden how much time and hard work it takes to generate EHTs and ML tissues.

I am thankful all my lab mates and colleagues from the institute of Experimental Pharmacology and Toxicology.

Some gold plated names like **Bernardo Dolce, Sharia Iqbal, and Anna Steenpas** will always come first on the list whenever I need help in my social, bureaucratic aspects of life. I cannot describe their loyalty, friendship, kindness and love in words.

I would like to thank peoples from Institute of Experimental Cardiovascular Research **Professor Viacheslav Nikolaev** and his lab members **Cristina E. Molina** and Hariharan Subramanian and I want to mention **Sophie Schobesberger** who gave me her precious time and trained me to use FRET to measure cAMP.

Finally, the biggest thank and gratitude is dedicated to **Prof. Thomas Eschenhagen** and my supervisor **Dr. Torsten Christ** for giving me the opportunity to undertake this PhD program and for always supporting my ideas. I have to confess that **Dr. Torsten Christ** was really kind and always supporting even when I did some blunders. I dedicate to **Dr. Torsten Christ** this quote from Galileo

“You cannot teach a man anything, you can only help him find it within himself.”

My stay at Hamburg and this PhD program was funded by German Academic Exchange Service (DAAD) and Higher Education Commission, Pakistan (HEC). I want to pay my thanks to all staff of my funding bodies i.e. DAAD and HEC.

11. Affidavit - Eidesstattliche Versicherung

I hereby expressly declare that I have written the work myself and without outside help, not used sources and tools other than those stated, and individually acknowledged the parts taken literally or in terms of content from the works used according to the edition (edition and year of publication), volume and page of the work used. Furthermore, I declare not to have submitted the dissertation to a subject representative at another university for review or otherwise applied for admission to a doctorate. I consent to my dissertation being examined by the Dean's Office of the Faculty of Medicine using a standard plagiarism detection software.

Signature: .....

Ich versichere ausdrücklich, dass ich die Arbeit selbständig und ohne fremde Hilfe verfasst, andere als die von mir angegebenen Quellen und Hilfsmittel nicht benutzt und die aus den benutzten Werken wörtlich oder inhaltlich entnommenen Stellen einzeln nach Ausgabe (Auflage und Jahr des Erscheinens), Band und Seite des benutzten Werkes kenntlich gemacht habe.

Ferner versichere ich, dass ich die Dissertation bisher nicht einem Fachvertreter an einer anderen Hochschule zur Überprüfung vorgelegt oder mich anderweitig um Zulassung zur Promotion beworben habe.

Ich erkläre mich einverstanden, dass meine Dissertation vom Dekanat der Medizinischen Fakultät mit einer gängigen Software zur Erkennung von Plagiaten überprüft werden kann.

Unterschrift: .....zafar.....